Strathclyde
Discussion Papers
in Economics

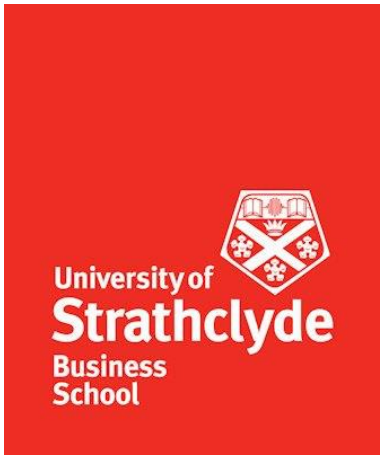

A Unified Framework to Estimate Macroeconomic Stars

Saeed Zaman

No. 21 – 6

Department of Economics
University of Strathclyde, Glasgow

A Unified Framework to Estimate Macroeconomic Stars

Saeed Zaman*
Federal Reserve Bank of Cleveland, USA
University of Strathclyde, UK

First draft: September 16, 2020
This version: June 30, 2021

Abstract

We develop a flexible semi-structural time series model to estimate jointly several macroeconomic *"stars"* — i.e., unobserved long-run equilibrium levels of output (and growth rate of output), unemployment rate, the real rate of interest, productivity growth, price inflation, and wage inflation. The ingredients of our model are in part motivated by economic theory and, in part, by the empirical features necessitated due to the changing economic environment. Following recent literature on inflation and interest rate modeling, we explicitly model the links between long-run survey expectations and stars to improve the stars' econometric estimation. Our approach permits time-variation in the relationships between various components, including time-variation in error variances. To tractably estimate our large multivariate model, we use a recently developed precision sampler that relies on Bayesian methods. Our approach's by-products are the time-varying estimates of the wage and price Phillips curves, passthrough between prices and wages, which provide new insights into these empirical relationships' instability in US data. Generally, the contours of our stars echo those documented elsewhere in the literature – estimated using smaller models – but at times the estimates of stars are different, and these differences can matter for policy. Furthermore, our estimates of the stars are among the most precise. Lastly, we document the competitive real-time forecasting properties of our model and, separately, the usefulness of stars' estimates if they were used as steady-state values in external models.

JEL classification: C5, E4, E31, E24, O4

Keywords: state-space model, Bayesian analysis, time varying parameters, natural rates, survey expectations, COVID-19 pandemic

I am extremely grateful to my advisors Gary Koop and Julia Darby for the valuable guidance and the feedback throughout the research process. I am indebted to Todd Clark, Ellis Tallman, and Randal Verbrugge for helpful comments on the first draft. This research has benefited from discussions with Fabio Canova, Olivier Coibion, Sharada Davidson, Jesus Fernandez-Villaverde, Paolo Gelain, Yuriy Gorodnichenko, Stuart McIntyre, Eric Sims, and Ping Wu. I also thank participants at the Society for Computational Economics 27th International Conference. The views expressed herein are those of the author and do not necessarily represent the views of the Federal Reserve Bank of Cleveland or the Federal Reserve System.

*Research department, Federal Reserve Bank of Cleveland, Ohio, USA; and Department of Economics, University of Strathclyde, Glasgow, United Kingdom; email: saeed.zaman@clev.frb.org

1. Introduction

The economic concept of a long-run equilibrium level (often denoted with the "star" symbol) is central to macroeconomics. This is because it provides a conceptual reference point (benchmark) to understand various macroeconomic developments. It is thought of as a reference point because it reflects the fundamental structural aspect of the economy. Hence, the deviations in real GDP from its long-run equilibrium path, or in deviations from equilibrium in other macroeconomic indicators, reflect cyclical and idiosyncratic fluctuations. The assumption is that these fluctuations die out in the long-run, and the economy gravitates to its long-run equilibrium. Dynamics of cyclical changes and the pace of their adjustment towards the long-run equilibrium are of interest to macroeconomists. However, effective identification of cyclical fluctuations in any macroeconomic aggregate requires knowledge of its long-run equilibrium.

In this paper, we consider the macroeconomic stars of broader interest to macroeconomists and policymakers: the equilibrium rate of productivity growth (p-star), the level of potential output (gdp-star), the growth rate of potential output (g-star), the equilibrium level of the unemployment rate (u-star), the equilibrium level of the real rate of interest (r-star), the equilibrium rate of price inflation (pi-star), and the equilibrium rate of nominal wage inflation (w-star).[1]

The very assumption that a long-run equilibrium exists implies that in the long-run, the economy is growing at potential, inflation is stable around its trend rate, the unemployment rate reflects a combination of structural and frictional factors, i.e., there is no cyclical pressure, nominal wages grow at a rate equal to the sum of trend productivity growth and trend inflation, which implies that real wages rise at the same rate as growth in labor productivity, and the real interest rate reflects the rate consistent with output growing at potential and stable inflation.[2]

As discussed in Weber et al. (2008), conceptually, determining stars' estimates appears straightforward. However, in practice, it is fraught with difficulties. The difficulties stem from the fact that the values of the stars and their determinants are unobserved. To infer the estimates of the stars, a range of statistical and econometric methods are applied to observable historical data. These methods range from statistical univariate filters (e.g., Hodrick and Prescott, 1997; Christiano and Fitzgerald, 2003; Ashley and Verbrugge, 2009) to multivariate models, including semi-structural time-series models (e.g., Pescatori and Turunen, 2016; Morley and Wong, 2020), and fully structural DSGE models (e.g., Del Negro et al., 2017).

Economic theory posits that the structural aspects of the economy, which inform the values of the stars, change slowly. Therefore, methods that deliver estimates of stars that change only

[1] The subset of these stars, p-star, g-star, u-star, and r-star, reflect the fundamental structural features of the economy whereas others, pi-star and w-star are thought to be influenced by centrals banks and monetary policy.

[2] The literature has referred to the concept of long-run equilibrium using different terminologies, such as "natural", "neutral", "trend", "steady-state", and "long-run". There are subtle differences among them, but they can be interpreted as the same for the purpose of this paper. In some studies, especially using Dynamic Stochastic General Equilibrium (DSGE) models, the concept of the natural rate refers to medium-horizon equilibrium, and in these same models, the concept of steady-state is used to refer to the long-run equilibrium.

gradually have more traction than methods that give less smooth estimates. According to this criterion, multivariate unobserved components (UC) models, which are statistical models that use economic theory to frame the empirical specification, have been shown to provide reasonable estimates of the stars (e.g., Kuttner, 1994; Basistha and Nelson, 2007; Laubach and Williams, 2003; Chan, Koop, and Potter, 2016). Hence, they are the dominant methods for obtaining time-varying estimates of the stars.

However, with few exceptions, the popular multivariate UC models that provide estimates of time-varying stars focus on a small number of observables, often just two or three, and have a minimal structure (e.g., Laubach and Williams, 2003). A priori, one would expect a specification based on greater amounts of information and a richer structure to provide more reliable estimates. Indeed, Taylor and Wieland (2016) make a similar argument in the importance of appropriately accounting for trends in the determinants of the r-star to estimate r-star correctly. Specifically, Taylor and Wieland (2016) point out, "What appear to be trends in the equilibrium interest rate may instead be trends in other policy variables that affect the economy." They emphasize that omitted variable(s) and relatedly omitted equation(s) problems can severely affect the reliability of the estimates of the r-star.

As a result, in the past few years, several papers have provided estimates of the stars using UC models with a larger number of indicators and an expanded structure. For example, Johannsen and Mertens (forthcoming) [henceforth JM], Pescatori and Turunen (2016), Del Negro et al. (2017), among others, have examined the roles of additional determinants in explaining r-star. Pescatori and Turunen (2016) enrich the underlying structure to estimate r-star. In particular, to extract a reliable estimate of the output gap, they bring additional information from the Congressional Budget Office (CBO)'s estimate of the output gap by treating it as a noisy measure of the "true" output gap. The improved estimate of the output gap affects the estimates of r-star and provides new insights about r-star estimates' movements.[3]

Similarly, Chan, Koop, and Potter (2016) – henceforth CKP – and Chan, Clark, and Koop (2018) – henceforth CCK – enrich the econometric specification to estimate pi-star. In particular, CCK introduces an explicit role for long-run survey expectations in influencing pi-star estimates. CKP illustrates the value of modeling u-star and pi-star as bounded random walk processes. More recently, Crump et al. (2019) combine a range of labor market indicators across demographic groups with survey expectations of inflation to pin down the estimates of u-star.

In this paper, we take on the challenge of jointly estimating several macroeconomic stars simultaneously, including g-star (and gdp-star), u-star, p-star, pi-star, w-star, and r-star, using a semi-structural time series model (aka multivariate UC model with a particular structure

[3]Morley and Wong (2020) and Chan (2019) propose alternative modeling framework based on VARs to estimate the long-run equilibrium values. The advantage of the VAR based framwork is the ability to handle larger amounts of information conveniently and flexibly compared to UC models. On the other hand, the advantage of UC modeling, as emphasized by Chan, Koop and Potter (2016), is the availability of the direct estimates of stars, which in our case proves quite convenient to allow for direct modeling of the relationships between various stars. In VARs, the long-run estimates are implied estimates, hence imposing long-run restricitions is not as straightforward.

informed from economic theory). For each star, we formulate a rich structure whose elements are guided by past research. In doing so, we contribute to the literature in six important ways. First, we develop a multivariate time-series model that provides direct estimates for all the stars that are of most relevance to macroeconomic policymakers. In principle, proceeding with the joint estimation of a framework that explicitly models the objects of interest and permits interactions among them (e.g., stars) has the potential to provide more reliable estimates of the objects compared than approaches that ignore them. The modeling of many variables directly addresses critiques of omitted variable and omitted equation bias pointed out by Taylor and Wieland (2016).

Our results indicate that specification choices matter for all stars considered, and there are payoffs to modeling them jointly. For r-star and u-star, the choice of specification matters the most, and least for g-star. Generally, the contours of our stars echo those documented elsewhere in the literature, but at times are different, and these differences can matter for policy. Interestingly, in the past decade, the estimates of r-star, pi-star, g-star (and output gap), p-star, and u-star from our baseline model indicate remarkably similar inferences to those documented elsewhere.

We also find that our models (with or without survey data) produce estimates of the output gap that are similar to the CBO estimate, which is based on a production function approach (see Shackleton, 2018). This result provides evidence supporting the common practice of using the output gap estimates from the CBO as an exogenous variable in empirical macroeconomic models (e.g., JM;Stock and Watson, 2020). We view this result as a useful contribution to the applied macro literature.

Second, in our medium-scale model, we allow for time-variation in the important macroeconomic relationships and in the error variances (i.e., stochastic volatility). Fernandez-Villaverde and Rubio-Ramirez (2010), Koop and Korobilis (2010), Carriero et al. (2019), among many others, highlight the importance of allowing for stochastic volatility in macroeconomic models. Permitting time-varying relationships between model components will potentially lead to more credible estimates and are arguably less susceptible to the Lucas critique. Also, new insights can be provided on time-varying nature of important empirical macroeconomic relationships such as the price Phillips curve, wage Phillips curve, passthrough between prices and wages, and persistence in price and wage inflation dynamics.

To the best of our knowledge, features such as time-varying parameters and stochastic volatility (SV) have not been implemented in a multivariate UC framework beyond a system consisting of at most four variables (e.g., Berger et al., 2016). In principle, these empirical features should help better distinguish between cyclical fluctuations and lower-frequency movements in the macroeconomic aggregates considered in this paper. Our results indicate economically and statistically significant evidence of time-variation in these important relationships and strong support for SV's inclusion in our model equations. It lends support to the popular narratives: "(price) Phillips curve has weakened over time," "wage Phillips curve is alive," and

"weakening in the procyclicality of labor productivity."

Third, we extend the CCK approach of using survey expectations to improve pi-star precision to other macroeconomic stars. Specifically, for each macroeconomic variable of interest, we explicitly model the link between the unobserved "star" and the expectations about the companion star contained in the Blue Chip survey of economic forecasters (or reported by the Congressional Budget Office [CBO] when the survey estimate is not available). The long-run survey expectations can be thought of as a hybrid forecast because it combines judgment based on a range of information and forecast derived from a range of modeling approaches. Our use of such a hybrid forecast implicitly serves as an additional channel through which the issue of omitted variable bias is mitigated. By bringing in additional information from survey expectations, we find significant improvements in the precisions of the stars' estimates. By-products are the results describing the nature of the relationship between survey expectations and stars. The results indicate that the relationship between the two is time-varying. In the context of inflation expectations, CCK finds similar results.

Fourth, we provide a model to obtain real-time estimates of w-star (the long-run equilibrium level of nominal wage inflation) and its determinants. Our choice of a particular specification for w-star permits a time-varying model-based decomposition of w-star into its determinants p-star and pi-star, as implied by economic theory. This specific decomposition is useful to monetary policymakers, who often refer to developments in nominal wages to support their forecasts and in related discussions on price inflation and employment.

Olivier Blanchard, recently suggested that the central bank, such as the Federal Reserve, should target nominal wage inflation instead of price inflation.[4] If in the future central banks define a longer run goal for nominal inflation in a measure of wage inflation, then the framework presented in this paper would prove valuable.

Our results provide strong evidence of time-varying wage Phillips curve in the post-1960 US data, and we find that compared to the price Phillips curve, the strength of the wage Phillips curve remains strong for longer, but has weakened since 1985.

Fifth, our empirical model can generate competitive real-time point and density forecasts of macroeconomic variables of broader interest. Sixth, the estimates of the stars from our model can potentially be used to inform the steady-state values for reduced-form VAR models (and/or DSGE models). Previous research has shown that forecasting models, such as VARs often benefit greatly from external information about steady-states informed by professional forecasters' long-run survey expectations (Wright, 2013; Tallman and Zaman, 2020). Using a real-time forecasting horse-race, we show that estimates of stars from our model are competitive relative to corresponding survey expectations (Blue Chip). Therefore, our framework provides a potential source for obtaining the stars' estimates in real-time. An advantage of our framework compared to surveys is that it offers both point and density estimates for the stars.

[4]See page 61 of the transcript from the Brookings Institution WHAT'S (NOT) UP WITH INFLATION? , October 3rd, 2019. https://www.brookings.edu/wpcontent/uploads/2019/10/es_20191003_inflation_transcript.pdf

Our desire to build an empirical model with an expanded list of features, specifically (1) the ability to produce estimates for several macroeconomic stars; (2) a richer structure underlying the determinants of each macroeconomic star; (3) the use of long-run survey expectations; and (4) allowing for time-varying parameters and stochastic volatility, leads to a very flexible but heavily parameterized model.

We estimate this high-dimensional model using Bayesian techniques, which is a coherent approach to account for uncertainty. A heavily parameterized UC model admits a high possibility that the estimates of the latent components (e.g., stars) will be subject to greater uncertainty (reflected in wider probability bands) than reported elsewhere in the literature. On the other hand, we are using more information that will likely help offset the increased parameter uncertainty arising from a large parameterized model. The net effect on uncertainty is difficult to know precisely a priori but can be determined empirically.

We find that the precision of the stars' estimates (measured as the width of 90% credible interval) from our model are on a par with recent studies highlighting the improved precision of stars derived from their approaches (e.g., r-star by Del Negro et al., 2017; u-star by Crump et al., 2019; pi-star by CCK). Our results indicate the crucial role of the long-run survey expectations in improving the precision of the estimates.

The paper is organized as follows. The next section describes in detail the econometric model and its variants. Section 3 describes the data and estimation. Section 4 presents and discusses in detail the estimates of stars and other model parameters. Section 5 reports the real-time forecasting results and a discussion comparing real-time and final estimates of stars. Section 6 illustrates the ability of the model to handle the COVID-19 pandemic data. Section 7 concludes. This paper has a hefty supplementary appendix, which lists detailed Bayesian estimation steps and many additional insightful results.

2. Empirical Macro Model and Variants

The ingredients of our macroeconomic econometric model are guided both by economic theory, and by empirical considerations – namely, features that previous research have demonstrated to be empirically relevant. These features include stochastic volatility and time-varying parameters, which in turn imply time-varying predictability. Collectively, these empirical features permit modeling changing macroeconomic relationships in a flexible way.

We represent our empirical model using six sets of equations, which we denote blocks. These six blocks, which allow for *contemporaneous interactions* between them, characterize the joint dynamics of the unemployment rate, output growth, labor productivity growth, price inflation, nominal wage inflation, nominal interest rate, and corresponding stars. To be sure, the model assumes that all innovations are uncorrelated both serially and across equations. However, we emphasize that any assumed current period correlations between the cyclical components and or between stars are directly modeled via the model equations that define the contempora-

neous relationships between the components (e.g., cyclical output gap at time t with cyclical unemployment gap at t; r-star and g-star).

Before we describe the model, we provide some necessary background information, including the econometric definition of the star and the usefulness of long-run survey expectations in the estimation of stars.

2.1. The econometric notion of a long-run equilibrium

Following CCK, Mertens (2016), Lee and Nelson (2007), Morley (2002), among many, this paper defines the long-run equilibrium (or star) of a particular macroeconomic series as its infinite-horizon forecast conditional on the current information set. This definition of a star is consistent with the notion of Beveridge-Nelson trend decomposition, and extensive literature has adopted this approach to estimate stars. Equivalently, as commonly defined in the trend estimation literature, the infinite horizon forecast could be viewed as an estimate of trend conditional on the current information set (e.g., CCK, Garcia and Poon (2018), Mertens (2016), Lee and Nelson (2007), Morley (2002)). As discussed in Mertens (2016), among others, different information sets would likely yield different estimates of the infinite-horizon forecast (or trend). Mertens showed that including survey projections of long-term inflation (hereafter long-run survey forecasts) in the information set led to more precise and forward-looking estimates of trend inflation.

The link between the infinite-horizon forecast and the underlying trend is described well by the unobserved components (UC) model (see Laubach and Williams, 2003; Lee and Nelson, 2007; Mertens, 2016; CCK). In a UC model, a series (Y_t) is typically represented as a sum of a nonstationary trend component Y_t^*, which is assumed to evolve slowly and a stationary cycle Y_t^c, whose infinite-horizon conditional expectation is assumed to be zero. Accordingly,

$$Y_t = Y_t^* + Y_t^c. \tag{1}$$

The trend component Y_t^* is interpreted as the limiting forecast of the series (conditional on the information set I_t) as the forecast horizon tends to infinity,

$$\lim_{j\to\infty} \mathbb{E}[Y_{t+j}|I_t] = Y_t^*. \tag{2}$$

Differencing the above equation yields,

$$Y_t^* = Y_{t-1}^* + \lim_{j\to\infty} \mathbb{E}[Y_{t+j}|I_t] - \lim_{j\to\infty} \mathbb{E}[Y_{t+j}|I_{t-1}] = Y_{t-1}^* + e_t, \;\; e_t \sim N(0, \sigma_e^2). \tag{3}$$

which suggests a random walk process for the trend Y_t^*.[5] It also suggests a stationary,

[5]The commonly adopted assumption of modeling Y_t^* as a random walk is partly due to consensus among macroeconomists that the factors driving the long-run equilibrium levels are perceived to be quite persistent (e.g., Lee and Nelson, 2007). In practice, the assumption of a (driftless) random walk has generally worked quite well, in that it has provided reasonable estimates of the stars (e.g., Clark, 1987; Kuttner, 1994; Laubach and

ergodic mean-zero process for Y_t^c.

Intuitively, the above set of assumptions imply that once the effects of the shocks have fully played out, the macroeconomic series of interest, Y_t gravitates to its underlying trend level, Y_t^*.

As discussed in CCK, various statistical and econometric models could fit within the above-specified decomposition. This paper formulates a specific unobserved components time series model and its variants.

2.2. The role of survey expectations

As discussed in the introduction, an important contribution of this paper is to provide a direct role for long-run survey expectations in refining the stars' estimates. Specifically, we follow the approach of CCK (and Pescatori and Turunen, 2016). These papers explicitly estimate an equation linking the observed measure of a long-run forecast obtained from external sources (survey in the case of CCK and CBO projection of the output gap in Pescatori and Turunen, 2016) to an unobserved object of interest. We extend their approach to the macroeconomic variables considered in this paper.

Several papers have documented an essential role of long-run survey (and institutional) forecasts in helping refine the econometric estimation of model parameters, including the latent components (e.g., pi-star: Kozicki and Tinsley, 2012; Mertens, 2016; CCK; Mertens and Nason, 2020; gdp-star: Pescatori and Turunen, 2016; r-star: Del Negro et al., 2017). Specifically, Mertens and Nason (2020), CCK, Mertens (2016), and Kozicki and Tinsley (2012), in using different methodologies (in combining survey data with model forecasts) to estimate trend in US inflation, show that long-run survey forecasts of inflation deliver crucial additional information (beyond the recent inflation history) in refining trend estimates and improving model fit. In a similar vein, Pescatori and Turunen (2016) document the usefulness of CBO's projection of the potential output gap in improving their model's output gap precision. It is this particular literature that motivates us to consider long-run survey forecasts in our large-scale econometric model.

The advantage of survey (and institutional) forecasts stems from the fact that they could be viewed as hybrid forecasts, i.e., a combination of judgment and forecasts derived from various modeling approaches. The fact that human judgment enters into survey expectations is an important reason for their success. As discussed by Kozicki and Tinsley (2012) and others, the good forecasting properties are partly because survey participants have at their disposal a wide range of indicators, including central bank communications, and information about changes in the tax laws, etc. The patterns gleaned from this large information set can help shape opinions, including any perceived structural change, which can immediately influence expectations about the long-run.

The usefulness of this hybrid forecast measure is appealing from both theoretical and practical perspectives. From a theoretical standpoint, the notion of such a type of hybrid forecast

Williams, 2003; Mertens, 2016).

is well-aligned with the New-Keynesian view that emphasizes the importance of allowing for interlinkages between the current state of the economic variables and their expectations about the future in determining the relevant stars (see Weber et al., 2008).

From a practical point of view, such a hybrid measure helps limit the number of variables (i.e., information) that need to be brought into the model. Put differently, explicitly utilizing long-run survey expectations through an equation linking these expectations to the corresponding model's latent objects could be thought of as a short-cut to enrich the necessary information set used in model estimation. Furthermore, in high-dimensional models, such as the one developed in this paper, the use of long-run survey projections, which are targeted and direct measures of stars, could help anchor model-based estimates of stars to reasonable values and have the potential to improve precision of the estimates.

Accordingly, in this paper, with the exceptions of nominal wage inflation and labor productivity, for each of the remaining four variables, we model a direct link between long-run survey projection (or the long-run CBO projection in the years for which survey projections are unavailable) and the corresponding star using the following econometric equations[6],

$$Z_t^j = C_t^j + \beta^j j_t^* + \varepsilon_t^{zj}, \;\; \varepsilon_t^{zj} \sim N(0, \sigma_{zj}^2), \;\; j = \pi, u, g, r \tag{4}$$

$$C_t^j = C_{t-1}^j + \varepsilon_t^{cj}, \;\; \varepsilon_t^{cj} \sim N(0, \sigma_{cj}^2), \;\; j = \pi, u, g, r \tag{5}$$

where π refers to price inflation, u refers to the unemployment rate, g refers to real GDP growth, r refers to the real interest rate, Z_t^j refers to the long-run survey forecast corresponding to the variable j, and j_t^* is the unobserved j star.

C_t^j is a time-varying intercept assumed to evolve as a RW process to possibly capture the permanent wedge between survey estimate and the model-based star. This wedge can arise due to several reasons, including the fact that star is assumed to be the infinite-horizon forecast, whereas the survey forecast refers to the average forecast for the five-year period starting seven years into the future in the case of BC and ten-year ahead forecast in the case of SPF (for price inflation).

The above set of equations define a simplistic and flexible relationship between the long-run survey expectations and the star. [7]

2.3. Unemployment block

The long-run equilibrium level of unemployment (u-star) is the unemployment rate that prevails when output is growing at potential, and the economy adds jobs so as to maintain the full-employment level. This nonzero equilibrium level of unemployment is primarily the result

[6] For the long-run inflation forecast, we use the Survey of Professional Forecasters (SPF)/PTR, and for the long-run forecasts of the other three variables, we use the Blue Chip (BC) survey.

[7] We note that we adopt a relatively less flexible relationship between survey forecasts and stars than CCK.

of labor-market imperfections caused by frictional and structural aspects of the labor markets.

As discussed in Crump et al. (2019), two approaches are commonly used to estimate u-star. The first approach applies UC modeling to detailed labor market data (such as job vacancies, firm's recruiting intensity, demographic changes, flows into and out of unemployment) to extract respective trends. These trends are used to construct implied estimates of u-star (e.g., Daly, Hobijn, Sahin, and Valleta, 2012; Davis, Faberman, and Haltiwinger, 2013; Barnichon and Mesters, 2018; Tasci, 2012). The second approach uses a combination of information from prices (and or nominal wages, survey expectations) and the estimated Phillips curve relationship between price inflation and the aggregate unemployment rate to backout the estimate of u-star.[8] Various modeling techniques ranging from parsimonious UC modeling to structural DSGE models are applied to estimate the Phillips curve relationship (e.g., Staiger, Stock, and Watson, 1997; Orphanides and Williams, 2002; Lee and Nelson, 2007; CKP; Gali, 2011).

Following CKP, we posit that the observed unemployment rate is decomposed into a (bounded) RW trend component (u-star) and a stationary cyclical component. The cyclical component is modeled as an AR(2) process. The use of a parsimonious (time-invariant) AR2 process to identify the cyclical component of the unemployment rate is a commonly used assumption, in our case motivated by a recent string of empirical studies, e.g., Lee and Nelson (2007), Gali (2011), Stock and Watson (2015), CKP, Tallman, and Zaman (2017), and Gali and Gambetti (2020), who all document reasonable patterns of the cyclical unemployment component (i.e., movements in this component correlate quite well with the NBER business cycle).[9]

More generally, the assumption of an AR2 to model the cyclical component of macroeconomic variables has a long tradition, at least going back to Clark (1987). However, because we are also modeling the output gap (i.e., level of real GDP minus level of potential real GDP), we depart from the previous literature by augmenting the AR2 unemployment gap with the output gap (denoted ogap) as an additional explanatory variable. Sinclair (2009), Grant and Chan (2017), and Berger, Everaert, and Vierke (2016), among several others, document the empirical importance of jointly modeling the unemployment rate gap and the output gap.

Similarly, as shown later, we add information from the unemployment gap when modeling the output gap. We find that the joint modeling of the output gap and the unemployment gap is empirically and economically useful (confirming previous research findings, e.g., Fleischman and Roberts, 2011). In addition, joint modeling of both the output gap and the unemployment gap allows us to estimate the strength in the relationship between the two cyclical components, popularly known as Okun's law. In equation (7), the coefficient ϕ_u captures the contempo-

[8] As mentioned in Crump et al. (2019), one of the criticisms of this approach is that it will be impacted by the breakdown of the Phillips curve relationship post 2007. However, by allowing time-variation in the coefficients capturing the price and wage Phillips curve relationships, as we do, our approach should face less of a problem. In addition, as illustrated in Del Negro, Giannoni, and Schorfheide (2015) and Clark (2014) bringing information from long-run survey expectations of inflation (as we do) should further help capture the inflation behavior in the post 2007 period.

[9] CKP explores the empirical importance of allowing for time-variation in the parameters of AR2 process, and finds that data prefers the time-invariant AR2 process, hence validating the widely used assumption of a simple AR2 process.

raneous relationship between the output gap and the cyclical unemployment rate gap. The estimate, $\frac{1-\rho_1^u-\rho_2^u}{\phi^u}$ could be interpreted as the Okun's law coefficient.

We note that when jointly modeling output and the unemployment rate, most researchers assume a common cyclical component between the two. However, in light of the empirical evidence that cyclical unemployment displays more persistence than the output gap (e.g., Berger et al., 2016), we model two separate cycles linked to each other via Okun's law relationship. As shown in Berger et al. (2016), a specification that entertains two separate cycles (cyclical unemployment and the output gap), the data support a time-invariant parameter describing the Okun's law relationship. In contrast, a specification with a common cyclical component favored a time-varying Okun's law relationship (adding support to Knotek, 2007).

In a nutshell, the inference of Berger et al. (2016) suggests that time-variation in the parameter capturing Okun's law reflects the sluggish response of the cyclical unemployment to movements in the output gap. Once they allowed for a sluggish response of the cyclical unemployment rate by adding persistence, via one-period lag of the cyclical unemployment rate, evidence of a time-varying Okun coefficient disappears. We found similar evidence. Hence, we adopt the modeling of two separate cycles and a time-invariant Okun's law relationship for our baseline setup; this has the added advantage of requiring estimation of significantly fewer parameters.[10]

With the exception of CKP, most of the literature models u-star as a driftless RW. The use of an unrestricted RW process has empirically been shown to work well, but CKP shows that modeling u-star as a bounded RW process is even better. Motivating their use of bounds is because, by construction, the unemployment rate is a bounded variable, which implies that the long-run equilibrium in the labor market would restrict the movements in u-star within a bounded interval.[11]

Accordingly, we model u-star as a bounded RW, where the bounds' values are fixed at 3.5% (lower bound) and 7.5% (upper bound).[12] Following Stella and Stock (2015), CKP, and Tallman and Zaman (2017), the variance of the error in the cyclical component is not allowed to vary over time.

$$U_t = U_t^* + U_t^c \tag{6}$$

$$U_t - U_t^* = \rho_1^u(U_{t-1} - U_{t-1}^*) + \rho_2^u(U_{t-2} - U_{t-2}^*) + \phi^u ogap_t + \varepsilon_t^u, \;\; \varepsilon_t^u \sim N(0, \sigma_u^2) \tag{7}$$

[10] Bayesian model comparison assessment slightly preferred the approach of two separate cycles with time-invariant Okun's law compared to common cycle with time-varying Okun's law parameter. Also, we note that Sinclair (2009) and Grant and Chan (2017) model two separate cycles, linked through a time-invariant parameter.

[11] CKP argue that economic forces that govern the movements in u-star are slow-moving and those forces would not cause the unemployment rate to fall to levels close to zero or to levels that are higher than the previous peaks caused by recessions.

[12] These values are informed by estimating the CKP model over our estimation sample, and are close to values reported in CKP based on their estimation sample. As a further check, most estimates of the u-star reported in commonly cited literature fall within the bounds we use in this paper.

where, $\rho_1^u + \rho_2^u < 1$, $\rho_2^u - \rho_1^u < 1$, and $|\rho_2^u| < 1$

$$U_t^* = U_{t-1}^* + \varepsilon_t^{u*}, \;\; \varepsilon_t^{u*} \sim TN(a_u - U_{t-1}^*, b_u - U_{t-1}^*; 0, \sigma_{u*}^2) \tag{8}$$

where the notation $TN(a, b; \mu, \sigma^2)$ refers to normal distribution with mean μ and variance σ^2 but truncated in the interval (a, b).

Lastly, the equation relating long-run survey projection of the unemployment rate, Z^u to U^*,

$$Z_t^u = C_t^u + \beta^u U_t^* + \varepsilon_t^{zu}, \;\; \varepsilon_t^{zu} \sim N(0, \sigma_{zu}^2) \tag{9}$$

$$C_t^u = C_{t-1}^u + \varepsilon_t^{cu}, \;\; \varepsilon_t^{cu} \sim N(0, \sigma_{cu}^2) \tag{10}$$

2.4. Output block

We are interested in both the potential output (i.e., gdp^*) and the growth rate in potential output (i.e., g^*). To feasibly estimate both these latent processes, we follow the commonly adopted approach, which decomposes the level of aggregate output into the level of potential output and a cyclical component (output gap), where the cyclical component is defined as the deviation of observed aggregate output level from potential output. This simple decomposition has a long tradition going back to Harvey (1985) and Clark (1987).

$$gdp_t = gdp_t^* + ogap_t \tag{11}$$

where $gdp \equiv log(GDP)$ and gdp^* refers to potential output, which is unobserved.

A common approach to model gdp^* is to assume a random walk with a time-varying drift term (i.e., the local level trend process), where the time-varying drift term (interpreted as g^*) is assumed to follow a random walk process (to allow for a stochastic g^*). More recently, Chan and Grant (2017) show that a model where gdp^* is assumed to follow a second-order Markov process fits the data better compared to the model where gdp^* is assumed as a random walk with time-varying drift. Hence, we follow Chan and Grant (2017) and model gdp^* as,

$$gdp_t^* = 2gdp_{t-1}^* - gdp_{t-2}^* + \varepsilon_t^{gdp*}, \;\; \varepsilon_t^{gdp*} \sim N(0, \sigma_{gdp*}^2) \tag{12}$$

Which can be re-written as,

$$\triangle gdp_t^* = \triangle gdp_{t-1}^* + \varepsilon_t^{gdp*}$$

If we define, $g_t^* \equiv \triangle gdp_t^*$, where $\triangle$ is the first difference operator. Then,

$$g_t^* = g_{t-1}^* + \varepsilon_t^{gdp*} \tag{13}$$

An advantage of modeling g^* as a second-order Markov process compared to RW with time-varying drift is that it requires estimating a single shock parameter (σ^2_{gdp*}), as opposed to two for the latter (one for the shock to gdp^* and the other for the shock to time-varying drift, aka g^*). This modeling assumption implies that all permanent shocks to output are attributed as shocks to g^*.[13]

The cyclical component, ogap, is assumed a stationary AR(2) process augmented with additional explanatory variables: the real interest rate gap and the unemployment gap,

$$ogap_t = \rho_1^g(ogap_{t-1}) + \rho_2^g(ogap_{t-2}) + a^r(r_t - r_t^*) + \lambda^g(U_t - U_t^*) + \varepsilon_t^{ogap} \tag{14}$$

where, $\varepsilon_t^{ogap} \sim N(0, \sigma^2_{ogap})$, $\rho_1^g + \rho_2^g < 1$, $\rho_2^g - \rho_1^g < 1$, and $|\rho_2^g| < 1$

Equation (14) could be interpreted as defining an IS-curve (as in LW and subsequent papers modeling r-star) that allows feedback from the real interest rate gap to the output gap (i.e., the real interest rate gap responds to economic slack). The IS equation is inspired by LW but with two modifications. First, instead of using the interest-rate gap based on the short-term real rate of interest, we use the long-term real interest rate (as in Gonzalez-Astudillo and Laforte, 2020). Specifically, the long-term real interest rate is constructed as the difference between the nominal yield on a 10-year Treasury bond and the 10-year inflation expectations (i.e., the PTR series for PCE inflation).[14]

In theoretical models, the long-term interest rate influences household consumption decisions and business investment decisions. Second, to improve the econometric estimation of the output gap, we enrich the IS equation by bringing in information from the unemployment gap (from the unemployment block) as an explanatory variable.[15] This latter addition is motivated by the approach taken in a long list of papers (e.g., Morley and Wong, 2020; Chan and Grant, 2017; Fleischman and Roberts, 2011; Sinclair, 2009; Clark, 1989) that demonstrate the usefulness of the unemployment rate in improving the econometric estimation of the output gap. As mentioned earlier, in the equation for the unemployment gap, we add the output gap to improve

[13]Note: the second-order Markov process for gdp* could be thought of as a limiting case of the process. Assuming gdp* as a RW with time-varying drift term, where the variance of shock to the gdp* goes to zero, and shock to the time-varying drift term (g-star) is the only relevant driver governing the evolution of gdp* and g-star (see Chan and Grant, 2017).

[14]We also experimented with an alternative specification, in which the interest rate gap is constructed as the difference between the short-term federal funds rate and first lag of four-quarter trailing PCE inflation, similar in spirit to LW. Based on model fit (log marginal likelihood), this specification was inferior compared to the Base specification. It is worth noting that had the longer history of long-term inflation expectations data available at the time of the writing, LW would have constructed the interest rate gap using the long-term interest rate (see page 1064 in LW).

[15]Model fit, the precision metric for u-star and the output gap, and the plausibility of the estimates of output gap strongly supports the joint modeling of output gap and unemployment gap. We note that LW estimated an alternative specification in which they added information from the labor market (hours worked) and found that doing so improved the precision of the estimated output gap, however, that improved precision did not spillover to r-star estimate (the focus of their paper) and therefore in their baseline specification they omit the labor market variable.

the former's estimation. The coefficient λ^g captures the contemporaneous relationship between the output gap and the unemployment gap. The parameter a^r relates the output gap to the real interest rate gap.

We note that innovations ε^2_{gdp*} and ε^2_{ogap} are uncorrelated. In an important contribution, Morley et al. (2003), who assume a deterministic g-star, show that this assumption matters for estimating potential output. However, Chan and Grant (2017) show that in their specification, once a stochastic g-star is allowed for, the correlation between ε^2_{gdp*} and ε^2_{ogap} goes to zero. They also show that the model without correlation performs comparably to the model with correlated innovations based on Bayesian model comparison. Accordingly, to keep estimation tractable, we assume uncorrelated innovations.

The equation linking survey projection of potential growth rate, Z^g to g^*,[16]

$$Z^g_t = C^g_t + \beta^g * 4 * g^*_t + \varepsilon^{zg}_t, \;\; \varepsilon^{zg}_t \sim N(0, \sigma^2_{zg}) \tag{15}$$

$$C^g_t = C^g_{t-1} + \varepsilon^{cg}_t, \;\; \varepsilon^{cg}_t \sim N(0, \sigma^2_{cg}) \tag{16}$$

2.5. Productivity block

Since the publication of Adam Smith's influential book, Wealth of Nations, it is widely acknowledged, that long-run productivity growth is the primary determinant of long-run changes in living standards. Therefore, estimates of the long-run level of (labor) productivity growth (p-star) have received considerable discussion in the past decades and are of great interest. Labor productivity is defined here as output per hour worked.

Furthermore, the estimates of p-star are an important input into policymaking, as they are used to gauge the appropriateness of the monetary policy stance. The importance of p-star for monetary policy is because standard macroeconomic models tightly connect p-star to the long-run level of real interest rate (i.e., r-star). In these models, a lower level of p-star implies a lower level of r-star, and a higher level of p-star implies a higher r-star (see Lunsford, 2017). However, based on post-1960 data, Lunsford (2017) found no statistical evidence supporting the link between p-star and r-star.

Several papers have endeavored to estimate the long-run level of productivity growth using various statistical and econometric models. A subset of those papers has documented support in favor of a regime-switching framework to model long-run labor productivity growth (e.g., Kahn and Rich, 2007). Also, to extract more precise and timely estimates of p-star, various authors

[16] We could potentially bring in additional information from the CBO's projection of the level of the potential GDP to improve the econometric estimation of the level of potential real GDP. However, as shown in the results section, the implied estimates of the output gap from our multivariate framework (with or without survey data) are remarkably similar to CBO's estimates suggesting the limited value of bringing additional information from CBO projections.

(e.g., Kahn and Rich, 2007; Roberts, 2001) have proposed using additional variables alongside labor productivity (e.g., real compensation, real consumption, and average hours worked). On the other hand, Edge et al. (2007) show that estimates of long-run productivity growth obtained from a simple trend-cycle univariate model solved with Kalman filter does an adequate job of mirroring the long-run projections of productivity growth reported in the survey of professional forecasters and institutional forecasts (e.g., CBO).[17]

On closer inspection, the ability of the Kalman filter to echo the predictions of the professional forecasters is not surprising. Productivity growth is a notoriously volatile series and is subject to extreme revisions from one vintage to another. So, distinguishing highly persistent fluctuations from truly permanent changes is a difficult job for professionals and models alike. Jacobs and van Nordern (2012) discuss in detail some of these challenges when working with productivity data.

The findings in Lunsford (2017), Edge et al. (2007), and Jacobs and van Norden (2012) motivates the formulation of a parsimonious structure for the productivity block relative to other blocks of the model. In particular, we abstract from explicit modeling of direct links between p-star and r-star and between p-star and g-star.[18] But along other dimensions, our formulation is richer than used in the cited literature, as we allow for time-varying parameters, including stochastic volatility. Specifically, the productivity gap, which is defined as (nonfarm) labor productivity growth[19] (quarterly annualized) less p-star, is modeled as a function of a one quarter lag in the productivity gap and the contemporaneous cyclical unemployment gap.

$$P_t - P_t^* = \rho^p(P_{t-1} - P_{t-1}^*) + \lambda_t^p(U_t - U_t^*) + \varepsilon_t^p, \;\; \varepsilon_t^p \sim N(0, e^{h_t^p}) \tag{17}$$

where, $|\rho^p| < 1$

The inclusion of the cyclical unemployment gap helps tease out movements in productivity associated with the business cycle. The growth in labor productivity (and more generally aggregate productivity) has been shown to be procyclical to some degree (e.g., Roberts 2001); it typically increases sharply at the onset of recoveries and falls during recessions. However, empirical evidence on the strength and the direction of the cyclical relationship is mixed. This mixed evidence stems from the use of different estimation samples and or cyclical indicators (employment-based or output-based). For instance, Gali and van Rens (2020), using split sample estimation, illustrate empirically the significant weakening in the correlation between labor

[17] It is worth emphasizing, in contrast to the regime-switching model (as used in Kahn and Rich, 2007), which allows for deterministic values of p-star, a random walk assumption for p-star (as in Edge et al., 2007) allows for the possibility that p-star may be changing (slowly) in every period.

[18] We implemented a model specification that allowed for a direct link between p-star and g-star. Doing so notably reduces the model fit to GDP, the unemployment rate, and the interest rate data. And it lowers the precision of the stars' estimates and the other model parameter estimates. The complete set of results corresponding to the model specification allowing for a link between p-star and g-star are available from the author.

[19] As discussed in Kahn and Rich (2007), the focus outside of the farm sector is primarily on avoiding short-term transitory volatility in the farm sector that is heavily driven by weather and other non-technological factors.

productivity and employment, especially post-1984. They find that the relationship has become countercyclical in the past three decades when using employment as the cyclical indicator.[20] But, it is slightly procyclical when using output as the cyclical indicator. This latter finding motivates our alternative specification that replaces cyclical unemployment with the output gap.

$$P_t - P_t^* = \rho^p(P_{t-1} - P_{t-1}^*) + \phi_t^p(ogap_t) + \varepsilon_t^p, \;\; \varepsilon_t^p \sim N(0, e^{h_t^p}) \tag{17b}$$

Gali and van Rens (2020) find weakening in the correlation between labor productivity and the cyclical indicator which motivates time-variation in the coefficients λ^p and ϕ^p.[21]

$$\lambda_t^p = \lambda_{t-1}^p + \varepsilon_t^{\lambda p}, \;\; \varepsilon_t^{\lambda p} \sim N(0, \sigma_{\lambda p}^2) \tag{18}$$

$$\phi_t^p = \phi_{t-1}^p + \varepsilon_t^{\phi p}, \;\; \varepsilon_t^{\phi p} \sim N(0, \sigma_{\phi p}^2) \tag{18b}$$

The variance of the error term ε_t^p is allowed to change over time.[22] Allowing for the time-variation in the cyclical relationship and the error term allows the model to better discriminate the cyclical movements and idiosyncratic movements in productivity from those associated with shifts in p-star.

The SV process is defined as a driftless random walk in the log-variance.

$$h_t^p = h_{t-1}^p + \varepsilon_t^{hp}, \;\; \varepsilon_t^{hp} \sim N(0, \sigma_{hp}^2) \tag{19}$$

P-star is modeled as a driftless random walk component, and the variance of the shocks to this component is assumed to be constant. By modeling p-star this way allows it to capture both unobserved and observed factors that are thought to be persistent but hard to measure. In particular, one factor is developments in fiscal policy; for example, high levels of government debt in the longer-term tend to crowd out private investment, thereby reducing longer-term productivity growth.

$$P_t^* = P_{t-1}^* + \varepsilon_t^{p*}, \;\; \varepsilon_t^{p*} \sim N(0, \sigma_{p*}^2) \tag{20}$$

Economic theory posits that the long-run nominal wage inflation equals the sum of long-run productivity growth and long-run price inflation. As discussed later in the wage inflation block, this theoretical restriction defines the law of motion for w-star and constitutes an additional

[20] Gali and van Rens (2020) using a structural macro model interpret the weakening procyclicality of labor productivity in part to increased flexibility of the US labor market post-1984, which has enabled firms to make adjustment at the extensive margin quickly and easily in response to shocks.

[21] Fernald and Wang (2016) documents weakening in the cyclicality of productivity at the industry level, suggesting that results of Gali and van Rens (2020) are not due to changes in the industry composition.

[22] Carriero, et al. (2019) and Tallman and Zaman (2020) document superior forecast accuracy of variables including labor productivity from Bayesian VARs with SV compared to VARs without SV; suggesting the usefulness of allowing for SV. We also find empirical support for the inclusion of SV.

channel influencing the dynamics of p-star.

2.6. Price inflation block

We use price inflation as measured by the Personal Consumption Expenditures (PCE) price index, the inflation measure that the Federal Reserve targets. Our formulation for price inflation block closely follows CKP and CCK, combining elements from both of these papers. Specifically, as in CKP, the stationary component, inflation gap (defined as the deviation of inflation from pi-star),[23] is modeled as a function of one-quarter lagged inflation gap, unemployment gap, and an error term, whose variance is allowed to vary over time.

The coefficient, ρ^{π} on the lagged inflation gap, which captures persistence in inflation dynamics (i.e., persistence in deviation of inflation from pi-star), is allowed to vary over time.[24] The motivation for time-variation stems from evidence in Weise (2012), who documents that in the period of Great Inflation, deviations of inflation from the desired target were very persistent because the Fed at the time either was unable or unwilling to enact policy to reduce inflation to its desired level. However, in the 1980s, the Fed was aggressive in returning inflation to the desired target; Ashley, Tsang, and Verbrugge (2020) also provide empirical evidence in support of this claim. Modeling time-variation in this parameter allows such contrasting behavior to be captured.

$$\pi_t - \pi_t^* = \rho_t^{\pi}(\pi_{t-1} - \pi_{t-1}^*) + \lambda_t^{\pi}(U_t - U_t^*) + \varepsilon_t^{\pi}, \;\; \varepsilon_t^{\pi} \sim N(0, e^{h_t^{\pi}}) \tag{21}$$

$$\rho_t^{\pi} = \rho_{t-1}^{\pi} + \varepsilon_t^{\rho\pi}, \;\; \varepsilon_t^{\rho\pi} \sim TN(0 - \rho_{t-1}^{\pi}, 1 - \rho_{t-1}^{\pi}; 0, \sigma_{\rho\pi}^2) \tag{22}$$

The innovations to the AR(1) coefficient, ρ^{π} are truncated so that $0 < \rho_t^{\pi} < 1$, ensuring that the inflation gap (in equation 21) is stationary at each point in time t.

$$\lambda_t^{\pi} = \lambda_{t-1}^{\pi} + \varepsilon_t^{\lambda\pi}, \;\; \varepsilon_t^{\lambda\pi} \sim TN(-1 - \lambda_{t-1}^{\pi}, 0 - \lambda_{t-1}^{\pi}; 0, \sigma_{\lambda\pi}^2) \tag{23}$$

λ^{π} is the slope of price Phillips curve and is constrained in the interval (-1,0).

The parameter λ estimates the price Phillips curve relationship (i.e., the relationship between the inflation gap and the unemployment gap at business cycle frequency). There is ample empirical evidence in support of a time-varying price Phillips curve (e.g., Stella and Stock, 2015; CKP; Del Negro et al., 2020) hence our choice of allowing for time-variation in the

[23] Modeling inflation in gap form, where gap is defined as the difference between inflation and slowly-moving trend, was popularized by Cogley, Primiceri and Sargent (2010), and since then has been a widely used approach to modeling inflation in macroeconomic models for policy and forecasting (e.g., Faust and Wright, 2013).

[24] Chan et al. (2013), CKP, and CCK have found strong empirical support for the time-variation in the coefficient of inflation gap. Our results reinforce the empirical importance of allowing for time-variation in this coefficient.

parameter λ^{π}.[25]

$$h_t^{\pi} = h_{t-1}^{\pi} + \varepsilon_t^{h\pi}, \;\; \varepsilon_t^{h\pi} \sim N(0, \sigma_{h\pi}^2) \tag{24}$$

The SV process is defined as a random walk in the log-variance.

Both the theoretical and empirical literature emphasizes the usefulness of the signal from fluctuations in labor costs for inflation dynamics. Post-Keynesian theory posits that excess wage inflation over labor productivity gains puts upward pressure on price inflation, i.e., causality runs from labor costs to price inflation. In comparison, the Neo-Classical theory suggests causality runs in the opposite direction, from price inflation to nominal wage inflation. The empirical evidence in the US data is inconclusive in that there is no clear evidence in the direction of the causality. If anything, the evidence suggests they co-move together (see Knotek and Zaman, 2014 and references therein).

Given the empirical evidence of co-movement, we explore an alternative specification in which we allow for a connection between two cyclical inflation components, nominal wage inflation gap and price inflation gap, by adding the nominal wage inflation gap as an explanatory variable in the equation describing price inflation gap. The parameter γ^{π} captures the strength of the relationship between the two cyclical inflation measures. The expression $\frac{\gamma^{\pi}}{1-\rho^{\pi}}$ can be interpreted as the passthrough from cyclical wage inflation to cyclical price inflation.[26]

$$\pi_t - \pi_t^* = \rho_t^{\pi}(\pi_{t-1} - \pi_{t-1}^*) + \lambda_t^{\pi}(U_t - U_t^*) + \gamma^{\pi}(W_t - W_t^*) + \varepsilon_t^{\pi}, \;\; \varepsilon_t^{\pi} \sim N(0, e^{h_t^{\pi}}) \tag{21b}$$

Similarly, as shown later, we add the price inflation gap to the equation describing the nominal wage inflation gap.

Pi-star is modeled as a driftless random walk component, and the variance of the shocks to this component is assumed to be constant (as in CKP). This latter assumption of homoscedastic errors is in contrast to Stock and Watson (2007), Mertens (2016), and several others. Our choice not to incorporate SV into shocks to pi-star is made to keep the estimation manageable and maintain consistency with our modeling assumptions for the stars.[27]

[25] See Del Negro et al. (2020) for a comprehensive literature review of the instability of the Phillips curve in the US data, and similarly Banbura and Bobeica (2020) for the euro area data. We note that the literature documenting empirical evidence in support of nonlinear Phillips curve (e.g., Ashley and Verbrugge, 2020) supports time variation in the parameter λ^{π}.

[26] We explored the possibility of allowing for time-variation in γ^{π} but the estimation ran into difficulties hence we resort to time-invariant γ^{π}.

[27] Allowing SV in the inflation gap component and not in the trend component is not without precedent. Besides CKP, Chan (2013) is a recent paper modeling SV only in the measurement equation (i.e., cyclical/transitory component). Berger et al. (2016) find support for SV in the inflation gap component but weak evidence for SV in the trend component. Our preliminary results indicate similar findings that adding SV to the pi-star equation neither helps nor hurts the model fit.

$$\pi_t^* = \pi_{t-1}^* + \varepsilon_t^{\pi*}, \;\; \varepsilon_t^{\pi*} \sim N(0, \sigma_{\pi*}^2) \tag{25}$$

Following CCK (and others, such as Mertens and Nason, 2020) to improve pi-star's econometric estimation, we bring in information from the long-run survey expectations (of PCE inflation). An important empirical finding of CCK is that long-run survey expectation of inflation is a biased measure of the underlying trend inflation, at least at some times. Hence, simply equating pi-star with the long-run survey expectation or assuming survey expectation as an unbiased measure of pi-star or calibrating econometric estimates of pi-star to surveys (as is commonly done) may not be a reasonable strategy.

Accordingly, we add an equation linking long-run survey expectations of inflation,Z^π to pi-star, where the intercept, C_t^π, is time-varying to capture possibly time-varying differential between the two.[28]

$$Z_t^\pi = C_t^\pi + \beta^\pi \pi_t^* + \varepsilon_t^{z\pi}, \;\; \varepsilon_t^{z\pi} \sim N(0, \sigma_{z\pi}^2) \tag{26}$$

$$C_t^\pi = C_{t-1}^\pi + \varepsilon_t^{c\pi}, \;\; \varepsilon_t^{c\pi} \sim N(0, \sigma_{c\pi}^2) \tag{27}$$

Our model specification modifies the baseline model of CCK in five important ways. First, we allow a time-varying Phillips curve relationship by adding the cyclical unemployment component (similar to CKP).[29] Second, we explore a model specification that allows for a link between the nominal-wage inflation gap and the price-inflation gap (capturing the evolving passthrough from labor costs to price inflation). Third, we adopt a more simplistic approach to modeling the link between survey expectations and pi-star. Fourth, the variance of the shocks to the pi-star process does not entertain SV. Fifth, pi-star is restricted to satisfy the long-run restriction informed by theory (see equation 28).

2.7. Wage inflation block

The long-run equilibrium level of nominal wage inflation (w-star) is the nominal wage growth rate consistent with its fundamentals – p-star and pi-star. As noted earlier, in the long-run, economic theory posits that the nominal wage inflation equals the sum of the long-run growth rate of labor productivity and the long-run level of price inflation. In other words, in the long-run, labor productivity growth is the only fundamental driver of real wages; therefore, price inflation and nominal wage inflation have to adjust relative to each other to maintain the

[28] Our formulation is flexible but less so than the one adopted by CCK. In addition to time-variation in the intercept, CCK add time-variation in the slope coefficient, and moving average (MA) in the error term. For PCE inflation, CCK did not find the addition of the MA in the error term useful. We think our relatively simplistic equation suffices in its aim of influencing econometric estimation of pi-star through the survey expectations.

[29] CCK explored an alternative specification in which they add cyclical unemployment but as an exogenous variable (constructed using the CBO estimate of the natural rate). CCK found that adding the cyclical unemployment slightly worsened the fit of their model.

fundamental relationship. In our setup, we impose this relationship to define w-star.

$$W_t^* = \pi_t^* + P_t^* + \varepsilon_t^{w*}, \;\; \varepsilon_t^{w*} \sim N(0, \sigma_{w*}^2) \tag{28}$$

The above equation implies that W^* is approximately equal to sum of $\pi_t^* + P_t^*$

In order to assess empirical support for the theoretical restriction defined by equation (28), we explore an alternative specification that models W^* as a RW process,

$$W_t^* = W_{t-1}^* + \varepsilon_t^{w*}, \;\; \varepsilon_t^{w*} \sim N(0, \sigma_{w*}^2) \tag{28b}$$

Equation (29) relates the nominal wage inflation gap – defined as the difference between the nominal wage inflation and w-star – to its one-quarter lagged gap, the cyclical unemployment gap, and the price inflation gap.[30] The variance of the error term, ε_t^w, is allowed to vary over time. The latter feature is motivated by findings in Tallman and Zaman (2020) and Peneva and Rudd (2017), who document better fit of the VAR with SV to nominal wage data compared to VAR without SV.

$$W_t - W_t^* = \rho_t^w (W_{t-1} - W_{t-1}^*) + \lambda_t^w (U_t - U_t^*) + \kappa_t^w (\pi_t - \pi_t^*) + \varepsilon_t^w, \;\; \varepsilon_t^w \sim N(0, e^{h_t^w}) \tag{29}$$

The SV process is defined as random walk in the log-variance.

$$h_t^w = h_{t-1}^w + \varepsilon_t^{hw}, \;\; \varepsilon_t^{hw} \sim N(0, \sigma_{hw}^2) \tag{30}$$

The findings in Knotek and Zaman (2014) motivate the inclusion of a one-quarter lagged nominal wage inflation gap, with time-variation in the parameter ρ^w; the latter quantifies the persistence in wage inflation dynamics.

$$\rho_t^w = \rho_{t-1}^w + \varepsilon_t^{\rho w}, \;\; \varepsilon_t^{\rho w} \sim TN(0 - \rho_{t-1}^w, 1 - \rho_{t-1}^w; 0, \sigma_{\rho w}^2) \tag{31}$$

The innovations to the AR(1) coefficient, ρ^w are truncated so that $0 < \rho_t^w < 1$, to ensure that the wage gap (in equation 29) is stationary at each point in time t.

The parameter λ^w in equation (29) measures the strength of the cyclical relationship between the nominal wage gap and labor market slack (aka the wage Phillips curve). Many studies, both theoretical (e.g., Gali, 2011) and empirical (e.g., Knotek and Zaman, 2014; Peneva and Rudd,

[30] Following the literature on modeling price inflation in the gap, Knotek and Zaman (2014) apply a similar transformation to modeling nominal wage inflation for the US. In particular, they construct the nominal wage inflation gap as nominal wage inflation less pi-star, where pi-star is survey expectations. They note the competitive forecasting properties of their model is due to modeling in gaps. Following Knotek and Zaman (2014), Bobeica, Ciccarelli, and Vansteenkiste (2019) construct a nominal wage inflation gap for the euro area data and find empirical support for the gap specification.

2017; Gali and Gambetti, 2019), have documented strong support for the existence of a wage Phillips curve in the US data. These studies have also demonstrated the instability of the wage Phillips curve, motivating the need for time-variation in the parameter λ^w.[31]

$$\lambda_t^w = \lambda_{t-1}^w + \varepsilon_t^{\lambda w}, \;\; \varepsilon_t^{\lambda w} \sim TN(-1 - \lambda_{t-1}^w, 0 - \lambda_{t-1}^w; 0, \sigma_{\lambda w}^2) \tag{32}$$

where λ^w is the slope of wage Phillips curve and is constrained in the interval (-1,0).

As discussed earlier in the price inflation block, both theory and empirical evidence point to the connection between price inflation and nominal wage inflation. The standard fully structural models describing the New Keynesian Phillips curve posit a tight relationship between price and wage inflation via the channel of current and expected future marginal costs. In these models, price inflation today is a function of expected price inflation and expected future marginal costs, where marginal costs are generally linked to wages. Knotek and Zaman (2014) provide empirical evidence of the connection between nominal wage and price inflation. In particular, they show no clear evidence of one Granger-causing the other; instead, both wage and price inflation generally tend to move together. This reasoning would suggest the importance of modeling the direct relationship between wage inflation and price inflation. Hence, this motivates the inclusion of the price inflation gap in the measurement equation (29).

Several studies document a significant weakening in the empirical link between price inflation and nominal wage inflation since the 1980s (e.g., Peneva and Rudd, 2017; Knotek and Zaman, 2014), motivating time-variation in the parameter κ^w.[32] The expression $\frac{\kappa_t^w}{1-\rho_t^w}$ could be interpreted as an estimate of the passthrough from price inflation to wage inflation.

$$\kappa_t^w = \kappa_{t-1}^w + \varepsilon_t^{\kappa w}, \;\; \varepsilon_t^{\kappa w} \sim N(0, \sigma_{\kappa w}^2) \tag{33}$$

To assess empirical support for the inclusion of the price inflation gap in the equation describing the nominal wage gap, we estimate an alternative model that replaces equation (29) with the following,

$$W_t - W_t^* = \rho_t^w (W_{t-1} - W_{t-1}^*) + \lambda_t^w (U_t - U_t^*) + \varepsilon_t^w, \;\; \varepsilon_t^w \sim N(0, e^{h_t^w}) \tag{29b}$$

2.8. Interest rate block

We close our model with the interest-rate block characterizing the interest rate dynamics and the law of motion for r-star (the long-run equilibrium real short-term interest rate).

Our first equation of the block brings information from the nominal short-term interest rate

[31] Literature has posited various explanations for the instability of the wage Phillips curve, including downward nominal wage rigidities, where the degree of rigidity varies with the phase of the business cycle (see Daly and Hobijn, 2014).

[32] Bobeica et al (2019) find that in the euro area the link between labor compensation and price inflation continues to remain strong post-1980.

via a Taylor-type rule (TR) to aid in identifying r-star. Past research has shown the TR's usefulness in characterizing the monetary policy reaction function over the past four decades. Specifically, this equation characterizes the dynamics of the short-term nominal interest rate gap, where the gap is the difference between the nominal short-term interest rate i, and the long-run level of the nominal neutral rate of interest, i-star. (i-star = pi-star + r-star). When modeling the nominal short-term interest rate, especially in a framework like ours, one must account for the effective lower bound (ELB) period.

Recent literature provides at least two options to handle the ELB. The first is to explicitly but separately model the observed short-term nominal rate, which cannot go below zero, and the "shadow interest rate," which is a hypothetical unobserved and unbounded counterpart. Wu and Xia (2016) popularized the concept of the shadow interest rate, and JM and Gonzalez-Astudillo and Laforte (2020) are two recent approaches well suited for inclusion in UC models. The second approach is to treat the estimate of the "shadow rate" obtained from Wu and Xia (2016) as the measure of the short-term nominal interest rate in measurement equations such as the TR (e.g., Pescatori and Turunen, 2016).[33]

Given our model's size and complexity, we adopt the latter approach, which is simpler though not perfect. Using a direct measure of the nominal shadow rate allows us to capture both conventional and unconventional monetary policy effects when the (observed) nominal federal funds rate is constrained at the ELB.[34]

Equation (34) relates the nominal interest rate gap (based on the shadow federal funds rate) to its one-period lag interest rate gap, current quarter inflation gap (i.e., deviation of inflation from pi-star), and unemployment rate gap (i.e., deviation of unemployment rate from u-star). This equation roughly characterizes the monetary policy reaction function as defined by Taylor (1999).[35] There is a broad consensus that policy adjustments outside of cyclical turning points are made very gradually. Hence, this motivates the inclusion of the lagged interest rate gap term.

Chan and Eisenstat (2018a; 2018b) and JM document strong empirical support for constant parameters in the Taylor rule equation while allowing for stochastic volatility in the errors. Accordingly, we allow for SV in the interest-rate equation. JM, Gonzalez-Astudillo and Laforte (2020), and Brand and Mazelius (2019) document the usefulness of adding the TR equation to identify r-star. The latter two do not entertain SV, which JM has found to be empirically important. As discussed later, we also found that adding the TR equation improves the precision of the r-star estimates significantly, and data strongly favors allowing for SV in the error process.

[33]The estimates from Wu and Xia (2016) are publicly available and regularly updated.Treating the shadow rate as the measure of the short-term nominal rate in place of the federal funds rate is commonly done, and often academic papers report results indicating robustness to the use of Wu and Xia (2016) shadow rate (e.g., Beyer and Wieland, 2019; Lewis and Vazquez-Grande, 2019)

[34]The nominal *shadow* federal funds rate is identical to the nominal federal funds rate when effective lower bound (ELB) is not binding.

[35]It is worth emphasizing that we denote this equation as a "Taylor-type rule" and not an exact Taylor-rule because in our equation, pi-star refers to the estimate of trend inflation which may or may not equal to central bank's long-run inflation goal.

$$i_t - \pi_t^* - r_t^* = \rho^i(i_{t-1} - \pi_{t-1}^* - r_{t-1}^*) + \lambda^i(U_t - U_t^*) + \kappa^i(\pi_t - \pi_t^*) + \varepsilon_t^i, \;\; \varepsilon_t^i \sim N(0, e^{h_t^i}) \quad (34)$$

where, ρ^i is truncated so that $0 < \rho^i < 1$.

$$h_t^i = h_{t-1}^i + \varepsilon_t^{hi}, \;\; \varepsilon_t^{hi} \sim N(0, \sigma_{hi}^2) \quad (35)$$

The SV process is defined as random walk in the log-variance.

Our second equation motivated by LW heeds to the economic theory suggesting the role of various real factors in influencing movements in r-star. These factors include long-run output growth (and long-run productivity growth), trend labor force growth (reflecting shifts in demographics and net migration), taxation structure, government expenditure shifts, and shifts in liquidity preferences (e.g., Del Negro et al., 2017; Bullard, 2018). Accordingly, equation (36) expresses r-star as a linear function of g-star and a "catch-all" component D. In our baseline specification, both g-star and D follow random walk processes similar to LW (and many other papers). The RW assumption for D is an appropriate one, given our focus is the long-run r-star that should, in principle, be influenced over time by permanent shifts in aggregate supply and demand (Laubach and Williams, 2016).[36]

$$r_t^* = \zeta g_t^* + D_t. \quad (36)$$

$$D_t = D_{t-1} + \varepsilon_t^d, \;\; \varepsilon_t^d \sim N(0, \sigma_d^2) \quad (37)$$

In more recent literature on long-run r-star, modeling r-star as a random walk process has performed better empirically than model specifications relying on the link between g-star and r-star.[37] Accordingly, we explore an additional specification that models r-star simply as the RW process (similar to g-star, p-star, pi-star, u-star). The RW assumption for r-star implies that we are agnostic about the underlying unobserved forces driving r-star but acknowledge those forces reflect persistent structural shifts in aggregate demand and supply that ought to have a bearing on r-star.

$$r_t^* = r_{t-1}^* + \varepsilon_t^{r*}, \;\; \varepsilon_t^{r*} \sim N(0, \sigma_{r*}^2) \quad (36b)$$

Lastly, the equations linking implied estimate of the long-run survey expectations of real

[36] Researchers have also explored AR process for component D, which would be consistent if the interest is in medium-term r-star (see Lewis and Vazquez-Grande, 2019), as this would allow r-star to be influenced by the transitory shocks to aggregate demand (via the AR process) and permanent shocks to aggregate supply (via the RW process for g-star). In studies focused on the long-run notion of r-star, such as LW, Laubach and Williams (2016), Clark and Kozicki (2005), and Kiley (2020) specification based on RW assumption has shown empirically to be favored by data compared to AR assumption.

[37] See Kiley (2020), Gonzael-Astudillo and Laforte (2020), JM, Orphanides and Williams (2002)

short-term interest rate, Z^r to r^* is defined as:[38]

$$Z_t^r = C_t^r + \beta^r r_t^* + \varepsilon_t^{zr}, \;\; \varepsilon_t^{zr} \sim N(0, \sigma_{zr}^2) \tag{38}$$

$$C_t^r = C_{t-1}^r + \varepsilon_t^{cr}, \;\; \varepsilon_t^{cr} \sim N(0, \sigma_{cr}^2) \tag{39}$$

All in all, information from six sources and or elements inform the econometric identification of r-star. These sources include: an IS equation (14)), TR equation (34), which allows for SV; an equation linking r-star to survey expectations; shadow rate; and an equation relating r-star to g-star. As we show shortly, all these sources play a role in improving r-star's precision. To reiterate, in our framework, we utilize information from both short-term nominal interest rates (via a TR equation) and long-term nominal interest rates (via an IS equation) to inform the estimation of r-star.[39]

2.9. Base model and its variants

The equations (6), (7)…(39) defines our baseline model formulation (denoted *Base*). Figure 1 provides a visual representation of our Base model. And section A1.a. of the appendix lists all the equations for the Base model for easy reference. To assess the usefulness of survey information in the econometric estimation of our multivariate UC model, we also estimate a variant of the baseline model that excludes the equations linking long-run survey expectations to stars (i.e., excluding equations 9, 10, 15, 16, 26, 27, 38, and 39). We denote the latter specification as *Base-NoSurv*. The model specifications Base and Base-NoSurv constitute our two main model specifications. To assess the empirical support for numerous additional features (informed from theory and past empirical research) embedded in our modeling framework, we formulate several additional model specifications, each of which is a restricted variant of the Base. For instance, to assess the empirical support of the theoretical restriction defined by equation 28 (which defines w-star as the sum of pi-star and p-star), we estimate a variant of the baseline model that replaces equation 28 with a random walk assumption for w-star as defined by the equation 28b. We denote this specification as *Base-W*RW*.

Similarly, to assess the empirical support for the theoretical restriction defined by equation 36 (the link between gstar and rstar), we estimate a model specification that replaces equation 36 with a random walk assumption for r-star as defined by the equation 36b. Table 1 reports the description of model specifications that are formulated to assess various features of importance.

[38] The r-star survey estimates are not direct estimates instead they are inferred from the Blue Chip survey long-run estimates of GDP deflator and short-term interest rates using the long-run Fisher equation. The survey expectations for r-star goes back to 1983.Q1. Please refer to the appendix A9 for details on the procedure to back cast estimates all the way back to 1959

[39] Del Negro et al. (2017), JM, Bauer and Rudebusch (2020), Gonzael-Astudillo and Laforte (2020) are recent studies that have highlighted the usefulness of exploiting information from both short-term and long-term interest rates in the identification of r-star.

We ran few additional specifications to explore the role of priors in influencing r-star, and for brevity purposes they are relegated to the appendix. To keep the length of paper manageable, we report selected results from the auxiliary model specifications in the main part of the paper with additional results included in the appendix.

3. Data and Bayesian Estimation

3.1. ***Data***

We estimate the empirical model using the following quarterly data: (1) the unemployment rate; (2) Real GDP growth; (3) Nonfarm labor productivity growth; (4) inflation rate in Personal Consumption Expenditures (PCE) price index; (5) Average Hourly Earnings (AHE) of production and nonsupervisory workers (total private industries);[40] (6) Federal funds rate; (7) Nominal yield on 10-year Treasury Bond; (8) Shadow federal funds rate from Wu and Xia (2016); (9) Blue Chip (real-time) long-run projections of 3-month Treasury Bill, real output growth, the unemployment rate, and GDP deflator inflation; (10) Long-run inflation expectations of PCE inflation (PTR series). We also collect the real-time long-run CBO projections of real output growth, level of real potential output, and the natural rate of unemployment. For forecast evaluation exercises, the real-time data vintages of real GDP growth, PCE inflation, the unemployment rate, AHE, and nonfarm labor productivity spanning 1998Q1 through 2019Q4 are downloaded from the ALFRED database maintained by the St. Louis Fed and the real-time database maintained by the Federal Reserve Bank of Philadelphia. For the data series labeled (1) through (7), which comprises our core dataset, we collect two vintages of revised data: 2020Q2 and 2020Q4 vintages, respectively. We use data starting 1959Q4 through 2019Q4 from the 2020Q2 vintage (which includes the third estimate of 2019Q4) as a featured sample for this paper. To show the implications of the COVID-19 data on our model estimates, we estimate our model(s) using the 2020Q4 vintage, which has data spanning from 1959Q4 through 2020Q3. The vintages corresponding to the revised data are downloaded from Haver Analytics.

3.2. ***Bayesian Estimation***

We use Bayesian estimation methods to fit our Base model and its variants. The use of inequality restrictions on latent parameters in our model(s) setup leads to a non-linear state-space model, which renders estimation using standard Kalman filter methods infeasible. Accordingly, we implement our Markov chain Monte Carlo (MCMC) posterior sampler based on computational methods developed in Chan, Koop, and Potter (2013) and CKP, which uses the band and sparse matrix algorithms detailed in Chan and Jeliazkov (2009). Specifically, the MCMC posterior sampler is a significantly scaled-up version of the sampler employed by CKP.

[40] Average Hourly Earnings (AHE) of production and nonsupervisory workers in total private industries goes back to 1964Q1. From 1959Q4 through 1963Q4, we use the AHE of production and nonsupervisory workers in goods producing industries. We splice them together.

The CKP posterior sample developed for a relatively smaller-scale nonlinear state-space model is carefully extended to accommodate the additional structure and numerous features of our model(s). Since the computational methods used in this paper are based on CKP, we relegate the specific details of the sampler to the appendix A1.

In a methodological sense, this paper's novelty is in assembling the existing sampling algorithms based on the fast band and sparse matrix routines to solve a large nonlinear and a high-dimensional UC model. We found that the use of inequality restrictions such as bounds on the u-star and other parameters is crucial to estimate the model, especially in the Base-NoSurv model. Intuitively, features such as truncated distributions that we implement for some of the time-varying parameters, e.g., the Phillips curve (price and wage), persistence, and bounds on u-star facilitate estimation by guiding the estimation procedure to the credible regions of the parameter space.

For each model, we simulate 1 million posterior draws from the MCMC posterior sampler. We then discard the first 500,000 draws, and of the remaining, we keep every 100th draw. Accordingly, all the reported results for the Base model and its variants are based on 5000 retained draws.

As emphasized by Chan (2017), the MCMC algorithm is considered efficient if the draws it produces have low autocorrelation – they are autocorrelated by construction – and the time it takes to sample a given number of posterior draws is reasonable. In the appendix, we report efficiency diagnostics of our MCMC algorithm. Those diagnostics, which include inefficiency factors and convergence metrics, indicate good convergence properties (and low autocorrelation) of our sampler for both Base and Base-NoSurv models.[41]

Bayesian model comparison is based on the marginal likelihood metric. In computing marginal likelihood for various models, we use the approach proposed by CCK, which decomposes the marginal density of the data (e.g., inflation) into the product of predictive likelihoods; see appendix A1.d for details.[42] An important advantage of the CCK approach is that it allows us to separately compute marginal data density for each variable of interest: inflation, nominal wages, interest rate, real GDP, the unemployment rate, and labor productivity. The variable specific marginal densities prove useful for us because it allows for deeper insights about the source of the deficiencies, which helps differentiate models at a more granular level.

We note that our prior settings are similar to those used in CKP, CCK, Gonzalez-Astudillo and Laforte (2020). As discussed in CCK, UC models with several unobserved variables, such as the one developed in this paper, require informative priors. That said, our priors settings for most variables are only slightly informative. The use of inequality restrictions on some

[41] Regarding computational time, given the high-dimensionality of our model(s) and the number of posterior simulations we require, the speed is quite fast (in our assessment). When applied to the Base model, the MCMC algorithm, which is implemented in Matlab, takes about 350 seconds to generate 10,000 posterior draws using a laptop computer with an Intel(R) Xeon(R) E-2176M CPU @ 2.70 GHz processor. To generate 1 million posterior draws, it takes less than 10 hours.

[42] Alternatively, one could use the cross-entropy (Kullback-Leibler divergence) approach proposed by Chan and Eisenstat (2018a,b). We leave this for future extension.

parameters such as the Phillips curve, persistence, and bounds on u-star could be viewed as additional sources of information that eliminates the need for tight priors, something also noted by CKP. The parameters for which there is a strong agreement in the empirical literature on their values, such as the Taylor-rule equation parameters, we use relatively tight priors, such that prior distributions are centered on prior means with small variance. In model comparison exercises, the priors are kept the same for the common parameters across models. We also perform some prior sensitivity analysis reported in the appendix A2.

4. Full Sample Estimation Results

This section sequentially discusses results for each of the six blocks, particularly the full-sample estimates of stars. Here, we briefly highlight some of the noteworthy findings. Comparing estimates of the stars between model specification Base and Base-NoSurv, a clear pattern emerges. The precision of the estimates, as measured by the width of the 90% credible intervals, indicates that the Base model, which explicitly accounts for the links between stars and survey data, yields more precise estimates of the stars than Base-NoSurv. Although the broader contours seen in the estimates of stars from our two main model specifications, Base and Base-NoSurv, are comparable, at times, the differences can be notable, especially in the case of r-star. In the case of g-star (and, in turn, the output gap), our two model specifications yield very similar trajectories as implied by the posterior mean estimates. This result suggests that data are very informative about g-star, and not so much about r-star, confirming Kiley's finding (2020).

Furthermore, the Bayesian model comparison indicates marginally higher support in data for Base over Base-NoSurv, as shown in table 3. The breakdown of the marginal data density by variables suggests that the Base model's improved fit over Base-NoSurv is due to its improved fit to inflation and nominal interest rate data. But that improved fit is offset mainly by worsening fit to the unemployment and wage data. The table also reports the marginal data density for two additional Base model variants that the Bayesian model comparison indicates a comparable fit to the data. Overall, we find that bringing additional information from surveys – by directly modeling the connection to the stars – leads to more reasonable values, provides more precise estimates, and marginally improves the model fit.

4.1. ***Estimation results for u-star***

Figure 2 plots the evolution of u-star (and its uncertainty) covering the period 1960 through 2019. Panel (a) plots the posterior estimates from the Base model and panel (b) from the Base-NoSurv model. Also plotted are the corresponding 90% credible intervals. Both models imply smooth evolution of u-star. In the past six decades, the (posterior mean of) u-star has fluctuated between 4.4% and 5.7%, peaking in the early-1980s and early-2010s; and troughs in the late-1990s and at the end of our sample period. The contours of u-star from both models

are generally similar (as can also be seen conveniently in panel d); however, the level of u-star can differ notably in some periods. From 1960 through the late-1970s, the u-star has gradually increased (from 5.4% to 5.7% in Base and 5.0% to 5.6% in Base-NoSurv). But, since the mid-1980s through the late-1990s, u-star has steadily drifted lower (to 4.5%). This downward trend in the later period is also documented in the u-star literature based on job-flows data, which attributes the decline in u-star to declining trends in job-separation and job-finding rates (e.g., Crump et al., 2019; Tasci, 2012).

From early-2000 through early 2010, the u-star has trended higher, with a sharp pickup during the Great Recession period. Since 2010, u-star has steadily drifted lower. By the end of 2019, Base has u-star at 4.4% (with a 90% interval covering 3.7% to 5.2%) and Base-NoSurv at 4.5% (with a 90% interval covering 3.7% to 5.4%). As shown in figure 3, at the end of 2019, the unemployment gap implied by both models is negative, i.e., the unemployment rate is below the estimated u-star.

The use of survey information in the Base model mainly contributes to the difference in the levels of the u-star across the two models. To facilitate comparison, panel (a) also plots u-star from the survey. As is evident from the plot, u-star from the survey displays more pronounced shifts in u-star than the model-based estimates. However, due to a strong estimated relationship between the survey u-star and Base u-star (i.e., posterior mean of $\beta^u = 0.988$), the Base estimate of u-star reflects the contours in survey u-star. As can be seen in panel (e), which plots the precision (measured as the width of the 90% intervals), taking onboard survey information improves the precision of u-star notably (comparing Base and Base-NoSurv).

Surprisingly, based on the Bayesian model comparison, the Base model has an inferior fit to the unemployment data compared to Base-NoSurv. As shown later, this result contrasts with the results for pi-star, r-star, and g-star, for which survey information helps improve the model fit or at least does not worsen the fit.[43]

Sensitivity of u-star to modeling assumptions including information set

Panel (c) plots additional estimates of u-star (posterior mean) from the variants of the Base model to highlight the sensitivity of u-star to modeling assumptions and the informational aspect of joint modeling. The plot denoted Base-NoBoundU* represents the Base model variant that eliminates the bound on the random walk process describing the u-star. Doing so has a trivial effect on the estimates of u-star, the precision of u-star, and model fit. Comparing between panels (a) and (c), the posterior mean estimate of u-star is quite similar across Base and Base-NoBoundU*. Similarly, there is little change in the u-star estimate's precision across the two models, with Base only marginally better in the latter part of the sample (as shown in panel e). Not surprisingly, the Bayesian model comparison suggests equal support for both Base and Base-NoBoundU*.

[43] Wright (2013) and Tallman and Zaman (2020) use long run survey information in an attempt to improve VAR model forecasts. In both cases, survey information did not improve unemployment rate forecast accuracy, although they found survey forecasts useful in improving accuracy for a range of other macroeconomic variables.

We highlight two noteworthy comments in regards to the implementation of bounds on u-star. First, the trivial difference in the estimates between Base and Base-NoBoundU* is because the bounds defined on u-star are wide. Put differently, the values of the bound we have set are not binding on the Base model. Second, we find that using bounds on u-star is extremely important in the Base-NoSurv, as it helps keep the estimation tractable. In other words, the advantages of using bounds on the random walk processes that were stressed in CKP were in full display in the estimation of Base-NoSurv. Hence, we prefer to keep bounds on u-star in our main models.

When writing this paper, the world was hit with a COVID-19 shock, an extreme and an unprecedented global health shock along various dimensions, leading several analysts to call it a "once-in-a-lifetime upheaval." As we will show in section 6, the implementation of bounds on u-star is part of the story in preventing our models from blowing up in response to COVID-19 data.

The other model variants plotted in Panel (c) are all nested specification of the Base model: the Bivariate model of GDP and the unemployment rate (a Base model that excludes survey information and everything else except the equations describing the dynamics of GDP and unemployment rate); Bivariate+Surv, which is Bivariate but adds survey data for GDP and unemployment; and CKP Adjusted, which is a bivariate model of inflation and the unemployment rate as in CKP but with no bounds on pi-star. For visual reasons (to limit the number of plots), u-star from Base in panel (c) is not shown. However, for the sake of discussion, we could treat the plot representing Base-NoBoundU* as the estimate for the Base model, since they are identical to each other (as discussed in the preceding paragraph).

These plots show that different model specifications could provide very different signals about the level of long-run unemployment, indicating the sensitivity of u-star to modeling assumptions. As evident from the figure, the small-scale model specifications indicate u-star range-bound between 5.3% and 6.5% over the sample. In contrast, the Base specification has u-star fluctuating over a broader range. A model specification that infers the estimate of u-star from inflation and unemployment data only, i.e., the price Phillips curve (CKP Adj. model), has a higher trajectory of u-star compared to Base. The story is similar in the case of the model specification that infers the estimate of u-star from GDP and the unemployment data only, i.e., the Okun's law relationship (Bivariate model), though the trajectory of u-star is lower than implied by the CKP-Adj model. Once the Bivariate model is augmented with survey data for GDP and unemployment, the trajectory is revised higher to resemble CKP-Adj, but with contours similar to Base (because of the survey data).

Panel (d) compares the u-star estimates from our main model specifications with the CBO estimate of the long-run unemployment rate. Interestingly, except for the 2000-2007 period, the CBO u-star's contour is similar to our model-based estimates, though the level of CBO u-star estimate is significantly higher from 1960 through the early-2000s. From 2000 to 2007, both Base and Base-NoSurv indicate a steadily rising u-star, whereas CBO has u-star trending lower.

At the onset of the Great Recession and through the early phase of the economic recovery, all three have u-star continuing to move higher. Whereas Base and Base-NoSurv peak in late 2010 at 5.5% and 5.2%, respectively, CBO has u-star peaking in late 2011 at 5.8%. Since then, u-star has steadily moved lower, with the pace of decline quite similar across CBO and Base. CBO has u-star at the end of 2019 at 4.4%, identical to Base and just a tenth shy of Base-NoSurv.

Precision of u-star

The panel (e) plots the precision of u-star estimates for Base, Base-NoSurv, Base-NoBoundU*, and Bivariate+Surv. We make several observations. First, comparing between Base and Bivariate+Surv, both these model specifications use information from the surveys and the Okuns relationship. However, Base relies on greater information and additional structure (e.g., wage Phillips curve, price Phillips curve, cyclical productivity, monetary policy stance via the Taylor-type policy rule) to infer the u-star compared to Bivariate+Surv, hence the more improved precision of the resulting u-star. The latter reasoning contributed to the very different estimate of u-star from the Base than Bivariate+Surv discussed earlier (and shown in panel c). And the model comparison indicates a significantly higher fit of the Base model to the unemployment data compared to the Bivariate+Surv.

Second, comparing with Base and Base-NoSurv, additional information from survey forecasts improve the precision of u-star, but this improved precision does not translate into the improved model fit, which instead worsens somewhat (as shown in table 4).

Panel (f) shows the precision of u-star for Base-NoSurv, Bivariate (GDP and unemployment), and CKP-Adj (which is bivariate model of price inflation and unemployment rate). As indicated earlier, the u-star from Base-NoSurv is inferred from a broader information set and structure than the other two small-scale models. Accordingly, Base-NoSurv estimate of u-star is, for the most part, more precise and the model comparison indicates a substantially higher fit to the unemployment data than the other two. The plots also show that u-star inferred from the Okun's law relationship (i.e., Bivariate model) is less precise than inferred from the price Phillips curve (i.e., CKP-Adj model). In contrast, the Bayesian model comparison lends support to the Bivariate model over the CKP-Adj model.

The results also provide evidence that adding survey data to the Bivariate model (Bivariate+Surv) improves further both the precision of the u-star (comparing Bivariate and Bivariate-Surv in panels e and f) and the fit to the unemployment data (Bivariate: -56.5 vs. Bivariate+Surv: -46.5, as shown in table 4). This latter finding of improved fit from adding survey data is interesting because in the case of Base, adding survey data worsens the model fit (Base: -24.6 vs. Base-NoSurv: -21.7). Importantly, it suggests that survey forecasts of u-star are likely useful in the case of parsimonious models but of limited use for models that already are utilizing various sources of information to infer u-star.

Cyclical unemployment

Figure 3 presents the posterior mean estimate of the unemployment gap (i.e., the cyclical component of the unemployment rate) and the corresponding 90% credible intervals. The top panel plots the estimates from the Base model, and the bottom panel from the Base-NoSurv model. A visual inspection indicates that the movements in the cyclical unemployment correspond quite well with the NBER's business cycle dating. For instance, cyclical unemployment falls in economic expansions and rises during recessions. Both models show a significant spike in the cyclical unemployment rate in the 1982-83 and 2007-09 recessions. And a sharper recovery following the 1982-83 recession but a more gradual recovery following the Great Recession. The figure also highlights that both models produce similar estimates of cyclical unemployment. Comparing estimates of (smoothly evolving) u-star in the previous figure to estimates of the cyclical unemployment rate indicates that fluctuations in the observed unemployment rate are attributed mainly to cyclical unemployment.

4.2. ***Estimation results for g-star and the output gap***

The panels (a) and (b) in figure 4 plot the g-star estimates from several sources, and panel (c) plots the corresponding precision. As is evident, g-star estimates from all sources shown indicate a steady decline throughout the sample, except a temporary rise in the late 1990s, which the literature has attributed to the technology boom. According to the posterior mean estimates of g-star from our Base and Base-NoSurv models, the growth rate of potential output has continuously drifted lower from an annualized rate of close to 4.5% in early 1960 to 1.4% by the end of 2019. The estimate of g-star fell to 1.2% in 2012 and remained there through 2015 and then began very slowly to move up. The story is generally similar based on the inference from simpler (nested) specifications of the Base model: (1) univariate model (which is Chan and Grant 2017 model); (2) the bivariate model of real GDP and unemployment rate; (3) and the bivariate model augmented to include survey data for g-star and u-star (denoted Bivariate+Surv).

This continuous reduction in the growth rate of potential output has been extensively documented elsewhere (e.g., Berger et al., 2016; Chan and Grant, 2017; Coibion et al., 2018) and in particular the decline since 2009 has been of great concern among the policymakers. Several other researchers including, Summers (2014), Eggertson, Mehrotra, and Summers (2016), Pescatori and Turunen (2016), LW (2016), Antolin-Diaz, Drechsel, and Petrella (2017) have also documented the secular decline in g-star over the past two decades.

Not surprisingly, the precision of the g-star estimates (and of the output gap) display patterns that align well with intuition. For instance, model specifications that incorporate survey expectations (i.e., Base and Bivariate + Surv) yield more precise estimates than specifications that ignore survey data. As discussed earlier, previous researchers have shown unemployment data to be the most critical indicator for the estimation of g-star and the output gap, and the plots provide evidence to that effect. For example, the model specification Bivariate, which builds on the univariate GDP model by adding the unemployment rate, yields a substantial

improvement in the precision of the g-star estimate. Interestingly, the g-star estimate's precision from Bivariate is about the same as the Base-NoSurv, suggesting that unemployment is the most crucial variable influencing estimation of g-star. However, as we show shortly, model comparison results indicate support for Base-NoSurv over Bivariate in the output gap case.

Output gap estimates

Next, we examine the estimates of the output gap. In figure 4, panels (d) and (e) plot the output gap estimates from the same sources as in the case of g-star, and panel (f) plots the corresponding precision. Overall, the estimates of the output gap from Base and Base-NoSurv are quite similar. They accord well with the NBER recession dates. Furthermore, as noted by Morley and Piger (2012) and Johannsen and Mertens (2015), our model-based estimates provide evidence of asymmetry in that recessions are shorter in duration but deeper than expansions in the US. It is instructive to highlight that estimates imply a more negative output gap (of -10.5%; posterior mean) during the 1981-82 recession compared to the Great Recession period (-7%) when output fell more dramatically. At a first pass, this may seem odd. But a closer inspection reveals that in comparison to the 1981-82 recession during the Great Recession, g-star fell significantly (as can be seen in panel a), resulting in a smaller negative output gap; in contrast, during the 1981-82 recession, g-star is estimated to have remained stable.

Bivariate models are consistent with a similar story, but there are notable differences in the estimates implied from a univariate model. For instance, the latter model suggests a less dramatic fall in the output gap in 1973-74, 1981-82, and 2007-09 recessions. In the mild 2001 recession, the univariate model estimates a positive output gap, although less positive than before the recession. Also, as of 2019, according to this model, the output gap remains negative, which is in sharp contrast to other models and the consensus view (e.g., CBO output gap).

The precision estimates and the Bayesian model comparison indicate the inferior quality of the univariate model's output gap estimate. Table 5 reports the assessment of model fit to the GDP data for the various model specifications discussed in this section. As in the case of g-star, the output gap estimate from the univariate model is subject to a great deal of uncertainty. The bivariate model, that brings additional information from the unemployment rate helps improve the precision significantly. This improved precision is also reflected in the bivariate model's substantially improved fit to GDP data compared to the univariate model (Bivariate: -280.4 vs. Univariate: -296.5). In our subjective assessment, the estimate of the bivariate model's output gap is more reasonable because its trajectory aligns well with Base and Base-NoSurv, and as shown shortly, with the consensus view.

Further improvements in precision are realized by bringing in additional information from the surveys (comparing Bivariate vs. Bivariate+Surv); however, the model fit, which reflects uncertainty about other model parameters in addition to g-star and the output gap, is little changed – in fact, it slightly deteriorates. The usefulness of survey data in improving the quality of the g-star and output gap estimates is also apparent comparing precision between Base

and Base-NoSurv; however, model fit is nearly similar. Contributing to comparable model-fit between the two models is that beginning 1990 onwards, the precision of output gap across the two models is identical. Unlike, in the case of g-star, the Base-NoSurv yields significantly more precise estimates of output gap than Bivariate, suggesting the usefulness of additional information and structure embedded in Base-NoSurv; hence, on-net the slightly better fit of the Base-NoSurv model to GDP data compared to Bivariate (Base-NoSurv: -279.1 vs. Bivariate: -280.4)

Posterior parameter estimates for the output block

Next, we discuss the Base model's parameter estimates of the output block that drive the dynamics of g-star and the output gap. The posterior mean estimates of parameters ρ_1^g and ρ_2^g indicate a high degree of persistence ($\rho_1^g + \rho_2^g = 0.74$) and suggest a hump-shaped response of output gap to shocks (as $\rho_1^g > 1$). These parameters are precisely estimated as evidenced by tight posterior credible intervals. The posterior estimate of parameter λ^g (the coefficient on the unemployment gap in the output gap equation) is negative and highly significant statistically. The estimated posterior mean of λ^g is -0.46 (with 90% interval -0.58 to -0.34). Similarly, the parameter ϕ^u (the coefficient on output gap in the unemployment equation), discussed earlier, is also negative and highly significant statistically. Together, these estimates indicate a strong Okun's law relationship in the data. The implied posterior mean estimate of the Okun's law coefficient, $\frac{(1-\rho_1^u-\rho_2^u)}{\phi_u}$ is -2.1, with 90% credible intervals spanning -2.3 to -1.8. This estimated coefficient is strikingly identical to the conventional estimate often discussed in macroeconomic textbooks. Therefore, not surprisingly, both the estimated output gap and unemployment gap (shown earlier) reveal similar cyclical dynamics. For instance, according to both cyclical measures, the 1981-82 recession is estimated to have been deeper than the Great Recession.

The parameter a^r, which relates the output gap to the real rate gap (characterizing the IS relation), is negative and much smaller than the prior mean. The estimated posterior mean of a^r is -0.07 (with 90% interval -0.14 to -0.00).

The posterior mean estimate of $E(\sigma^2_{gdp*})$, the variance parameter of the innovations to the process governing the evolution of the g-star (and gdp-star), is nearly identical across the Base and Base-NoSurv models: 0.02^2. For comparison, the prior mean $E(\sigma^2_{gdp*})$ is 0.01^2. Similarly, for the output gap, the posterior mean estimate of $E(\sigma^2_{ogap})$, the variance parameter of the innovations to the IS equation, is also identical across the two models: 0.72^2 (compared with a prior of 1^2).[44] The estimation results suggest that data is quite informative in influencing the dynamics of both output gap and g-star, confirming Kiley (2020).

[44]Note, our prior setting implying a high ratio of $\frac{\sigma^2_{ogap}}{\sigma^2_{gdp*}}$ is consistent with the high noise to signal ratio suggested in Kamber et al. (2016). Specifically, they recommend fixing the noise-to-signal ratio to a high value to obtain large and more persistent cycles when estimating output using Morley et al. (2003) UC model with maximum likelihood estimation.

Model-based estimates of output gap vs. CBO and others

Figure 5 presents estimates from outside sources, CBO, and LW model to gauge how our model-based output gap estimates compare to measures from other sources. Also plotted are estimates from Base and Base-NoSurv in panel (a) and from the Bivariate and Bivariate+Surv models in panel (b) to facilitate comparison with the outside estimates. A few observations immediately stand out. First, the output gap estimate implied from the LW model is notably different over most of the sample period. In particular, during the Great Recession period, the output gap from LW turned slightly negative, while other estimates implied larger negative gaps. The slight negative gap in the LW model is the result of the LW model estimating a dramatic fall in potential output, in line with the collapse in the actual output.

Second, both Base and Base-NoSurv models produce estimates of the output gap generally similar to the CBO estimate. This close similarity is notable because the CBO approach is based upon an entirely different methodology, a production function approach (see Shackleton, 2018).[45] Note that the Bivariate models of real GDP and the unemployment rate (with and without survey), which are nested specifications of our bigger Base model, produce estimates of the output gap broadly similar, though not identical, to our two main model specifications. Interestingly, in periods when the output gap estimates from our Base (and Base-NoSurv) differ from the CBO estimates, the Bivariate models' estimates are identical to the CBO's. And in periods when Bivariate models differ from CBO, the Base (and Base-NoSurv) estimates are identical to CBO's.

The estimation results suggest an important takeaway: that joint modeling of real GDP and the unemployment rate is the key to obtaining credible output gap estimates. Morley and Wong (2020), who estimate the output gap using a large BVAR, also found that the unemployment rate is the most crucial indicator for the output gap. (In section 6, we compare our model estimates with additional estimates, including Morley and Wong's). Recently, Barbarino et al. (2020) use a range of small-scale UC models to estimate the output gap and similarly find that the unemployment rate is the most valuable indicator.

Our paper's result indicating a close resemblance of our models' output gap estimates to the CBO's output gap provides evidence supporting the common practice of using output gap estimates from the CBO as an exogenous variable in empirical macroeconomic models (e.g., JM; Stock and Watson, 2020). We view this result as a useful contribution to the applied macroeconomics literature.

On the one hand, the fact that model-based estimates of the output gap bear a strong resemblance to institutional forecasts, i.e., CBO, are encouraging and lends credibility to our model(s). However, on the other hand, in light of the evidence reported in Coibion et al. (2018), the strong resemblance to outside estimates is an unfortunate outcome. We say this for the following reason. Coibion et al. (2018) examine estimates of potential output taken from a

[45] We note that in recent years, more and more papers using UC models, which jointly models real GDP growth and unemployment rate, yield estimates of output gap similar to CBO output gap (e.g., Johannsen and Mertens, 2015; Berger et al., 2016; Kiley, 2020; Gonzalez-Astudillo and Laforte, 2020).

variety of model-based and external sources, including CBO and survey forecasts, and based on a range of shock measures, find that (in real-time) the estimates of potential output are unable to distinguish between transitory and permanent shocks effectively. Put differently, they find that their estimates of potential output respond "gradually and similarly" to both supply shocks and demand shocks that drive cyclical fluctuations in real GDP. This is unfortunate, since, by definition, potential output (and g-star) should only adjust in response to permanent shocks.

Coibion et al. (2018) in their conclusion postulate whether a framework that jointly estimates the dynamics of potential output with other relevant stars (as theory would imply) better distinguish between permanent and transitory components and hence lead to more credible estimates of potential output. Unfortunately, our model estimates, both based on full sample and real-time (shown in section 5) suggest otherwise.

4.3. ***Estimation results for p-star***

Figure 6 presents posterior estimates of p-star and other parameters of the productivity block. The panels (a), (b), and (c) present p-star estimates from the Base, Base-NoSurv, and Base-W*RW models, respectively. Both the posterior mean and the 90% credible intervals are shown. Also plotted is the actual labor productivity series. A visual inspection of the actual series indicates the unusually high volatility of the quarterly productivity data. In addition, this series is subject to a high-degree of revisions in subsequent data vintages, suggesting the extreme difficulties of its measurement in real-time (see Jacobs and van Norden, 2016). Perhaps, a quote from the former Chair of the Federal Reserve, Alan Greenspan (courtesy of Jacobs and van Norden, 2016), would be instructive to reflect a general sentiment about the productivity data,

"The productivity numbers are very rough estimates because we are measuring a whole set of production outputs from one set of data and a whole set of labor inputs from a different set. That they come out even remotely measuring actual labor productivity is open to question..."
(Transcript: Meeting of the Federal Open Market Committee, March 25, 1998, p. 96)

Not surprisingly, researchers have emphasized that these difficulties of extreme volatility, extensive revisions, and real-time measurement issues with productivity data complicate its trend-cycle decomposition (e.g., Edge, Laubach and Williams, 2007; Kahn and Rich, 2007). Our model-based estimates reflect these challenges. For instance, the estimate of the parameter ρ^p, reported in table 2, indicates close to zero persistence in the labor productivity data, defined as the difference between the growth rate in labor productivity and p-star. Similarly, our estimation indicates that labor productivity data has very little influence on the estimate of p-star. Put differently, the data is so volatile to allow for a meaningful identification of trend in the productivity data. The posterior mean of $E(\sigma^2_{p*})$, the variance of the shock process for p-star, is essentially the same as the prior mean.[46] As a result, the degree of time-variation

[46] We tried different values for the prior mean on this parameter, and found that posterior moves with the

in p-star is primarily influenced by the prior setting. So conditional on our prior belief, which allows p-star to evolve slowly from one quarter to the next, we find considerable evidence of gradual time-variation in p-star over the post-war sample. The evidence of time-variation is economically significant and is consistent with the findings of Roberts (2001), Benati (2007), Edge, Laubach and Williams (2007), and Fernald (2007).

Comparing across the three top panels in the figure, the paths of p-star (posterior mean estimates) from Base and Base-NoSur are lower than Base-W*RW. The latter model removes the restriction that the long-run w-star grows at a rate equal to the sum of pi-star and p-star. So removing this restriction eliminates the direct influence on p-star from wages and prices and helps raise the level of p-star. As evident from the Bayesian model comparison reported in table 6, the elimination of this restriction improves the fit of the model to the productivity data but reduces the overall model fit to other data, particularly interest rates – via the changes in pi-star and u-star in the Taylor-type rule equation. That said, all three models generally indicate similar broad patterns in p-star.

After averaging between 2% and 3% in the 1960s, the models indicate that p-star experienced a sharp deceleration in the 1970s through mid-1980s, mirroring the dramatic fall in productivity growth. Both Base and Base-NoSurv estimates show p-star trending lower from 2.4% (2.3%) in early 1970 to 0.5% by mid-1980, whereas Base-W*RW has it falling close to 1.5%, with wide 90% credible intervals that range from 0.4% to 2.3%. From there on through to the late 1990s, p-star increased sharply, at a pace roughly equivalent to its deceleration in prior periods, to reach a level of 2.0 to 2.4% by 1999. The literature attributes part of this acceleration in the latter half of the 1990s to the information technology boom. Roberts (2001), Edge, Laubach, and Williams (2007), and Benati (2007) document estimates of trend productivity generally similar to the p-star implied from the Base-W*RW model.[47]

In the 2000s, the models have p-star gradually declining to a level close to 1.0%-1.2% by 2010. It remained close to that level through most of the past decade, but since 2018, it has steadily increased. At the end of our sample, all three models estimate the posterior mean of p-star at, or close to, 1.5%. As we show in appendix A12, these estimates of p-star are consistent with the narrative implied by the two-regime Markov-switching model of Kahn and Rich (2007), an influential contribution in the trend productivity literature.

The uncertainty around the posterior mean estimates of p-star is large. Panel (d) quantifies this uncertainty by reporting the width of the 90% credible intervals corresponding to all three models. The plots provide evidence that the theoretical restriction (defined by eq. 28) contributes to a substantially improved precision of p-star (just like it does for pi-star and w-star), as evident by Base and Base-NoSurv plots lying below the Base-W*RW. Interestingly, the estimate of p-star from the Base is more precise than Base-NoSurv in 1960 through the mid-1980s, even though we do not utilize survey based long-run expectations of productivity in

prior.

[47] Edge et al. (2007), who collect real-time estimates of long-run productivity from various sources, including historical Economic Reports of the President, document a similar pattern in the trend productivity estimates.

the estimation of our model. Based on the Bayesian model comparison, the Base model's fit to productivity data is marginally better than Base-NoSurv. The improved precision and better fit of the Base model to productivity data suggest there are important spillover effects in the estimation from survey forecasts of other stars.

Cyclical dynamics of labor productivity

Panel (e) plots the estimate of the parameter λ^p, which relates cyclical unemployment to the productivity gap, from all three models. The plots indicate a high level of uncertainty around the estimates of λ^p. The 90% credible intervals are wide, such that they include both positive and negative values complicating reliable inference. Going just by the posterior mean estimate, the evidence suggests a counter-cyclical behavior of labor productivity, with this relationship weakening over time.

The model specification Base-P*CycOutputgap, which relates productivity to output gap instead of unemployment gap (through parameter ϕ^p), provides generally similar inference about the cyclical nature of labor productivity. The plot for the time-varying parameter ϕ^p is relegated to appendix A13 to conserve space. The credible intervals are wide and include both positive and negative values. Based on the posterior estimate of parameter ϕ^p, productivity is procyclical in the 1960s and post-2010, but it is either acyclical or countercyclical in other periods. Overall, the empirical evidence generally corroborates the evidence presented in Gali and van Rens (2020). The model comparison results indicate a slightly inferior fit of the Base-P*CycOutputgap model compared to Base (-608.1 vs. -606.9 in the case of productivity data and -1773.8 vs. -1771.7 for the overall fit).

The importance of SV in productivity equation

An essential element of our decomposition of labor productivity into the trend, cyclical, and idiosyncratic components, which others have abstracted from, is that we permit a time-varying variance of the idiosyncratic component. Empirically, our results show this to be an important extension, as shown in the SV plots included in panel (f) and the model comparison results reported in table 6. The plots indicate statistically significant evidence of time-variation in the volatility of the idiosyncratic component. The model comparison further provides evidence supporting SV inclusion, as the Base-NoSV is the worst performing and has a significantly worse fit to productivity data compared to Base.

We also explored the possibility that the SV may be soaking up the variation in productivity, which otherwise would have been attributed to the cyclical component of productivity. The model specification Base-NoSV, which shuts down SV in the idiosyncratic component of productivity (and other model equations), yields estimates of λ^p similar to Base, suggesting that SV is not contributing to the ambiguous result on the cyclicality of labor productivity.

4.4. ***Estimation results for π-star***

Figure 7, panels (a) and (b) plot the posterior mean estimates of pi-star along with the 90% credible intervals from the Base and Base-NoSurv model specifications, respectively. Panel (c) plots the corresponding precision estimates, defined as the width of the 90% intervals. A quick visual inspection shows that the pi-star from the Base specification is significantly more precise than Base-NoSurv, as evidenced by narrower credible bands and the precision plot corresponding to Base lying below the Base-NoSurv plot. Based on the marginal likelihood criteria, the fit of the inflation equation to the data in the case of Base is substantially greater than Base-NoSurv (as reported in Table 8). The fit of the overall Base model to the data is also higher than Base-NoSurv. Our finding that adding survey expectations improves both the model fit and the precision of pi-star is consistent with CCK.

The broad contours reflected in the posterior mean pi-star from the two models are similar to those documented elsewhere in the literature (e.g., CCK). For instance, pi-star was low in the 1960s, high in the 1970s, fell sharply in the 1980s, continued a steady deceleration in the 1990s, fluctuated in a narrow range between 2.0% and 2.5% in the 2000s, and has been below 2% since 2012. This general pattern is consistent with the widely held view. Focusing on the specifics, unlike some papers (e.g., Stock and Watson, 2007; Mertens, 2016), which show two peaks in pi-star, one in the mid-1970s and another in the early 1980s, our model-based estimates (both with and without survey data) do not show the earlier peak (similar to CCK). Relatedly, in those same papers, the pi-star is estimated to peak at a level of 10% or higher; in contrast, the mean estimate of pi-star in our model specifications peak at a lower level (similar to CCK and Mertens, 2016 – in his model spec that augments survey data).[48]

Comparing estimates from Base and Base-NoSurv specifications, the level of pi-star is similar in the 1960s but starting in early 1970, pi-star from the Base specification sharply accelerates to peak at 6% in early 1980, whereas, while the estimates of pi-star from Base-NoSurv specification also accelerate but peaks at a lower level of 4.5%. As shown, uncertainty about pi-star increases sharply in early 1980, with the Base-NoSurv estimates experiencing a much more dramatic rise. It is the case that uncertainty around pi-star (as measured by the width of 90% credible intervals) inferred from the Base-NoSurv is higher compared to the Base throughout the estimation sample. But in early 1980, the differential in uncertainty is twice as large, as can be seen comparing dotted and solid plots in panel (c).

A similar rise in model-based estimates of pi-star uncertainty in the late 1970s through early 1980 (known as the Great Inflation period) has been noted elsewhere (e.g., Mertens, 2016). A subset of literature attributes the rise in pi-star uncertainty to un-anchoring of inflation expectations during the Great Inflation period. Beginning early 1980 through early 2000, both models have (posterior mean of) pi-star steadily declining to 2%. Between 2000 and 2012,

[48] Since both Stock and Watson (2007) and Mertens (2016) endow SV to the RW process governing the pi-star whereas we do not, this difference in the modeling assumption may explain why the difference in the pi-star estimates around the Great Inflation period. However, CCK, who also allows SV in the pi-star process, yields pi-star generally similar to our pi-star estimates suggest that the SV assumption is likely not the answer.

whereas in the case of Base, pi-star is flat at 2%, in Base-NoSurv, it is stable at a slightly higher level of 2.3%. Since 2012, pi-star has slowly moved down to reach 1.5% (in Base) and 1.4% (in Base-NoSurv).

Inflation gap persistence

Panel (d) shows the posterior mean estimates of parameter ρ^{π} for Base (solid line) and Base-NoSurv (dotted line). Also plotted are the 90% credible intervals from the Base model. As is evident, the uncertainty around the posterior mean is high. That said, both models indicate quite similar estimates of persistence in the deviations of inflation from pi-star. There is also strong evidence of time-variation in inflation gap persistence. For example, gap persistence was low (0.25 to 0.35) in early 1960, but from thereon began to increase steadily, reaching close to 0.85 by early 1970, and remained at that level through the early 1980s. Subsequently, the persistence declined steadily to 0.4 by the early 1990s. From the late 1990s to the early 2000s, persistence fell further to 0.3, and it remains at that level.

Price Phillips curve

Panel (e) plots the posterior mean estimate of parameter λ^{π}, which is the slope of the price Phillips curve. As before, the plots from the main model specifications are shown. (The 90% credible intervals are from the Base model). The plots indicate both model specifications yield very similar estimates of the parameter linking the inflation gap to the unemployment gap. The estimates also indicate strong evidence of time-variation in the slope of the Phillips curve. For example, both models estimate a steeper Phillips curve in the 1960s that subsequently weakens (becomes less negative) over time through 2010. From thereon, it slowly begins to become steeper (more negative), ending 2019 at -0.23, which is still weak historically speaking and is surrounded by wide intervals spanning -0.05 to -0.52. This pattern is consistent with the familiar narrative (also documented in several other papers) that the *"Phillips curve has weakened over time."*

SV in price inflation equation

Panel (f) plots the volatility estimates (i.e., the standard deviation of the shocks to the inflation gap, $e^{h_t^{\pi}}$) corresponding to the two model specifications. The figure shows that the posterior mean estimates are quite similar. The estimates imply high volatility during the period of Great Inflation that fell subsequently. Inflation volatility increased sharply again during the Great Recession but has trended lower since then. By 2019, inflation volatility had returned to the low levels of the early 2000s but remains shy of historic lows of the mid-1960s and mid-1990s. The contours of the volatility in the inflation gap are generally similar to those reported in CCK and Chan, Koop and Potter (2013). Bayesian model comparison indicates strong evidence supporting the inclusion of SV in the price inflation equation.

Link between survey and pi-star

In figure A6 (appendix), panels (a) and (b) plot the posterior estimates of the coefficients C^{π} and β^{π} that provide a sense of the estimated relationship between survey forecast and pi-star. The prior assumes an unbiased relationship between survey forecasts and pi-star (i.e., prior mean $\beta^{\pi} = 1$ and at all periods $C_t^{\pi} = 0$). The model estimation yields posterior mean estimate of 0.99 for β^{π}, with 90% credible interval spanning 0.91 to 1.07 (also reported in table 2). The posterior mean of C_t^{π} displays considerable time-variation; however, the 90% credible intervals, for the most part, include zero. Taken together, the posterior estimates of β^{π} and C_t^{π} imply that the survey forecast, on average, is somewhat a biased measure of pi-star. This latter result confirms the findings of CCK.

In the appendix A11.a, we include the results and discussion comparing pi-star estimates from the Base model to external models: CCK, CKP, and UCSV. The estimates indicate that the CCK model generates the most precise pi-star, followed by the Base model, CKP, and UCSV. The latter model yields volatile and erratic estimates of pi-star (and precision).

Summary: pi-star

All told, we summarize the analysis of the inflation block as follows. First, the Base model and its variants indicate contours of pi-star that corroborate the narrative documented elsewhere in the literature. However, in some periods, pi-star estimates can differ notably across models, and as emphasized in CCK, these differences can have important implications for monetary policy. Second, comparing across Base and Base-NoSurv specifications, and comparing the Base specification with outside models, strongly suggests the usefulness of survey forecasts in improving the econometric estimation of pi-star (i.e., survey forecast information yields sensible estimates of pi-star and improved precision); hence, corroborating evidence in CCK, Mertens (2016), and Nason and Smith (2020). Third, we find evidence in support of incorporating time-variation in the price Phillips curve. Specifically, suggesting, in a broad sense, weakening of the relationship between inflation and labor market slack since the 1960s, something also documented by several others (e.g., CKP; Stella and Stock, 2015; Del Negro et al., 2020).

Fourth, as found by CKP, CCK, Mertens and Nason (2020), among others, we find evidence supporting time-variation in the persistence of the inflation gap. Fifth, as noted by many, including Stock and Watson (2007) and Clark and Doh (2014), we find strong evidence of SV in the innovations of the inflation equation. Sixth, as in CCK, we find evidence that the survey forecast of PCE inflation is a biased measure of pi-star. Lastly, the Base model's improved fit to inflation data compared to some of its variants provides evidence supporting the long-run theoretical restriction defined by equation (28), which imposes w-star = pi-star + p-star.

4.5. ***Estimation results for W-star***

In modeling w-star, a novel feature of our framework is the decomposition of w-star into its fundamental components, pi-star and p-star. Figure 8 presents posterior estimates of w-star along with the decomposition. The first row in the figure plots estimates from the Base model, and the second-row plots estimates from the Base-NoSurv. Third-row plots p-star estimates from other model variants alongside Base and Base-NoSurv models, and also presents precision estimates of the w-star.

The estimates imply w-star increased steadily in the 1970s and peaked in the early 1980s. This increasing w-star reflected upward drift in pi-star that more than offset the downward drift in p-star, as evidenced by the widening in the shaded area representing pi-star and slight narrowing of the shaded area representing p-star. Base model implies w-star peaked at 7.3% in the early 1980s, while Base-NoSurv has w-star peaking at 6%. Both models have w-star sharply drifting lower through much of the 1980s to reach near 4% by early 1990. From thereon, the path of w-star across the two models is very similar and indicates a gradual slowing to 2.5% by the end of 2017. W-star moved up to 3.0% by the end of 2018, only to fall back to 2.8% in 2019.

Not surprisingly, w-star is more precisely estimated in the Base model than in the Base-NoSurv model, as shown in panel (f). The considerable uncertainty around w-star, implied by the Base-NoSurv model during the 1970s, is mostly driven by pi-star. As noted earlier, the pi-star estimate from the Base-NoSurv was highly imprecise during the 1970s. Interestingly, despite the inferior precision of the Base-NoSurv compared to Base, the Bayesian model comparison suggests a better fit of the Base-NoSurv model to the nominal wage data than Base (see Table 7). However, the overall fit of the Base-NoSurv to data (which includes data beyond nominal wage) is slightly worse than Base.

Sensitivity of w-star to modeling assumptions

Panel (e) plots estimates of w-star from two additional Base model variants, Base-W*RW and Base-NoPT. The Base-W*RW model eliminates the long-run restriction that w-star is the sum of p-star and pi-star (on average) and instead models w-star as a RW process. Interestingly, the path of w-star implied by Base-W*RW is similar to Base-NoSurv through the mid-1980s. From thereon, w-star from Base-W*RW is below the Base-NoSurv through early 2010. Since then, it is identical to Base and Base-NoSurv. Although in the first half of the estimation sample, the w-star from Base-W*RW is less precisely estimated than Base, in the second half of the sample, it is more precise. According to the Bayesian model comparison, the fit of the Base-W*RW to the nominal wage data is inferior to both Base-NoSurv and Base. However, compared to Base, the degree of inferiority is only slight. The overall fit of the Base-W*RW model to the data is substantially worse than achieved by either the Base and Base-NoSurv model.

The Base-NoPT model eliminates the passthrough from prices, i.e., it removes the price

inflation gap from the equation describing the wage inflation gap. In other words, the direct link between the cyclical components of prices and nominal wages is eliminated, but the connection between the permanent components pi-star and w-star remains. Doing so has notable implications for the estimate of w-star and the model's fit. As shown in panel (e), the w-star implied from Base-NoPT is higher than that implied by the other models through the first half of the sample. While the Base model has w-star peaking at a little above 7% in the early 1980s, the Base-NoPT model implies a higher peak of 8.2%. The acceleration in w-star implied by the Base-NoPT model during the 1970s is much stronger than that implied by the Base model estimates. This stronger path of w-star is associated with more precise estimates of w-star in the 1970s compared to the Base and other models, as can be seen in panel (f). However, according to the Bayesian model comparison reported in table 7, removing the connection between the cyclical components negatively impacts the model fit, as evidenced by the substantially inferior fit of the Base-NoPT model to data compared to the Base model.

Wage persistence, Wage Phillips curve, Passthrough from prices, and SV in wage equation

Figure 9 presents the time-varying posterior estimates of the parameters describing the persistence in the nominal wage gap, the wage Phillips curve, the short-run passthrough from prices to wages, and stochastic volatility of the shocks to the nominal wage equation. Estimates from three models, Base, Base-NoSurv, and Base-W*RW are presented. A quick visual inspection indicates both statistically and economically significant evidence of time-variation in these parameters that capture important empirical relationships.

Wage gap persistence

Panel (a) plots the posterior estimates of the parameter ρ^w, capturing the persistence in the nominal wage inflation gap. Also included are the 90% credible intervals from the Base model. The posterior mean estimates for the three models indicate increasing persistence in the wage inflation gap beginning in early 1960 and peaking in mid-1980. The Base model shows a notably higher peak at 0.45 compared to 0.39 and 0.33 for Base-NoSurv and Base-W*RW, respectively. The higher peak suggests that the Base model attributes a higher share of fluctuations in the cyclical nominal wages to the persistence component than that implied by the other two models. From the mid-1980 to the early 1990s, the persistence steadily declines but after that increases through the mid-2000s; from there on through the early 2010s, the estimated persistence in the nominal wage gap falls to levels seen in the mid-1970s. Since then, it has been slowly increasing. It is worth noting that credible intervals around the posterior mean are wide, suggesting high uncertainty in the inference about the estimated persistence.

Wage Phillips curve

In Figure 9, panel (b) plots the estimates of parameter λ^w, which captures the wage Phillips curve relationship in the US data. The plot provides strong evidence supporting the existence of

the wage Phillips curve in the post-war data. Notably, the plot also offers convincing evidence of a time-variation in this relationship. According to the posterior mean estimate, from the early 1960s through mid-1970s, our models imply the strength of the wage Phillips curve at a moderate level, but from thereon through the mid-1980s, the wage Phillips curve steepened sharply in Base and Base-NoSurv (less steep in Base-W*RW). By the mid-1980s, in the Base model, the posterior mean of the wage Phillips curve parameter is estimated to be -0.5, with 90% credible intervals ranging from -0.23 to -0.75. From thereon, it gradually flattened until the mid-2000s, but soon afterward, it began to flatten more rapidly through to early 2010. In 2010, all three models estimate the posterior mean of the Phillips curve parameter at -0.2. The prevalence of the downward wage rigidities during the Great Recession is among the primary explanations for the flattening wage Phillips curve (see Daly and Hobijn, 2014).

From 2010 onwards, with an improving economy, the estimated wage Phillips curve has steadily steepened. Our empirical evidence on the wage Phillips curve is consistent with the findings of Knotek and Zaman (2014), Peneva and Rudd (2017), and Gali and Gambetti (2019), who all document strong support for the continuing existence of a wage Phillips curve in the US data.

Passthrough from prices

Panel (c) plots the estimates of the short-run passthrough from prices to wages defined as $\frac{\kappa_t^w}{1-\rho_t^w}$. The posterior estimates of passthrough indicate a weakening relationship between cyclical nominal wage inflation and cyclical price inflation over the estimation sample, confirming the evidence presented in Peneva and Rudd (2017) and Knotek and Zaman (2014). The relationship between the two was strong in the 1970s through to the mid-80s, but since then, it has gradually weakened such that it has been nonexistent (i.e., the passthrough is estimated to be zero) for the past decade. This period of the breakdown in the relationship between the two cyclical components has coincided with low and stable price inflation. Literature has attributed various explanations to this breakdown in the relationship that includes improved anchoring of inflation expectations (Peneva and Rudd, 2017) and amplification of downward wage rigidities during low levels of price inflation (Daly and Hobijn, 2014).

Our empirical finding also supports the results of Bobeica et al. (2019), who show using euro area and US data that the link between labor compensation and price inflation in the short-run importantly depends on the prevailing inflation regime. They find a high inflation regime associated with a tighter connection between labor costs and price inflation and a low inflation regime associated with a weaker link. All three of our models imply similar inference. Both Base-NoSurv and Base-W*RW indicate a stronger passthrough than the Base model in the 1970s and 1980s, periods associated with high inflation in the US. Comparing between panels (a) and (c) suggests that during that period, Base attributes more of the increase in nominal wage inflation to increase in persistence than to the passthrough from price inflation, hence the less strong passthrough estimate than seen in the Base-NoSurv and Base-W*RW models.

SV in the wage equation

Panel (d) plots the time-varying standard deviation of the innovations to the nominal wage inflation gap. The plot indicates the importance of allowing for SV in the equation for nominal wage inflation. All three models show very similar posterior mean estimates of SV. The estimates suggest that volatility in the early 1960s was high but then subsequently fell to rise back up again in the late 1960s and early 1970s. From thereon through the mid-1970s, it fell steeply. It increased in the early 1980s, but less sharply than in the previous decades. From the mid-1980s through the early 1990s, volatility moderated to low levels, and since then, it remains flat at that low level. The Bayesian model comparison indicates further evidence supporting the inclusion of SV in the wage equation, as evident by the substantially inferior fit of the Base-NoSV model to nominal wage inflation data compared to Base and Base-NoSurv models (Base-NoSV: -344.3 vs. Base: -277.5; see table 7).

4.6. ***Estimation results for r-star***

Figure 10 presents r-star and the "catch-all" component D estimates for our two main model specifications. The top row of the figure plots the estimates of r-star (panel a) and component D (panel b) from the Base model. Also included in panel (a) are the survey expectations of r-star (which enters our Base model). As can be seen, the contours of (posterior mean) r-star from the Base model track the survey estimate; this suggests that survey data plays an influential role in guiding the model's assessment of r-star. The posterior mean estimate from the Base model shows r-star staying relatively flat at 3.5% in the 1960s, and then slowly trends down through the 1970s to reach 3% by early 1980. Thereafter, it fluctuates in a range between 2.8% and 3.5% through to the beginning of 2000. From there on, it steadily declines to reach 1.1% at the end 2019.

Panel (b) plots the estimate of component D, whose dynamics are shaped by the survey expectations data and by information from the Taylor rule and IS equations. As can be seen in the figure, component D is imprecisely estimated. According to the posterior mean estimate, in the 1960s, component D exerts slight upward pressure on r-star that is mostly offset by downward pressure coming from g-star (via equation 36), helping keep r-star relatively flat. After that, with D remaining flat through 2000, developments in g-star shape the trajectory of r-star. Beginning in 2000 and onwards, all forces (as captured through the model structure) work in the same direction to push r-star steadily downwards. The estimated link between r-star and g-star is of moderate strength (posterior mean of parameter $m = \frac{\zeta}{4} = 0.701$); see table 2); therefore, movements in g-star play an influential role in driving r-star.

Moving on to the Base-NoSurv model specification, in panel (c), the mean estimate shows r-star rising from 2% in early 1960 to 3.5% through early 1980 and then remaining stable through early 2000. This trajectory is similar to Gonzalez-Astudillo and Laforte (2020), who also utilize the Taylor-rule and information from long-term interest rates in their estimation.

Beginning 2000 onwards, r-star steadily declines to reach 1.4% at the end 2019. The trajectory of r-star from 2000 onwards is similar to that from the Base model. It is worth noting that our models' indication of a secular decline in the r-star beginning in 2000 is also documented elsewhere in the literature tackling r-star (the exception being JM).[49] However, the extent of decline varies considerably across studies. The literature attributes this secular decline in r-star to various explanations, including: a trend decline in g-star (e.g., LW, 2016); rising premiums for convenience yield, i.e., increased demand for safety and liquidity Treasury bonds (see Del Negro et al., 2017; Bullard, 2018); and excess global savings (Pescatori and Turunen, 2016).

The uncertainty around the r-star estimate from the Base-NoSurv model is substantially higher than Base, as can be seen by comparing panel (a) and panel (c) of figure 10, and also shown in panel (b) of figure 11. The increased uncertainty in r-star comes from component D, which is imprecisely estimated without the survey data. Furthermore, based on the marginal likelihood criteria, the Base model is favored over the Base-NoSurv model (see table 9).

Without the survey information about r-star, the estimated link between g-star and r-star is significantly weaker (posterior mean of $m = \frac{\zeta}{4} = 0.390$; see table 2), which is consistent with the evidence documented in Hamilton et al. (2016) and Lunsford and West (2019). Therefore, the movements in component D significantly dominate the contours of r-star in Base-NoSurv model. Both the IS curve and Taylor rule equations shape the evolution of component D. The hump-shaped patterns in both D and r-star reflect the trends in real long-term interest rates (informed from the IS equation) and short-term interest rates (from the Taylor-rule equation). It is interesting to note that the r-star estimate from JM (and Gonzalez-Astudillo and Laforte (2020)) – who use the Taylor-rule equation and information from both short and long-term interest rates – also exhibit hump-shaped behavior (though, in the case of JM, it is only slight). As we show shortly, the prior setting on the shock process for r-star (in our Base and Base-NoSurv cases, component D) plays an essential role in shaping the contours of r-star.

As discussed earlier, the estimates of g-star from both Base and Base-NoSurv models are quite similar. Therefore, the primary source of the differential in the r-star estimates between Base and Base-NoSurv is the quantitatively weaker relation estimated between r-star and g-star in Base-NoSurv than Base.

Assessment of policy stance

Panel (e) of figure 10 provides an assessment of the stance of monetary policy. Following Pescatori and Turunen (2016), we gauge monetary policy's stance as the deviation of the short-term nominal interest rate from the long-run nominal neutral rate of interest (defined as the sum of r* and pi*) – this is the interest rate gap from the Taylor rule equation. A positive interest rate gap characterizes a restrictive monetary policy stance, and a negative interest rate

[49] JM document that r-star from their preferred specification (which allows for SV in TR equation) is generally flat over their sample spanning 1960 through 2018. However, in an alternative specification, which does not permit SV, the r-star estimate exhibits decline in r-star similar to that documented elsewhere. In our examination, r-star trajectory is little changed comparing between Base specification and Base without SV (i.e., Base-NoSV).

gap implies a stimulative stance. The solid line corresponds to the policy stance inferred from the Base model and the dashed line to that inferred from the Base-NoSurv model. Even with notable differences in the estimates of r-star across the two models, the assessment of the policy stance is remarkably similar throughout the sample. So why are they so similar?

The answer lies in the differences in pi-star estimates across two model specifications, as shown in figure 7 (panels a and b). In other words, the differences between r-star estimates across the two models are compensated (i.e., offset) by the differences between pi-star, such that assessment about the stance of monetary policy across the two models is strikingly similar. For instance, in the 1960s, the r-star estimate from the Base is on average 1.34 percentage points (ppts) higher than that of Base-NoSurv. However, over the same period, the pi-star estimate from the Base model is 0.54 ppt lower than that of the Base-NoSurv model, which reduces the difference between their associated assessments of policy stance.

According to our model(s) estimates, the policy stance appeared to be slightly restrictive before the Great Recession, but at the onset of the Great Recession, the policy stance immediately turned accommodative. Since then, it has remained very accommodative (reflecting the effects of unconventional monetary policy). After peaking in late 2015, the degree of accommodation has gradually declined (i.e., the interest rate gap has become less negative), such that, by the end of 2019, it has edged closer to the neutral threshold.

A closer inspection of the figure reveals an interesting insight. Since 1990, both the degree and duration of policy accommodation in response to the recession have been more significant than the previous recession. For instance, the monetary policy stance was more accommodative both in terms of level and duration following the 2001 recession than the 1990-1991 recession. Similarly, during and following the Great Recession, the policy stance in terms of level and duration was more significant than following the 2001 recession. Broadly speaking, our model implied assessment of the stance of monetary policy mirrors that in the assessment documented in Brand and Mazelis (2019).

Random walk assumption for r vs. Base (and Base-NoSurv)*

As is commonly done when estimating stars, a random walk assumption for r-star is a popular choice (e.g., Kiley, 2020; JM). Accordingly, we explore this particular modeling choice's fit to the data and empirical properties by replacing the equation linking r-star to g-star and the RW component D with an equation that assumes a random walk process for r-star in our main model specifications (Base and Base-NoSurv). We denote these specifications, Base-R*RW and Base-NoSurv-R*RW. By adopting a RW assumption for r-star, the models will be unable to attribute any specific causes of movements in estimates of r-star.

Figure 11, panel (a) plots the posterior mean r-star estimates from the Base-R*RW and Base-NoSurv-R*RW models. To facilitate comparison, also shown are estimates from Base and Base-NoSurv models. Panel (b) plots the corresponding r-star precision estimates (defined as the width of 90% credible intervals). A few observations immediately stand out. First,

the estimated r-star from model specifications with the RW assumption, although exhibiting broadly similar contours, are higher than those obtained from the specifications that impose a relation between r-star and g-star. Second, beginning 2000 and onwards, r-star estimates from the specifications with the assumed link between r-star and g-star experience a more stark decline than those from the specifications with the RW assumption. For instance, by late 2019, the estimates of r-star from both the Base-R*RW and Base-NoSurv-R*RW models settle at close to 2%, whereas those from the Base and Base-NoSurv models fall further to the range of 1.2 to 1.4%. This differential is mostly explained by the lack of direct downward pressure from g-star in the specifications with RW assumption.

Fourth, bringing information from the survey improves the precision of the r-star estimates substantially, irrespective of whether r-star is modeled simply as RW process or the combination of RW component and a component linking r-star to g-star. Fifth, the specifications that allow for a link between r-star and g-star are more precise than those that do not. The Base specification generates the most precise r-star estimates relative to those obtained from the other three specifications.

Based on the model comparison metric reported in table 9, the model indicating the most precise r-star does not necessarily rank as the best fitting model. The fit of the Base specification is slightly inferior to that of both the Base-R*RW specification and the Base-NoSurv-R*RW, but not by very much. This evidence nicely illustrates that the marginal likelihood metric has a built-in penalty that increases as the model complexity goes up. When comparing between Base-NoSurv-R*RW and Base-R*RW specifications, the addition of survey data increases the model's fit to the interest rate data slightly from -215.58 to -214.04 (but reduces overall model fit marginally from -1769.3 to -1770.8). In comparison, moving from the Base-NoSurv to the Base specification, the fit to the interest rate data increases, from -221.98 to -216.4 (and the overall model fit from -1772.8 to -1771.7).

Taken together, the evidence described above suggests that the RW assumption for r-star is a viable option, but bringing in information from surveys helps improve precision of the estimates of r-star substantially. Another result worth highlighting from the model comparison exercise concerns the marginal value of survey information in the estimation of r-star. In a model specification that imposes a relationship between r-star and g-star (e.g., Base; Base-NoSurv), adding survey information is crucial in making the model a competitive alternative. By bringing in survey information, which has a high correlation between g-star and r-star survey expectations (0.8), the estimated link between g-star and r-star in the model becomes stronger ($m = \frac{\zeta}{4} = 0.701$ in Base vs. $m = \frac{\zeta}{4} = 0.390$ in Base-NoSurv).

Given the evidence on model comparison and the precision of r-star estimates, our preferred choice is the Base model because its fit to the data is competitive (just marginally inferior to spec with RW assumption). And it produces the most precise r-star estimate compared to the alternative specifications. An additional factor that influences our choice is the ability to provide an explanation for movements in r-star, which is made possible due to its direct link to

g-star.

In a supplementary set of exercises, we illustrate the usefulness of the Taylor-type rule equation and the equation linking r-star to survey expectations for identifying r-star. The addition of the Taylor-type rule equation turns out to be crucial to yield plausible and precise estimates of r-star (see appendix A10.d).

We also explored the role of data versus prior in determining r-star, and in the interest of brevity, the results of the exercises are relegated to the appendix (see A10.a). Here, we briefly mention that results indicate that in the case of the Base-NoSurv model, the prior views determine the shape of the posterior for r-star, confirming Kiley (2020). However, in the Base model, which links r-star to survey expectations, the data does have some influence. In the case of the Base-NoSurv model, we also find that if we loosen the prior on the variance of the r-star process (to values similar to Kiley, 2020), then the data begin to shape the posterior. But, this comes at the cost of worsening fit to the interest rate data.

Overall, we find that when it comes to r-star, specification choices matter a lot (something also highlighted by Clark and Kozicki (2005), Beyer and Wieland (2019), and Kiley (2020)). The model specifications that include survey expectations yield estimates that are both reasonable and the most precise. In our examinations, the Base specification, which allows the link between g-star and r-star, is equally preferred by the data to variant of the Base specification that assumes r-star as a RW. Since 2000, the best fitting model specifications indicate a steady decline in r-star, similar to documented elsewhere in the literature.

5. Real-time Estimates and Forecasting

In this section, we perform two real-time, out-of-sample, forecasting exercises. In the first exercise, we compare the real-time forecasting performance of our two main models, Base and Base-NoSurv. We evaluate both the point and density forecast accuracy for real GDP growth, PCE inflation, the unemployment rate, nominal wage inflation, labor productivity growth, and the shadow federal funds rate. We show that the Base model is more accurate on average compared to Base-NoSurv for all variables of interest except the unemployment rate. We also document our Base model's superior forecasting properties relative to "hard to beat" benchmarks, including some of the recently proposed UC models for inflation forecasting. By-products of our real-time forecasting exercise are the real-time estimates of the stars from 1999 through 2019. We compare these real-time estimates to the final (smoothed) estimates – based on the entire sample spanning 1959Q4 through 2019Q4.

In the second forecasting exercise, we illustrate the efficacy of the stars' estimates produced from our models by demonstrating their usefulness in forecasting with external models (e.g., steady-state VARs). We find that the quality of our estimates of the stars from the Base model is generally competitive to the survey estimates, which are commonly used as proxies for stars in VAR forecasting models. For brevity purposes, we relegate the discussion of this latter exercise

to the appendix A5.

Table 10 presents the results from comparing the out-of-sample forecasting performance (both point and density) between the two models over the forecast evaluation sample spanning 1999Q1 through 2019Q4. The forecast evaluation is based on real-time data vintages and uses a recursively expanding estimation window, where each recursive run uses an additional quarterly data point in the estimation sample.[50] The forecast accuracy (point and density) is computed from one-quarter ahead to 20 quarters out. Partly due to our focus on the medium-term horizon and partly in the interest of space, we report accuracy metrics for four, eight, twelve, sixteen, and twenty quarters ahead. We evaluate the forecast accuracy using real-time data; specifically, we treat the "actual" as the *third* release of a given quarterly estimate.[51] For instance, in the case of real GDP, the third estimate for 2018Q4 corresponds to the GDP data available in late 2019Q1. The point forecast accuracy is assessed using the root mean squared error (RMSE) metric, and the density forecast accuracy is evaluated using the log predictive score (LPS). The statistical significance of the point forecast accuracy is gauged using the Diebold-Mariano and West test and in the case of density forecast accuracy based on the likelihood-ratio test of Amisano and Giacomini (2007).

The top panel of the table reports the results corresponding to the point forecast accuracy, while the lower panel for the density forecast accuracy. The numbers reported in the table correspond to relative RMSE –RMSE Base relative to RMSE of Base-NoSurv – in point forecast comparison, and relative mean LPS – LPS Base minus LPS Base-NoSurv – in the case of density forecast comparison. Hence, numbers less than one in the top panel suggest that point forecast accuracy of the Base forecast is more accurate on average, and positive numbers in the bottom panel suggest that density forecast accuracy of the Base forecast is more accurate than Base-NoSurv forecast.

As is evident by the numbers reported in the table, except for point forecast accuracy of the unemployment rate, the evidence generally favors the Base model as more accurate than Base-NoSurv. The evidence in support of the Base model is strongest for PCE inflation and labor productivity growth. In the case of the unemployment rate, as was the case with the in-sample model fit (see table 3), the Base-NoSurv model outperforms the Base model in point forecast accuracy. However, over the forecast evaluation sample, the uncertainty around the point forecast of unemployment rate implied by the Base-NoSurv model was higher than the Base model (on average). This higher uncertainty contributed to inferior density forecasts from the Base-NoSurv model compared to the Base model, as is evident by the positive numbers in

[50] Going back in time means that we are using relatively fewer observations to estimate model(s). As is commonly done when performing real-time forecasting using multivariate UC models, we need to tighten priors on the shocks' variances driving the latent components (see, for instance, Barbarino et al., 2020). Accordingly, we devise a systematic approach to adjusting the prior on the Scale parameters of the inverse gamma distributions defining the variances of the stars. We multiply the Scale parameter with the $factor = (\frac{2T}{N} - 1) * (\frac{T}{N+5(N-T)})$, where N is total sample size from 1959Q4 through 2019Q4, and T refers to the number of data points in a given data vintage. At the end of the sample,the $factor = 1$ because $T = N$.

[51] Results are qualitatively similar if we instead use the revised data (2020Q1 vintage data) as the actual values in the forecast evaluation exercises. The results are available on request from the author.

the row corresponding to the unemployment rate. It is generally the case across all variables, except the real GDP growth, the accuracy of the density forecasts from the Base model are more accurate than Base-NoSurv. In the case of real GDP growth, even though, for the most part, the point forecast accuracy between the two models are similar on average, the density forecasts from the Base-NoSurv model are more accurate than the Base model.

We also compared the forecasting performance of our Base model to the outside benchmark models, which forecasting literature has shown to be useful forecasting devices. Specifically, we compare the accuracy of the inflation forecasts from our Base model to the following three models, UCSV of Stock and Watson (2007) [UCSV], Chan, Koop, and Potter (2016) [CKP], and Chan, Clark, and Koop (2018) [CCK]. We compare the accuracy of the unemployment rate forecasts from our Base model to the Chan, Koop, and Potter (2016), and the accuracy of the nominal wage inflation from the Base model to the UCSV model applied to the nominal wage inflation – motivated by Knotek (2015). Our forecasting results provide strong evidence in support of our Base model's competitive forecasting properties. For the sake of brevity, the results are included in the appendix A4 table A3.

Real-time versus final estimates

Up to this point, we only examined the smoothed estimates of the stars inferred using all the sample data, i.e., from 1959Q4 through 2019Q4, which we denote here as final estimates. As discussed in CKP and Clark and Kozicki (2005), the examination of final estimates is beneficial for "historical analysis," such as the evaluation of past policy. But for real-time analysis, such as forecasting and policy-making, real-time estimates at time t – estimates based on data and model estimation through time t (instead of through 1:T) – are the relevant measures. In estimating the stars, a voluminous number of papers have documented the typical pattern of notable differences between real-time and final estimates, e.g., see Clark and Kozicki (2005) and Beyer and Wieland (2019) for r-star and Tasci (2019) for u-star.[52]

Relatedly, several researchers have attributed the inability to precisely know the location of these stars in real-time to past policy mistakes, see Powell (2018) and references therein. The documented differences between the real-time and final estimates, which at times could be dramatic, and the recognition of these differences by policymakers have been the primary reason limiting the usefulness of real-time estimates of the stars in policy discussions in recent years (see Powell, 2018). Hence, there is a strong preference for methods that can provide more credible inferences about stars in real-time.[53]

[52]Both revisions to past data and the accrual of additional data could contribute to the observed differences between the real-time and final estimates. The estimation with additional data has been found by many to be the primary factor causing revisions to historical estimates of the stars and contributing to divergence between the real-time and final estimates (see Tasci, 2019; Clark and Kozicki, 2005).

[53]The issue of imprecision in the estimation of stars is an important one. It has been long recognized that considerable uncertainty surrounds the estimated stars complicating reliable inference (e.g., Cross, Darby and Ireland, 2005). Despite the stars' imprecision, they continue to be used as inputs into policymaking and for other purposes (see Williams, 2018; for r-star). After all, as discussed in Mester (2018), uncertainty about the stars is just one source of uncertainty among many that confront policymakers.

Comparing real-time and final estimates of the stars from our Base model suggests that we have made some progress in mitigating the difficulties in previous real-time estimation of the stars. However, in the Base-NoSurv model, there is less success in mitigating this issue. We believe a big reason for this lack of success in the latter case is that we estimate a very high-dimensional model with a lot less data (as will be the case when stopping estimation at earlier periods). An artifact of this is that it requires the imposition of very tight priors in earlier periods than when estimating with more recent periods, which, in turn, impacts on the posterior estimates of model parameters and the stars. This latter fact mechanically contributes to more considerable observed differences between real-time and final estimates in the first half of the sample period analyzed. In the case of the Base model, the use of survey information helps anchor the estimates to more reasonable values even in the face of tight priors.

Figure 12 plots the real-time posterior mean estimates of the stars from 1999Q1 to 2019Q4. Also plotted are the corresponding final (posterior mean) smoothed estimates and the 68% and 90% credible bands, respectively. The real-time estimates are the end-sample posterior mean (of the smoothed) estimates at any given period, e.g., 1999Q1 estimate corresponds to estimating the model(s) from 1959Q4 to 1999Q1; similarly, 1999Q2 estimate corresponds to estimating the models from 1959Q4 to 1999Q2. As can be seen, for the most part, the real-time estimates of the stars generally remain within the credible intervals, especially the 68% credible sets implied based on full sample information. The exception is the g-star, and in turn, the output gap, the latter shown in figure A3 of the appendix for brevity purpose. In the case of g-star, the real-time estimate, which before 2007 is not aware that the Great Recession (GR) is about to occur, is relatively upbeat like the survey estimate (at 2.9% vs. 2.25% for the final). Between 2007 and 2011, the real-time estimate gradually decelerates to 2.5%, but from thereon through 2015, it declines very rapidly, catching up to the final estimate.

Interestingly, the BC survey (which is real-time data) fell by only two-tenths over this period, but between 2015 and 2017, it dropped another three-tenths to 2.0% and remained at that level through the end of 2019. Whereas beyond 2017, the survey estimate remained flat, the real-time model estimate gradually moved back up partly in response to stronger realizations in real GDP growth than the implied g-star. The more gradual decline in the real-time g-star during the GR implies a larger (negative) output gap estimate than is indicated by the final estimate.

In the case of u-star, interestingly, in the first half of the forecast evaluation sample, the real-time estimate generally fell outside the 68% credible intervals but inside the 90% intervals. In contrast, in the second half, it remained inside the 68% intervals and tracked quite closely the posterior mean of the final estimate. In the case of p-star, the real-time posterior mean estimate largely remained inside the 68% intervals, and post-2007, the implied inference on p-star is consistent with the final estimate, as evident by similar contours of the real-time and final estimates. It is worth noting that both the real-time and final estimates of p-star are notably lower than the survey estimate of p-star; recall that the survey estimate of p-star is not used in the estimation of the Base model.

In the case of pi-star, the real-time estimate closely tracked the final estimate from 1999 through 2004, and from thereon through 2016, it averaged three tenths higher. From 2017 through 2019, the real-time estimate once again closely tracked the final estimate. The contours of the real-time and final estimates are similar, and the real-time estimate remained within the 90% credible intervals throughout the sample period analyzed. Consistent with a generally higher real-time estimate of p-star and pi-star than the final estimate, the real-time estimate of w-star is higher than the final. Just as in the case of p-star and pi-star, the contours of the real-time and final estimates of w-star are similar, and the real-time estimate of w-star remained within the 90% credible intervals. Also plotted are the implied survey estimates of the w-star, constructed by adding p-star and pi-star survey estimates. Arguably, these implied estimates are implausibly high given that the actual realizations of nominal wage inflation in the post-2007 period were mostly below these implied estimates. The results of a forecasting exercise presented in the appendix further confirm the implausibility of the implied survey estimate.

In the case of r-star, the contours of the real-time and final estimates are remarkably similar. Between 2000 and 2005, and post-2014, the real-time estimate closely tracked the final estimate. From 2006 through 2013, the real-time estimate averaged 35 basis points higher than the final estimate. In our assessment, the magnitude of the gap between real-time and final estimates is relatively small compared to the uncertainty estimate around the posterior mean and estimates of uncertainty typically reported in papers estimating r-star, e.g., Clark and Kozicki (2005), Laubach and Williams (2016), and Lubik and Matthes (2015). Furthermore, the real-time estimate of r-star remained within the 68% credible intervals throughout the sample period considered. The width of the estimated 68% (and 90%) intervals from the Base model has been remarkably stable between 0.9 and 1.2 percent (1.5 and 2.0 percent) in the last 25 years. For reference, the typical estimates of 90% bands from popular models such as LW and Lubik and Matthes (2015) have a width averaging more than 4% and 3.5%, respectively.[54] Given that the 68% and 90% credible intervals are significantly narrower compared to typical estimates reported elsewhere in the literature, we view the evidence of our real-time r-star remaining inside the estimated credible intervals as encouraging.

Overall, the real-time estimates of stars and forecast evaluation based on the past twenty years of data provide empirical evidence supporting the competitive forecasting and real-time properties of the Base model. Unfortunately, the high dimensionality of our models and the limited availability of real-time data on nominal wage inflation prevent the evaluation of models' forecasting properties over a more extended historical sample.

[54] We note that recent approaches to model r-star such as JM and Del Negro et al. (2017) also generate precise intervals similar to ours, with JM marginally less precise and Del Negro and all measurably more precise than ours.

6. The implications of COVID-19 Pandemic on Stars

At the time of writing this paper, the global economy is in the midst of an ongoing global pandemic crisis (GPC), which has continued to inflict significant disruption to economic activity both here in the US and globally. The GPC, which started in early 2020, contributed to extreme movements in many US macroeconomic indicators, including those used in this paper. For instance, the US real GDP growth in quarterly annualized term declined from -5% in Q1 to -31% in Q2, the deepest contraction in post-war data (COVID-19 recession). And in Q3, growth rebounded to +33%, a record increase in the post-war data. These extreme movements, which were several standard deviations away from their historical averages, contributed to the breakdown of many conventional time series models, especially the time-invariant VAR models estimated with monthly data, see Lenza and Primiceri (2020) and Carriero et al. (2021).

Up to this point, our analysis has focused on the pre-GPC data. In light of the recent work documenting the difficulties of the standard time-series models handling pandemic data, we are naturally curious to see how our two main models respond to the COVID-19 GPC data. What do data during the pandemic imply for the estimates of the stars, or, in other words, what are the estimated long-run consequences of the GPC data? As we illustrate shortly, the short answer to the first question is that both models, Base and Base-NoSurv, handled the pandemic data well; but the Base model, in our judgment, did a better job than the Base-NoSurv.

The answer to the second question is a bit complicated. But, briefly, the models indicate that, at the moment, the long-run consequences of the economic developments related to the pandemic are highly uncertain. We view this latter characterization as a reasonable one. Let's take long-term productivity growth. Based on past research, pandemics are associated with a notable hit to long-term productivity growth; think of disruptions to schools and universities, the loss of skilled and knowledgeable workers, and dramatic shifts in demand and supply that necessitate costly and time-consuming adjustments.[55] On the other hand, the current research argues that recent technological advances and the unique nature of the GPC – which has raised prospects of recurrent pandemics – will lead to an acceleration in automation (see Leduc and Liu, 2020) and, in turn, boost long-term productivity. The net effect of these opposing factors on p-star is uncertain, and our model-based estimates of p-star reflect this via increased assessment of uncertainty around p-star, as shown in the appendix A8.

We believe that the rich features of our models helped position our models, especially the Base model, to handle the pandemic data quite well.[56] In the interests of brevity, we refer to appendix A8 for the results comparing pre-pandemic and pandemic periods, and results comparing estimates from the Base model to outside sources including CBO and Morley and Wong (2020).

[55] Aucejo et al.(2020) document negative impact of the COVID-19 on the students' academic performance.

[56] The rich features include: (1) modeling the changing economic relationships via the implementation of time-varying parameters; (2) allowing for changing variance of the innovations to various equations (i.e., SV); (3) imposing bounds on some of the random walk processes; (4) joint modeling of the output gap and unemployment gap in particular; (5) and the use of survey forecasts;

7. Conclusion

This paper takes up the challenge of developing a large-scale UC model to jointly estimate the dynamics of inflation, nominal wages, labor productivity, the unemployment rate, real GDP, interest rates, and their respective survey expectations to back out the estimates of long-run counterparts of these variables. These long-run counterparts include potential output (gdp-star), the growth rate of potential output (g-star), the equilibrium level of the unemployment rate (u-star), the equilibrium real rate of interest (r-star), the trend in inflation (pi-star), the trend in labor productivity (p-star), and the trend in nominal wage inflation (w-star). The structure of our UC model is guided by economic theory and past empirical research. Past research has highlighted strong evidence of changing macroeconomic relationships and allowing for stochastic volatility in the shocks to cyclical components of a range of macroeconomic indicators. Accordingly, our model structure permits time-varying parameters and stochastic volatility in most model equations.

An essential feature of our model structure is the explicit role of the long-run survey forecasts in possibly informing the econometric estimation of the stars. Like other researchers, we find adding information from surveys to be an important element in yielding reasonable and credible estimates of the stars. Incorporating a rich set of empirical features leads to a very flexible but heavily parameterized model. To feasibly estimate this model (and its variants), we use Bayesian techniques, specifically the efficient sampling techniques developed in Chan, Koop, and Potter (2013), and the precision sampler proposed in Chan and Jeliazkov (2009).

We explore the empirical relevance of various features incorporated in our baseline model by estimating several variants of the baseline model. The Bayesian model comparison results provide strong support to model features informed based on past research and confirm findings documented elsewhere. For instance, we find that allowing for SV in the model equations to be very important. Similarly, we find economically and statistically significant evidence of time-varying price Phillips curve, wage Phillips curve, the evolving cyclicality of labor productivity, a changing passthrough relationship between wages and prices, and evolving persistence in price inflation and wage inflation gaps. Given the richness of our model, we document an expansive set of empirical results that we hope will prove helpful for both applied and theoretical macroeconomists alike.

The estimates of the stars from our modeling framework generally echo the contours of stars documented elsewhere in the literature utilizing smaller-scale models. However, they are more precise, a consequence of the use of surveys, a flexible multivariate approach, and jointly modeling the dynamics of several stars. We also show that our baseline model held up well when including the COVID-19 pandemic data. The rich set of features endowed in our UC model helped handle the pandemic data without any difficulties. Lastly, we document the competitive real-time forecasting properties of both our main model and, separately, the estimates of the stars, if they were to be used as steady-state values in external models.

Fig. 1. Visual Overview of Interactions Between Blocks

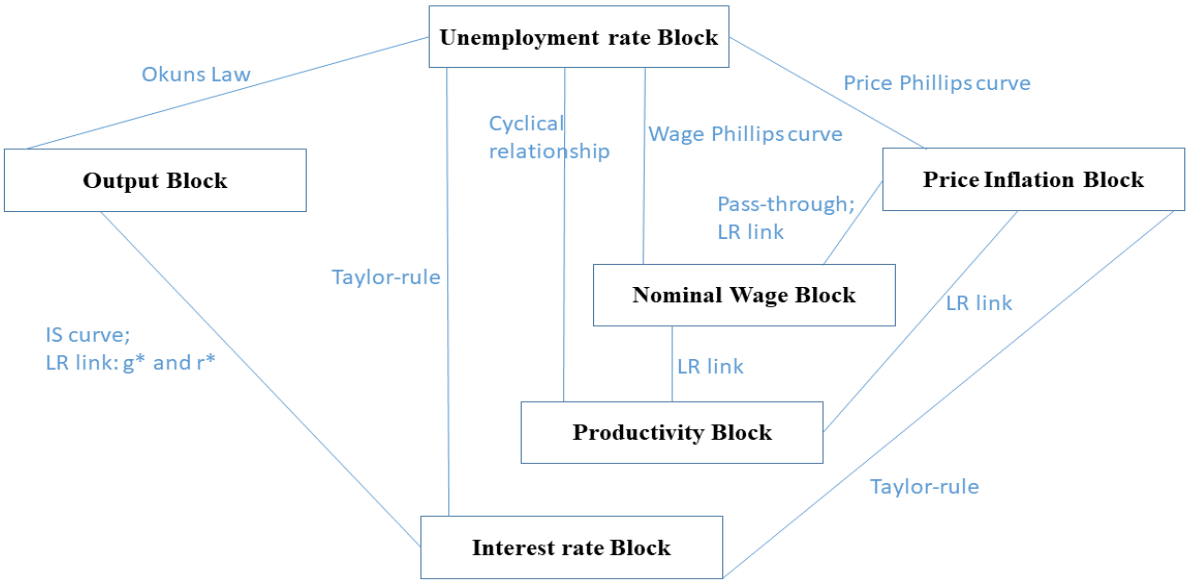

Notes: The solid lines represent contemporaneous relationship between the element(s) of the blocks. LR link denotes long-run relationship, i.e., link between stars.

Table 1: Description of Model Specifications

Panel (a): Main Models

Model	**Description**
Base	Full model as formulated in equations (6) through (39)
Base-NoSurv	Model as defined by baseline but excluding equations linking surveys to stars (i.e., excluding 9, 10, 15, 16, 26, 27, 38 and 39). Aim: assess the usefulness of survey data

Panel (b): Auxiliary Models

Base-W*RW	Base but replaces eq. (28) with a RW assumption for W^* as defined eq. (28b). Aim: assess the support for the theoretical restriction $W^* = \pi^* + P^*$
Base-PT-Wages-to-Prices	Base but replaces eq. (21) with eq. (21b) . Aim: asses the usefulness of allowing for pass-through from wages to prices (for reference, Base allows for pass-through from prices to wages)
Base-NoPT	Base but replaces eq. (29) with eq. (29b). Aim: assess the usefulness of inclusion of wage inflation in the price equation AND the inclusion of price inflation in the wage equation.
Base-NoSurv-NoPT	Base w/o surveys and replaces eq. (29) with eq. (29b). Aim: usefulness of inclusion of wage inflation in the price equation AND the inclusion of price inflation in the wage equation in a Base-NoSurv.
Base-P*CycOutputGap	Base but replaces eq. (17) with eq. (17b). Aim: assess empirical link between output gap and productivity gap and whether data support inclusion of output gap instead of unemployment gap.
Base-NoR*Surv	Base but excludes survey expectations of r^*; i.e., removes eq. (38) and eq. (39). Aim: assess specifically the marginal value of survey expectations of r^*
Base-NoR*Surv-NoTRule	Base but excludes (1) survey expectations of r^*, i.e., removes eq. (38) and eq. (39); and (2) policy rule eq. (34). Aim: assess the marginal value of the policy rule equation to the model.
Base-R*RW	Base but replaces eq.(36) and eq.(37) with a RW assumption for r^* as in eq. (36b). Aim: assess the support for the theoretical link between r^* and g^*.
Base-NoSurv-R*RW	Base-NoSurv but replaces eq.(36) and eq.(37) with a RW for r^* as in eq. (36b). Aim: assess support for the link between r^* and g^* in a spec. w/o survey data.
Base-R*AR	Base but replaces eq. (37) with AR assumption for D. Aim: support of r^* defined as comb. of permanent and transitory components.
Base-NoSurv-R*AR	Base-NoSurv but replaces eq. (37) with AR assumption for D Aim: support of r^* defined as comb. of permanent and transitory components.
Base-NoSurv-R*TightPrior	Base specification but tighter prior for std. of the shock to process D. Aim: assess the impact on r^* estimate of using a tighter prior for D.
Base-NoSV	Base specification but with no SV in any of the measurement equations. Aim: assess the importance of stochastic volatility in shock variances.
Base-NoBoundU*	Base specification without the bounds on the U^* process in eq. (8). Aim: assess empirical support for imposing bounds on U^*.

Table 2: Parameter Estimates

Parameter	Parameter description	Posterior estimates					
		Base			Base-NoSurv		
		Mean	5%	95%	Mean	5%	95%
a^r	Coefficient on interest-rate gap	-0.069	-0.141	0.002	-0.054	-0.130	0.015
$\rho_1^g + \rho_2^g$	Persistence in output gap	0.738	0.678	0.797	0.732	0.669	0.794
ρ_1^u	Lag 1 coefficient on UR gap	1.283	1.238	1.327	1.277	1.232	1.322
ρ_2^u	Lag 2 coefficient on UR gap	-0.504	-0.542	-0.466	-0.503	-0.540	-0.466
$\rho_1^u + \rho_2^u$	Persistence in UR gap	0.778	0.736	0.821	0.774	0.733	0.814
ρ^p	Persistence in productivity gap	-0.005	-0.118	0.110	-0.001	-0.119	0.115
$m = \frac{\zeta}{4}$	Relationship between r* and g*	0.701	0.621	0.784	0.390	0.270	0.560
ρ^i	Persistence in interest-rate gap	0.879	0.838	0.917	0.860	0.816	0.904
λ^i	Interest rate sensitivity to UR gap	-0.229	-0.278	-0.180	-0.243	-0.293	-0.194
κ^i	Interest rate sensitivity to inflation	0.061	0.014	0.107	0.085	0.035	0.134
λ^g	Output gap response to UR gap	-0.457	-0.580	-0.339	-0.454	-0.575	-0.333
ϕ^u	UR gap response to Output gap	-0.108	-0.130	-0.086	-0.118	-0.140	-0.096
$\frac{(1-\rho_1^u-\rho_2^u)}{\phi_u}$	Implied Okuns Law	-2.054	-2.327	-1.803	-1.929	-2.179	-1.699
β^g	Link between g* and survey	0.929	0.774	1.082	—	—	—
β^u	Link between u* and survey	0.988	0.919	1.055	—	—	—
β^r	Link between r* and survey	1.018	0.923	1.117	—	—	—
β^π	Link between π^* and survey	0.991	0.912	1.070	—	—	—
$\sigma^2_{\pi^*}$	Variance of the shocks to π^*	0.121^2	0.100^2	0.141^2	0.127^2	0.084^2	0.182^2
$\sigma^2_{p^*}$	Variance of the shocks to p^*	0.145^2	0.111^2	0.183^2	0.141^2	0.109^2	0.176^2
$\sigma^2_{u^*}$	Variance of the shocks to u^*	0.075^2	0.064^2	0.089^2	0.084^2	0.071^2	0.100^2
$\sigma^2_{gdp^*}$	Variance of the shocks to gdp^*	0.018^2	0.014^2	0.021^2	0.021^2	0.016^2	0.026^2
σ^2_d	Variance of the shocks to d	0.093^2	0.077^2	0.110^2	0.114^2	0.084^2	0.148^2
$\sigma^2_{w^*}$	Variance of the shocks to w^*	0.158^2	0.112^2	0.215^2	0.158^2	0.111^2	0.220^2
σ^2_{ogap}	Variance of the shocks to Output gap	0.725^2	0.672^2	0.781^2	0.723^2	0.669^2	0.780^2
σ^2_u	Variance of the shocks to UR gap	0.268^2	0.248^2	0.289^2	0.265^2	0.245^2	0.286^2
σ^2_{hp}	Var. of the Volatility – Productivity eq.	0.274^2	0.219^2	0.336^2	0.273^2	0.220^2	0.335^2
σ^2_h	Var. of the Volatility – Price Inf. eq.	0.297^2	0.237^2	0.364^2	0.298^2	0.238^2	0.365^2
σ^2_{hw}	Var. of the Volatility – Wage Inf. eq.	0.301^2	0.237^2	0.374^2	0.303^2	0.239^2	0.373^2
σ^2_{hi}	Var. of the Volatility – Interest rate eq.	0.377^2	0.293^2	0.469^2	0.369^2	0.287^2	0.454^2
$\sigma^2_{\lambda\pi}$	Var. of the shocks to TVP λ^π	0.041^2	0.032^2	0.052^2	0.041^2	0.032^2	0.051^2
$\sigma^2_{\lambda w}$	Var. of the shocks to TVP λ^w	0.041^2	0.032^2	0.051^2	0.040^2	0.032^2	0.050^2
$\sigma^2_{\lambda p}$	Var. of the shocks to TVP λ^p	0.044^2	0.034^2	0.057^2	0.045^2	0.034^2	0.057^2
$\sigma^2_{\kappa w}$	Var. of the shocks to TVP κ^w, PT	0.041^2	0.032^2	0.052^2	0.041^2	0.032^2	0.052^2
$\sigma^2_{\rho w}$	Var. of the shocks to TVP ρ^w	0.042^2	0.033^2	0.053^2	0.042^2	0.032^2	0.052^2
$\sigma^2_{\rho\pi}$	Var. of the shocks to TVP ρ^π	0.048^2	0.037^2	0.062^2	0.047^2	0.036^2	0.060^2

Table 3: Bayesian Model Comparison: Main Models and selected variants

	Base	**Base-NoSurv**	Base-R*RW	Base-NoSurv-R*RW
MDD of Inflation	-366.6	-368.6	-366.8	-370.1
MDD of Productivity	-606.9	-607.1	-607.5	-607.4
MDD of Nominal Wage	-277.5	-274.3	-278.0	-274.9
MDD of Unemployment	-24.6	-21.7	-24.7	-21.8
MDD of Interest rate	-216.4	-222.0	-214.0	-215.6
MDD of GDP	-279.7	-279.1	-279.8	-279.5
MDD	-1771.7	-1772.8	-1770.8	-1769.3

Table 4: Model Comparison: Variants focused on Unemployment rate (UR)

	Base	Base-NoSurv	Base-NoBoundU*	Bivariate	Bivariate+Surv	CKP-Adj
MDD of UR	-24.6	-21.7	-25.0	-56.5	-46.5	-61.9

Table 5: Model Comparison: Variants focused on GDP

	Base	Base-NoSurv	Univariate	Bivariate	Bivariate+Surv
MDD of GDP	-279.7	-279.1	-296.5	-280.4	-281.9

Table 6: Model Comparison: Variants focused on labor productivity

	Base	Base-NoSurv	Base-W*RW	Base-P*CycOutputGap	Base-NoSV
MDD of Productivity	-606.9	-607.1	-603.5	-608.1	-633.4
MDD of model	-1771.7	-1772.8	-1790.8	-1773.8	-2024.3

Table 7: Model Comparison: Variants focused on nominal wages

	Base	Base-NoSurv	Base-W*RW	Base-NoPT	Base-NoSV
MDD of Nominal wages	-277.5	-274.3	-277.7	-281.5	-344.3
MDD of model	-1771.7	-1772.8	-1790.8	-1776.3	-2024.3

Fig. 2. Full Sample Estimates for Unemployment rate block

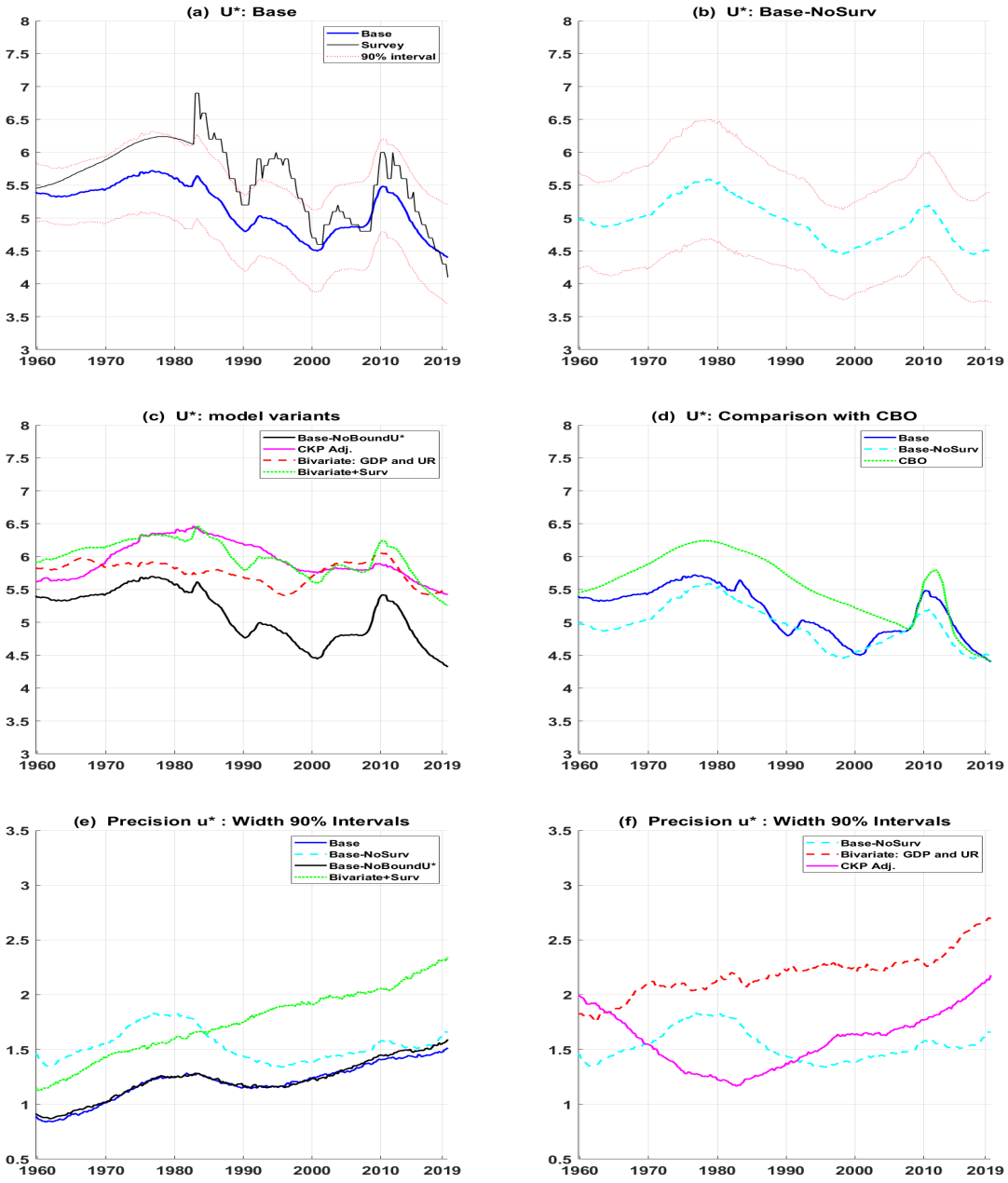

Notes: The posterior estimates are based on the full sample (from 1959Q4 through 2019Q4). In panel (e), CKP Adj. refers to the bivariate model of inflation and the unemployment rate as in CKP but with no bounds on pi-star.

Fig. 3. Full Sample Estimates for Cyclical Unemployment

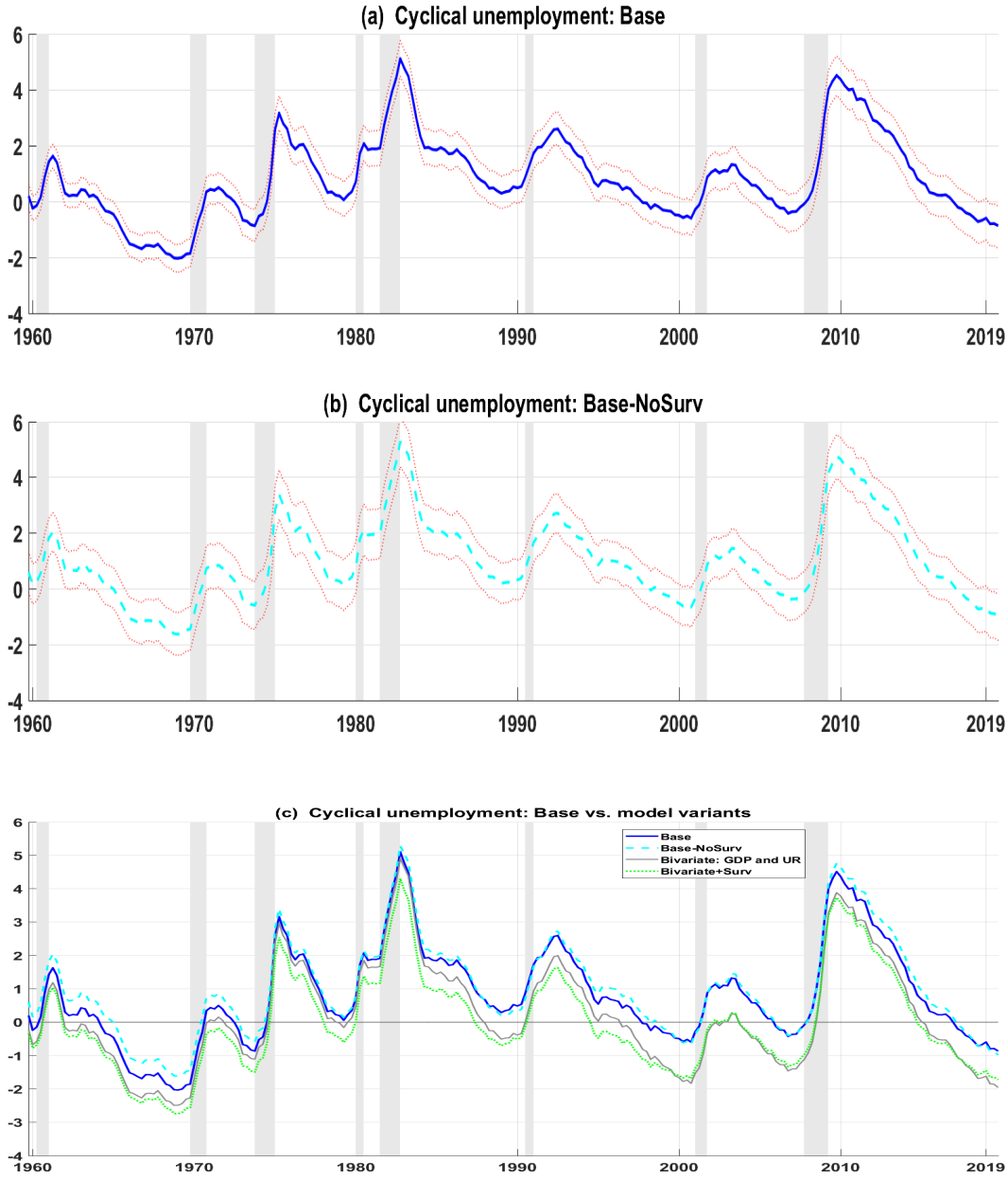

Notes: The posterior estimates are based on the full sample (from 1959Q4 through 2019Q4). The shaded areas represent the NBER recession dates.

Fig. 4. Full Sample Estimates for Output block

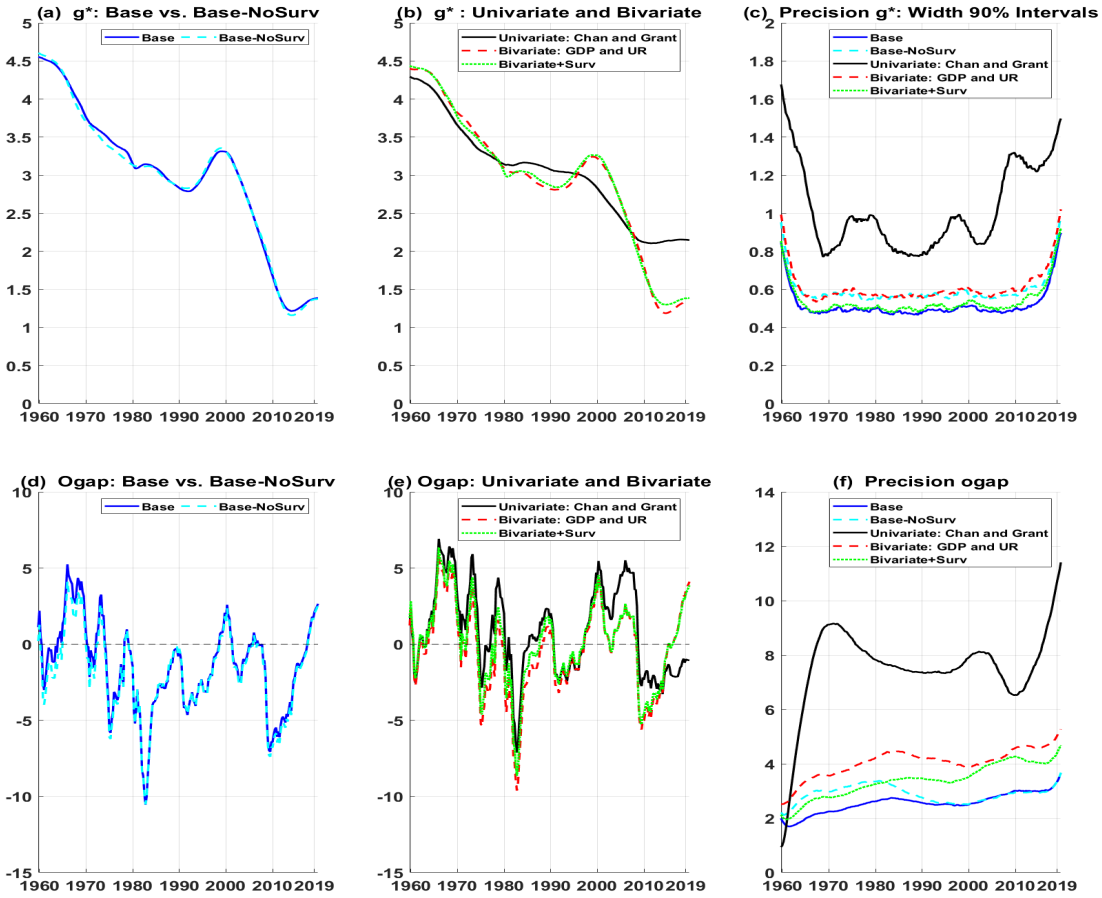

Fig. 5. Model-based output gap vs. CBO

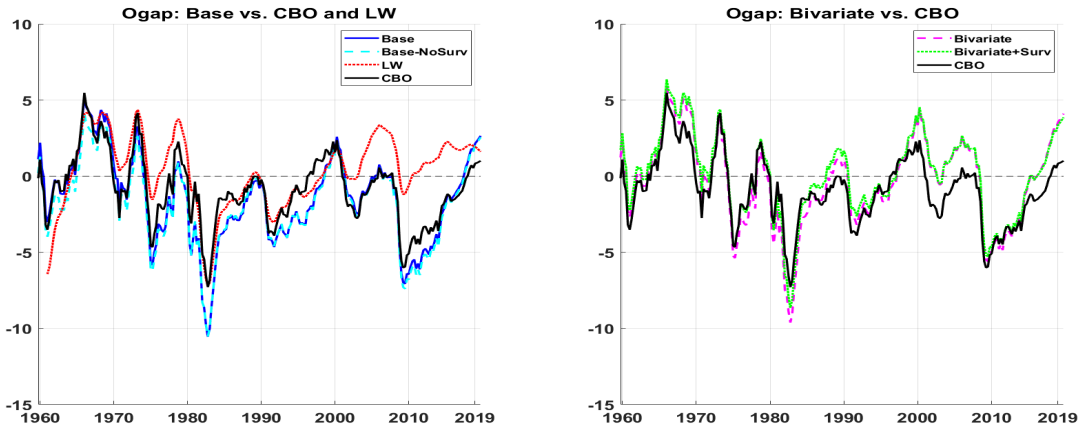

Fig. 6. Full Sample Estimates for Productivity block

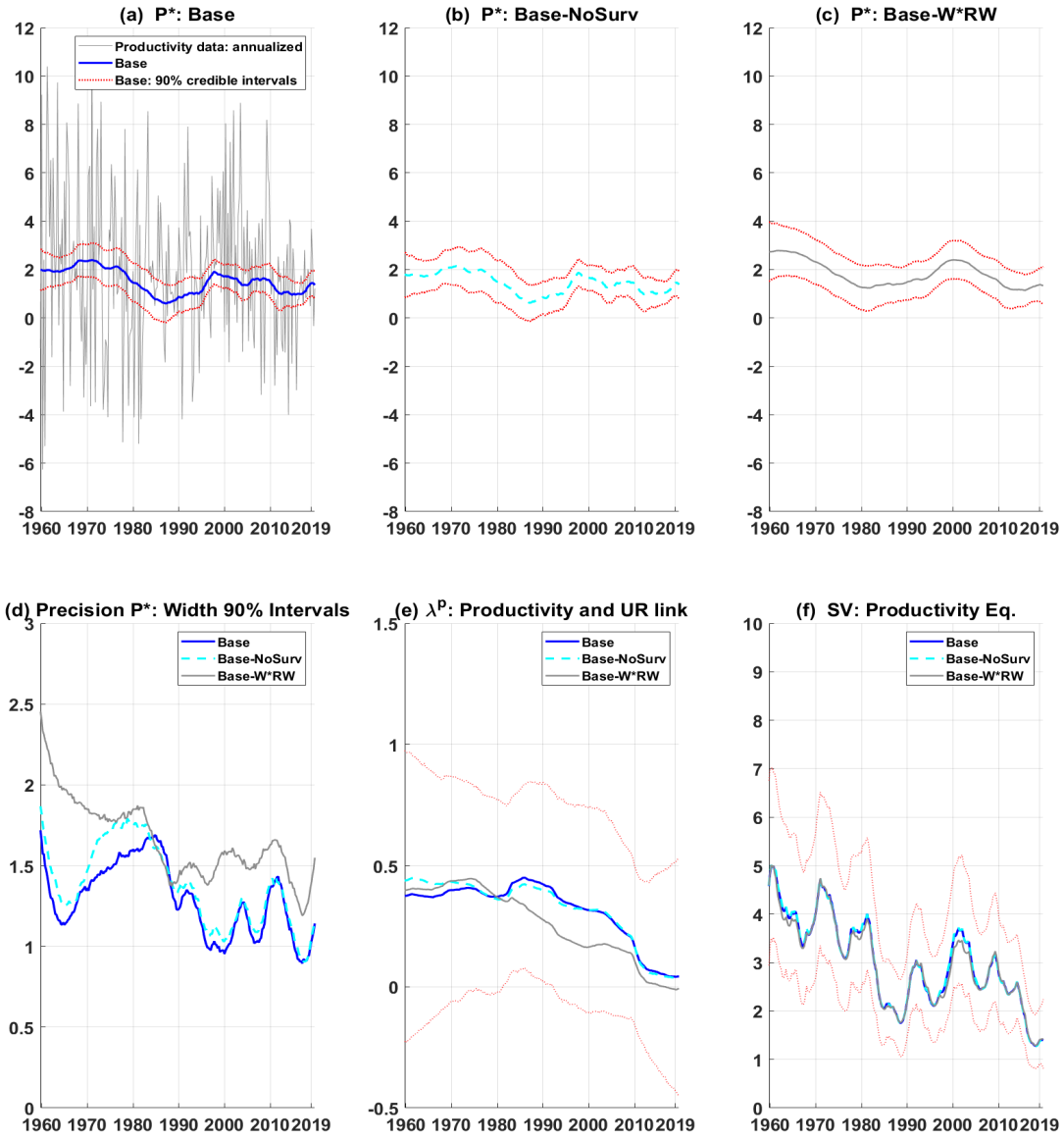

Notes: The posterior estimates are based on the full sample (from 1959Q4 through 2019Q4).

Fig. 7. Full Sample Estimates for Price inflation block

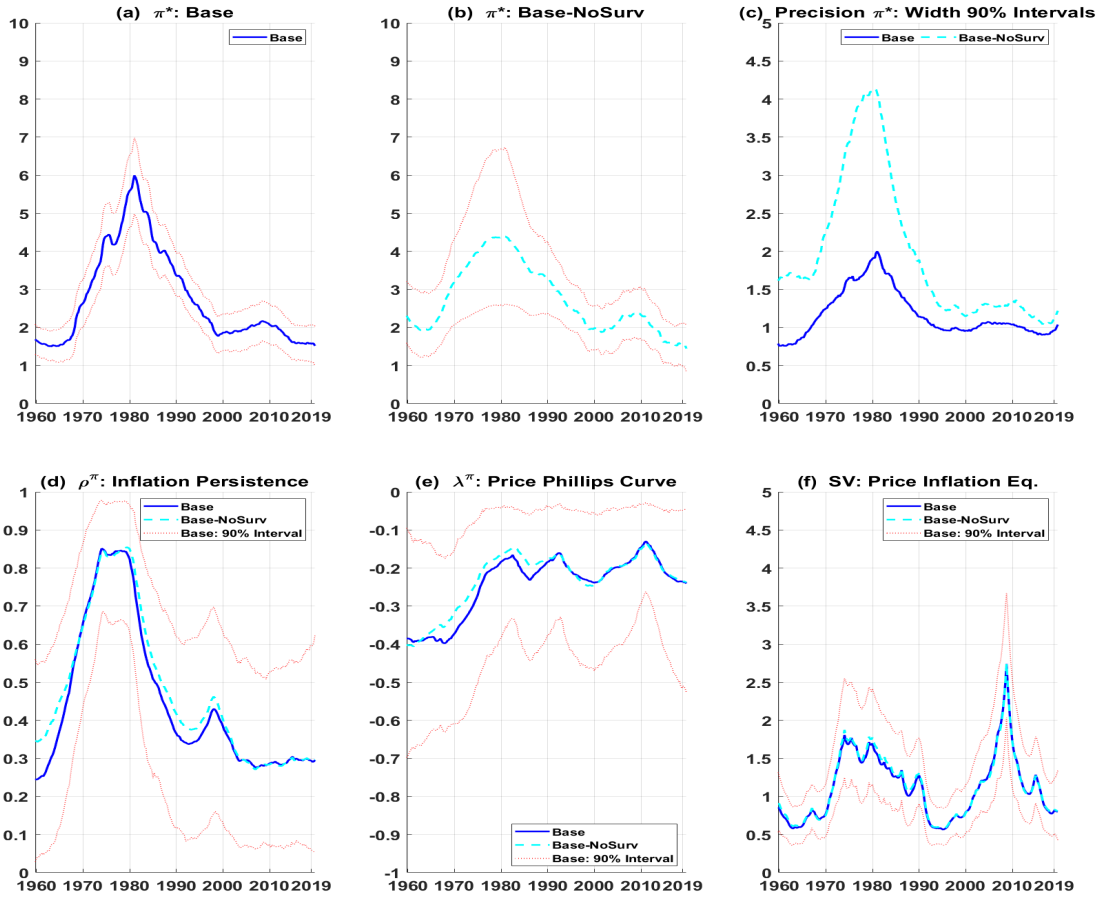

Notes: The posterior estimates are based on the full sample (from 1959Q4 through 2019Q4).

Table 8: Model variants for price inflation

Model variant	MDD of Price inflation	MDD Model
Base	-366.6	-1771.7
Base-NoSurv	-368.6	-1772.8
Base-W*RW	-367.0	-1790.8
Base-PT-Wages-to-Prices	-366.7	-1771.4
Base-NoPT	-365.2	-1776.3
Base-NoSV	-413.9	-2024.3

Fig. 8. Full Sample Estimates for Nominal Wage block

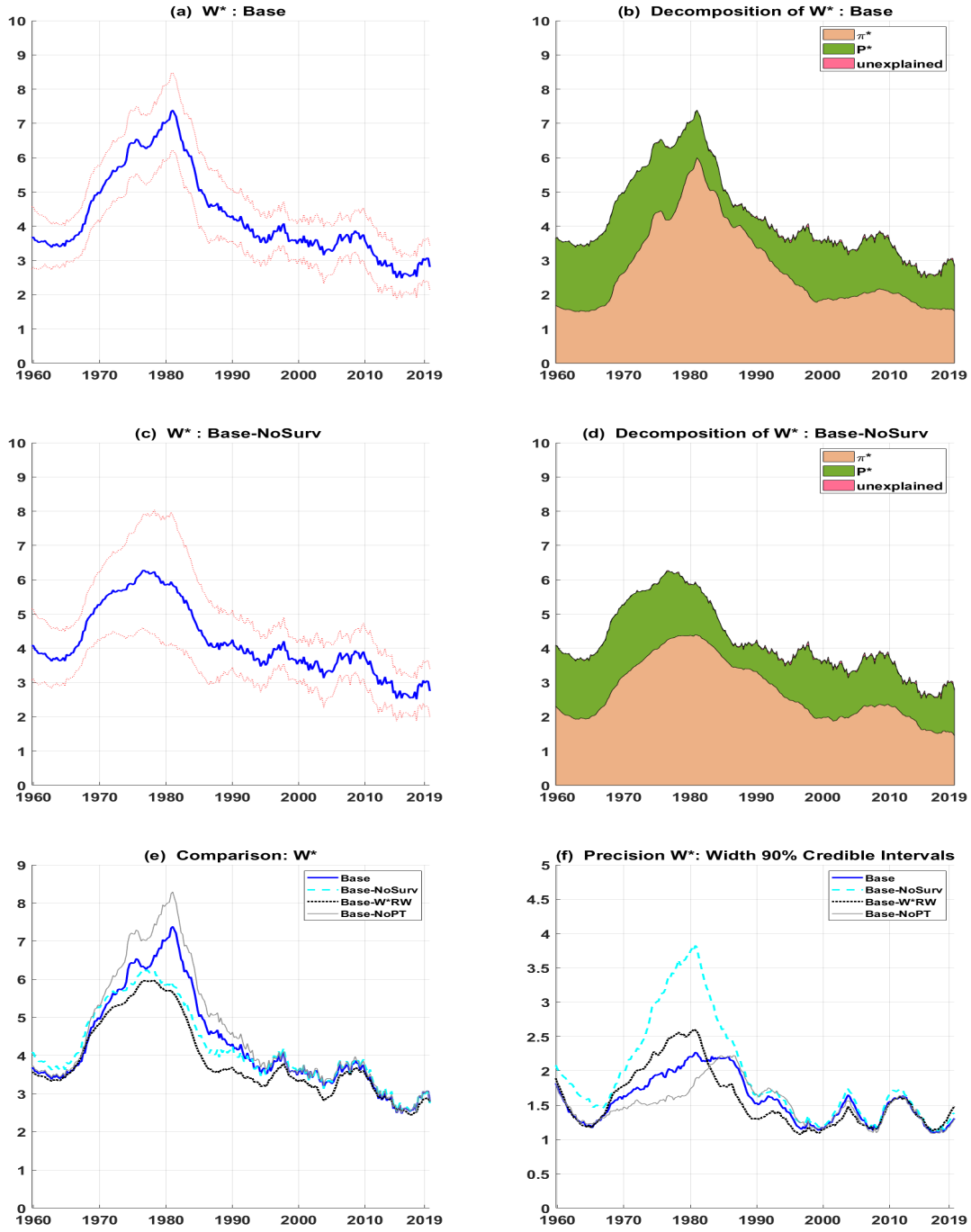

Notes: The posterior estimates are based on the full sample (from 1959Q4 through 2019Q4).

Fig. 9. Wage Persistence, Wage Phillips Curve, Passthrough from Prices, and SV

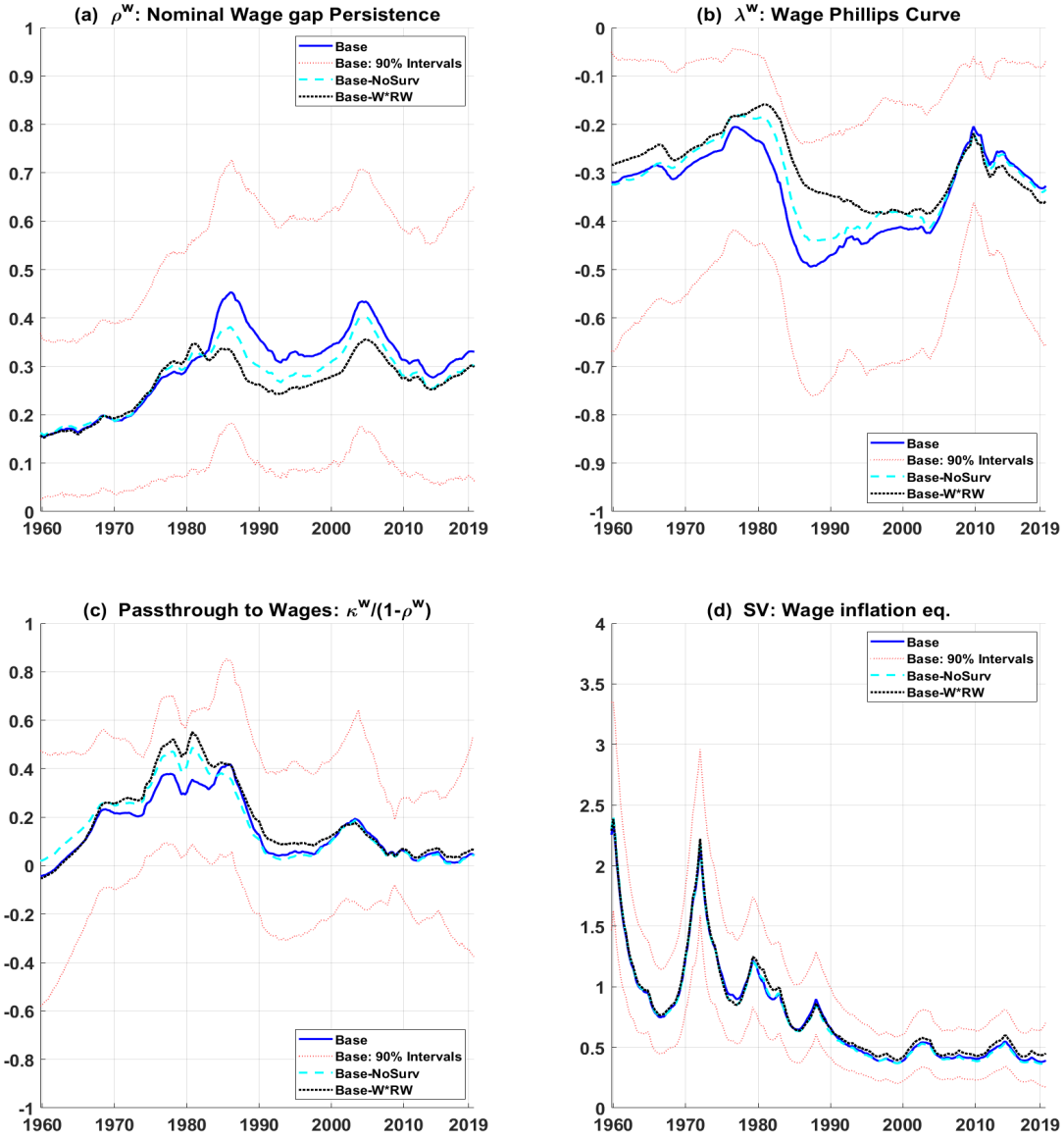

Notes: The posterior estimates are based on the full sample (from 1959Q4 through 2019Q4).

Fig. 10. Full Sample Estimates for interest rate block

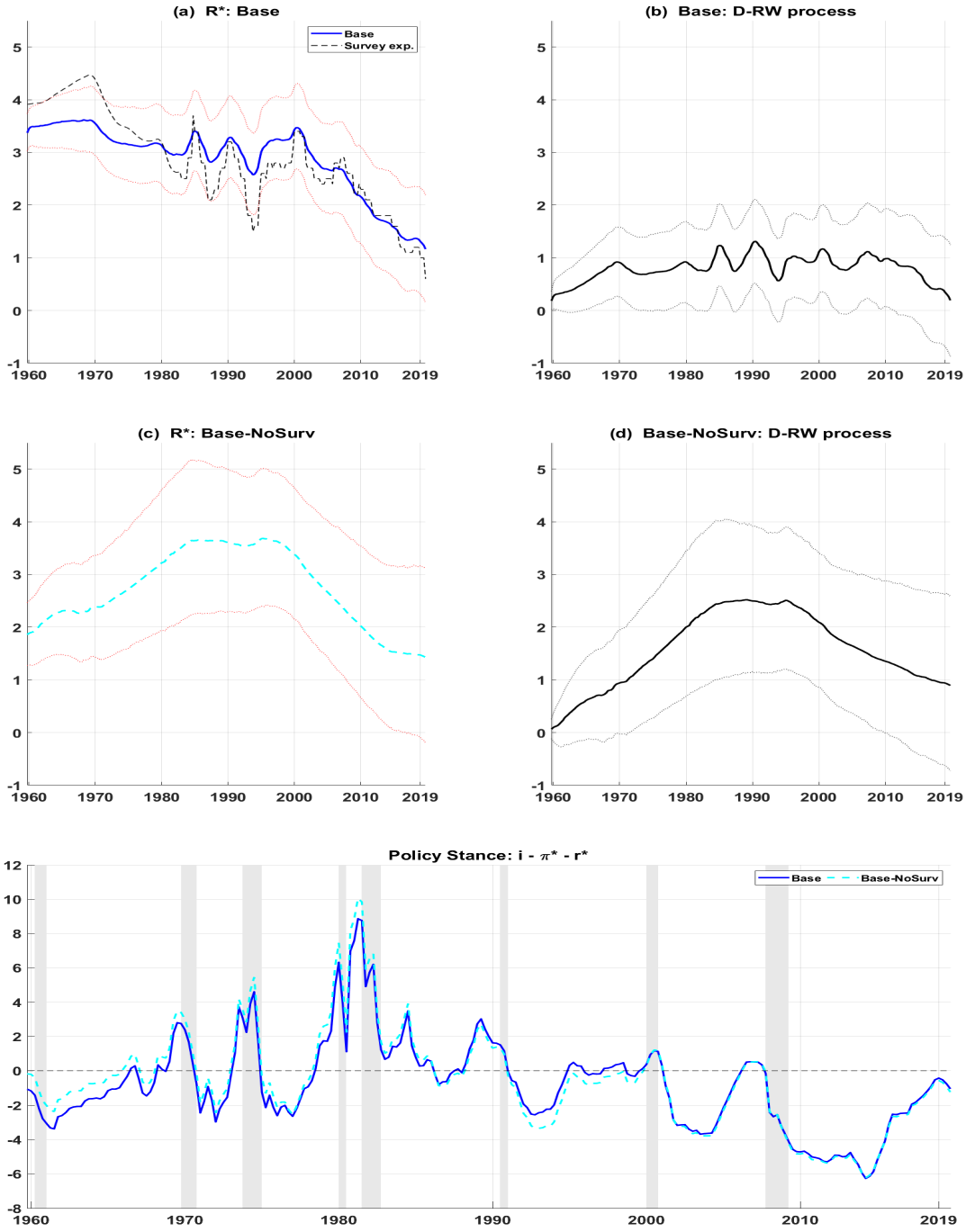

Notes: The posterior estimates are based on the full sample (from 1959Q4 through 2019Q4). In top panel, the plot labeled "survey exp." is an implied estimate: inferred from the Blue Chip survey long-run estimates of GDP deflator and short-term interest rates (3-month Treasury bill) using the long-run Fisher equation. Specifically, the long-run forecast of 3-month Treasury bill less the long-run forecast of GDP deflator. To this differential, we add +0.3 to reflect the average differential between the federal funds rate and the 3-month Treasury bill.

Fig. 11. More Estimates for interest rate block

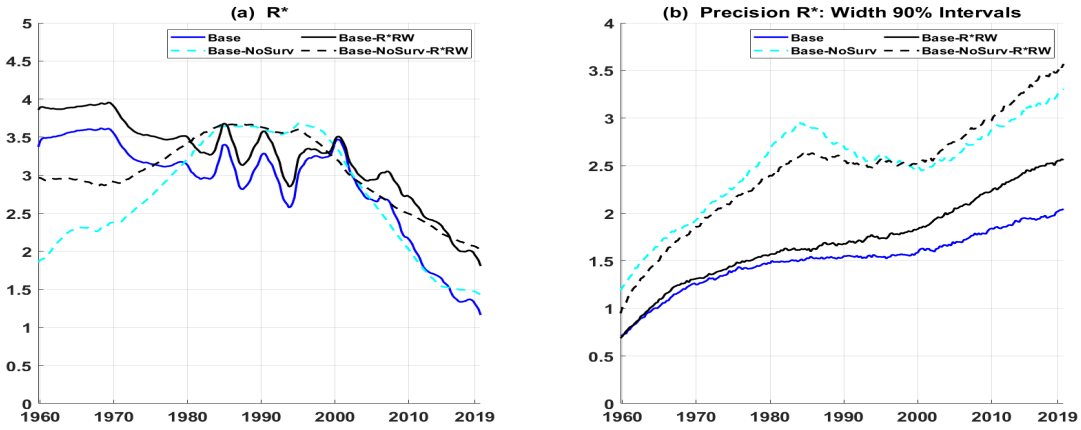

Table 9: Model variants for interest rate

Model variant	MDD of Interest rate	MDD Model
Base	-216.4	-1771.7
Base-NoSurv	-222.0	-1772.8
Base-R*RW	-214.0	-1770.8
Base-NoSurv-R*RW	-215.6	-1769.3
Base-NoSurv-R*TightPrior	-232.0	-1773.6

Fig. 12. Real-time Recursive Estimates of Stars: Base model

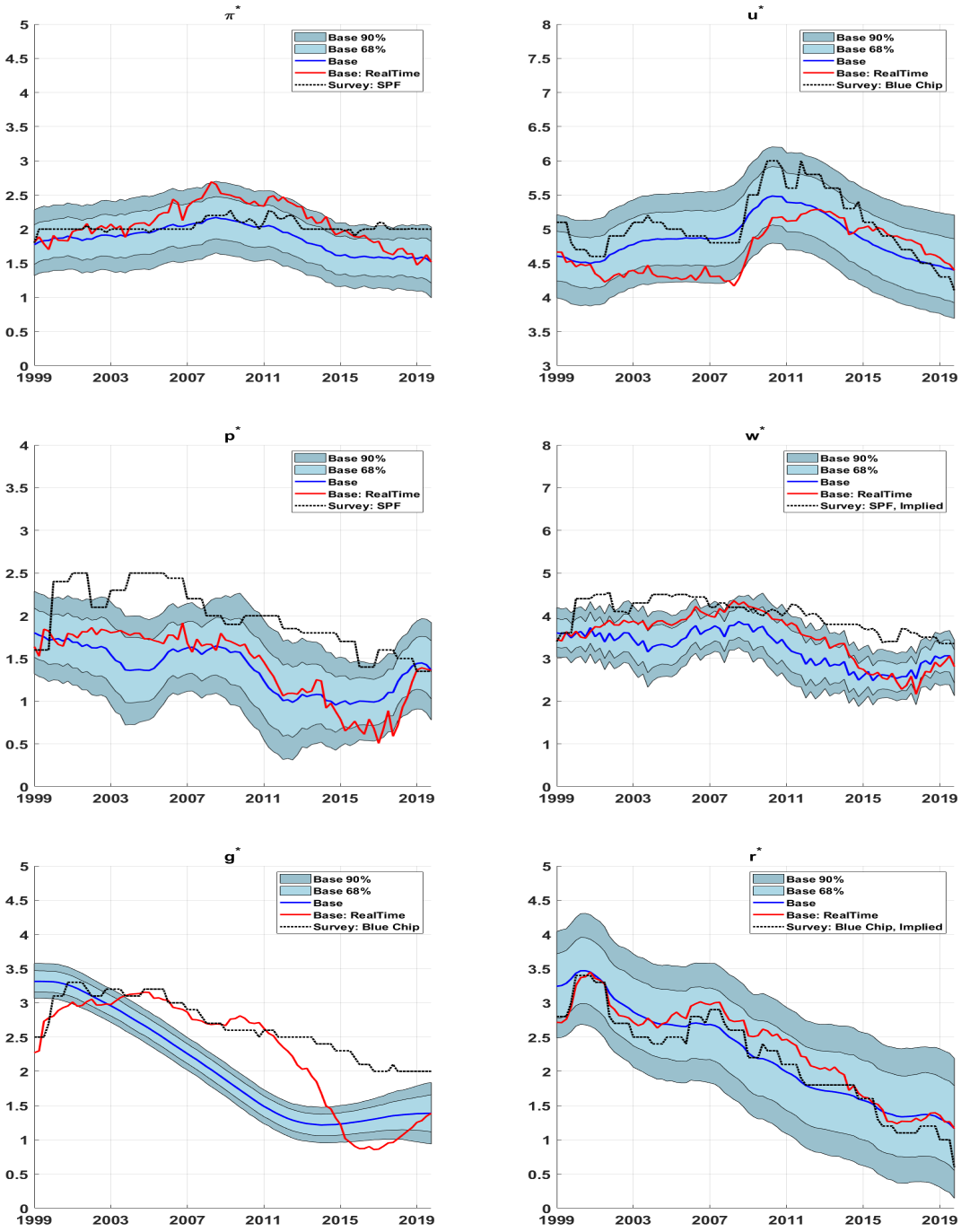

Notes: The plots labeled Base are posterior estimates reflecting information in the full sample (from 1959Q4 through 2019Q4). The plots labeled Base:RealTime are posterior estimates reflecting information available at a given point in time (i.e., truly real-time).

Table 10: Real-Time Forecasting Accuracy: Base vs. Base-NoSurv

Panel A: Point Forecast Accuracy (Recursive evaluation: 1999.Q1-2019.Q4)

Relative RMSE: RMSE **Base** / RMSE **BaseNoSurv**

	h=4Q	h=8Q	h=12Q	h=16Q	h=20Q
Real GDP	1.07*	1.03	1.01	1.00	0.99
PCE Inflation	0.96	0.94*	0.91*	0.89	0.88*
Productivity	0.98*	0.98	0.97	0.98*	0.97
Nominal Wage (AHE)	0.98	1.01	1.05	1.05	1.02
Unemployment Rate	1.07*	1.05*	1.03*	1.02*	1.00
Shadow FFR	0.98	1.00	1.00	0.99	0.98

Panel B: Density Forecast Accuracy (Recursive evaluation: 1999.Q1-2019.Q4)

Relative Log Predictive Score (LPS): LPS Base - LPS BaseNoSurv

	h=4Q	h=8Q	h=12Q	h=16Q	h=20Q
Real GDP	-0.003*	-0.002*	-0.002*	-0.001*	-0.001*
PCE Inflation	0.018*	0.020*	0.025*	0.027*	0.026*
Productivity	0.001	0.002*	0.002*	0.002*	0.003*
Nominal Wage (AHE)	0.017*	0.016*	0.018*	0.018*	0.019*
Unemployment Rate	-0.003	0.005	0.009*	0.012*	0.013*
Shadow FFR	0.020*	0.007*	0.003	0.000	0.000

Notes for Table: The top panel compares the point forecast accuracy of Base model with Base-NoSurv model. The numbers less than 1 indicates that Base model is more accurate on average. The bottom panel reports the corresponding density forecast accuracy performance. A positive value (for the relative mean predictive log score) suggests that Base model is on average more accurate. The log predictive scores are computed using parametric normal approximation. The table reports statistical significance based on the likelihood-ratio test of Amisano and Giacomini (2007) for the density forecast accuracy, and based on the Diebold-Mariano and West test (with the lag $h-1$ truncation parameter of the HAC variance estimator) for the point forecast accuracy. The test statistics for likelihood-ratio test use two-sided t-test. In the case of the Diebold-Mariano and West test, the test statistics use two-sided standard normal critical values for horizons less than equal to 8 quarters, and two-sided t-statistics for horizons greater than 8 quarters. *up to 10% significance level.

References

[1] Amisano, Gianni, & Raffaella Giacomini (2007). Comparing density forecasts via weighted likelihood ratio tests. *Journal of Business and Economic Statistics*, 25(2), 177-190

[2] Antolin-Diaz, Juan, Drechsel, Thomas, & Ivan Petrella (2017). Tracking the slowdown in long-run GDP growth. *Review of Economics and Statistics*, 99(2): 343–356

[3] Ashley, Richard, Tsang, Kwok P., & Randal J. Verbrugge (2020). A new look at historical monetary policy (and the Great Inflation) through the lens of a persistence-dependent policy rule. *Oxford Economic Papers*, 72(3): 672–691

[4] Ashley, Richard, & Randal J. Verbrugge (2009). Frequency dependence in regression model coefficients: an alternative approach for modeling nonlinear dynamic relationships in time series. *Econometric Reviews*, 28(1–3): 4–20

[5] Ashley, Richard, & Randal J. Verbrugge (2020). Finding a stable Phillips curve relationship: A persistence-dependent regression model. Federal Reserve Bank of Cleveland, Working Paper no. 19-09R

[6] Aucejo, Esteban M., French, Jacob, Araya, Maria P.,& Basit Zafar (2020). The impact of COVID-19 on student experiences and expectations: evidence from a survey. *Journal of Public Economics*, 191: 104271. https://doi.org/10.1016/j.jpubeco.2020.104271.

[7] Banbura, Marta, & Elena Bobeica (2020). Does the Phillips curve help to forecast euro area inflation? European Central Bank Working Paper Series No 20202471

[8] Barbarino, Alessandro, Berge, Travis J., Chen, Han, & Andrea Stella (2020). Which output gap estimates are stable in real time and why? Finance and Economics Discussion Series 2020-102. Washington: Board of Governors of the Federal Reserve System

[9] Barnichon, Regis., & Geert Mesters (2018). On the demographic adjustment of unemployment. *Review of Economics and Statistics*, 100: 219-231.

[10] Basistha, Arabinda, & Charles R. Nelson (2007). New measures of the output gap based on the forward-looking new Keynesian Phillips curve. *Journal of Monetary Economics*, 54:498-511.

[11] Bauer, Michael D., & Glenn D. Rudebusch (2020). Interest rates under falling stars. *American Economic Review*, 110(5): 1316:1354.

[12] Benati, Luca (2007). Drift and breaks in labor productivity. *Journal of Economic Dynamics & Control*, 31(8): 2847-2877.

[13] Berger, Tino, Evaraert, Gerdie, & Hauke Vierke (2016). Testing for time variation in an unobserved components model for the U.S. economy. *Journal of Economic Dynamics & Control*, 179-208.

[14] Beveridge, Stephen, & Charles R. Nelson (1981). A new approach to decomposition of economic time series into permanent and transitory components with particular attention to measurement of the business cycle. *Journal of Monetary Economics*, 7:151-174

[15] Beyer, Robert C.M., & Volker Wieland. (2019). Instability, imprecision and inconsistent use of equilibrium real interest rate estimates. *Journal of International Money and Finance*,

94:1–14

[16] Bobeica, Elena., Ciccarelli, Matteo, & Isabel Vansteenkiste (2019). The link between labor cost and price inflation in the euro area. European Central Bank Working Paper 2235

[17] Brand, Claus, & Falk Mazelis. (2019). Taylor-rule consistent estimates of the natural rate of interest. European Central Bank Working Paper 2257

[18] Carriero, Andrea, Clark, Todd E., & Massimiliano Marcellino (2019). Large Bayesian vector autoregressions with stochastic volatility and non-conjugate priors. *Journal of Econometrics*, 212: 137–154, https://doi.org/10.1016/j.jeconom.2019.04.024

[19] Carriero, Andrea, Clark, Todd E., Marcellino, Massimiliano, & Elmar Mertens (2021). Addressing COVID-19 outliers in BVARs with stochastic volatility. Federal Reserve Bank of Cleveland, Working Paper No.21-02. https://doi.org/10.26509/frbc-wp-202102

[20] Chan, Joshua (2013). Moving average stochastic models with application to inflation forecast. *Journal of Econometrics*, 176: 162-172

[21] Chan, Joshua (2017). The stochastic volatility in mean model with time-varying parameters: An application to inflation modeling. *Journal of Business & Economic Statistics*, 35(1): 17-28

[22] Chan, Joshua (2019). Large Hybrid Time-Varying Parameter VARs. CAMA paper 77

[23] Chan, Joshua, Clark, Todd E., & Gary Koop (2018). A new model of inflation, trend inflation, and long-run inflation expectations. *Journal of Money, Credit, and Banking*, 50(1): 5-53

[24] Chan, Joshua, & Eric Eisenstat (2018a). Comparing hybrid time-varying parameter VARs. *Economics Letters*, 171:1-5

[25] Chan, Joshua, & Eric Eisenstat (2018b). Bayesian model comparison for time-varying parameter VARs with stochastic volatility. *Journal of Applied Econometrics*, 33(4): 509-532

[26] Chan, Joshua, & Angelia L. Grant (2017). A Bayesian model comparison for trend-cycle decompositions of output. *Journal of Money, Credit and Banking* 49(2-3): 525-552

[27] Chan, Joshua, & Ivan Jeliazkov (2009). Efficient simulation and integrated likelihood estimation in state space models. *International Journal of Mathematical Modeling and Numerical Optimisation* 1: 101-120

[28] Chan, Joshua, Koop, Gary, & Simon M. Potter (2013). A new model of trend inflation. *Journal of Business and Economic Statistics* 31: 94-106

[29] Chan, Joshua, Koop, Gary, & Simon M. Potter (2016). A bounded model of time variation in trend inflation, NAIRU and the Phillips curve. *Journal of Applied Econometrics* 31: 551-565

[30] Christiano, Lawrence J., & Terry J. Fitzgerald (2003). The band pass filter. *International Economic Review* 44:435-465

[31] Clark, Peter K. (1987). The Cyclical component of U.S. economic activity. *Quarterly Journal of Economics*, 10(4): 797-814

[32] Clark, Todd E. (2014). The importance of trend inflation in the search for missing disin-

flation. Federal Reserve Bank of Cleveland *Economic Commentary*, No. 2014-16

[33] Clark, Todd E., & Taeyoung Doh (2014). Evaluating alternative models of trend inflation. *International Journal of Forecasting* 30: 426-448

[34] Clark, Todd E., & Sharon Kozicki (2005). Estimating equilibrium real interest rates in real time. *North American Journal of Economics and Finance* 16: 395-413

[35] Cogley, Timothy, Primiceri, Giorgio, & Thomas J. Sargent (2010). Inflation-gap persistence in the U.S. *American Economic Journal: Macroeconomics* 2: 43-69

[36] Coibion, Olivier, Gorodnichenko, Yuriy, & Mauricio Ulate (2018). The cyclical sensitivity in estimates of potential output. *Brookings Papers on Economic Activity*, Fall 2018

[37] Cross, Rod, Darby, Julia, & Jonathan Ireland (2005). Uncertainties surrounding natural rate estimates in the G7. *Advances in Computational Economics*, Quantitative Economic Policy Vol 20: 337-361

[38] Crump, Richard K., Eusepi, Stefano, Giannoni, Marc, & Aysegul Sahin (2019). A unified approach to measuring u*. *Brookings Papers on Economic Activity*

[39] Daly, Mary, & Bart Hobijn (2014). Downward nominal wage rigidities bend the Phillips curve *Journal of Money, Credit and Banking* 46(2): 51-93

[40] Daly, Mary, Hobijn, Bart, Sahin, Ayse, & Rob G. Valletta (2012). A search and matching approach to labor markets: did the natural rate of unemployment rise?. *Journal of Economic Perspectives* 26: 3-26

[41] Davis, Steven J., Faberman, Jason R., & John Haltiwanger (2013). The establishment-level behavior of vacancies and hiring. *Quarterly Journal of Economics* 128(2): 581-622

[42] Del Negro, Marco, Giannoni, Marc, & Frank Schorfheide (2015). Inflation in the great recession and New Keynesian models. *American Economic Journal: Macroeconomics*, 7:168-196

[43] Del Negro, Marco, Giannone, Domenico, Giannoni, Marc, & Andrea Tambalotti (2017). Safety, liquidity, and the natural rate of interest. *Brookings Papers on Economic Activity*

[44] Del Negro, Marco, Giannoni, Marc, Lenza, Michele, & Andrea Tambalotti (2020). What's up with the Phillips curve?. *Brookings Papers on Economic Activity*

[45] Edge, Rochelle M., Laubach, Thomas & John C. Williams (2007). Learning and shifts in long-run productivity growth. *Journal of Monetary Economics* 54: 2421-2438

[46] Eggertsson, Gauti B., Mehrotra, Neil R., Singh, Sanjay R., and Lawrence H. Summers (2016). A Contagious malady? Open economy dimensions of secular stagnation. *IMF Economic Review* 64 (4): 581–634

[47] Faust, Jon, & Jonathan Wright (2013). Forecasting inflation. *In Handbook of Economic Forecasting*, Vol. 2, edited by Graham Elliot and Allan Timmermann, pp: 3-56

[48] Fernald, John G. (2007). Trend breaks, long-run restrictions, and contractionary technology improvements. *Journal of Monetary Economics*, 54(8): 2467-2485

[49] Fernald, John G.& Christina Wang (2016). Why has the cyclicality of productivity changed? What does it mean? *Annual Review of Economics*, 8(1): 465–96

[50] Fernandez-Villaverde, Jesus, & Juan Rubio-Ramirez (2010). Macroeconomics and volatility: data, models, and estimation. NBER Working Papers, 16618, DOI 10.3386/w16618

[51] Fleischman, Charles A., & John M. Roberts (2011). From many Series, one cycle: improved estimates of the business cycle from a multivariate unobserved components model. Federal Reserve Board Working paper no 2011-46

[52] Gali, Jorda (2011). The return of the wage Phillips Curve. *Journal of the European Economic Association*, 9(3): 436-461

[53] Gali, Jorda, & Luca Gambetti (2019). Has the U.S. wage Phillips curve flattened? A semi-structural exploration. *NBER Working Paper series*, No. 25476

[54] Gali, Jorda, & Thijs van Rens (2020). The vanishing procyclicality of labour productivity. *The Economic Journal*, pp 1-25

[55] Garcia, Juan A., & Aubrey Poon (2018). Trend inflation and inflation compensation. IMF Working Paper series, WP/18/154

[56] Gonzalez-Astudillo, Manuel, & Jean-Philippe Laforte (2020). Estimates of r* consistent with a supply-side structure and a monetary policy rule for the U.S. economy. Finance and Economics Discussion Series Paper 2020-085.

[57] Grant, Angelia L., and Joshua Chan (2017). Reconciling output gaps: unobserved components model and Hodrick-Prescott filter. *Journal of Economic Dynamics and Control* 114-121

[58] Hamilton, James., Harris, Ethan, Hatzius, Jan, & Ken West (2016). The equilibrium real funds rate: past, present and future. *IMF Economic Review*, 64(4): 660-707.

[59] Harvey, David, Leybourne, Stephen, & Paul Newbold (1997). Testing the equality of prediction mean squared errors. *International Journal of Forecasting*, 13: 281-291.

[60] Hodrick, Robert J., & Edward C. Prescott (1997). Postwar US business cycles: an empirical investigation *Journal of Money, Credit and Banking*, 29:1-16.

[61] Holston, Kathryn, Thomas Laubach, & John Williams. (2017). Measuring the natural rate of interest: international trends and determinants. *Journal of International Economics*, 108: 59-75.

[62] Jacobs, Jan P.A.M., & Simon van Norden (2016). Why are initial estimates of productivity growth so unreliable? *Journal of Macroeconomics*, 47:200-213

[63] Johannsen, Benjamin K., & Elmar Mertens (2015).The shadow rate of interest, macroeconomic trends, and time-varying uncertainty. Unpublished manuscript

[64] Johannsen, Benjamin K., & Elmar Mertens (forthcoming). A time series model of interest rates with the effective lower bound. *Journal of Money, Credit, and Banking*

[65] Kahn, James A., & Robert W. Rich (2007). Tracking the new economy: Using growth theory to detect changes in trend productivity. *Journal of Monetary Economics* 54: 1670-1701

[66] Kamber, Gunes, Morley, James, & Benjamin Wong (2018). Intuitive and reliable estimates of the output gap from a Beveridge-Nelson filter. *Review of Economics and Statistics* 100(3):

550-566

[67] Kiley, Michael T. (2020). What can data tell us about the equilibrium real interest rate? *International Journal of Central Banking*, June 2020

[68] Knotek, Edward S. (2007). How useful is Okun's Law. Federal Reserve Bank of Kansas City *Economic Review*, Fourth Quarter 2007

[69] Knotek, Edward S. (2015). Difficulties forecasting wage growth. Federal Reserve Bank of Cleveland *Economic Trends*

[70] Knotek, Edward S., & Saeed Zaman (2014). On the relationships between wages, prices, and economic activity. Federal Reserve Bank of Cleveland *Economic Commentary*, No. 2014-14

[71] Koop, Gary, & Dimitris Korobilis (2010). Bayesian multivariate time series methods for empirical macroeconomics. *Foundations and Trends in Econometrics*, *3*, 267-358

[72] Kozicki, Sharon, & Peter A. Tinsley (2012). Effective use of survey information in estimating the evolution of expected inflation. *Journal of Money, Credit and Banking*, 44(1): 145-169

[73] Kuttner, Kenneth N. (1994). Estimating potential output as a latent variable. *Journal of Business and Economic Statistics*, 12(3): 361-368

[74] Laubach, Thomas (2001). Measuring the NAIRU: Evidence from seven economies. *The Review of Economics and Statistics* 83(2): 218-231

[75] Laubach, Thomas & John C. Williams (2003). Measuring the natural rate of interest. *The Review of Economics and Statistics*, 85(4): 1063-1070

[76] Laubach, Thomas & John C. Williams (2016). Measuring the natural rate of interest redux. *Business Economics*, 51(2): 57-67

[77] Leduc, Sylvain, & Zheng Liu. (2020). Can Pandemic-Induced Job Uncertainty Stimulate Automation? San Francisco Fed Working paper 2020-19

[78] Lee, Jaejoon & Charles R. Nelson (2007). Expectation horizon and the Phillips curve: the solution to an empirical puzzle. *Journal of Applied Econometrics* 22(1): 161-178

[79] Lewis, Kurt F. & Francisco Vazquez-Grande (2019). Measuring the natural rate of interest: A note on transitory shocks. *Journal of Applied Econometrics* 34: 425-436

[80] Lubik, Thomas A. & Christian Matthes (2015). Calculating the natural rate of interest: A comparison of two alternative approaches. *Richmond Fed Economic Brief*

[81] Lunsford, Kurt (2017). Productivity growth and real interest rates in the long run. Federal Reserve Bank of Cleveland *Economic Commentary*, No. 2017-20

[82] Lunsford, Kurt, & Kenneth D. West (2019). Some evidence on secular drivers of US safe real rates. *American Economic Journal: Macroeconomics*, AEA, 11(4): 113-139

[83] Mertens, Elmar (2016). Measuring the level and uncertainty of trend inflation. *The Review of Economics and Statistics*, 98: 950-967

[84] Mertens, Elmar, & James M. Nason (2020). Inflation and professional forecast dynamics: An evaluation of stickiness, persistence and volatility. *Quantitative Economics*, 11:1485-1520. https://doi.org/10.3982/QE980

[85] Mester, Loretta J. (2018). Demographics and their implications for the economy and policy. *Cato Journal*, 38(2): 399-413

[86] Morley, James (2002). A state-space approach to calculating the Beveridge-Nelson decomposition. *Economics Letters*, 75: 123-127

[87] Morley, James, Nelson, Charles R. & Eric Zivot (2003). Why are the Beveridge-Nelson and unobserved components decompositions of GDP so different?. *Review of Economics and Statistics*, 85: 235-243

[88] Morley, James, & Jeremy Piger (2012). The asymmetric business Cycle. *Review of Economics and Statistics*, 94: 208-221

[89] Morley, James, & Benjamin Wong (2020). Estimating and accounting for the output gap with large Bayesian vector autoregressions. *Journal of Applied Econometrics*, 35: 1-18

[90] Nason, James M., & Gregor W. Smith (2020). Measuring the slowly evolving trend in US inflation with professional forecasts. *Journal of Applied Econometrics*

[91] Orphanides, Athanasios., & John C. Williams (2002). Robust monetary policy rules with unknown natural rates. Working paper 2003-01, Federal Reserve Bank of San Francisco

[92] Peneva, Ekaterina V., & Jeremy B. Rudd (2017). The passthrough of labor costs to price inflation. *Journal of Money, Credit, and Banking*, 49(8): 1777-1802

[93] Pescatori, Andrea, & Jarkko Turunen (2016). Lower for longer: Neutral rate in the U.S. *IMF Economic Review*, 64(4): 708-731

[94] Primiceri, Giorgio E. (2005). Time varying structural vector autoregressions and monetary policy. *Review of Economic Studies*, 72, 821-852 doi:10.1111/j.1467-937x.2005.00353.x

[95] Powell, Jerome H. (2018). Changing market structure and implication for monetary policy. Speech at the Jackson Hole Symposium organized by the Federal Reserve Bank of Kansas City, August 24, 2018.

[96] Roberts, John. (2001). Estimates of the productivity trend using time-varying parameter techniques. *Contributions to Macroeconomics*, 1(1):3

[97] Shackleton, Robert (2018). Estimating and projecting potential output using CBO's forecasting growth model. Congressional Budget Office, Working Paper 2018-03

[98] Sinclair, Tara M. (2009). The relationships between permanent and transitory movements in U.S. output and the unemployment Rate. *Journal of Money, Credit and Banking* 41(2-3): 529-542

[99] Staiger, Douglas O., Stock, James H., & Mark W. Watson (1997). How precise are estimates of the natural rate of unemployment?. *In Romer, C, Romer, D. (Eds.), Reducing Inflation: Motivation and Strategy*, pp. 195-242, University of Chicago Press

[100] Stella, Andrea, & James H. Stock (2015). A state-dependent model for inflation forecasting. *In S. J. Koopman, & N. Shephard (Eds.), Unobserved components and time series econometrics*, (pp, 14-29), Oxford University Press

[101] Stock, James H., & Mark W. Watson (2007). Why has U.S. inflation become harder to forecast? *Journal of Money, Credit and Banking*, 39: 3-33

[102] Stock, James H., & Mark W. Watson (2020). Slack and cyclically sensitive inflation. *Journal of Money, Credit and Banking*, 52(S2): 393-428, https://doi.org/10.1111/jmcb.12757

[103] Summers, Lawrence H. (2014). US economic prospects: Secular stagnation, hysteresis and the zero lower bound. *Business Economics*, 49(2): 65-73

[104] Tallman, Ellis W., & Saeed Zaman (2017). Forecasting inflation: Phillips curve effects on services price measures. *International Journal of Forecasting*, 33(2): 442-457

[105] Tallman, Ellis W., & Saeed Zaman (2020). Combining survey long-run forecasts and nowcasts with BVAR forecasts using relative entropy. *International Journal of Forecasting*, 36(2): 373-398

[106] Taylor, John B. (1999). A historical analysis of monetary policy rules. *University of Chicago Press*, Chapter 7: 319-348

[107] Taylor, John B. & Volker Wieland (2016). Finding the equilibrium real interest rate in a fog of policy deviations. *Business Economics*, 51(3): 147-154

[108] Tasci, Murat (2012).The ins and outs of unemployment in the long run: Unemployment flows and the natural rate. Federal Reserve Bank of Cleveland Working paper

[109] Tasci, Murat (2019). Challenges with estimating u star in real time. Federal Reserve Bank of Cleveland *Economic Commentary*, 2019-18

[110] Weber, Axel A., Lemke, Wolfgang, & Andreas Worms (2008). How useful is the concept of the natural real rate of interest for monetary policy? *Cambridge Journal of Economics*, 32:49-63

[111] Weise, Charles L. (2012). Political pressures on monetary policy during the US Great Inflation. *American Economic Journal: Macroeconomics*, 4:33-64

[112] Williams, John C. (2018). The future fortunes of r-star: Are they really rising? Federal Reserve Bank of San Francisco *Economic Letter*, No. 2018-13

[113] Wright, Jonathan (2013). Evaluating real-time VAR forecasts with an informative democratic prior. *Journal of Applied Econometrics*, 28: 762-776 doi:10.1002/jae.2268

[114] Wu, Jing C., & Fan Dora Xia (2016). Measuring the macroeconomic impact of monetary policy at the ZLB. *Journal of Money, Credit, and Banking*, 48(2-3): 253-291

Supplementary Appendix

A Unified Framework to Estimate Macroeconomic Stars

Saeed Zaman*
Federal Reserve Bank of Cleveland, USA
University of Strathclyde, UK

This version: June 11, 2021
Original version: September 16, 2020

I am extremely grateful to my advisors Gary Koop and Julia Darby for the valuable guidance and the feedback throughout the research and writing process. The views expressed herein are those of the author and do not necessarily represent the views of the Federal Reserve Bank of Cleveland or the Federal Reserve System.

*Research department, Federal Reserve Bank of Cleveland, Ohio, USA; and Department of Economics, University of Strathclyde, Glasgow, United Kingdom; email: saeed.zaman@clev.frb.org

Contents

A1. Bayesian Estimation Details **3**
A1.a. Base Model equations 3
A1.b. Prior Elicitation 5
A1.c. MCMC Algorithm 7
A1.d Marginal likelihood computation 40

A2. Prior Sensitivity Analysis **40**

A3. MCMC Convergence Diagnostics **42**

A4. Additional Forecasting Results: Base vs. Benchmarks **45**

A5. Additional Forecasting Results: Steady-State BVAR, Base stars vs. Survey **47**

A6. Additional Real-time Estimates Stars **50**

A7. Estimated relationship between Survey and Stars **53**

A8. Additional COVID-19 Pandemic Results **54**

A9. Backcast: Survey R* from 1959-1982 **60**

A10. R* : Additional Full Sample Results **61**
A10.a. Role of data vs. prior in shaping r-star 61
A10.b. Base vs. External models 61
A10.c. Sensitivity of r-star to the prior setting 62
A10.d. The usefulness of the Taylor-rule equation 64

A11. Pi* : Additional Full Sample Results **65**
A11.a. Pi-star comparison Base vs. outside models 65
A11.b. Sensitivity of pi-star to modeling assumptions 67
A11.c. Pi-star estimates for some variants of the Base model 68

A12. P*: comparison with Kahn and Rich (2007) **69**

A13. P* : Additional Full Sample Results **71**
A13.a. Cyclical Productivity based on Output gap 71

A1. Bayesian Estimation Details

A1.a. Base Model equations

For convenience, we list all model equations keeping the numbering as in the main text.

$$U_t = U_t^* + U_t^c \tag{6}$$

$$U_t - U_t^* = \rho_1^u(U_{t-1} - U_{t-1}^*) + \rho_2^u(U_{t-2} - U_{t-2}^*) + \phi^u ogap_t + \varepsilon_t^u,\ \ \varepsilon_t^u \sim N(0, \sigma_u^2) \tag{7}$$

where, $\rho_1^u + \rho_2^u < 1$, $\rho_2^u - \rho_1^u < 1$, and $|\rho_2^u| < 1$; $\phi^u < 0$

$$U_t^* = U_{t-1}^* + \varepsilon_t^{u*},\ \ \varepsilon_t^{u*} \sim TN(a_u - U_{t-1}^*, b_u - U_{t-1}^*; 0, \sigma_{u*}^2) \tag{8}$$

$$Z_t^u = C_t^u + \beta^u U_t^* + \varepsilon_t^{zu},\ \ \varepsilon_t^{zu} \sim N(0, \sigma_{zu}^2) \tag{9}$$

$$C_t^u = C_{t-1}^u + \varepsilon_t^{cu},\ \ \varepsilon_t^{cu} \sim N(0, \sigma_{cu}^2) \tag{10}$$

$$gdp_t = gdp_t^* + ogap_t \tag{11}$$

$$gdp_t^* = 2gdp_{t-1}^* - gdp_{t-2}^* + \varepsilon_t^{gdp*},\ \ \varepsilon_t^{gdp*} \sim N(0, \sigma_{gdp*}^2) \tag{12}$$

$$g_t^* \equiv \triangle gdp_t^*$$

$$g_t^* = g_{t-1}^* + \varepsilon_t^{gdp*} \tag{13}$$

$$ogap_t = \rho_1^g(ogap_{t-1}) + \rho_2^g(ogap_{t-2}) + a^r(r_t - r_t^*) + \lambda^g(U_t - U_t^*) + \varepsilon_t^{ogap} \tag{14}$$

where, $\varepsilon_t^{ogap} \sim N(0, \sigma_{ogap}^2)$, $\rho_1^g + \rho_2^g < 1$, $\rho_2^g - \rho_1^g < 1$, and $|\rho_2^g| < 1$; $\lambda^g < 0$

$$Z_t^g = C_t^g + \beta^g * 4 * g_t^* + \varepsilon_t^{zg},\ \ \varepsilon_t^{zg} \sim N(0, \sigma_{zg}^2) \tag{15}$$

$$C_t^g = C_{t-1}^g + \varepsilon_t^{cg},\ \ \varepsilon_t^{cg} \sim N(0, \sigma_{cg}^2) \tag{16}$$

$$P_t - P_t^* = \rho^p(P_{t-1} - P_{t-1}^*) + \lambda_t^p(U_t - U_t^*) + \varepsilon_t^p,\ \ \varepsilon_t^p \sim N(0, e^{h_t^p}) \tag{17}$$

where, $|\rho^p| < 1$

$$\lambda_t^p = \lambda_{t-1}^p + \varepsilon_t^{\lambda p},\ \ \varepsilon_t^{\lambda p} \sim N(0, \sigma_{\lambda p}^2) \tag{18}$$

$$h_t^p = h_{t-1}^p + \varepsilon_t^{hp},\ \ \varepsilon_t^{hp} \sim N(0, \sigma_{hp}^2) \tag{19}$$

$$P_t^* = P_{t-1}^* + \varepsilon_t^{p*},\ \ \varepsilon_t^{p*} \sim N(0, \sigma_{p*}^2) \tag{20}$$

$$\pi_t - \pi_t^* = \rho_t^\pi(\pi_{t-1} - \pi_{t-1}^*) + \lambda_t^\pi(U_t - U_t^*) + \varepsilon_t^\pi,\ \ \varepsilon_t^\pi \sim N(0, e^{h_t^\pi}) \tag{21}$$

$$\rho_t^\pi = \rho_{t-1}^\pi + \varepsilon_t^{\rho\pi},\ \ \varepsilon_t^{\rho\pi} \sim TN(0 - \rho_{t-1}^\pi, 1 - \rho_{t-1}^\pi; 0, \sigma_{\rho\pi}^2) \tag{22}$$

where, ρ^π are truncated so that $0 < \rho_t^\pi < 1$.

$$\lambda_t^\pi = \lambda_{t-1}^\pi + \varepsilon_t^{\lambda\pi},\ \ \varepsilon_t^{\lambda\pi} \sim TN(-1 - \lambda_{t-1}^\pi, 0 - \lambda_{t-1}^\pi; 0, \sigma_{\lambda\pi}^2) \tag{23}$$

λ^π is the slope of price Phillips curve and is constrained in the interval (-1,0).

$$h_t^\pi = h_{t-1}^\pi + \varepsilon_t^{h\pi},\ \ \varepsilon_t^{h\pi} \sim N(0, \sigma_{h\pi}^2) \tag{24}$$

$$\pi_t^* = \pi_{t-1}^* + \varepsilon_t^{\pi*},\ \ \varepsilon_t^{\pi*} \sim N(0, \sigma_{\pi*}^2) \tag{25}$$

$$Z_t^{\pi} = C_t^{\pi} + \beta^{\pi}\pi_t^* + \varepsilon_t^{z\pi},\ \ \varepsilon_t^{z\pi} \sim N(0, \sigma_{z\pi}^2) \tag{26}$$

$$C_t^{\pi} = C_{t-1}^{\pi} + \varepsilon_t^{c\pi},\ \ \varepsilon_t^{c\pi} \sim N(0, \sigma_{c\pi}^2) \tag{27}$$

$$W_t^* = \pi_t^* + P_t^* + \varepsilon_t^{w*},\ \ \varepsilon_t^{w*} \sim N(0, \sigma_{w*}^2) \tag{28}$$

$$W_t - W_t^* = \rho_t^w(W_{t-1} - W_{t-1}^*) + \lambda_t^w(U_t - U_t^*) + \kappa_t^w(\pi_t - \pi_t^*) + \varepsilon_t^w,\ \ \varepsilon_t^w \sim N(0, e^{h_t^w}) \tag{29}$$

$$h_t^w = h_{t-1}^w + \varepsilon_t^{hw},\ \ \varepsilon_t^{hw} \sim N(0, \sigma_{hw}^2) \tag{30}$$

$$\rho_t^w = \rho_{t-1}^w + \varepsilon_t^{\rho w},\ \ \varepsilon_t^{\rho w} \sim TN(0 - \rho_{t-1}^w, 1 - \rho_{t-1}^w; 0, \sigma_{\rho w}^2) \tag{31}$$

$$\lambda_t^w = \lambda_{t-1}^w + \varepsilon_t^{\lambda w},\ \ \varepsilon_t^{\lambda w} \sim TN(-1 - \lambda_{t-1}^w, 0 - \lambda_{t-1}^w; 0, \sigma_{\lambda w}^2) \tag{32}$$

λ^w is the slope of wage Phillips curve and is constrained in the interval (-1,0).

$$\kappa_t^w = \kappa_{t-1}^w + \varepsilon_t^{\kappa w},\ \ \varepsilon_t^{\kappa w} \sim N(0, \sigma_{\kappa w}^2) \tag{33}$$

$$i_t - \pi_t^* - r_t^* = \rho^i(i_{t-1} - \pi_{t-1}^* - r_{t-1}^*) + \lambda^i(U_t - U_t^*) + \kappa^i(\pi_t - \pi_t^*) + \varepsilon_t^i,\ \ \varepsilon_t^i \sim N(0, e^{h_t^i}) \tag{34}$$

where, ρ^i is truncated so that $0 < \rho^i < 1$.

$$h_t^i = h_{t-1}^i + \varepsilon_t^{hi},\ \ \varepsilon_t^{hi} \sim N(0, \sigma_{hi}^2) \tag{35}$$

$$r_t^* = \zeta g_t^* + D_t. \tag{36}$$

$$D_t = D_{t-1} + \varepsilon_t^d,\ \ \varepsilon_t^d \sim N(0, \sigma_d^2) \tag{37}$$

$$Z_t^r = C_t^r + \beta^r r_t^* + \varepsilon_t^{zr},\ \ \varepsilon_t^{zr} \sim N(0, \sigma_{zr}^2) \tag{38}$$

$$C_t^r = C_{t-1}^r + \varepsilon_t^{cr},\ \ \varepsilon_t^{cr} \sim N(0, \sigma_{cr}^2) \tag{39}$$

A1.b. Prior Elicitation

Our prior settings are similar to those used in Chan, Koop, and Potter (2016) [CKP], Chan, Clark, and Koop (2018) [CCK], and Gonzalez-Astudillo and Laforte (2020). As discussed in CCK, UC models with several unobserved variables, such as the one developed in this paper, require informative priors. That said, our priors settings for most variables are only slightly informative. The use of inequality restrictions on some parameters such as the Phillips curve, persistence, bounds on u-star could be viewed as additional sources of information that eliminates the need for tight priors, something also noted by CKP. The parameters for which there is a strong agreement in the empirical literature on their values, such as the Taylor-rule equation parameters, we use relatively tight priors, such that prior distributions are centered on prior means with small variance.

In the table below, the notation $N(a, b)$ denotes Normal distribution with mean a, and variance b; and $IG(\nu, S)$ denotes Inverse Gamma distribution with degrees of freedom parameter ν, and scale parameter S.

Table A1: Prior settings

Parameter	**Parameter Description**	**Prior**
a^r	Coefficient on interest-rate gap in output gap equation	$N(0, 1)$
ρ_1^g	Persistence in output gap: lag 1	$N(1.3, 0.1^2)$
ρ_2^g	Persistence in output gap: lag 2	$N(-0.5, 0.1^2)$
ρ_1^u	Persistence in UR gap: lag 1	$N(1.3, 0.1^2)$
ρ_2^u	Persistence in UR gap: lag 2	$N(-0.5, 0.1^2)$
ρ^p	Persistence in productivity gap	$N(0.1, 1)$
ζ	Relationship between r* and g*	$N(1, 0.1)$
ρ^i	Persistence in interest-rate gap	$N(0.85, 0.1^2)$
λ^i	Interest rate sensitivity to UR gap: $(-2 * (1 - \rho^i))$	$N(-0.3, 0.1^2)$
κ^i	Interest rate sensitivity to inflation: $(0.5 * (1 - \rho^i))$	$N(0.075, 0.1^2)$
λ^g	Output gap response to UR gap	$N(-0.02, 1)$
ϕ^u	UR gap response to Output gap	$N(-0.02, 1)$
β^g	Link between g* and survey	$N(1, 0.1^2)$
β^u	Link between u* and survey	$N(1, 0.05^2)$
β^r	Link between r* and survey	$N(1, 0.1^2)$
β^π	Link between π^* and survey	$N(1, 0.05^2)$
$\sigma^2_{\pi^*}$	Var. of the shocks to π^*	$IG(10, 0.1^2 \times 9)$
$\sigma^2_{p^*}$	Var. of the shocks to p^*	$IG(10, 0.142^2 \times 9)$
$\sigma^2_{u^*}$	Var. of the shocks to u^*	$IG(10, 0.1^2 \times 9)$
$\sigma^2_{gdp^*}$	Var. of the shocks to gdp^*	$IG(10, 0.01^2 \times 9)$
σ^2_d	Var. of the shocks to d	$IG(10, 0.1^2 \times 9)$
$\sigma^2_{w^*}$	Var. of the shocks to w^*	$IG(10, 0.142^2 \times 9)$
σ^2_{ogap}	Var. of the shocks to Ogap	$IG(10, 1 \times 9)$
σ^2_u	Var. of the shocks to UR gap	$IG(10, 0.707^2 \times 9)$
σ^2_{hp}	Var. of the volatility – Productivity eq.	$IG(10, 0.316^2 \times 9)$
σ^2_h	Var. of the volatility – Price Inf. eq.	$IG(10, 0.316^2 \times 9)$
σ^2_{hw}	Var. of the volatility – Wage Inf. eq.	$IG(10, 0.316^2 \times 9)$

Continued on next page

Table A1 – continued from previous page

Parameter	Parameter Description	Prior
σ^2_{hi}	Var. of the volatility – Interest rate eq.	$IG(10, 0.316^2 \times 9)$
$\sigma^2_{\lambda\pi}$	Var. of the shocks to TVP λ^π, Price Phillips curve	$IG(10, 0.04^2 \times 9)$
$\sigma^2_{\lambda w}$	Var. of the shocks to TVP λ^w, Wage Phillips curve	$IG(10, 0.04^2 \times 9)$
$\sigma^2_{\lambda p}$	Var. of the shocks to TVP λ^p, Cyc. Productivity	$IG(10, 0.04^2 \times 9)$
$\sigma^2_{\kappa w}$	Var. of the shocks to TVP κ^w, PT: π to Wages	$IG(10, 0.04^2 \times 9)$
$\sigma^2_{\rho w}$	Var. of the shocks to TVP ρ^w, Persist. Wage-gap	$IG(10, 0.04^2 \times 9)$
$\sigma^2_{\rho\pi}$	Var. of the shocks to TVP ρ^π, Persist. Inflation-gap	$IG(10, 0.04^2 \times 9)$
C^π_0	Time-varying Intercept in eq. linking survey to pi-star	$N(0, 0.1)$
C^u_0	Time-varying Intercept in eq. linking survey to u-star	$N(0, 0.1)$
C^g_0	Time-varying Intercept in eq. linking survey to g-star	$N(0, 0.1)$
C^r_0	Time-varying Intercept in eq. linking survey to r-star	$N(0, 0.1)$
$\sigma^2_{c\pi}$	Var. of the shocks to TVP C^π	$IG(10, 0.1^2 \times 9)$
σ^2_{cu}	Var. of the shocks to TVP C^u	$IG(10, 0.1^2 \times 9)$
σ^2_{cg}	Var. of the shocks to TVP C^g	$IG(10, 0.1^2 \times 9)$
σ^2_{cr}	Var. of the shocks to TVP C^r	$IG(10, 0.1^2 \times 9)$
$\sigma^2_{z\pi}$	Var. of the shocks in measurement eq. Z^π,	$IG(10, 0.2 \times 9)$
σ^2_{zu}	Var. of the shocks in measurement eq. Z^u,	$IG(10, 0.3 \times 9)$
σ^2_{zg}	Var. of the shocks in measurement eq. Z^g,	$IG(10, 0.1 \times 9)$
σ^2_{zr}	Var. of the shocks in measurement eq. Z^r,	$IG(10, 0.2 \times 9)$
π^*_0	Initial value of pi-star	$N(3, 5^2)$
u^*_0	Initial value of u-star, $t = 0$	$N(5, 5^2)$
u^*_{-1}	Initial value of u-star, $t = -1$	$N(5, 5^2)$
p^*_0	Initial value of p-star	$N(3, 5^2)$
w^*_0	Initial value of w-star, $E(p^*_0) + E(\pi^*_0) = 6$	$N(6, 5^2)$
D_0	Initial value of D, "catch-all" component of r-star	$N(0, 0.3162^2)$
gdp^*_0	Initial value of gdp-star, $t = 0$	$N(750, 10^2)$
gdp^*_{-1}	Initial value of gdp-star, $t = -1$	$N(750, 10^2)$

A1.c. MCMC Algorithm

The estimation of our complex UC model and sampling from its joint posterior distribution reduces to sequentially drawing from a set of conditional posterior densities, some of which are standard and some that are non-standard.

Collect all the time-invariant model parameters into θ:
$\theta = (\rho_1^u, \rho_2^u, \sigma_u^2, \phi_u, \sigma_{u*}^2, \beta^u, \sigma_{zu}^2, \sigma_{cu}^2, \sigma_{gdp*}^2, \rho_1^g, \rho_2^g, a^r, \lambda^g, \sigma_{ogap}^2, \sigma_{zg}^2, \sigma_{cg}^2, \beta^g, \rho^p, \sigma_{hp}^2, \sigma_{p*}^2, \sigma_{\lambda\pi}^2, ...$
$\sigma_{\rho\pi}^2, \sigma_{h\pi}^2, \sigma_{\pi*}^2, \sigma_{z\pi}^2, \sigma_{c\pi}^2, \beta^\pi, \sigma_{w*}^2, \sigma_{hw}^2, \sigma_{\rho w}^2, \sigma_{\lambda w}^2, \sigma_{\kappa w}^2, \rho^i, \lambda^i, \kappa^i, \sigma_{hi}^2, \sigma_{zr}^2, \sigma_{cr}^2, \beta^r, \sigma_d^2)$

We denote $\bullet$ as representing all other model parameters.
1. $p(U^*|Y,\bullet)$ 2. $p(gdp^*|Y,\bullet)$ 3. $p(P^*|Y,\bullet)$ 4. $p(\pi^*|Y,\bullet)$ 5. $p(w^*|Y,\bullet)$ 6. $p(r^*|Y,\bullet)$
7. $p(\lambda^p|Y,\bullet)$ 8. $p(\rho^\pi|Y,\bullet)$ 9. $p(\lambda^\pi|Y,\bullet)$ 10. $p(\rho^w|Y,\bullet)$ 11. $p(\lambda^w|Y,\bullet)$ 12. $p(\kappa^w|Y,\bullet)$
13. $p(h^p, h^\pi, h^w, h^i|Y,\bullet)$ 14. $p(C^u, C^g, C^\pi, C^r|Y,\bullet)$ 15. $p(D|Y,\bullet)$ 16. $p(\theta|Y,\bullet)$

Step 1. Derive the conditional distribution $p(U^*|Y,\bullet)$

The derivation of this distribution is most complex because the information about U^* comes from eight sources (i.e., model equations). Below, we derive an expression for each of the eight sources.

The first source is the state equation of U^*. We rewrite it in a matrix notation as follows,

$$HU^* = \alpha_u + \varepsilon^{u*} \quad \varepsilon^{u*} \sim N(0, \Omega_{u*}), \quad where\ \Omega_{u*} = diag(\omega_{u*}^2, \sigma_{u*}^2, ..., \sigma_{u*}^2) \tag{40}$$

where,

$$\alpha_u = \begin{pmatrix} U_0^* \\ 0 \\ 0 \\ \vdots \\ 0 \end{pmatrix}, \quad H = \begin{pmatrix} 1 & 0 & 0 & \cdots & 0 \\ -1 & 1 & 0 & \cdots & 0 \\ 0 & -1 & 1 & \cdots & 0 \\ \vdots & & & \ddots & \vdots \\ 0 & 0 & \cdots & -1 & 1 \end{pmatrix}$$

That is, the prior density for U^* is given by

$$p(U^*|\sigma_{U*}^2) \propto -\tfrac{1}{2}(U^* - H^{-1}\alpha_u)' H' \Omega_{u*}^{-1} H (U^* - H^{-1}\alpha_u) + g_{u*}(U^*, \sigma_{u*}^2)$$

where,
$a_u < U^* < b_u$ for $t = 1, ..., T$, and

$$g_{u*}(U^*, \sigma_{u*}^2) = -log\left(\Phi\left(\frac{b_u}{\omega_{u_*}}\right) - \Phi\left(\frac{a_u}{\omega_{u_*}}\right)\right) - \sum_{t=2}^{T} log\left(\Phi\left(\frac{b_u - U_{t-1}^*}{\sigma_{u_*}}\right) - \Phi\left(\frac{a_u - U_{t-1}^*}{\sigma_{u_*}}\right)\right)$$

The second source of information comes from the unemployment measurement equation. Rewrite

the equation in a matrix notation,

$$K_u U = \mu^u + K_u U^* + \varepsilon^u \qquad \varepsilon^u \sim N(0, \Omega_u), \quad where\ \ \Omega_u = I_T \otimes \sigma_u^2 \tag{41}$$

and,

$$\mu_u = \begin{pmatrix} \rho_1^u(U_0 - U_0^*) + \rho_2^u(U_{-1} - U_{-1}^*) \\ \rho_2^u(U_0 - U_0^*) \\ 0 \\ \vdots \\ 0 \end{pmatrix}, \quad K_u = \begin{pmatrix} 1 & 0 & 0 & \cdots & 0 \\ -\rho_1^u & 1 & 0 & \cdots & 0 \\ -\rho_2^u & -\rho_1^u & 1 & \cdots & 0 \\ \vdots & & & \ddots & \vdots \\ 0 & \cdots & -\rho_2^u & -\rho_1^u & 1 \end{pmatrix}$$

Ignoring any terms not involving U^*, we have

$$log\ \ p(U|U^*, \bullet) \propto -\tfrac{1}{2}(U - K_u^{-1}\mu_u - U^*)' K_u' \Omega_u^{-1} K_u (U - K_u^{-1}\mu_u - U^*)$$

The third source of information comes from the inflation measurement equation. Rewrite the equation in a matrix notation,

$$Z = \Lambda^\pi U^* + \varepsilon^\pi \qquad \varepsilon^\pi \sim N(0, \Omega_\pi), \quad where\ \ \Omega_\pi = diag(e^{h_1^\pi}, e^{h_2^\pi}, ..., e^{h_T^\pi}) \tag{42}$$

where,

$z_t = (\pi_t - \pi_t^*) - \rho_t^\pi(\pi_{t-1} - \pi_{t-1}^*) - \lambda_t^\pi U_t,$

$Z = (z_1, ..., z_T)'$ and $\Lambda^\pi = diag(-\lambda_1^\pi, ..., -\lambda_T^\pi)$

Ignoring any terms not involving U^*, we have

$$log\ \ p(\pi|U^*, U, \pi^*, h^\pi, \rho^p, \bullet) \propto -\tfrac{1}{2}(Z - \Lambda^\pi U^*)' \Omega_\pi^{-1} (Z - \Lambda^\pi U^*)$$

The fourth source of information comes from the productivity measurement equation. Rewrite the equation in a matrix notation,

$$M^P = \Lambda^P U^* + \varepsilon^P \qquad \varepsilon^P \sim N(0, \Omega_P), \quad where\ \ \Omega_P = diag(e^{h_1^p}, e^{h_2^p}, ..., e^{h_T^p}) \tag{43}$$

where,

$m_t = (P_t - P_t^*) - \rho^P(P_{t-1} - P_{t-1}^*) - \lambda_t^P U_t,$

$M^P = (m_1, ..., m_T)'$ and $\Lambda^P = diag(-\lambda_1^P, ..., -\lambda_T^P)$

Ignoring any terms not involving U^*, we have

$$log\ \ p(P|U^*, U, P^*, h^p, \rho^p, \bullet) \propto -\tfrac{1}{2}(M^P - \Lambda^P U^*)' \Omega_P^{-1} (M^P - \Lambda^P U^*)$$

The fifth source of information comes from the wage measurement equation. Rewrite the equation in a matrix notation,

$$M^w = \Lambda^w U^* + \varepsilon^w \qquad \varepsilon^w \sim N(0, \Omega_w), \quad where\ \ \Omega_w = diag(e^{h_1^w}, e^{h_2^w}, ..., e^{h_T^w}) \tag{44}$$

where,

$m_t^w = (W_t - W_t^*) - \rho_t^W (W_{t-1} - W_{t-1}^*) - \lambda_t^W U_t - \kappa_t^W (\pi_t - \pi_t^*)$,

$M^w = (m_1^w, ..., m_T^w)'$ and $\Lambda^w = diag(-\lambda_1^W, ..., -\lambda_T^W)$

Ignoring any terms not involving U^*, we have

$log\ \ p(W|U^*, W, W^*, h^w, \rho^W, \bullet) \propto -\frac{1}{2}(M^w - \Lambda^w U^*)' \Omega_w^{-1} (M^w - \Lambda^w U^*)$

The sixth source of information comes from the output gap measurement equation. Rewrite the equation in a matrix notation,

$$M^g = \Lambda^g U^* + \varepsilon^g \qquad \varepsilon^g \sim N(0, \Omega_{ogap}), \quad where\ \ \Omega_{ogap} = diag(\sigma_{ogap}^2, ..., \sigma_{ogap}^2) \tag{45}$$

where,

$m_t^g = ogap_t - \rho_1^g (ogap_{t-1}) - \rho_2^g (ogap_{t-2}) - \lambda^g U_t - a^r (r_t - r_t^*)$,

$M^g = (m_1^g, ..., m_T^g)'$ and $\Lambda^g = diag(-\lambda^g, ..., -\lambda^g)$

Ignoring any terms not involving U^*, we have

$log\ \ p(ogap|U^*, U, \bullet) \propto -\frac{1}{2}(M^g - \Lambda^g U^*)' \Omega_{ogap}^{-1} (M^g - \Lambda^g U^*)$

The seventh source of information comes from the Taylor-type rule measurement equation. Rewrite the equation in a matrix notation,

$$M^{ui} = \Gamma^{ui} U^* + \varepsilon^i \qquad \varepsilon^i \sim N(0, \Omega_i), \quad where\ \ \Omega_i = diag(e^{h_1^i}, e^{h_2^i}, ..., e^{h_T^i}) \tag{46}$$

where,

$m_t^{ui} = i_t - \pi_t^* - r_t^* - \rho^i (i_{t-1} - \pi_{t-1}^* - r_{t-1}^*) - \kappa^i (\pi_t - \pi_t^*) - \lambda^i U_t$,

$M^{ui} = (m_1^{ui}, ..., m_T^{ui})'$ and $\Gamma^{ui} = diag(-\lambda^i, ..., -\lambda^i)$

Ignoring any terms not involving U^*, we have

$log\ \ p(i|U^*, U, \pi, \bullet) \propto -\frac{1}{2}(M^{ui} - \Gamma^{ui} U^*)' \Omega_i^{-1} (M^{ui} - \Gamma^{ui} U^*)$

The eighth source of information comes from the measurement equation that links survey to

U^*. Rewrite the equation in a matrix notation,

$$F^u = \beta^u U^* + \varepsilon^{zu} \qquad \varepsilon^{zu} \sim N(0, \Omega_{zu}), \quad where \ \ \Omega_{zu} = diag(\sigma^2_{zu}, ..., \sigma^2_{zu}) \tag{47}$$

where,

$f^u_t = Z^u_t - C^u_t,$

$F^u = (f^u_1, ..., f^u_T)'$

Ignoring any terms not involving U^*, we have

$log \ \ p(Z^u|U^*, U, \pi, \bullet) \propto -\frac{1}{2}(F^u - \beta^u U^*)'\Omega^{-1}_{zu}(F^u - \beta^u U^*)$

Combining the above eight conditional densities we obtain,

$log \ \ p(U^*|Y, \bullet) \propto -\frac{1}{2}(U^* - \hat{U}^*)' D^{-1}_{U^*}(U^* - \hat{U}^*) + g_{u*}(U^*, \sigma^2_{u*})$

where,

$D_{U*} = (H'\Omega^{-1}_{U^*}H + K^{'}_u\Omega^{-1}_u K_u + \Lambda^{\pi'}\Omega^{-1}_\pi\Lambda^\pi + \Lambda^{w'}\Omega^{-1}_w\Lambda^w + \Lambda^{g'}\Omega^{-1}_{ogap}\Lambda^g + \Gamma^{ui'}\Omega^{-1}_i\Gamma^{ui} + \Lambda^{P'}\Omega^{-1}_P\Lambda^P + (\beta^u)^2\Omega^{-1}_{zu})^{-1}$

$\hat{U}^* = D_{U*}(H'\Omega^{-1}_{U^*}\alpha_u + K^{'}_u\Omega^{-1}_u K_u(U - K^{-1}_u\mu_u) + \Lambda^{\pi'}\Omega^{-1}_\pi Z + \Lambda^{w'}M^w + \Lambda^w + \Lambda^{g'}\Omega^{-1}_{ogap}M^g + \Gamma^{ui'}\Omega^{-1}_i M^{ui} + \Lambda^{P'}\Omega^{-1}_P M^P + \beta^u\Omega^{-1}_{zu}F^u)$

The addition of the term $g_{u*}(U^*, \sigma^2_{u*})$ leads to a non-standard density. Accordingly, we sample U^* using an independence-chain Metropolis-Hastings (MH) procedure. This involves first generating candidate draws from $N(\hat{U}^*, D_{U*})$ using the precision based algorithm that are then accepted or rejected based on accept-reject Metropolis-Hastings (ARMH) algorithm (discussed in Chan and Strachan, 2012).

Step 2. Derive the conditional distribution $p(gdp^*|Y, \bullet)$

The information about gdp^* comes from five sources. Below, we derive an expression for each of these sources.

The first source is the state equation of gdp^*. We rewrite it in a matrix notation as follows,

$$H_2 gdp^* = \alpha_{gdp*} + \varepsilon^{gdp*} \qquad \varepsilon^{gdp*} \sim N(0, \Omega_{gdp*}), \quad where \ \ \Omega_{gdp*} = diag(\omega^2_{gdp*}, \sigma^2_{gdp*}, ..., \sigma^2_{gdp*}) \tag{48}$$

where,

$$\alpha_{gdp*} = \begin{pmatrix} gdp_0^* + \triangle gdp_0^* \\ -gdp_0^* \\ 0 \\ \vdots \\ 0 \end{pmatrix}, \quad H_2 = \begin{pmatrix} 1 & 0 & 0 & 0 & \cdots & 0 \\ -2 & 1 & 0 & 0 & \cdots & 0 \\ 1 & -2 & 1 & 0 & \cdots & 0 \\ 0 & 1 & -2 & 1 & \cdots & 0 \\ \vdots & & & & \ddots & \vdots \\ 0 & \cdots & 0 & 1 & -2 & 1 \end{pmatrix}$$

H_2 is a band matrix with unit determinant and hence is invertible.

The prior density for gdp^* is given by

$$p(gdp^*|\sigma^2_{gdp*}) \propto -\tfrac{1}{2}(gdp^* - H_2^{-1}\alpha_{gdp*})' H_2' \Omega^{-1}_{gdp*} H_2 (gdp^* - H_2^{-1}\alpha_{gdp*})$$

The second source of information about gdp^* is from the output gap measurement equation. Rewrite in matrix form,

$$H_{rhog} gdp = H_{rhog} gdp^* + a^r \tilde{r} + \lambda^g \tilde{u} + \alpha_{gmore} + \varepsilon^{ogap} \qquad \varepsilon^{ogap} \sim N(0, \Omega_{ogap}), \quad where \ \Omega_{ogap} = diag(\sigma^2_{ogap}, ..., \sigma^2_{ogap}) \tag{49}$$

where,

$$\alpha_{gmore} = \begin{pmatrix} \rho_1^g(gdp_0 - gdp_0^*) + \rho_2^g(gdp_{-1} - gdp_{-1}^*) \\ \rho_2^g(gdp_0 - gdp_0^*) \\ 0 \\ \vdots \\ 0 \end{pmatrix}, \quad H_{rhog} = \begin{pmatrix} 1 & 0 & 0 & 0 & \cdots & 0 \\ -\rho_1^g & 1 & 0 & 0 & \cdots & 0 \\ -\rho_2^g & -\rho_1^g & 1 & 0 & \cdots & 0 \\ 0 & -\rho_2^g & -\rho_1^g & 1 & \cdots & 0 \\ \vdots & \ddots & \ddots & \ddots & \ddots & 0 \\ 0 & \cdots & 0 & -\rho_2^g & -\rho_1^g & 1 \end{pmatrix},$$

$$\tilde{r} = \begin{pmatrix} r_1 - r_1^* \\ r_2 - r_2^* \\ r_3 - r_3^* \\ \vdots \\ r_T - r_T^* \end{pmatrix} \quad \tilde{u} = \begin{pmatrix} U_1 - U_1^* \\ U_2 - U_2^* \\ U_3 - U_3^* \\ \vdots \\ U_T - U_T^* \end{pmatrix}$$

$log\ \ p(gdp|gdp^*, \bullet) \propto -\frac{1}{2}(gdp - H^{-1}_{rhog}(H_{rhog} gdp^* + a^r \tilde{r} + \lambda^g \tilde{u} + \alpha_{gmore}))' H'_{rhog} \Omega^{-1}_{ogap} H_{rhog} (gdp - H^{-1}_{rhog}(H_{rhog} gdp^* + a^r \tilde{r} + \lambda^g \tilde{u} + \alpha_{gmore}))$

The third source of information comes from the unemployment gap measurement equation. Rewrite that equation in matrix notation,

$$Y^{ugdp} = \Gamma^u gdp^* + \varepsilon^u \qquad \varepsilon^u \sim N(0, \Omega_u), \quad where \ \Omega_u = diag(\sigma_u^2, ..., \sigma_u^2) \tag{50}$$

where,

$y_t^{ugdp} = \tilde{u_t} - \rho_1^u \tilde{u_{t-1}} - \rho_2^u \tilde{u_{t-2}} - \phi^u gdp$, where $\tilde{u_t} = (U_t - U_t^*)$

$Y^{ugdp} = (y_1^{ugdp}, ..., y_T^{ugdp})'$

Ignoring any terms not involving gdp^*, we have

$$log\ \ p(U|gdp^*, \bullet) \propto -\tfrac{1}{2}(Y^{ugdp} - \Gamma^u gdp^*)'\Omega_u^{-1}(Y^{ugdp} - \Gamma^u gdp^*)$$

The fourth source of information comes from the equation linking r-star to g-star, i.e.,

$$r_t^* = \zeta(gdp_t^* - gdp_{t-1}^*) + D_t \tag{51}$$

Rewrite this equation in matrix notation,

$$r^* = \zeta H gdp^* + \alpha_{gr} + D \tag{52}$$

where,

$\alpha_{gr} = (-\zeta gdp_0^*, 0, 0, ..., 0)'$

Ignoring any terms not involving gdp^*, we have

$$log\ \ p(r^*|gdp^*, D, \bullet) \propto -\tfrac{1}{2}(r^* - (\zeta H gdp^* + \alpha_{gr} + D))'(r^* - (\zeta H gdp^* + \alpha_{gr} + D))$$

The fifth source of information comes from the measurement equation that links survey to g^*. Rewrite the equation in a matrix notation,

$$F^g = \beta^g(H gdp^* - \alpha_g) + \varepsilon^{zg} \qquad \varepsilon^{zg} \sim N(0, \Omega_{zg}), \quad where\ \ \Omega_{zg} = diag(\sigma_{zg}^2, ..., \sigma_{zg}^2) \tag{53}$$

where,

$f_t^g = Z_t^g - C_t^g$, $F^g = (f_1^g, ..., f_T^g)'$

$\alpha_g = (gdp_0^*, 0, 0, ..., 0)'$ is a $T \times 1$ vector.

Ignoring any terms not involving gdp^*, we have

$$log\ \ p(Z^g|gdp^*, \bullet) \propto -\tfrac{1}{2}(F^g - \beta^g(H gdp^* - \alpha_g))'\Omega_{zg}^{-1}(F^g - \beta^g(H gdp^* - \alpha_g))$$

Combining the above five conditional densities we obtain,

$$log\ \ p(gdp^*|Y, \bullet) \propto -\tfrac{1}{2}(gdp^* - \hat{gdp}^*)' D_{gdp*}^{-1}(gdp^* - \hat{gdp}^*)$$

where,

$D_{gdp*} = (H_2'\Omega_{gdp*}^{-1}H_2 + H_{rhog}'\Omega_{ogap}^{-1}H_{rhog} + \Gamma^{u'}\Omega_u^{-1}\Gamma^u + (\zeta H)'(\zeta H) + \beta^g H'\Omega_{zg}^{-1}\beta^g H)^{-1}$

$\hat{gdp}^* = D_{gdp*}(H_2'\Omega_{gdp*}^{-1}H_2\alpha_{gdp*} + H_{rhog}'\Omega_{ogap}^{-1}(H_{rhog}gdp - a^r\tilde{r} - \lambda^g\tilde{u} - \alpha_{gmore}) + \Gamma^{u'}\Omega_u^{-1}Y^{ugdp} + (\zeta H)'(r^* - \alpha_{gr} + D) + \beta^g H'\Omega_{zg}^{-1}F^g)$

Step 3. Derive the conditional distribution $p(P^*|Y, \bullet)$

First, rewrite the productivity measurement eq. as

$$K_p P = \mu_p + K_p P^* + \varepsilon^P \qquad \varepsilon^P \sim N(0, \Omega_P), \quad where \ \ \Omega_P = diag(e^{h_1^p}, e^{h_2^p}, ..., e^{h_T^p}) \tag{54}$$

$$\mu_p = \begin{pmatrix} \rho_1^P(P_0 - P_0^*) + \lambda_1^P(U_1 - U_1^*) \\ \lambda_2^P(U_2 - U_2^*) \\ \lambda_3^P(U_3 - U_3^*) \\ \vdots \\ \lambda_T^P(U_T - U_T^*) \end{pmatrix}, \quad K_P = \begin{pmatrix} 1 & 0 & 0 & \cdots & 0 \\ -\rho_2^P & 1 & 0 & \cdots & 0 \\ 0 & -\rho_3^P & 1 & \cdots & 0 \\ \vdots & & & \ddots & \vdots \\ 0 & 0 & \cdots & -\rho_T^P & 1 \end{pmatrix}, \quad P^* = \begin{pmatrix} P_1^* \\ P_2^* \\ P_3^* \\ \vdots \\ P_T^* \end{pmatrix}$$

Since $\mid K_P \mid = 1$ for any ρ_P, K_P is invertible. Therefore, we have likelihood

$$p(P|P^*, U, \bullet) \sim N(K_P^{-1}\mu_P + P^*, \ \ (K_P^{'}\Omega_P^{-1}K_P)^{-1})$$

i.e.,

$$log \ \ p(P|U, \bullet) \propto -\tfrac{1}{2}\iota_T h^P - \tfrac{1}{2}(P - K_P^{-1}\mu_P - P^*)^{'} K_P^{'}\Omega_P^{-1}K_P(P - K_P^{-1}\mu_P - P^*),$$

where ι_T is a $T \times 1$ columns of ones.

Similarly, rewrite the state equation for P^* as

$$HP^* = \alpha_p + \varepsilon^{P*} \qquad \varepsilon^{P*} \sim N(0, \Omega_{P*}), \quad where \ \ \Omega_{P*} = diag(\omega_{P*}^2, \sigma_{P*}^2, ..., \sigma_{P*}^2) \tag{55}$$

where,

$$\alpha_p = \begin{pmatrix} P_0^* \\ 0 \\ 0 \\ \vdots \\ 0 \end{pmatrix}, \quad K_P = \begin{pmatrix} 1 & 0 & 0 & \cdots & 0 \\ -1 & 1 & 0 & \cdots & 0 \\ 0 & -1 & 1 & \cdots & 0 \\ \vdots & & & \ddots & \vdots \\ 0 & 0 & \cdots & -1 & 1 \end{pmatrix}$$

That is, the prior density for P^* is given by

$$p(P^*|\sigma_{P*}^2) \propto -\tfrac{1}{2}(P^* - H^{-1}\alpha_p)^{'} H^{'}\Omega_{P*}^{-1}H(P^* - H^{-1}\alpha_p)$$

Now account for the third source of information about P* in the equation $W^* = P^* + \pi^* + \varepsilon^{w*}$,

$$p(P^*|W^*, \pi^*, \sigma_{W*}^2) \propto -\tfrac{1}{2}(P^* - (W^* - \pi^*))^{'}\Omega_{W*}^{-1}(P^* - (W^* - \pi^*))$$

where,

$$\Omega_{W*} = diag(\sigma^2_{W*}, \sigma^2_{W*}, ..., \sigma^2_{W*}),\ \ W^* = (W^*_1, ..., W^*_T)',\ \ \pi^* = (\pi^*_1, ..., \pi^*_T)'$$

Combining the above three conditional densities we obtain,

$$log\ \ p(P^*|Y, \bullet) \propto -\tfrac{1}{2}(P^* - \hat{P}^*)' D^{-1}_{P*}(P^* - \hat{P}^*)$$

where,

$$D_{P*} = (H' \Omega^{-1}_{P*} H + K'_P \Omega^{-1}_P K_P + \Omega^{-1}_{W*})^{-1}$$

$$\hat{P}^* = D_{P*}(H^{-1}\Omega^{-1}_{P*}\alpha_p + K'_P \Omega^{-1}_P K_P(P - K^{-1}_P \mu_P) + \Omega^{-1}_{W*}(W^* - \pi^*))$$

The candidate draws are sampled from $N(\hat{P}^*, D_{P*})$ using the precision based algorithm.

Step 4. Derive the conditional distribution $p(\pi^*|Y, \bullet)$

The information about π^* comes from six sources. Below, we derive an expression for each of these sources.

The first source is the inflation measurement equation. Rewrite it in a matrix notation as,

$$K_\pi \pi = \mu_\pi + K_\pi \pi^* + \varepsilon^\pi \qquad \varepsilon^\pi \sim N(0, \Omega_\pi), \quad where\ \ \Omega_\pi = diag(e^{h^\pi_1}, e^{h^\pi_2}, ..., e^{h^\pi_T}) \tag{56}$$

where,

$$\mu_\pi = \begin{pmatrix} \rho^\pi_1(\pi_0 - \pi^*_0) + \lambda^\pi_1(U_1 - U^*_1) \\ \lambda^\pi_2(U_2 - U^*_2) \\ \lambda^\pi_3(U_3 - U^*_3) \\ \vdots \\ \lambda^\pi_T(U_T - U^*_T) \end{pmatrix}, \quad K_\pi = \begin{pmatrix} 1 & 0 & 0 & \cdots & 0 \\ -\rho^\pi_2 & 1 & 0 & \cdots & 0 \\ 0 & -\rho^\pi_3 & 1 & \cdots & 0 \\ \vdots & & & \ddots & \vdots \\ 0 & 0 & \cdots & -\rho^\pi_T & 1 \end{pmatrix}$$

Since $\mid K_\pi \mid = 1$ for any ρ_π, K_π is invertible. Therefore, we have likelihood

$$log\ \ p(\pi|U, U^*, \bullet) \propto -\tfrac{1}{2}\iota_T h^\pi - \tfrac{1}{2}(\pi - (K^{-1}_\pi \mu_\pi + \pi^*))' K'_\pi \Omega^{-1}_\pi K_\pi (\pi - (K^{-1}_\pi \mu_\pi + \pi^*))$$

The second source of information is from the state equation of π^*. Rewrite it in a matrix notation,

$$H\pi^* = \alpha_\pi + \varepsilon^{\pi*} \qquad \varepsilon^{\pi*} \sim N(0, \Omega_{\pi*}), \quad where\ \ \Omega_{\pi*} = diag(\omega^2_{\pi*}, \sigma^2_{\pi*}, ..., \sigma^2_{\pi*}) \tag{57}$$

where,

$$\alpha_\pi = \begin{pmatrix} \pi_0^* \\ 0 \\ 0 \\ \vdots \\ 0 \end{pmatrix}$$

That is, the prior density for π^* is given by

$$p(\pi^*|\sigma^2_{\pi*}) \propto -\tfrac{1}{2}(\pi^* - H^{-1}\alpha_\pi)' H' \Omega^{-1}_{\pi*} H(\pi^* - H^{-1}\alpha_\pi)$$

Now account for the third source of information about π^* in the equation $W^* = P^* + \pi^* + \varepsilon^{w*}$,

$$p(\pi^*|W^*, P^*, \sigma^2_{W*}) \propto -\tfrac{1}{2}(\pi^* - (W^* - P^*))' \Omega^{-1}_{W*}(\pi^* - (W^* - P^*))$$

where,

$$\Omega_{W*} = diag(\sigma^2_{W*}, \sigma^2_{W*}, ..., \sigma^2_{W*}), \;\; W^* = (W_1^*, ..., W_T^*)', \;\; P^* = (P_1^*, ..., P_T^*)'$$

The fourth source of information is from the wage measurement equation. Rewrite in matrix notation,

$$M^{w\pi} = X_{w\pi}\pi^* + \varepsilon^w \qquad \varepsilon^w \sim N(0, \Omega_w), \quad where \;\; \Omega_w = diag(e^{h_1^w}, e^{h_2^w}, ..., e^{h_T^w}) \tag{58}$$

where,

$$m_t^{w\pi} = w_t - w_t^* - \rho_t^w(w_{t-1} - w_{t-1}^*) - \lambda_t^w(U_t - U_t^*) - \kappa_t^w \pi_t$$
$$M^{w\pi} = (m_1^{w\pi}, m_2^{w\pi}, ..., m_T^{w\pi})$$

$$X_{w\pi} = \begin{pmatrix} -\kappa_1^w & 0 & 0 & \cdots & 0 \\ 0 & -\kappa_2^w & 0 & \cdots & 0 \\ 0 & 0 & -\kappa_3^w & \cdots & 0 \\ \vdots & & & \ddots & \vdots \\ 0 & 0 & \cdots & 0 & -\kappa_T^w \end{pmatrix}$$

$$log \;\; p(W|\pi^*, \bullet) \propto -\tfrac{1}{2}(M^{w\pi} - X_{w\pi}\pi^*)' \Omega_w^{-1}((M^{w\pi} - X_{w\pi}\pi^*)$$

The fifth source is the Taylor-rule equation. Rewrite the equation in the matrix notation,

$$M^{\pi i} = \alpha_{\pi i} + (K_{\pi i} + \Gamma_\pi)\pi^* + \varepsilon^i \qquad \varepsilon^i \sim N(0, \Omega_i), \quad where \;\; \Omega_i = diag(e^{h_1^i}, e^{h_2^i}, ..., e^{h_T^i}) \tag{59}$$

where,

$$m_t^{\pi i} = i_t - \rho^i i_{t-1} - r_t^* + \rho^i r_{t-1}^* - \lambda^i (U_t - U_t^*) - \kappa^i \pi_t$$
$$M^{\pi i} = (m_1^{\pi i}, m_2^{\pi i}, ..., m_T^{\pi i})'$$

$$K_{\pi i} = \begin{pmatrix} 1 & 0 & 0 & \cdots & 0 \\ -\rho^i & 1 & 0 & \cdots & 0 \\ 0 & -\rho^i & 1 & \cdots & 0 \\ \vdots & & & \ddots & \vdots \\ 0 & 0 & \cdots & -\rho^i & 1 \end{pmatrix}, \quad \Gamma_\pi = \begin{pmatrix} -\kappa^i & 0 & 0 & \cdots & 0 \\ 0 & -\kappa^i & 0 & \cdots & 0 \\ 0 & 0 & -\kappa^i & \cdots & 0 \\ \vdots & & & \ddots & \vdots \\ 0 & 0 & \cdots & 0 & -\kappa^i \end{pmatrix}, \quad \alpha_{\pi i} = \begin{pmatrix} -\rho^i \pi_0^* \\ 0 \\ 0 \\ \vdots \\ 0 \end{pmatrix}$$

$$log\ \ p(i|\pi^*, \pi, \bullet) \propto -\tfrac{1}{2}(M^{\pi i} - (\alpha_{\pi i} + (K_{\pi i} + \Gamma_\pi)\pi^*))' \Omega_i^{-1} (M^{\pi i} - (\alpha_{\pi i} + (K_{\pi i} + \Gamma_\pi)\pi^*))$$

The sixth source of information comes from the measurement equation that links survey to π^*. Rewrite the equation in a matrix notation,

$$F^\pi = \beta^\pi \pi^* + \varepsilon^{z\pi} \qquad \varepsilon^{z\pi} \sim N(0, \Omega_{z\pi}), \quad where\ \ \Omega_{z\pi} = diag(\sigma_{z\pi}^2, ..., \sigma_{z\pi}^2) \tag{60}$$

where,

$$f_t^\pi = Z_t^\pi - C_t^\pi,$$

$$F^\pi = (f_1^\pi, ..., f_T^\pi)'$$

Ignoring any terms not involving π^*, we have

$$log\ \ p(Z^\pi|\pi^*, \pi, \bullet) \propto -\tfrac{1}{2}(F^\pi - \beta^\pi \pi^*)' \Omega_{z\pi}^{-1} (F^\pi - \beta^\pi \pi^*)$$

Combining the above six conditional densities we obtain,

$$log\ \ p(\pi^*|Y, \bullet) \propto -\tfrac{1}{2}(\pi^* - \hat{\pi}^*)' D_{\pi^*}^{-1} (\pi^* - \hat{\pi}^*)$$

where,

$D_{\pi^*} = (H'\Omega_{\pi^*}^{-1} H + K_\pi' \Omega_\pi^{-1} K_\pi + \Omega_{w^*}^{-1} + X_{w\pi}' \Omega_w^{-1} X_{w\pi} + (K_{\pi i}' + \Gamma_\pi)') \Omega_i^{-1} (K_{\pi i}' + \Gamma_\pi)' + (\beta^\pi)^2 \Omega_{zr}^{-1})^{-1}$

$\hat{\pi}^* = D_{\pi^*}(H'\Omega_{\pi^*}^{-1}\alpha_\pi + K_\pi' \Omega_\pi^{-1} K_\pi(\pi - K_\pi^{-1}\mu_\pi) + \Omega_{w^*}^{-1}(W^* - P^*) + X_{w\pi}' \Omega_w^{-1} M^{w\pi} + (K_{\pi i}' + \Gamma_\pi)' \Omega_i^{-1} (M^{\pi i} - \alpha_{\pi i}) + \beta^\pi \Omega_{zr}^{-1} F^\pi)$

The candidate draws are sampled from $N(\hat{\pi}^*, D_{\pi^*})$ using the precision based algorithm.

Step 5. Derive the conditional distribution $p(w^*|Y, \bullet)$

The information about w^* comes from two sources. Below, we derive an expression for each of these sources.

The first source is the nominal wage measurement equation. Rewrite it in a matrix notation as,

$$K_w W = \mu_w + K_w W^* + \varepsilon^w \qquad \varepsilon^w \sim N(0, \Omega_w), \quad where\ \Omega_w = diag(e^{h_1^w}, e^{h_2^w}, ..., e^{h_T^w}) \tag{61}$$

where,

$$\mu_w = \begin{pmatrix} \rho_1^w(W_0 - W_0^*) + \lambda_1^w(U_1 - U_1^*) + \kappa_1^w(\pi_1 - \pi_1^*) \\ \lambda_2^w(U_2 - U_2^*) + \kappa_2^w(\pi_2 - \pi_2^*) \\ \lambda_3^w(U_3 - U_3^*) + \kappa_3^w(\pi_3 - \pi_3^*) \\ \vdots \\ \lambda_T^w(U_T - U_T^*) + \kappa_T^w(\pi_T - \pi_T^*) \end{pmatrix}, \quad K_w = \begin{pmatrix} 1 & 0 & 0 & \cdots & 0 \\ -\rho_2^w & 1 & 0 & \cdots & 0 \\ 0 & -\rho_3^w & 1 & \cdots & 0 \\ \vdots & & & \ddots & \vdots \\ 0 & 0 & \cdots & -\rho_T^w & 1 \end{pmatrix}$$

Since $\mid K_w \mid = 1$ for any ρ_w, K_w is invertible. Therefore, we have likelihood

Ignoring any terms not involving w^*, we have

$$log\ \ p(W|W^*, \bullet) \propto -\tfrac{1}{2}\iota_T h^w - \tfrac{1}{2}(W - (K_w^{-1}\mu_w + W^*))' K_w^{'} \Omega_w^{-1} K_w (W - (K_w^{-1}\mu_w + W^*))$$

The second source is the state equation of W^*, which describes W^* as the sum of P^* and π^*. This equation can be thought of describing prior density for W^*. Rewrite it in a matrix form.

$$W^* = P^* + \pi^* + \varepsilon^{w*} \qquad \varepsilon^{w*} \sim N(0, \Omega_{w*}) \tag{62}$$

$$p(W^*|P^*, \pi^*, \sigma_{w*}^2) \propto -\tfrac{1}{2}(W^* - (P^* + \pi^*))' \Omega_{w*}^{-1} (W^* - (P^* + \pi^*))$$

Combining the above two conditional densities we obtain,

$$log\ \ p(W^*|Y, \bullet) \propto -\tfrac{1}{2}(W^* - \hat{W}^*)' D_{W*}^{-1} (W^* - \hat{W}^*)$$

where,

$$D_{W*} = (K_w^{'} \Omega_w^{-1} K_w + \Omega_{W*}^{-1})^{-1}$$

$$\hat{W}^* = D_{W*}(K_w^{'} \Omega_w^{-1}(K_w W - \mu_w) + \Omega_{w*}^{-1}(P^* + \pi^*))$$

The candidate draws are sampled from $N(\hat{W}^*, D_{W*})$ using the precision based algorithm.

Step 6. Derive the conditional distribution $p(r^*|Y, \bullet)$

The information about r^* comes from four sources. Below, we derive an expression for each of

these sources.

The first source is the output gap measurement equation. We rewrite it in a matrix notation as follows,

$$H_{rhog}ogap = \alpha_{ogap} - a^r r^* + \varepsilon^{ogap} \qquad \varepsilon^{ogap} \sim N(0, \Omega_{ogap}) \tag{63}$$

where,

$$\alpha_{ogap} = \begin{pmatrix} \rho_1^g(ogap_0) + \rho_2^g(ogap_{-1}) + a^r r_1 + \lambda^g(U_1 - U_1^*) \\ \rho_2^g(ogap_0) + a^r r_2 + \lambda^g(U_2 - U_2^*) \\ a^r r_3 + \lambda^g(U_3 - U_3^*) \\ \vdots \\ a^r r_T + \lambda^g(U_T - U_T^*) \end{pmatrix}$$

Ignoring any terms not involving r^*, we have
$log\ \ p(ogap|r^*, \bullet) \propto -\frac{1}{2}(ogap - H_{rhog}^{-1}(\alpha_{ogap} - a^r r^*))' H_{rhog}^{'} \Omega_{ogap}^{-1} H_{rhog}(ogap - H_{rhog}^{-1}(\alpha_{ogap} - a^r r^*))$

The second source is the state equation linking r^* to g^*. We rewrite it in a matrix notation as follows,

$$r^* = \zeta \triangle gdp^* + H^{-1}\varepsilon^d \qquad \varepsilon^d \sim N(0, \Omega_d), \quad where\ \ \Omega_d = diag(\omega_d^2, \sigma_d^2, ..., \sigma_d^2) \tag{64}$$

Ignoring any terms not involving r^*, the prior density for r^* is given by
$log\ \ p(r^*|gdp^*, \sigma_d^2, \bullet) \propto -\frac{1}{2}(r^* - \zeta \triangle gdp^*)' H' \Omega_d^{-1} H(r^* - \zeta \triangle gdp^*)$

The third source is the Taylor-type rule equation. We rewrite it in a matrix notation as follows,

$$M^{ri} = \alpha_{ri} + K_{\pi i} r^* + \varepsilon^i \quad \varepsilon^i \sim N(0, \Omega_i), \quad where\ \ \Omega_i = diag(e^{h_1^i}, e^{h_2^i}, ..., e^{h_T^i}) \tag{65}$$

where,

$$m_t^{ri} = i_t - \rho^i i_{t-1} - \pi_t^* + \rho^i \pi_{t-1}^* - \lambda^i(U_t - U_t^*) - \kappa^i(\pi_t - \pi_t^*),$$

$$M^{ri} = (m_1^{ri}, m_2^{ri}, ..., m_T^{ri})'$$

$$\alpha_{ri} = \begin{pmatrix} -\rho^i r_0^* \\ 0 \\ 0 \\ \vdots \\ 0 \end{pmatrix}, \quad K_{\pi i} = \begin{pmatrix} 1 & 0 & 0 & \cdots & 0 \\ -\rho^i & 1 & 0 & \cdots & 0 \\ 0 & -\rho^i & 1 & \cdots & 0 \\ \vdots & & & \ddots & \vdots \\ 0 & 0 & \cdots & -\rho^i & 1 \end{pmatrix}$$

Ignoring any terms not involving r^*, we have
$log\ \ p(i|r^*, \bullet) \propto -\frac{1}{2}\iota_T h^i - \frac{1}{2}(M^{ri} - (\alpha_{ri} + K_{\pi i} r^*))' \Omega_i^{-1}(M^{ri} - (\alpha_{ri} + K_{\pi i} r^*))$

The fourth source of information comes from the measurement equation that links survey to r^*. Rewrite the equation in a matrix notation,

$$F^r = \beta^r r^* + \varepsilon^{zr} \qquad \varepsilon^{zr} \sim N(0, \Omega_{zr}), \quad where \ \Omega_{zr} = diag(\sigma_{zr}^2, ..., \sigma_{zr}^2) \tag{66}$$

where,

$f_t^r = Z_t^r - C_t^r,$

$F^r = (f_1^r, ..., f_T^r)'$

Ignoring any terms not involving r^*, we have

$log \ p(Z^r|r^*, \bullet) \propto -\frac{1}{2}(F^r - \beta^r r^*)'\Omega_{zr}^{-1}(F^r - \beta^r r^*)$

Combining the above four conditional densities we obtain,

$log \ p(r^*|Y, \bullet) \propto -\frac{1}{2}(r^* - \hat{r}^*)' D_{r*}^{-1}(r^* - \hat{r}^*)$

where,

$D_{r*} = ((-a^r)^2\Omega_{ogap}^{-1} + H'\Omega_d^{-1}H + K_{\pi i}'\Omega_i^{-1}K_{\pi i} + (\beta^r)(2)\Omega_{zr}^{-1})^{-1}$

$\hat{r}^* = D_{r*}(-a^r\Omega_{ogap}^{-1}(H_{rhog}ogap - \alpha_{ogap}) + H'\Omega_d^{-1}H\zeta\triangle gdp^* + K_{\pi i}'\Omega_i^{-1}(M^{ri} - \alpha_{ri}) + \beta^r\Omega_{zr}^{-1}F^r)$

The candidate draws are sampled from $N(\hat{r}^*, D_{r*})$ using the precision based algorithm.

Step 7. Derive the conditional distribution $p(\lambda^p|Y, \bullet)$

The information about λ^p comes from two sources. Below, we derive an expression for each of these two sources.

The first source is the productivity measurement equation. Rewrite it in a matrix notation,

$$B = X_u\lambda^p + \varepsilon^p \qquad \varepsilon^p \sim N(0, \Omega_p) \tag{67}$$

where,

$B = (\tilde{p}_1 - \rho^p\tilde{p}_0, ..., \tilde{p}_T - \rho^p\tilde{p}_{T-1})$
$\tilde{p}_t = p_t - p_t^*$
$\tilde{u}_t = U_t - U_t^*$
$X_u = diag(\tilde{u}_1, ..., \tilde{u}_T)$

Ignoring any terms not involving λ^p, we have the likelihood

$$log\ \ p(p|\lambda^p, \bullet) \propto -\tfrac{1}{2}(B - X_u\lambda^p)'\Omega_p^{-1}(B - X_u\lambda^p)$$

The second source of information comes from state equation for λ^p. We rewrite it in a matrix notation as follows,

$$H\lambda^p = \varepsilon^{\lambda p} \qquad \varepsilon^{\lambda p} \sim N(0, \Omega_{\lambda p}), \quad where\ \ \Omega_{\lambda p} = diag(\omega_{\lambda p}^2, \sigma_{\lambda p}^2, ..., \sigma_{\lambda p}^2) \tag{68}$$

Ignoring any terms not involving λ^p, the prior density for λ^p is given by

$$log\ \ p(\lambda^p|\sigma_{\lambda p}^2, \Omega_{\lambda p}) \propto -\tfrac{1}{2}(\lambda^p)'H'\Omega_{\lambda p}^{-1}H(\lambda^p)$$

Combining the above two conditional densities we obtain,

$$log\ \ p(\lambda^p|Y, \bullet) \propto -\tfrac{1}{2}(\lambda^p - \hat{\lambda}^p)' D_{\lambda^p}^{-1}(\lambda^p - \hat{\lambda}^p)$$

where,

$D_{\lambda^p} = (H'\Omega_{\lambda p}^{-1}H + X_u'\Omega_p^{-1}X_u)^{-1}$

$\hat{\lambda}^p = D_{\lambda^p}(X_u'\Omega_p^{-1}B)$

The candidate draws are sampled from $N(\hat{\lambda}^p, D_{\lambda^p})$ using the precision based algorithm.

Step 8. Derive the conditional distribution $p(\rho^\pi|Y, \bullet)$

The information about ρ^π comes from two sources. Below, we derive an expression for each of these two sources.

First, we define some notation,

$\tilde{\pi}_t = \pi_t - \pi_t^*$
$\tilde{u}_t = U_t - U_t^*$
$\tilde{\Pi} = (\tilde{\pi}_1, ..., \tilde{\pi}_T)'$
$\tilde{u} = (\tilde{u}_1, ..., \tilde{u}_T)'$

The first source is the price inflation measurement equation. Rewrite it in a matrix notation,

$$\tilde{\Pi} + \Lambda\tilde{u} = X_\pi\rho^\pi + \varepsilon^\pi \qquad \varepsilon^\pi \sim N(0, \Omega_\pi) \tag{69}$$

where,

$X_\pi = diag(\tilde{\pi}_0, ..., \tilde{\pi}_{T-1})$
$\Lambda = diag(-\lambda_1^\pi, ..., -\lambda_T^\pi)$

Ignoring any terms not involving ρ^π, we have the likelihood

$log\ \ p(\pi|\rho^{\pi},\bullet) \propto -\frac{1}{2}(\tilde{\Pi} - (X_{\pi}\rho^{\pi} - \Lambda\tilde{u}))'\Omega_{\pi}^{-1}(\tilde{\Pi} - (X_{\pi}\rho^{\pi} - \Lambda\tilde{u}))$

The second source comes from state equation for ρ^{π}. We rewrite it in a matrix notation as follows,

$$H\rho^{\pi} = \varepsilon^{\rho\pi} \qquad \varepsilon^{\rho\pi} \sim N(0, \Omega_{\rho\pi}), \quad where\ \ \Omega_{\rho\pi} = diag(\omega_{\rho\pi}^2, \sigma_{\rho\pi}^2, ..., \sigma_{\rho\pi}^2) \tag{70}$$

$0 < \rho_t^{\pi} < 1$ for t=1,....,T

Ignoring any terms not involving ρ^{π}, the prior density for ρ^{π} is given by

$log\ \ p(\rho^{\pi}|\sigma_{\rho\pi}^2, \Omega_{\rho\pi}) \propto -\frac{1}{2}(\rho^{\pi})'H'\Omega_{\rho\pi}^{-1}H(\rho^{\pi}) + g_{\rho\pi}(\rho^{\pi}, \sigma_{\rho\pi}^2)$

where,

$$g_{\rho\pi}(\rho^{\pi}, \sigma_{\rho\pi}^2) = -\sum_{t=2}^{T} log\left(\Phi\left(\frac{1-\rho_{t-1}^{\pi}}{\sigma_{\rho\pi}}\right) - \Phi\left(\frac{0-\rho_{t-1}^{\pi}}{\sigma_{\rho\pi}}\right)\right)$$

Combining the above two conditional densities we obtain,

$log\ \ p(\rho^{\pi}|Y,\bullet) \propto -\frac{1}{2}(\rho^{\pi} - \hat{\rho}^{\pi})' D_{\rho^{\pi}}^{-1}(\rho^{\pi} - \hat{\rho}^{\pi}) + g_{\rho\pi}(\rho^{\pi}, \sigma_{\rho\pi}^2)$

where,

$D_{\rho^{\pi}} = (H'\Omega_{\rho\pi}^{-1}H + X_{\pi}'\Omega_{\pi}^{-1}X_{\pi})^{-1}$

$\hat{\rho}^{\pi} = D_{\rho^{\pi}}(X_{\pi}'\Omega_{\pi}^{-1}(\tilde{\Pi} + \Lambda\tilde{u}))$

The addition of the term $g_{\rho\pi}(\rho^{\pi}, \sigma_{\rho\pi}^2)$ leads to a non-standard density. Accordingly, we sample ρ^{π} using an independence-chain Metropolis-Hastings (MH) procedure. This involves first generating candidate draws from $N(\hat{\rho}^{\pi}, D_{\rho^{\pi}})$ using the precision based algorithm that are then accepted or rejected based on accept-reject Metropolis-Hastings (ARMH) algorithm (discussed in Chan and Strachan, 2012).

Step 9. Derive the conditional distribution $p(\lambda^{\pi}|Y,\bullet)$

The information about λ^{π} comes from two sources. Below, we derive an expression for each of these two sources.

First, we define some notation,

$\tilde{\pi}_t = \pi_t - \pi_t^*$
$\tilde{u}_t = U_t - U_t^*$
$NW = (\tilde{\pi}_1 - \rho_1^{\pi}\tilde{\pi}_0, ..., \tilde{\pi}_T - \rho_T^{\pi}\tilde{\pi}_{T-1})'$

The first source is the price inflation measurement equation. Rewrite it in a matrix notation,

$$NW = X_u\lambda^\pi + \varepsilon^\pi \qquad \varepsilon^\pi \sim N(0, \Omega_\pi) \tag{71}$$

where,

$X_u = diag(\tilde{u}_1, ..., \tilde{u}_T)$

Ignoring any terms not involving λ^π, we have the likelihood

$$log\ \ p(\pi|\lambda^\pi, \bullet) \propto -\tfrac{1}{2}(NW - X_u\lambda^\pi)'\Omega_\pi^{-1}(NW - X_u\lambda^\pi)$$

The second source comes from state equation for λ^π. We rewrite it in a matrix notation as follows,

$$H\lambda^\pi = \varepsilon^{\lambda\pi} \qquad \varepsilon^{\lambda\pi} \sim N(0, \Omega_{\lambda\pi}), \quad where\ \ \Omega_{\lambda\pi} = diag(\omega^2_{\lambda\pi}, \sigma^2_{\lambda\pi}, ..., \sigma^2_{\lambda\pi}) \tag{72}$$

$-1 < \lambda^\pi_t < 0$ for t=1,....,T

Ignoring any terms not involving λ^π, the prior density for λ^π is given by

$log\ \ p(\lambda^\pi|\sigma^2_{\lambda\pi}, \Omega_{\lambda\pi}) \propto -\frac{1}{2}(\lambda^\pi)'H'\Omega^{-1}_{\lambda\pi}H(\lambda^\pi) + g_{\lambda\pi}(\lambda^\pi, \sigma^2_{\lambda\pi})$

where,

$$g_{\lambda\pi}(\lambda^\pi, \sigma^2_{\lambda\pi}) = -\sum_{t=2}^{T} log\left(\Phi\left(\frac{0 - \lambda^\pi_{t-1}}{\sigma_{\lambda\pi}}\right) - \Phi\left(\frac{-1 - \lambda^\pi_{t-1}}{\sigma_{\lambda\pi}}\right)\right)$$

Combining the above two conditional densities we obtain,

$$log\ \ p(\lambda^\pi|Y, \bullet) \propto -\tfrac{1}{2}(\lambda^\pi - \hat{\lambda}^\pi)'D^{-1}_{\lambda^\pi}(\lambda^\pi - \hat{\lambda}^\pi) + g_{\lambda\pi}(\lambda^\pi, \sigma^2_{\lambda\pi})$$

where,

$D_{\lambda^\pi} = (H'\Omega^{-1}_{\lambda\pi}H + X'_u\Omega^{-1}_\pi X_u)^{-1}$

$\hat{\lambda}^\pi = D_{\lambda^\pi}(X'_u\Omega^{-1}_\pi NW)$

The addition of the term $g_{\lambda\pi}(\lambda^\pi, \sigma^2_{\lambda\pi})$ leads to a non-standard density. Accordingly, we sample λ^π using an independence-chain Metropolis-Hastings (MH) procedure. This involves first generating candidate draws from $N(\hat{\lambda}^\pi, D_{\lambda^\pi})$ using the precision based algorithm that are then accepted or rejected based on accept-reject Metropolis-Hastings (ARMH) algorithm (discussed in Chan and Strachan, 2012).

Step 10. Derive the conditional distribution $p(\rho^w|Y,\bullet)$

The information about ρ^w comes from two sources. Below, we derive an expression for each of these two sources.

First, we define some notation,

$\tilde{w}_t = w_t - w_t^*$
$\tilde{u}_t = U_t - U_t^*$
$\tilde{w} = (\tilde{w}_1, ..., \tilde{w}_T)'$
$\tilde{u} = (\tilde{u}_1, ..., \tilde{u}_T)'$
$\tilde{\pi}_t = \pi_t - \pi_t^*$
$\tilde{\pi} = (\tilde{\pi}_1, ..., \tilde{\pi}_T)'$

The first source is the wage inflation measurement equation. Rewrite it in a matrix notation,

$$\tilde{w} + \Lambda^w \tilde{u} + \Lambda^{w\pi}\tilde{\pi} = X_w \rho^w + \varepsilon^{\rho w} \qquad \varepsilon^{\rho w} \sim N(0, \Omega_w) \tag{73}$$

where,

$X_w = diag(\tilde{w}_0, ..., \tilde{w}_{T-1})$
$\Lambda^w = diag(-\lambda_1^w, ..., -\lambda_T^w)$
$\Lambda^{w\pi} = diag(-\kappa_1^w, ..., -\kappa_T^w)$

Ignoring any terms not involving ρ^w, we have the likelihood

$$log\ \ p(w|\rho^w, \bullet) \propto -\tfrac{1}{2}(\tilde{w} - (X_w\rho^w - \Lambda^w\tilde{u} - \Lambda^{w\pi}\tilde{\pi}))'\Omega_w^{-1}(\tilde{w} - (X_w\rho^w - \Lambda^w\tilde{u} - \Lambda^{w\pi}\tilde{\pi}))$$

The second source comes from state equation for ρ^w. We rewrite it in a matrix notation as follows,

$$H\rho^w = \varepsilon^{\rho w} \qquad \varepsilon^{\rho w} \sim N(0, \Omega_{\rho w}), \quad where\ \ \Omega_{\rho w} = diag(\omega_{\rho w}^2, \sigma_{\rho w}^2, ..., \sigma_{\rho w}^2) \tag{74}$$

$0 < \rho_t^w < 1$ for t=1,....,T

Ignoring any terms not involving ρ^w, the prior density for ρ^w is given by

$log\ \ p(\rho^w|\sigma_{\rho w}^2, \Omega_{\rho w}) \propto -\tfrac{1}{2}(\rho^w)'H'\Omega_{\rho w}^{-1}H(\rho^w) + g_{\rho w}(\rho^w, \sigma_{\rho w}^2)$

where,

$$g_{\rho w}(\rho^w, \sigma^2_{\rho w}) = -\sum_{t=2}^{T} log\left(\Phi\left(\frac{1-\rho^w_{t-1}}{\sigma_{\rho w}}\right) - \Phi\left(\frac{0-\rho^w_{t-1}}{\sigma_{\rho w}}\right)\right)$$

Combining the above two conditional densities we obtain,

$$log\ \ p(\rho^w|Y,\bullet) \propto -\tfrac{1}{2}(\rho^w - \hat{\rho}^w)' D^{-1}_{\rho^w}(\rho^w - \hat{\rho}^w) + g_{\rho w}(\rho^w, \sigma^2_{\rho w})$$

where,

$D_{\rho^w} = (H'\Omega^{-1}_{\rho w} H + X'_w \Omega^{-1}_w X_w)^{-1}$

$\hat{\rho}^w = D_{\rho^w}(X'_w \Omega^{-1}_w(\tilde{w} + \Lambda^w \tilde{u} + \Lambda^{w\pi}\tilde{\pi}))$

The addition of the term $g_{\rho\pi}(\rho^\pi, \sigma^2_{\rho\pi})$ leads to a non-standard density. Accordingly, we sample ρ^π using an independence-chain Metropolis-Hastings (MH) procedure. This involves first generating candidate draws from $N(\hat{\rho}^\pi, D_{\rho^\pi})$ using the precision based algorithm that are then accepted or rejected based on accept-reject Metropolis-Hastings (ARMH) algorithm (discussed in Chan and Strachan, 2012).

Step 11. Derive the conditional distribution $p(\lambda^w|Y,\bullet)$

The information about λ^w comes from two sources. Below, we derive an expression for each of these two sources.

First, we define some notation,

$\tilde{w}_t = w_t - w^*_t$
$\tilde{u}_t = U_t - U^*_t$
$\tilde{\pi}_t = \pi_t - \pi^*_t$
$B^w = (\tilde{w}_1 - \rho^w_1 \tilde{w}_0 - \kappa^w_1 \tilde{\pi}_1, ..., \tilde{w}_T - \rho^w_T \tilde{w}_{T-1} - \kappa^w_{T-1}\tilde{\pi}_T)'$

The first source is the wage inflation measurement equation. Rewrite it in a matrix notation,

$$B^w = X_u \lambda^w + \varepsilon^w \qquad \varepsilon^w \sim N(0, \Omega_w) \tag{75}$$

where,

$X_u = diag(\tilde{u}_1, ..., \tilde{u}_T)$

Ignoring any terms not involving λ^w, we have the likelihood

$$log\ \ p(w|\lambda^w,\bullet) \propto -\tfrac{1}{2}(B^w - X_u\lambda^w)'\Omega^{-1}_w(B^w - X_u\lambda^w)$$

The second source comes from state equation for λ^w. We rewrite it in a matrix notation

as follows,

$$H\lambda^w = \varepsilon^{\lambda w} \qquad \varepsilon^{\lambda w} \sim N(0, \Omega_{\lambda w}), \quad where\ \ \Omega_{\lambda w} = diag(\omega^2_{\lambda w}, \sigma^2_{\lambda w}, ..., \sigma^2_{\lambda w}) \tag{76}$$

$-1 < \lambda^w_t < 0$ for t=1,....,T

Ignoring any terms not involving λ^w, the prior density for λ^w is given by

$log\ \ p(\lambda^w|\sigma^2_{\lambda w}, \Omega_{\lambda w}) \propto -\frac{1}{2}(\lambda^w)' H' \Omega^{-1}_{\lambda w} H(\lambda^w) + g_{\lambda w}(\lambda^w, \sigma^2_{\lambda w})$

where,

$$g_{\lambda w}(\lambda^w, \sigma^2_{\lambda w}) = -\sum_{t=2}^{T} log\left(\Phi\left(\frac{0 - \lambda^w_{t-1}}{\sigma_{\lambda w}}\right) - \Phi\left(\frac{-1 - \lambda^w_{t-1}}{\sigma_{\lambda w}}\right)\right)$$

Combining the above two conditional densities we obtain,

$log\ \ p(\lambda^w|Y, \bullet) \propto -\frac{1}{2}(\lambda^w - \hat{\lambda}^w)' D^{-1}_{\lambda^w}(\lambda^w - \hat{\lambda}^w) + g_{\lambda w}(\lambda^w, \sigma^2_{\lambda w})$

where,

$D_{\lambda^w} = (H' \Omega^{-1}_{\lambda w} H + X'_u \Omega^{-1}_w X_u)^{-1}$

$\hat{\lambda}^w = D_{\lambda^w}(X'_u \Omega^{-1}_w B^w)$

The addition of the term $g_{\lambda w}(\lambda^w, \sigma^2_{\lambda w})$ leads to a non-standard density. Accordingly, we sample λ^w using an independence-chain Metropolis-Hastings (MH) procedure. This involves first generating candidate draws from $N(\hat{\lambda}^w, D_{\lambda^w})$ using the precision based algorithm that are then accepted or rejected based on accept-reject Metropolis-Hastings (ARMH) algorithm (discussed in Chan and Strachan, 2012).

Step 12. Derive the conditional distribution $p(\kappa^w|Y, \bullet)$

The information about $kappa^w$ comes from two sources. Below, we derive an expression for each of these two sources.

First, we define some notation,

$\tilde{w}_t = w_t - w^*_t$
$\tilde{u}_t = U_t - U^*_t$
$\tilde{\pi}_t = \pi_t - \pi^*_t$
$B^{\kappa w} = (\tilde{w}_1 - \rho^w_1 \tilde{w}_0 - \lambda^w_1 \tilde{u}_1, ..., \tilde{w}_T - \rho^w_T \tilde{w}_{T-1} - \lambda^w_{T-1} \tilde{u}_T)'$

The first source is the wage inflation measurement equation. Rewrite it in a matrix notation,

$$B^{\kappa w} = X_\pi \kappa^w + \varepsilon^w \qquad \varepsilon^w \sim N(0, \Omega_w) \tag{77}$$

where,

$X_\pi = diag(\tilde{\pi}_1, ..., \tilde{\pi}_T)$

Ignoring any terms not involving κ^w, we have the likelihood

$$log\ \ p(w|\kappa^w, \bullet) \propto -\tfrac{1}{2}(B^{\kappa w} - X_\pi \kappa^w)' \Omega_w^{-1} (B^{\kappa w} - X_\pi \kappa^w)$$

The second source comes from state equation for κ^w. We rewrite it in a matrix notation as follows,

$$H\kappa^w = \varepsilon^{\kappa w} \qquad \varepsilon^{\kappa w} \sim N(0, \Omega_{\kappa w}), \quad where\ \ \Omega_{\kappa w} = diag(\omega_{\kappa w}^2, \sigma_{\kappa w}^2, ..., \sigma_{\kappa w}^2) \tag{78}$$

Ignoring any terms not involving κ^w, the prior density for κ^w is given by

$$log\ \ p(\kappa^w | \sigma_{\kappa w}^2, \Omega_{\kappa w}) \propto -\tfrac{1}{2}(\kappa^w)' H' \Omega_{\kappa w}^{-1} H(\kappa^w)$$

Combining the above two conditional densities we obtain,

$$log\ \ p(\kappa^w | Y, \bullet) \propto -\tfrac{1}{2}(\kappa^w - \hat{\kappa}^w)' D_{\kappa^w}^{-1} (\kappa^w - \hat{\kappa}^w)$$

where,

$D_{\kappa^w} = (H' \Omega_{\kappa w}^{-1} H + X_\pi' \Omega_w^{-1} X_\pi)^{-1}$

$\hat{\kappa}^w = D_{\kappa^w} (X_\pi' \Omega_w^{-1} B^{\kappa w})$

The candidate draws are sampled from $N(\hat{\kappa}^w, D_{\kappa^w})$ using the precision based algorithm.

Step 13. Derive the conditional distribution $p(h^p, h^\pi, h^w, h^i | Y, \bullet)$

Given parameters and other latent states, the stochastic volatility, h^p, h^π, h^w, h^i are conditionally independent and so can be drawn separately. Following, Chan, Koop, and Potter (2013; 2016), we draw h^p, h^π, h^w, h^i using the Accept-Reject independence-chain Metropolis Hastings (ARMH) algorithm of Chan and Strachan (2012; page 32-34).

Step 14. Derive the conditional distribution $p(C^u, C^g, C^\pi, C^r | Y, \bullet)$

Given parameters and other latent states, C^u, C^g, C^π, C^r are conditionally independent and so can be drawn separately.

Beginning with C^u, the information about it comes from two sources. Below, we derive an expression for each of these two sources.

The first source is the measurement equation linking survey to U^*. Rewrite it in a matrix notation,

$$N^{zu} = C^u + \varepsilon^{zu} \qquad \varepsilon^{zu} \sim N(0, \Omega_{zu}) \tag{79}$$

where,

$n_t^{zu} = Z_t^u - \beta^u U^*$
$N^{zu} = (n_1^{zu}, n_2^{zu}, ..., n_T^{zu})'$
$\Omega_{zu} = diag(\sigma_{zu}^2, ..., \sigma_{zu}^2)$

Ignoring any terms not involving C^u, we have the likelihood

$$log\ \ p(Z^u|C^u, \bullet) \propto -\tfrac{1}{2}(N^{zu} - C^u)'\Omega_{zu}^{-1}(N^{zu} - C^u)$$

The second source comes from state equation for C^u. We rewrite it in a matrix notation as follows,

$$HC^u = \alpha_{cu} + \varepsilon^{cu} \qquad \varepsilon^{cu} \sim N(0, \Omega_{cu}), \quad where\ \ \Omega_{cu} = diag(\omega_{cu}^2, \sigma_{cu}^2, ..., \sigma_{cu}^2) \tag{80}$$

where,

$$\alpha_{cu} = \begin{pmatrix} C_0^u \\ 0 \\ 0 \\ \vdots \\ 0 \end{pmatrix}$$

Ignoring any terms not involving C^u, the prior density for C^u is given by

$$log\ \ p(C^u|\sigma_{cu}^2, \Omega_{cu}) \propto -\tfrac{1}{2}(C^u - H^{-1}\alpha_{cu})'H'\Omega_{cu}^{-1}H(C^u - H^{-1}\alpha_{cu})$$

Combining the above two conditional densities we obtain,

$$log\ \ p(C^u|Y, \bullet) \propto -\tfrac{1}{2}(C^u - \hat{C}^u)'D_{C^u}^{-1}(C^u - \hat{C}^u)$$

where,

$D_{C^u} = (H'\Omega_{cu}^{-1}H + \Omega_{zu}^{-1})^{-1}$

$\hat{C}^u = D_{C^u}(H'\Omega_{cu}^{-1}\alpha_{cu} + \Omega_{zu}^{-1}N^{zu})$

The candidate draws are sampled from $N(\hat{C}^u, D_{C^u})$ using the precision based algorithm.

Following similar logic,

$N(\hat{C}^r, D_{C^r})$

$D_{C^r} = (H'\Omega_{cr}^{-1}H + \Omega_{zr}^{-1})^{-1}$

$\hat{C}^r = D_{C^r}(H'\Omega_{cr}^{-1}\alpha_{cr} + \Omega_{zr}^{-1}N^{zr})$

where,

$n_t^{zr} = Z_t^r - \beta^r r^*$
$N^{zr} = (n_1^{zr}, n_2^{zr}, ..., n_T^{zr})'$
$\Omega_{zr} = diag(\sigma_{zr}^2, ..., \sigma_{zr}^2)$

$N(\hat{C}^\pi, D_{C^\pi})$

$D_{C^\pi} = (H'\Omega_{c\pi}^{-1}H + \Omega_{z\pi}^{-1})^{-1}$

$\hat{C}^\pi = D_{C^\pi}(H'\Omega_{c\pi}^{-1}\alpha_{c\pi} + \Omega_{z\pi}^{-1}N^{z\pi})$

where,

$n_t^{z\pi} = Z_t^\pi - \beta^\pi \pi^*$
$N^{z\pi} = (n_1^{z\pi}, n_2^{z\pi}, ..., n_T^{z\pi})'$
$\Omega_{z\pi} = diag(\sigma_{z\pi}^2, ..., \sigma_{z\pi}^2)$

$N(\hat{C}^g, D_{C^g})$

$D_{C^g} = (H'\Omega_{cg}^{-1}H + \Omega_{zg}^{-1})^{-1}$

$\hat{C}^g = D_{C^g}(H'\Omega_{cg}^{-1}\alpha_{cg} + \Omega_{zg}^{-1}N^{zg})$

where,

$n_t^{zg} = Z_t^g + \beta^g \alpha_g - \beta^g gdp^*$
$N^{zg} = (n_1^{zg}, n_2^{zg}, ..., n_T^{zg})'$
$\Omega_{zg} = diag(\sigma_{zg}^2, ..., \sigma_{zg}^2)$
$\alpha_g = (gdp_0^*, 0, 0, ..., 0)'$

Step 15. Derive the conditional distribution $p(D|Y, \bullet)$

Given the posterior draws of r^*, ζ, and g^*, the posterior draw for D is constructed as,

$$D = r^* - \zeta g^* \tag{81}$$

Step 16. Derive the conditional distribution $p(\theta|Y, \bullet)$

There are 40 parameters in the vector θ. These parameters are drawn in 38 separate blocks using standard regression procedures. Following similar notation to Chan, Koop, and Potter (2016), we denote θ_{-x} to refer all parameters in θ except the parameter x.

Substep 16.1 Derive the conditional distribution $p(\rho^u|Y, \bullet)$

Given the stationary constraints, $\rho_1^u + \rho_2^u < 1$, $\rho_2^u - \rho_1^u < 1$, and $|\rho_2^u| < 1$

$\rho^u = (\rho_1^u, \rho_2^u)'$ is a bivariate truncated normal. To obtain draws from this truncated normal distribution, ARMH sampling algorithm is applied to the candidate draws from the proposal density, $N(\hat{\rho}^u, D_{\rho u})$.

$D_{\rho u} = (V_{\rho u}^{-1} + X_u^{'} X_u/\sigma_u^2)^{-1}$

$\hat{\rho}^u = D_{\rho u}(V_{\rho u}^{-1}\rho_0^u + X_u^{'}(\tilde{u} - \phi^u ogap)/\sigma_u^2)$

where,

$V_{\rho u}^{-1}$ is the prior variance and ρ_0^u is the prior mean,

$$X_u = \begin{pmatrix} \tilde{u}_0 & \tilde{u}_{-1} \\ \tilde{u}_1 & \tilde{u}_0 \\ \vdots & \\ \tilde{u}_{T-1} & \tilde{u}_{T-2} \end{pmatrix}$$

Substep 16.2 Derive the conditional distribution $p(\sigma_u^2|Y, \bullet)$

$p(\sigma_u^2|Y, \bullet)$ is a standard inverse-Gamma density,

$$p(\sigma_u^2|Y, \bullet) \sim IG(\nu_{u0} + \tfrac{T}{2}, S_{u0} + \tfrac{1}{2}\sum_{t=1}^{T}(\tilde{u}_t - \rho_1^u \tilde{u}_{t-1} - \rho_2^u \tilde{u}_{t-2} - \phi^u ogap_t)^2)$$

Substep 16.3 Derive the conditional distribution $p(\phi^u|Y, \bullet)$

Given the constraint $\phi^u < 0$, the conditional distribution $p(\phi^u|Y, \bullet)$ is a truncated normal density. The candidate draws are sampled from the proposal distribution $N(\hat{\phi}^u, D_{\phi u})$ using the precision based algorithm, and simple Accept-Reject step is applied to the candidate draws.

Rewrite the unemployment rate (gap) measurement equation in matrix notation as

$$Y^{\phi} = \phi^{u} ogap + \varepsilon^{u} \qquad \varepsilon^{u} \sim N(0, \sigma_u^2) \tag{82}$$

where,

$y_t^{\phi} = \tilde{u}_t - \rho_1^u \tilde{u}_{t-1} - \rho_2^u \tilde{u}_{t-2}$
$Y^{\phi} = (y_1^{\phi}, ..., y_T^{\phi})'$

$D_{\phi u} = (V_{\phi u}^{-1} + ogap^{'} ogap/\sigma_u^2)^{-1}$

$\hat{\phi}^u = D_{\phi u}(V_{\phi u}^{-1}\phi_0^u + ogap^{'} Y^{\phi}/\sigma_u^2)$

where,

$V_{\phi u}^{-1}$ is the prior variance and ϕ_0^u is the prior mean,

Substep 16.4 Derive the conditional distribution $p(\sigma_{u*}^2|Y, \bullet)$

$p(\sigma_{u*}^2|Y, \bullet)$ is a non-standard density because U^* is a bounded random walk,

$log\ \ p(\sigma_{u*}^2|Y, \bullet) \propto -(\nu_{u*0}+1) log\ \ \sigma_{u*}^2 - \frac{S_{u*0}}{\sigma_{u*}^2} - \frac{T-1}{2} log\ \ \sigma_{u*}^2 - \frac{1}{2\sigma_{u*}^2}\sum_{t=2}^{T}(U_t^* - U_{t-1}^*)^2 + g_{u*}(U^*, \sigma_{u*}^2)$

The candidate draws from $p(\sigma_{u*}^2|Y, \bullet)$ are obtained via the MH step with the proposal density

$$IG(\nu_{u*0} + \tfrac{T-1}{2}, S_{u*0} + \tfrac{1}{2}\sum_{t=2}^{T}(U_t^* - U_{t-1}^*)^2)$$

Substep 16.5 Derive the conditional distribution $p(\beta^u|Y, \bullet)$

Candidate draws are sampled from $N(\hat{\beta}^u, D_{\beta u})$ using the precision based algorithm.

where,

$D_{\beta u} = (V_{\beta u}^{-1} + U^{*'}\Omega_{zu}^{-1}U^*)^{-1}$

$\hat{\beta}^u = D_{\beta u}(V_{\beta u}^{-1}\beta_0^u + U^{*'}\Omega_{zu}^{-1}J^{zu})$

$j_t^{zu} = Z_t^u - C_t^u$
$J^{zu} = (j_1^{zu}, ..., j_T^{zu})'$

$V_{\beta u}^{-1}$ is the prior variance and β_0^u is the prior mean for β^u

Substep 16.6 Derive the conditional distribution $p(\sigma_{zu}^2|Y, \bullet)$

$p(\sigma^2_{zu}|Y,\bullet)$ is a standard inverse-Gamma density,

Candidate draws are sampled from

$$p(\sigma^2_{zu}|Y,\bullet) \sim IG(\nu_{zu0} + \tfrac{T}{2}, S_{zu0} + \tfrac{1}{2}\sum_{t=1}^{T}(Z^u_t - C^u_t - \beta^u U^*)^2)$$

Substep 16.7 Derive the conditional distribution $p(\sigma^2_{cu}|Y,\bullet)$

$p(\sigma^2_{cu}|Y,\bullet)$ is a standard inverse-Gamma density,

Candidate draws are sampled from

$$p(\sigma^2_{cu}|Y,\bullet) \sim IG(\nu_{cu0} + \tfrac{T-1}{2}, S_{cu0} + \tfrac{1}{2}\sum_{t=2}^{T}(C^u_t - C^u_{t-1})^2)$$

Substep 16.8 Derive the conditional distribution $p(\sigma^2_{gdp*}|Y,\bullet)$

$p(\sigma^2_{gdp*}|Y,\bullet)$ is a standard inverse-Gamma density,

Candidate draws are sampled from

$$p(\sigma^2_{gdp*}|Y,\bullet) \sim IG(\nu_{gdp*0} + \tfrac{T-1}{2}, S_{gdp*0} + (gdp^* - \alpha_{gdp*})' * H_2 H_2 * (gdp^* - \alpha_{gdp*})/2)$$

where (although they are defined above but for convenience we redefine them),

$$\alpha_{gdp*} = \begin{pmatrix} gdp^*_0 + \triangle gdp^*_0 \\ -gdp^*_0 \\ 0 \\ \vdots \\ 0 \end{pmatrix}, \quad H_2 = \begin{pmatrix} 1 & 0 & 0 & 0 & \cdots & 0 \\ -2 & 1 & 0 & 0 & \cdots & 0 \\ 1 & -2 & 1 & 0 & \cdots & 0 \\ 0 & 1 & -2 & 1 & \cdots & 0 \\ \vdots & & & & \ddots & \vdots \\ 0 & \cdots & 0 & 1 & -2 & 1 \end{pmatrix}$$

H_2 is a band matrix with unit determinant and hence is invertible.

Substep 16.9 Derive the conditional distribution $p(\rho^g|Y,\bullet)$

Given the stationary constraints, $\rho^g_1 + \rho^g_2 < 1$, $\rho^g_2 - \rho^g_1 < 1$, and $|\rho^g_2| < 1$

$\rho^g = (\rho^g_1, \rho^g_2)'$ is a bivariate truncated normal. To obtain draws from this truncated normal distribution, ARMH sampling algorithm is applied to the candidate draws from the proposal density, $N(\hat{\rho}^g, D_{\rho g})$.

$$D_{\rho g} = (V^{-1}_{\rho g} + X'_{\rho g} X_{\rho g}/\sigma^2_{ogap})^{-1}$$

$$\hat{\rho}^g = D_{\rho g}(V^{-1}_{\rho g}\rho^g_0 + X'_{\rho g} Y_{ogap}/\sigma^2_{ogap})$$

where,

$V_{\rho g}^{-1}$ is the prior variance and ρ_0^g is the prior mean,

$$X_{\rho g} = \begin{pmatrix} 0 & 0 \\ ogap_1 & 0 \\ ogap_2 & ogap_1 \\ \vdots & \\ ogap_{T-1} & ogap_{T-2} \end{pmatrix}$$

$y_t^{ogap} = ogap_t - a^r(r_t - r_{t-1}) - \lambda^g \tilde{u}_t)$
$Y_{ogap} = (y_1^{ogap}, ..., y_T^{ogap})'$

Substep 16.10 Derive the conditional distribution $p(a^r|Y, \bullet)$

Candidate draws are sampled from $N(\hat{a}^r, D_{ar})$ using the precision based algorithm.

where,

$D_{ar} = (V_{ar}^{-1} + X_{ar}^{'}\Omega_{ogap}^{-1}X_{ar})^{-1}$

$\hat{a}^r = D_{ar}(V_{ar}^{-1}a_0^r + X_{ar}^{'}\Omega_{ogap}^{-1}J^{ar})$

$j_t^{ar} = ogap_t - \rho_1^g ogap_{t-1} - \rho_2^g ogap_{t-2} - \lambda^g \tilde{u}_t$
$J^{ar} = (j_1^{ar}, ..., j_T^{ar})'$
$X_{ar} = (\tilde{r}_1, ..., \tilde{r}_T)'$
$\tilde{r}_t = r_t - r_t^*$

V_{ar}^{-1} is the prior variance and a_0^r is the prior mean for a^r

Substep 16.11 Derive the conditional distribution $p(\lambda^g|Y, \bullet)$

Given the constraint $\lambda^g < 0$, the conditional distribution $p(\lambda^g|Y, \bullet)$ is a truncated normal density. The candidate draws are sampled from the proposal distribution $N(\hat{\lambda}^g, D_{\lambda g})$ using the precision based algorithm, and simple Accept-Reject step is applied to the candidate draws.

where,

$D_{\lambda g} = (V_{\lambda g}^{-1} + X_u^{'}\Omega_{ogap}^{-1}X_u)^{-1}$

$\hat{\lambda}^g = D_{\lambda g}(V_{\lambda g}^{-1}\lambda_0^g + X_u^{'}\Omega_{ogap}^{-1}B^g)$

$b_t^g = ogap_t - \rho_1^g ogap_{t-1} - \rho_2^g ogap_{t-2} - a^r \tilde{r}_t$
$B^g = (b_1^g, ..., b_T^g)'$
$X_u = diag(\tilde{u}_1, ..., \tilde{u}_T)'$
$\tilde{r}_t = r_t - r_t^*$

$V_{\lambda g}^{-1}$ is the prior variance and λ_0^g is the prior mean for λ^g

Substep 16.12 Derive the conditional distribution $p(\sigma_{ogap}^2|Y,\bullet)$

$p(\sigma_{ogap}^2|Y,\bullet)$ is a standard inverse-Gamma density,

Candidate draws are sampled from

$$p(\sigma_{ogap}^2|Y,\bullet) \sim IG(\nu_{ogap0}+\tfrac{T}{2}, S_{ogap0}+\tfrac{1}{2}\sum_{t=1}^{T}(ogap_t-\rho_1^g ogap_{t-1}-\rho_2^g ogap_{t-2}-\lambda^g\tilde{u}_t-a^r\tilde{r}_t)^2)$$

Substep 16.13 Derive the conditional distribution $p(\sigma_{zg}^2|Y,\bullet)$

$p(\sigma_{zg}^2|Y,\bullet)$ is a standard inverse-Gamma density,

Candidate draws are sampled from

$$p(\sigma_{zg}^2|Y,\bullet) \sim IG(\nu_{zg0}+\tfrac{T}{2}, S_{zg0}+\tfrac{1}{2}\sum_{t=1}^{T}(Z_t^g-C_t^g-\beta^g gdp_{t-1}^*+\beta^g gdp_t^*)^2)$$

Substep 16.14 Derive the conditional distribution $p(\sigma_{cg}^2|Y,\bullet)$

$p(\sigma_{cg}^2|Y,\bullet)$ is a standard inverse-Gamma density,

Candidate draws are sampled from

$$p(\sigma_{cg}^2|Y,\bullet) \sim IG(\nu_{cg0}+\tfrac{T-1}{2}, S_{cg0}+\tfrac{1}{2}\sum_{t=2}^{T}(C_t^g-C_{t-1}^g)^2)$$

Substep 16.15 Derive the conditional distribution $p(\beta^g|Y,\bullet)$

Candidate draws are sampled from $N(\hat{\beta}^g, D_{\beta g})$ using the precision based algorithm.

where,

$$D_{\beta g} = (V_{\beta g}^{-1}+(Hgdp^*-\alpha_g)'\Omega_{zg}^{-1}(Hgdp^*-\alpha_g))^{-1}$$

$$\hat{\beta}^g = D_{\beta g}(V_{\beta g}^{-1}\beta_0^g+(Hgdp^*-\alpha_g)\Omega_{zg}^{-1}J^{zg})$$

$j_t^{zg} = Z_t^g - C_t^g$
$J^{zg} = (j_1^{zg},...,j_T^{zg})'$
$\alpha_g = (gdp_0^*,0,0,....,0)'$

$V_{\beta g}^{-1}$ is the prior variance and β_0^g is the prior mean for β^g

Substep 16.16 Derive the conditional distribution $p(\rho^p|Y,\bullet)$

Given the stationary constraint, $|\rho^p| < 1$

ρ^p is a truncated normal. To obtain draws from this truncated normal distribution, AR sampling step is applied to the candidate draws from the proposal density, $N(\hat{\rho}^p, D_{\rho p})$.

$D_{\rho p} = (V_{\rho p}^{-1} + X_{prod}^{'}\Omega_P^{-1}X_{prod})^{-1}$

$\hat{\rho}^p = D_{\rho p}(V_{\rho p}^{-1}\rho_0^p + X_{prod}^{'}\Omega_P^{-1}Y^{prod})$

where,

$V_{\rho p}^{-1}$ is the prior variance and ρ_0^p is the prior mean,

$\tilde{p}_t = P_t - P_t^*$

$X_{prod} = (\tilde{p}_0, ..., \tilde{p}_{T-1})'$

$y_t^{prod} = \tilde{p}_t - \lambda_t^p \tilde{u}_t$

$Y^{prod} = (y_1^{prod}, ..., y_T^{prod})'$

Substep 16.17 Derive the conditional distribution $p(\sigma_{hp}^2|Y,\bullet)$

$p(\sigma_{hp}^2|Y,\bullet)$ is a standard inverse-Gamma density,

Candidate draws are sampled from

$p(\sigma_{hp}^2|Y,\bullet) \sim IG(\nu_{hp0} + \frac{T-1}{2}, S_{hp0} + \frac{1}{2}\sum_{t=2}^{T}(h_t^p - h_{t-1}^p)^2)$

Substep 16.18 Derive the conditional distribution $p(\sigma_{p*}^2|Y,\bullet)$

$p(\sigma_{p*}^2|Y,\bullet)$ is a standard inverse-Gamma density,

Candidate draws are sampled from

$p(\sigma_{p*}^2|Y,\bullet) \sim IG(\nu_{p*0} + \frac{T-1}{2}, S_{p*0} + \frac{1}{2}\sum_{t=2}^{T}(P_t^* - P_{t-1}^*)^2)$

Substep 16.19 Derive the conditional distribution $p(\sigma_{\lambda\pi}^2|Y,\bullet)$

$p(\sigma_{\lambda\pi}^2|Y,\bullet)$ is a non-standard density because of the constraints on λ^π,

$log\ \ p(\sigma^2_{\lambda\pi}|Y,\bullet) \propto -(\nu_{\lambda\pi 0}+1)log\ \ \sigma^2_{\lambda\pi} - \frac{S_{\lambda\pi 0}}{\sigma^2_{\lambda\pi}} - \frac{T-1}{2} log\ \ \sigma^2_{\lambda\pi} - \frac{1}{2\sigma^2_{\lambda\pi}} \sum_{t=2}^{T} (\lambda^{\pi}_t - \lambda^{\pi}_{t-1})^2 + g_{\lambda\pi}(\lambda^{\pi}, \sigma^2_{\lambda\pi})$

The candidate draws from $p(\sigma^2_{\lambda\pi}|Y,\bullet)$ are obtained via the MH step with the proposal density

$$IG(\nu_{\lambda\pi 0} + \tfrac{T-1}{2}, S_{\lambda\pi 0} + \tfrac{1}{2} \sum_{t=2}^{T} (\lambda^{\pi}_t - \lambda^{\pi}_{t-1})^2)$$

Substep 16.20 Derive the conditional distribution $p(\sigma^2_{\rho\pi}|Y,\bullet)$

$p(\sigma^2_{\rho\pi}|Y,\bullet)$ is a non-standard density because of the constraints on ρ^{π},

$log\ \ p(\sigma^2_{\rho\pi}|Y,\bullet) \propto -(\nu_{\rho\pi 0}+1)log\ \ \sigma^2_{\rho\pi} - \frac{S_{\rho\pi 0}}{\sigma^2_{\rho\pi}} - \frac{T-1}{2} log\ \ \sigma^2_{\rho\pi} - \frac{1}{2\sigma^2_{\rho\pi}} \sum_{t=2}^{T} (\rho^{\pi}_t - \rho^{\pi}_{t-1})^2 + g_{\rho\pi}(\rho^{\pi}, \sigma^2_{\rho\pi})$

The candidate draws from $p(\sigma^2_{\rho\pi}|Y,\bullet)$ are obtained via the MH step with the proposal density

$$IG(\nu_{\rho\pi 0} + \tfrac{T-1}{2}, S_{\rho\pi 0} + \tfrac{1}{2} \sum_{t=2}^{T} (\rho^{\pi}_t - \rho^{\pi}_{t-1})^2)$$

Substep 16.21 Derive the conditional distribution $p(\sigma^2_{h\pi}|Y,\bullet)$

$p(\sigma^2_{h\pi}|Y,\bullet)$ is a standard inverse-Gamma density,

Candidate draws are sampled from

$$p(\sigma^2_{h\pi}|Y,\bullet) \sim IG(\nu_{h\pi 0} + \tfrac{T-1}{2}, S_{h\pi 0} + \tfrac{1}{2} \sum_{t=2}^{T} (h^{\pi}_t - h^{\pi}_{t-1})^2)$$

Substep 16.22 Derive the conditional distribution $p(\sigma^2_{\pi *}|Y,\bullet)$

$p(\sigma^2_{\pi *}|Y,\bullet)$ is a standard inverse-Gamma density,

Candidate draws are sampled from

$$p(\sigma^2_{\pi *}|Y,\bullet) \sim IG(\nu_{\pi *0} + \tfrac{T-1}{2}, S_{\pi *0} + \tfrac{1}{2} \sum_{t=2}^{T} (\pi^{*}_t - \pi^{*}_{t-1})^2)$$

Substep 16.23 Derive the conditional distribution $p(\sigma^2_{z\pi}|Y,\bullet)$

$p(\sigma^2_{z\pi}|Y,\bullet)$ is a standard inverse-Gamma density,

Candidate draws are sampled from

$$p(\sigma^2_{z\pi}|Y,\bullet) \sim IG(\nu_{z\pi 0} + \tfrac{T}{2}, S_{z\pi 0} + \tfrac{1}{2}\sum_{t=1}^{T}(Z_t^{\pi} - C_t^{\pi} - \beta^{\pi}\pi^*)^2)$$

Substep 16.24 Derive the conditional distribution $p(\sigma^2_{c\pi}|Y,\bullet)$

$p(\sigma^2_{c\pi}|Y,\bullet)$ is a standard inverse-Gamma density,

Candidate draws are sampled from

$$p(\sigma^2_{c\pi}|Y,\bullet) \sim IG(\nu_{c\pi 0} + \tfrac{T-1}{2}, S_{c\pi 0} + \tfrac{1}{2}\sum_{t=2}^{T}(C_t^{\pi} - C_{t-1}^{\pi})^2)$$

Substep 16.25 Derive the conditional distribution $p(\beta^{\pi}|Y,\bullet)$

Candidate draws are sampled from $N(\hat{\beta}^{\pi}, D_{\beta\pi})$ using the precision based algorithm.

where,

$$D_{\beta\pi} = (V_{\beta\pi}^{-1} + \pi^{*'}\Omega_{z\pi}^{-1}\pi^*)^{-1}$$

$$\hat{\beta}^{\pi} = D_{\beta\pi}(V_{\beta\pi}^{-1}\beta_0^{\pi} + \pi^{*'}\Omega_{z\pi}^{-1}J^{z\pi})$$

$j_t^{z\pi} = Z_t^{\pi} - C_t^{\pi}$
$J^{z\pi} = (j_1^{z\pi}, ..., j_T^{z\pi})'$

$V_{\beta\pi}^{-1}$ is the prior variance and β_0^{π} is the prior mean for β^{π}

Substep 16.26 Derive the conditional distribution $p(\sigma^2_{w*}|Y,\bullet)$

$p(\sigma^2_{w*}|Y,\bullet)$ is a standard inverse-Gamma density,

Candidate draws are sampled from

$$p(\sigma^2_{w*}|Y,\bullet) \sim IG(\nu_{w*0} + \tfrac{T-1}{2}, S_{w*0} + \tfrac{1}{2}\sum_{t=2}^{T}(w_t^* - \pi_t^* - P_t^*)^2)$$

Substep 16.27 Derive the conditional distribution $p(\sigma^2_{hw}|Y,\bullet)$

$p(\sigma^2_{hw}|Y,\bullet)$ is a standard inverse-Gamma density,

Candidate draws are sampled from

$$p(\sigma^2_{hw}|Y,\bullet) \sim IG(\nu_{hw0} + \tfrac{T-1}{2}, S_{hw0} + \tfrac{1}{2}\sum_{t=2}^{T}(h_t^w - h_{t-1}^w)^2)$$

Substep 16.28 Derive the conditional distribution $p(\sigma^2_{\rho w}|Y,\bullet)$

$p(\sigma^2_{\rho w}|Y,\bullet)$ is a non-standard density because of the constraints on ρ^w,

$log\ \ p(\sigma^2_{\rho w}|Y,\bullet) \propto -(\nu_{\rho w0}+1)log\ \ \sigma^2_{\rho w} - \frac{S_{\rho w0}}{\sigma^2_{\rho w}} - \frac{T-1}{2} log\ \ \sigma^2_{\rho w} - \frac{1}{2\sigma^2_{\rho w}} \sum_{t=2}^{T} (\rho^w_t - \rho^w_{t-1})^2 + g_{\rho w}(\rho^w, \sigma^2_{\rho w})$

The candidate draws from $p(\sigma^2_{\rho w}|Y,\bullet)$ are obtained via the MH step with the proposal density

$$IG(\nu_{\rho w0} + \tfrac{T-1}{2}, S_{\rho w0} + \tfrac{1}{2} \sum_{t=2}^{T} (\rho^w_t - \rho^w_{t-1})^2)$$

Substep 16.29 Derive the conditional distribution $p(\sigma^2_{\lambda w}|Y,\bullet)$

$p(\sigma^2_{\lambda w}|Y,\bullet)$ is a non-standard density because of the constraints on λ^w,

$log\ \ p(\sigma^2_{\lambda w}|Y,\bullet) \propto -(\nu_{\lambda w0}+1)log\ \ \sigma^2_{\lambda w} - \frac{S_{\lambda w0}}{\sigma^2_{\lambda w}} - \frac{T-1}{2} log\ \ \sigma^2_{\lambda w} - \frac{1}{2\sigma^2_{\lambda w}} \sum_{t=2}^{T} (\lambda^w_t - \lambda^w_{t-1})^2 + g_{\lambda w}(\lambda^w, \sigma^2_{\lambda w})$

The candidate draws from $p(\sigma^2_{\lambda w}|Y,\bullet)$ are obtained via the MH step with the proposal density

$$IG(\nu_{\lambda w0} + \tfrac{T-1}{2}, S_{\lambda w0} + \tfrac{1}{2} \sum_{t=2}^{T} (\lambda^w_t - \lambda^w_{t-1})^2)$$

Substep 16.30 Derive the conditional distribution $p(\sigma^2_{\kappa w}|Y,\bullet)$

The candidate draws are obtained from

$$IG(\nu_{\kappa w0} + \tfrac{T-1}{2}, S_{\kappa w0} + \tfrac{1}{2} \sum_{t=2}^{T} (\kappa^w_t - \kappa^w_{t-1})^2)$$

Substep 16.31 Derive the conditional distribution $p(\rho^i|Y,\bullet)$

Given the constraint $|\rho^i| < 1$, the conditional distribution $p(\rho^i|Y,\bullet)$ is a truncated normal density. The candidate draws are sampled from the proposal distribution $N(\hat{\rho}^i, D_{\rho i})$ using the precision based algorithm, and simple Accept-Reject step is applied to the candidate draws.

where,

$D_{\rho i} = (V^{-1}_{\rho i} + X'_{\rho i} \Omega^{-1}_i X_{\rho i})^{-1}$

$\hat{\rho}^i = D_{\rho i}(V^{-1}_{\rho i} \rho^i_0 + X'_{\rho i} \Omega^{-1}_i M^{\rho i})$

$m^{\rho i}_t = i_t - \pi^*_t - r^*_t - \lambda^i \tilde{u}_t - \kappa^i \tilde{\pi}_t$
$M^{\rho i} = (m^{\rho i}_1, ..., m^{\rho i}_T)'$

$X_{\rho i} = (i_0 - \pi_0^* - r_0^*, ..., i_{T-1} - \pi_{T-1}^* - r_{T-1}^*)'$

$V_{\rho i}^{-1}$ is the prior variance and ρ_0^i is the prior mean for ρ^i

Substep 16.32 Derive the conditional distribution $p(\lambda^i|Y, \bullet)$

The candidate draws are sampled from the proposal distribution $N(\hat{\lambda}^i, D_{\lambda i})$ using the precision based algorithm.

where,

$D_{\lambda i} = (V_{\lambda i}^{-1} + X_{\lambda i}' \Omega_i^{-1} X_{\lambda i})^{-1}$

$\hat{\lambda}^i = D_{\lambda i}(V_{\lambda i}^{-1} \lambda_0^i + X_{\lambda i}' \Omega_i^{-1} M^{\lambda i})$

$m_t^{\lambda i} = i_t - \pi_t^* - r_t^* - \rho^i(i_{t-1} - \pi_{t-1}^* - r_{t-1}^*) - \kappa^i \tilde{\pi}_t$
$M^{\lambda i} = (m_1^{\lambda i}, ..., m_T^{\lambda i})'$
$X_{\lambda i} = (\tilde{u}_1, ..., \tilde{u}_T)'$

$V_{\lambda i}^{-1}$ is the prior variance and λ_0^i is the prior mean for λ^i

Substep 16.33 Derive the conditional distribution $p(\kappa^i|Y, \bullet)$

The candidate draws are sampled from the proposal distribution $N(\hat{\kappa}^i, D_{\kappa i})$ using the precision based algorithm.

where,

$D_{\kappa i} = (V_{\kappa i}^{-1} + X_{\kappa i}' \Omega_i^{-1} X_{\kappa i})^{-1}$

$\hat{\kappa}^i = D_{\kappa i}(V_{\kappa i}^{-1} \kappa_0^i + X_{\kappa i}' \Omega_i^{-1} M^{\kappa i})$

$m_t^{\kappa i} = i_t - \pi_t^* - r_t^* - \rho^i(i_{t-1} - \pi_{t-1}^* - r_{t-1}^*) - \lambda^i \tilde{u}_t$
$M^{\kappa i} = (m_1^{\kappa i}, ..., m_T^{\kappa i})'$
$X_{\kappa i} = (\tilde{\pi}_1, ..., \tilde{\pi}_T)'$

$V_{\kappa i}^{-1}$ is the prior variance and κ_0^i is the prior mean for κ^i

Substep 16.34 Derive the conditional distribution $p(\sigma_{hi}^2|Y, \bullet)$

$p(\sigma_{hi}^2|Y, \bullet)$ is a standard inverse-Gamma density,

Candidate draws are sampled from

$$p(\sigma_{hi}^2|Y,\bullet) \sim IG(\nu_{hi0} + \tfrac{T-1}{2}, S_{hi0} + \tfrac{1}{2}\sum_{t=2}^{T}(h_t^i - h_{t-1}^i)^2)$$

Substep 16.35 Derive the conditional distribution $p(\sigma_{zr}^2|Y,\bullet)$

$p(\sigma_{zr}^2|Y,\bullet)$ is a standard inverse-Gamma density,

Candidate draws are sampled from

$$p(\sigma_{zr}^2|Y,\bullet) \sim IG(\nu_{zr0} + \tfrac{T}{2}, S_{zr0} + \tfrac{1}{2}\sum_{t=1}^{T}(Z_t^r - C_t^r - \beta^r r_t^*)^2)$$

Substep 16.36 Derive the conditional distribution $p(\sigma_{cr}^2|Y,\bullet)$

$p(\sigma_{cr}^2|Y,\bullet)$ is a standard inverse-Gamma density,

Candidate draws are sampled from

$$p(\sigma_{cr}^2|Y,\bullet) \sim IG(\nu_{cr0} + \tfrac{T-1}{2}, S_{cr0} + \tfrac{1}{2}\sum_{t=2}^{T}(C_t^r - C_{t-1}^r)^2)$$

Substep 16.37 Derive the conditional distribution $p(\beta^r|Y,\bullet)$

Candidate draws are sampled from $N(\hat{\beta}^r, D_{\beta r})$ using the precision based algorithm.

where,

$$D_{\beta r} = (V_{\beta r}^{-1} + r^{*\prime}\Omega_{zr}^{-1}r^*)^{-1}$$

$$\hat{\beta}^r = D_{\beta r}(V_{\beta r}^{-1}\beta_0^r + r^{*\prime}\Omega_{zr}^{-1}J^{zr})$$

$j_t^{zr} = Z_t^r - C_t^r$
$J^{zr} = (j_1^{zr}, ..., j_T^{zr})'$

$V_{\beta r}^{-1}$ is the prior variance and β_0^r is the prior mean for β^r

Substep 16.38 Derive the conditional distribution $p(\sigma_d^2|Y,\bullet)$

$p(\sigma_d^2|Y,\bullet)$ is a standard inverse-Gamma density,

Candidate draws are sampled from

$$p(\sigma_d^2|Y,\bullet) \sim IG(\nu_{d0} + \tfrac{T-1}{2}, S_{d0} + \tfrac{1}{2}\sum_{t=2}^{T}(D_t - D_{t-1})^2)$$

A1.d Marginal likelihood computation

Bayesian model comparison is based on the marginal likelihood (marginal data density) metric. In computing marginal likelihood for various models, we use the approach proposed by CCK, which decomposes the marginal density of the data (e.g., inflation) into the product of predictive likelihoods. This approach allows us to separately compute marginal data density for each variable of interest: inflation, nominal wages, interest rate, real GDP, the unemployment rate, and labor productivity. The variable specific marginal densities prove quite useful because it allows for deeper insights about the source of the deficiencies, which in turn helps differentiate models at a more disaggregated level.

Specifically, marginal data density of the variables of interest is computed as follows,

$$p(y^j|X_i^j, M_i) = \prod_{t=3}^{T} p(y_t^j|y_{1:t-1}^j, X_{1:t,i}^j, M_i) \tag{83}$$

where, $j =$ PCE inflation (π), unemployment rate(ur), real GDP(gdp), labor productivity($prod$), nominal wage inflation($wage$), nominal short-term interest rate(int) ;
$p(y_t^j|y_{1:t-1}^j, X_{1:t,i}^j, M_i)$ is the predictive likelihood for variable j, and X_i^j is set of covariates that influences variable j in model M_i. For example, in the case of short-term interest rate, the covariates in the Base model include ur, π, gdp, and survey data. Whereas, in the Base-NoSurv model, the covariates will not include the survey data.

To compute the overall marginal data density of $Y = (y^{\pi}, y^{ur}, y^{gdp}, y^{prod}, y^{wage}, y^{int})'$ for model M_i,

$$\begin{aligned} p(Y|X_i, M_i) = p(y^{\pi}|X_i^{\pi}, M_i) \times p(y^{ur}|X_i^{ur}, M_i) \times p(y^{gdp}|X_i^{gdp}, M_i)... \\ \times p(y^{prod}|X_i^{prod}, M_i) \times p(y^{wage}|X_i^{wage}, M_i) \times p(y^{int}|X_i^{int}, M_i) \end{aligned} \tag{84}$$

A2. Prior Sensitivity Analysis

In the paper, we noted that our prior settings are similar to those used in CKP, CCK, Gonzalez-Astudillo and Laforte (2020). As discussed in CCK, UC models with several unobserved variables, such as the one developed in this paper, require informative priors. That said, our priors settings for most variables are only slightly informative. The use of inequality restrictions on some parameters such as the Phillips curve, persistence, bounds on u-star could be viewed as additional sources of information that eliminates the need for tight priors, something also noted by CKP. The parameters for which there is a strong agreement in the empirical literature on their values, such as the Taylor-rule equation parameters, we use relatively tight priors, such that prior distributions are centered on prior means with small variance. So besides the prior on the Taylor-rule equation parameters, all other prior settings are taken from related papers.

Here, we examine the sensitivity of loosening the priors on the variances of the shocks to the pi-star, p-star, u-star, and r-star (i.e., for the process D). Specifically, we double the prior mean of the variances from 0.01 to 0.03. Table A2 reports the posterior estimates. The top panel reports the posterior estimates from the main text to facilitate easy comparison, and the bottom panel reports the posterior estimates of re-running the models with these new prior values. The

results for p-star are as expected. In the paper, we noted that the prior view primarily shapes p-star, and we see that manifest here too; prior ($E(\sigma^2_{p*})$) and posterior ($E(\sigma^2_{p*}|Data)$) are fairly identical. Similar evidence is seen in the case of r-star (i.e., D) for the Base-NoSurv model. For pi-star, u-star, and r-star (in the case of Base), the posterior mean estimates' differences between the two panels are small. In fact, the posterior mean estimates from the runs with looser prior are pushed toward values that are closer to the prior mean estimates used in the main paper, lending credibility to our default prior settings used in the main paper.

Table A2: Parameter Estimates

Panel A: From the main paper, where prior $E(\sigma^2_{\pi^*}) = E(\sigma^2_{u^*}) = E(\sigma^2_d) = 0.1^2$ and $E(\sigma^2_{p^*}) = 0.14^2$

Parameter	Parameter description	Posterior estimates					
		Base			Base-NoSurv		
		Mean	5%	95%	Mean	5%	95%
$\sigma^2_{\pi^*}$	Variance of the shocks to π^*	0.121^2	0.100^2	0.141^2	0.127^2	0.084^2	0.182^2
$\sigma^2_{p^*}$	Variance of the shocks to p^*	0.145^2	0.111^2	0.183^2	0.141^2	0.109^2	0.176^2
$\sigma^2_{u^*}$	Variance of the shocks to u^*	0.075^2	0.064^2	0.089^2	0.084^2	0.071^2	0.100^2
σ^2_d	Variance of the shocks to d	0.093^2	0.077^2	0.110^2	0.114^2	0.084^2	0.148^2

Panel B: Prior sensitivity, where prior $E(\sigma^2_{\pi^*}) = E(\sigma^2_{u^*}) = E(\sigma^2_d) = E(\sigma^2_{p^*}) = 0.173^2$

Parameter	Parameter description	Posterior estimates					
		Base			Base-NoSurv		
		Mean	5%	95%	Mean	5%	95%
$\sigma^2_{\pi^*}$	Variance of the shocks to π^*	0.143^2	0.124^2	0.163^2	0.190^2	0.145^2	0.236^2
$\sigma^2_{p^*}$	Variance of the shocks to p^*	0.172^2	0.134^2	0.214^2	0.166^2	0.130^2	0.207^2
$\sigma^2_{u^*}$	Variance of the shocks to u^*	0.102^2	0.090^2	0.115^2	0.121^2	0.103^2	0.140^2
σ^2_d	Variance of the shocks to d	0.122^2	0.106^2	0.140^2	0.175^2	0.136^2	0.218^2

A3. MCMC Convergence Diagnostics

In this section, we document the diagnostic properties of our MCMC algorithm in the Base and Base-NoSurv models. Following Primiceri (2005), Koop, Leon-Gonzalez, and Strachan (2010), and Korobilis (2017), we report the autocorrelation functions of the posterior draws (10th and 50th order sample autocorrelation), inefficiency factors (IFs), and convergence diagnostic (CD) of Geweke (1992).[1]

One of the most common metrics examined to assess the efficiency of the MCMC sampler is to look at the autocorrelation function of the draws, which indicates how well the chain is mixing. Low autocorrelations are preferred to higher because the lower the autocorrelation, the closer the draws are to being independent and higher the efficiency of the algorithm. The plots shown in the top panel of the figures correspond to 10th and 50th order autocorrelations in the draws, and as can be seen, they indicate very low autocorrelation. In the case of 50th order autocorrelation, all of them indicate close to zero, and in the case of 10th order except for a couple most indicate correlation below 0.2.

The inefficiency factor related to the autocorrelation functions is the inverse of Geweke's (1992) relative numerical efficiency measure (RNE). It is computed using the following formula, $(1 + 2\sum_{i=1}^{\infty} \rho_i)$, where ρ_i refers to the $k - th$ order autocorrelation of the chain. The middle panel in the figures plots the IF for each of the parameters. The values lower than or close to 20 are considered desirable. As shown, in the case of the Base model, all the IFs are below 20, and most at below 10. Similarly, in the case of Base-NoSurv, except one, for all other parameters, IFs are below 20. (Note: IFs are computed using the default setting in LeSage's toolbox: estimation of spectral density at frequency zero uses a tapered window of 4%)

As discussed in Koop, Leon-Gonzalez, and Strachan (2010), to assess whether the MCMC sampler has converged, a rough rule of thumb is to look at the CDs and see whether 95% of them are less than 2. If they are, then convergence is likely achieved. Based on the plots in figures A1 and A2 (third-panel), most CDs are within +/- 2. The very few that exceed 2 are only slightly larger than 2.

We also note that the results are fairly identical to the different initial conditions of the chain (picked randomly) and to a significantly lower number of simulations (and burn-in). For example, a run using 320K posterior draws with a burn-in of the first 300K and retaining all the remaining draws provide similar inference. However, the MCMC convergence properties favor higher simulations because it allows for a greater degree of thinning.

Overall, these diagnostic measures provide us confidence in the good convergence properties of our MCMC algorithm in both the Base and Base-NoSurv models.

[1] In computing some of these metrics, we have benefitted from the Matlab toolbox developed by James P. LeSage. Detailed explanation including intuition for these convergence diagnostics are provided in Koop (2006; page 67-68) and Chan, Koop, Poirier, and Tobias (2019; page 209).

Figure A1: MCMC Diagnostics of Base Model

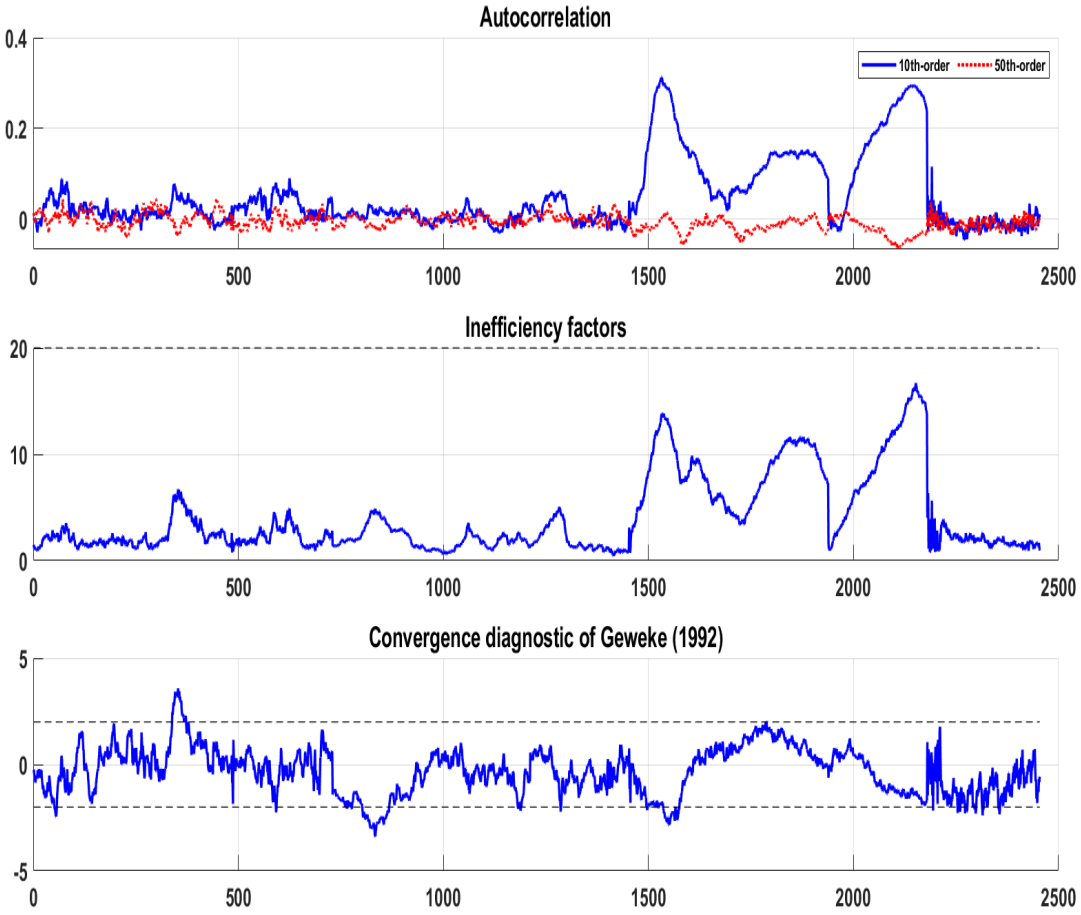

Figure A2: MCMC Diagnostics of Base-NoSurv Model

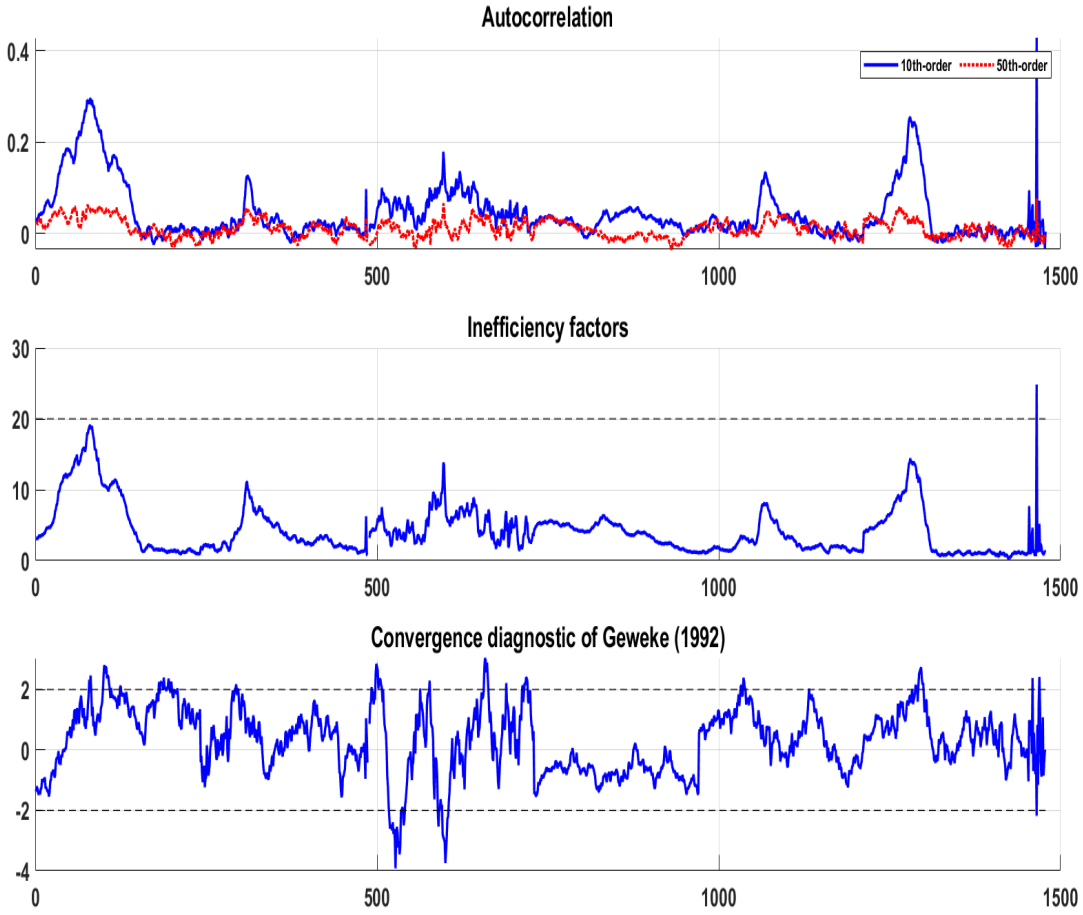

A4. Additional Forecasting Results: Base vs. Benchmarks

In this section we compare the real-time forecasting performance of our Base model to the outside benchmark models, which forecasting literature has shown to be useful forecasting devices. Specifically, we compare the accuracy of the inflation forecasts from our Base model to the following three models, UCSV of Stock and Watson (2007) [UCSV], Chan, Koop, and Potter (2016) [CKP], and Chan, Clark, and Koop (2018) [CCK]. We compare the accuracy of the unemployment rate forecasts from our Base model to the CKP, and the accuracy of the nominal wage inflation from the Base model to the UCSV model applied to the nominal wage inflation – motivated by Knotek (2015).

Table A3 presents the forecast evaluation results for headline PCE inflation, nominal wage inflation, and the unemployment rate. These results indicate following three observations. First, in terms of point forecast accuracy, inflation forecasts from all the four models considered are competitive to each other. There is some statistically significant evidence that the Base model is more accurate than UCSV at h=12Q. Regarding the density forecast accuracy, the Base model is more accurate than the UCSV but inferior to CCK, as the latter produces more precise intervals than the Base model. Second, in the case of nominal wage inflation, the Base model generates more accurate forecasts (both point and density) than UCSV, and the gains are statistically significant for the most part.

Third, the accuracy of the unemployment forecasts from the Base model is competitive to the CKP model statistically speaking, even though the relative numbers favor CKP. A closer inspection of the forecast errors reveals that the Base model, which incorporates survey forecasts of the unemployment rate, experienced significantly bigger misses than the CKP model around the Great Recession period. Outside of this period, the Base model is slightly more accurate than the CKP, and when combined with the Great Recession period, on the net, the much bigger misses of the Base model results in overall higher RMSE.

As illustrated in Tallman and Zaman (2020), just before and at the onset of the Great Recession, the survey participants projected relatively upbeat long-run forecasts of unemployment, which indicated a declining natural rate of unemployment. It was not until few months into the recession that survey participants recognized the extent of the labor market damage and began to revise their estimates of the long-run unemployment higher. Hence, models such as the Base model that take signals from the survey forecasts experienced big misses.

To sum up, we view these forecasting results as providing evidence supporting our Base model's competitive forecasting properties.

Table A3: Out-of-Sample **F**orecasting Performance: **Base vs. Benchmarks**

Full Sample (Recursive evaluation: 1999.Q1-2019.Q4)

	Point forecasting					Density forecasting			
	4Q	8Q	12Q	20Q		4Q	8Q	12Q	20Q
PCE Inflation									
Relative RMSE					Relative Log Score				
Base/UCSV	0.95	0.97	0.93*	0.96	Base - UCSV	0.013*	0.023*	0.028*	0.041*
Base/CCK	1.01	1.04	1.01	1.04*	Base - CCK	-0.018*	-0.030*	-0.046*	-0.058*
Base/CKP	0.98	0.99	0.97	1.02	Base - CKP	0.002	0.001	-0.003*	-0.008*
Nominal Wage									
Relative RMSE					Relative Log Score				
Base/UCSV	0.89*	0.87*	0.92	0.64	Base - UCSV	0.012	0.027*	0.037*	0.041*
Unemployment Rate									
Relative MSE					Relative Log Score				
Base/CKP	1.08	1.12	1.15	1.24	Base - CKP	0.001	0.000	-0.004	-0.007

Notes for Table: For variables PCE inflation and nominal wage (i.e., average hourly earnings), the forecasts and associated accuracy correspond to the quarterly annualized rate. Base forecast is defined as the Steady-State (SS) VAR forecast in which the steady states are assumed to be the estimates of the stars from the Base model. UCSV forecast corresponds to the forecast from the univariate unobserved component stochastic volatility model similar to Stock and Watson (2007). The model is used to construct forecasts of PCE inflation and nominal wage inflation. CCK forecast corresponds to the forecast from the bivariate unobserved component stochastic volatility model of Chan, Clark and Koop (2018). CKP forecast corresponds to the forecast from the bivariate unobserved component stochastic volatility model of Chan, Koop and Potter (2016), with the bounds on u-star fixed to values identical to the Base model. The left panel reports results for the point forecast accuracy (relative root mean squared errors) and the right panel reports the corresponding density forecast accuracy (mean of the relative log predictive score). The table reports statistical significance based on the Diebold-Mariano and West test with the lag $h-1$ truncation parameter of the HAC variance estimator and adjusts the test statistic for the finite sample correction proposed by Harvey, Leybourne, and Newbold (1997); *up to 10% significance level. The test statistics use two-sided standard normal critical values for horizons less than equal to 8 quarters, and two-sided t-statistics for horizons greater than 8 quarters.

A5. Additional Forecasting Results: SSBVAR, Base stars vs. Survey

In macroeconomic forecasting, research by Wright (2013) and Tallman and Zaman (2020), among others, show using workhorse Bayesian VAR models that the predictive performance boils down to good starting conditions (i.e., nowcasts) and terminal conditions (i.e., steady-states proxied by stars). Survey forecasts provide both nowcasts and long-run projections, whose accuracy has been shown by past research to be quite good. Wright (2019) emphasizes the desirable forecasting properties of the survey forecasts and highlights that econometric approaches utilizing survey projections are at the forecasting frontier, especially in inflation forecasting. Most empirical research on forecasting has focused on proposing methods to improve the accuracy of the nowcast estimates relative to survey nowcasts' accuracy, but only little effort has been dedicated to improving estimates of long-run projections. Hence, this paper raises the natural curiosity in the usefulness of the stars' estimates from our modeling framework for macroeconomic forecasting using Bayesian VARs (via the imposition of steady-states).

To assess the efficacy of our star's estimates for the external VAR models, we perform a real-time out-of-sample forecasting evaluation similar to Wright (2013) and Tallman and Zaman (2020). These studies informed the time-varying steady-states for the steady-state (SS) BVAR using the long-run survey projections and found that doing so leads to significant accuracy gains. Accordingly, the design of our forecasting examination is as follows. We take the SSBVAR from Tallman and Zaman (2020) and perform three sets of recurive real-time out-of-sample forecasting runs. In the first run, we inform the steady-states for real GDP growth, PCE inflation, core PCE inflation, the unemployment rate, nominal wage inflation, and labor productivity growth using the long-run survey projections. For the latter two variables, we use the survey expectations from the SPF.[2] The forecasts from this run are denoted 'Survey' in table A4. In the second run, we repeat the exercise, but this time inform the steady-states using the real-time estimates of the stars from the Base-NoSurv model, denoted 'BaseNoSurv'. In the third run, we inform the steady-states using the real-time estimates of stars from the Base model, denoted 'Base'.

Each of the three forecasting runs is based on estimating the SSBVAR with a recursively expanding sample, i.e., the recursive execution uses an additional quarterly data point in the estimation. The SSBVAR is estimated with quarterly data beginning 1959Q2. The model consists of ten variables: (1) real GDP growth; (2)real consumption expenditures; (3) headline PCE inflation; (4) core PCE inflation; (5) labor productivity growth; (6) growth in average hourly earnings; (7) growth in payroll employment; (8) the unemployment rate; (9) the shadow federal funds rate; (10) and the risk spread, defined as the difference between the yield on 10-year Treasury Bond and yield on BAA Bond. The out-of-sample forecasting period spans 1999Q1 through 2019Q4. The forecast accuracy (point and density) is computed from one-quarter ahead to 20 quarters out. Partly due to focus on the medium-term horizon and partly in the interest of space, we report accuracy metrics for four, eight, twelve, and twenty quarters ahead.

We evaluate the forecast accuracy using real-time data; specifically, we treat the "actual" as the third quarterly estimate. For instance, in the case of real GDP, the third estimate for 2018Q4 corresponds to the GDP data available in late 2019Q1. The point forecast accuracy is assessed using the root mean squared error (RMSE) metric, and the density forecast accuracy

[2]In the case of nominal wage inflation, we construct an implied survey projection by adding the survey expectation of PCE inflation and productivity, both of which are obtained from the SPF.

is assessed using either the continuous ranked probability score (CRPS). Forecasts with lower RSME and CRPS are preferred. The statistical significance of the point and density forecast accuracy is gauged using the Diebold-Mariano and West test. The description of these tests is listed in the notes accompanying the tables reporting forecast accuracy.

Table A4 reports forecast evaluation results corresponding to this exercise. The left panel reports the point forecast accuracy results, while the right panel results for the density forecast accuracy. We evaluate and compare the point, and density forecast accuracies among the Base, BaseNosurv, and Survey forecasts in a pairwise fashion. For each variable, the three rows report the relative RMSE (for point forecast accuracy) and the relative CRPS (for density forecast accuracy). The first row reports the RMSE of the Base relative to Survey, the second row reports the RMSE of BaseNoSurv to Survey, and the third row reports the RMSE of BaseNoSurv relative to Base. A model with a lower values of RMSE and CRPS is preferred to a model with higher values. These relative metrics indicate the following. First, for real GDP growth, statistically speaking, Survey outperforms both Base and BaseNoSurv. A closer inspection of the errors reveals that most of the gains of Survey over Base and BaseNoSurv are achieved over the post-Great Recession period.

As indicated in the figures plotting real-time estimates (see figure A5), starting in 2011 onwards, while both Base and Base-NoSurv have g-star falling sharply in the vicinity of 1.0%, the Survey has g-star falling only a little to 2.0%. This more rapid deceleration in g-star inferred by our models hurts the forecast accuracy of real GDP forecasts. This particular forecasting result suggests that our models misleadingly attribute a higher portion of the low GDP growth realizations in the post-Great Recession period to a trend decline in real GDP growth instead of cyclical fluctuations.

For headline PCE inflation, all three are competitive to each other, with some statistically significant gains in the density forecast accuracy of Base and Base-NoSurv over Survey. In the case of nominal wage inflation, both Base and Base-NoSurv generate forecasts that are substantially more accurate than Survey on average. The gains are statistically significant for the most part. In the case of labor productivity, while Base is more accurate than BaseNoSurv, both are inferior to the Survey. This result suggests that maybe bringing in survey information about productivity in the Base model may improve the econometric estimation of p-star.

For the unemployment rate, both Base and BaseNoSurv are inferior to the Survey, but the gains are not statistically significant for the most part. The SSBVAR with steady-states informed from the Base model generates more accurate unemployment forecasts than Base-NoSurv, but the forecast gains are statistically significant only for the very long horizons. In the case of the shadow federal funds rate, both Base and Survey are competitive but are inferior to BaseNoSurv for h=4Q and h=8Q.

Overall, these forecasting results lend credibility to our stars' estimates (except for g-star) in their use to inform steady-states for VAR forecasting models. We also note the results of this section lend support to the survey projections in their use as proxies for stars, something also documented by Tallman and Zaman (2020), among others.

The fact that the estimates of stars from our models are generally competitive to survey long-run projections we believe is a good outcome. It has been well-established that survey expectations are at the frontier of forecasting (e.g., Wright, 2019). However, the preference is for forecasts (or estimates of stars) obtained using a single multivariate model because the resulting forecasts will be coherent and allow for a credible narrative in a systematic manner.

Table A4: Out-of-Sample **F**orecasting Performance: **Steady-State BVAR**

Full Sample (Recursive evaluation: 1999.Q1-2019.Q4)

	Point forecasting					Density forecasting			
	4Q	8Q	12Q	20Q		4Q	8Q	12Q	20Q
Real GDP									
Relative RMSE					Relative CRPS				
Base/Survey	1.05*	1.07*	1.06*	1.01	Base - Survey	0.09*	0.09*	0.07*	0.01
BaseNoSurv/Survey	1.04	1.09*	1.07*	1.03*	BaseNoSurv - Survey	0.06	0.12*	0.09*	0.03
BaseNoSurv/Base	0.98	1.02	1.01	1.02*	BaseNoSurv - Base	-0.02	0.03	0.01	0.02
PCE Inflation									
Relative RMSE					Relative CRPS				
Base/Survey	0.99*	0.98	1.00	1.05	Base - Survey	-0.02*	-0.02*	-0.01	0.04
BaseNoSurv/Survey	0.97	1.00	1.04	1.06	BaseNoSurv - Survey	-0.03*	-0.01	0.02	0.04
BaseNoSurv/Base	0.99	1.02	1.04	1.01	BaseNoSurv - Base	-0.02	0.01	0.03	0.00
Productivity									
Relative RMSE					Relative CRPS				
Base/Survey	1.04*	1.08*	1.05*	1.00	Base - Survey	0.04*	0.08*	0.06*	0.00
BaseNoSurv/Survey	1.06*	1.13*	1.12*	1.05	BaseNoSurv - Survey	0.07*	0.13*	0.12*	0.05
BaseNoSurv/Base	1.02	1.05*	1.06*	1.05*	BaseNoSurv - Base	0.02	0.05*	0.06*	0.05*
Nominal Wage									
Relative RMSE					Relative CRPS				
Base/Survey	0.73*	0.77*	0.84*	0.92*	Base - Survey	-0.08*	-0.09*	-0.09*	-0.08*
BaseNoSurv/Survey	0.72*	0.76*	0.93*	1.06	BaseNoSurv - Survey	-0.08*	-0.09*	-0.05*	0.03
BaseNoSurv/Base	0.98	0.99	1.10	1.16	BaseNoSurv - Base	0.00	0.00	0.04	0.11
Unemployment Rate									
Relative MSE					Relative CRPS				
Base/Survey	1.05	1.08*	1.09	1.11	Base - Survey	0.03	0.09*	0.13*	0.18*
BaseNoSurv/Survey	1.07	1.13	1.19	1.27*	BaseNoSurv - Survey	-0.08	-0.15	-0.10	0.20*
BaseNoSurv/Base	1.02	1.05	1.09	1.14*	BaseNoSurv - Base	0.02	0.10	0.19	0.31
Shadow FFR									
Relative RMSE					Relative CRPS				
Base/Survey	0.98	0.99	1.01	1.06	Base - Survey	-0.02	-0.02	0.02	0.18
BaseNoSurv/Survey	0.91*	0.92	0.96	1.07	BaseNoSurv - Survey	-0.08*	-0.15	-0.10	0.20
BaseNoSurv/Base	0.93*	0.93*	0.95	1.01	BaseNoSurv - Base	-0.06*	-0.13*	-0.12	0.02

Notes for Table: For the variables real GDP, PCE inflation, productivity, nominal wage (i.e., average hourly earnings), the forecasts and the associated accuracy correspond to the quarterly annualized rate. Base forecast is defined as the Steady-State (SS) VAR forecast in which the steady states are assumed to be the estimates of the stars from the Base model. BaseNoSurv forecast is defined as the SS-VAR forecast in which the steady states are taken from the Base-NoSurv model. The left panel reports results for the point forecast accuracy (relative root mean squared errors) and the right panel reports the corresponding density forecast accuracy (mean of the relative continuous ranked probability score). The table reports statistical significance based on the Diebold-Mariano and West test with the lag $h-1$ truncation parameter of the HAC variance estimator and adjusts the test statistic for the finite sample correction proposed by Harvey, Leybourne, and Newbold (1997); *up to 10% significance level. The test statistics use two-sided standard normal critical values for horizons less than equal to 8 quarters, and two-sided t-statistics for horizons greater than 8 quarters.

A6. Additional Real-time Estimates Stars

Figure A3: Real-time Recursive Estimates of Output gap: Base model

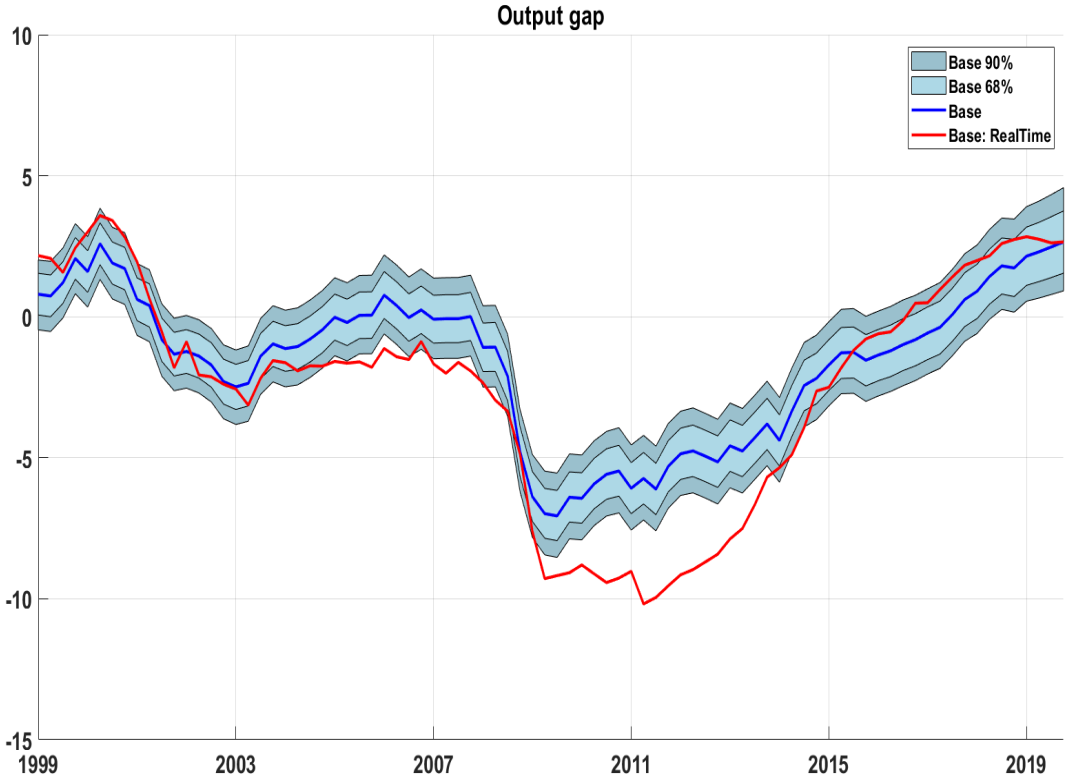

Notes: The plot denoted Base corresponds to smoothed (posterior mean) estimates which are based on the full sample information, i.e., 1959.Q4 through 2019.Q4. The plot denoted Base: RealTime corresponds to real-time recursive (posterior mean) estimate generated by estimating Base model at different points in time, specifically 1999.Q1 through 2019.Q4. The credible intervals reflect the uncertainty around the posterior mean smoothed estimates.

Figure A4: Real-time Recursive Estimates of Stars: Base-NoSurv model

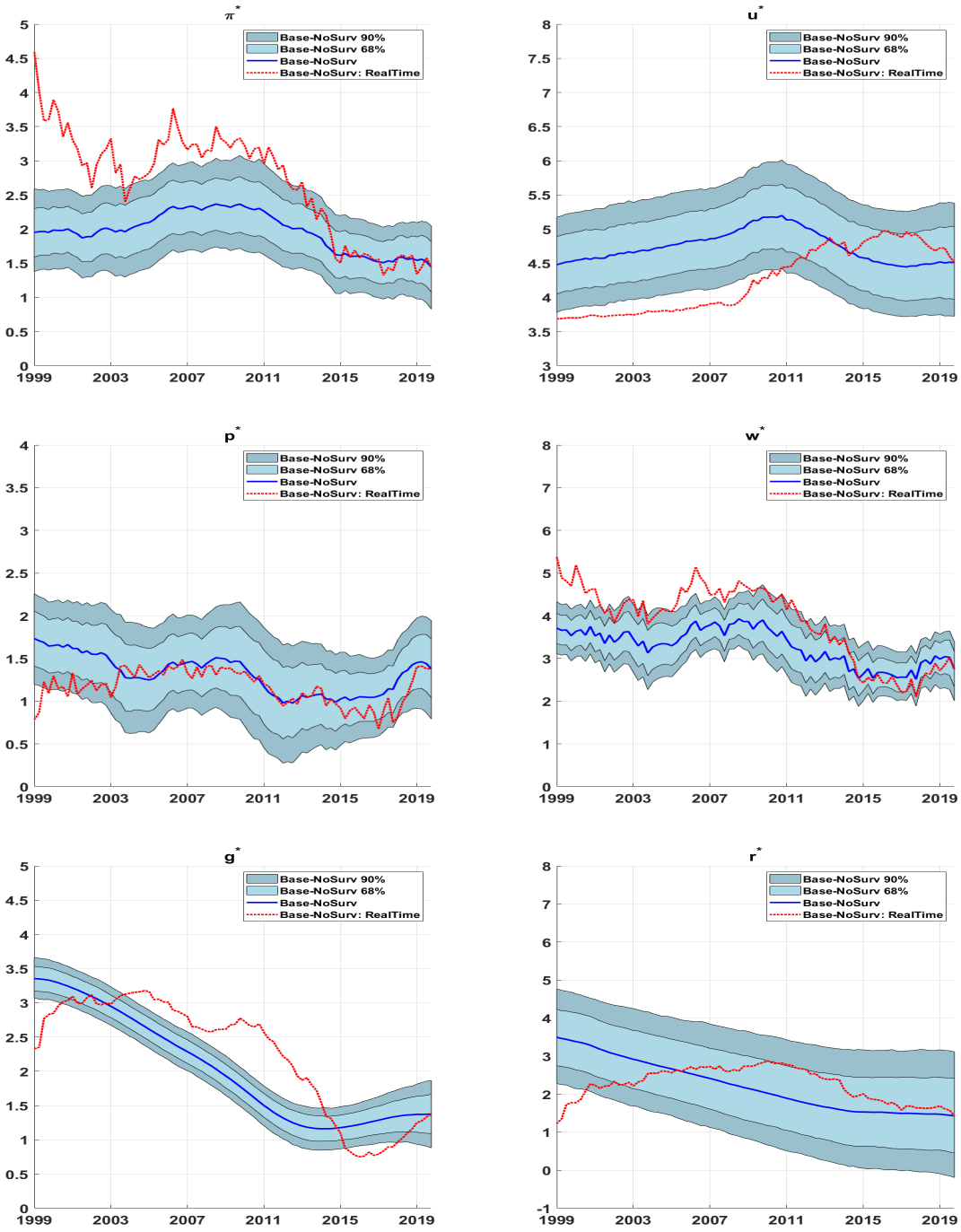

Notes: The plots denoted Base-NoSurv correspond to smoothed estimates which are based on the full sample information, i.e., 1959.Q4 through 2019.Q4. The plots denoted Base-NoSurv: RealTime correspond to real-time recursive estimates generated by estimating Base-NoSurv model at different points in time, specifically 1999.Q1 through 2019.Q4.

Figure A5: Real-time Recursive Estimates of Stars: Base model vs. Base-NoSurv model

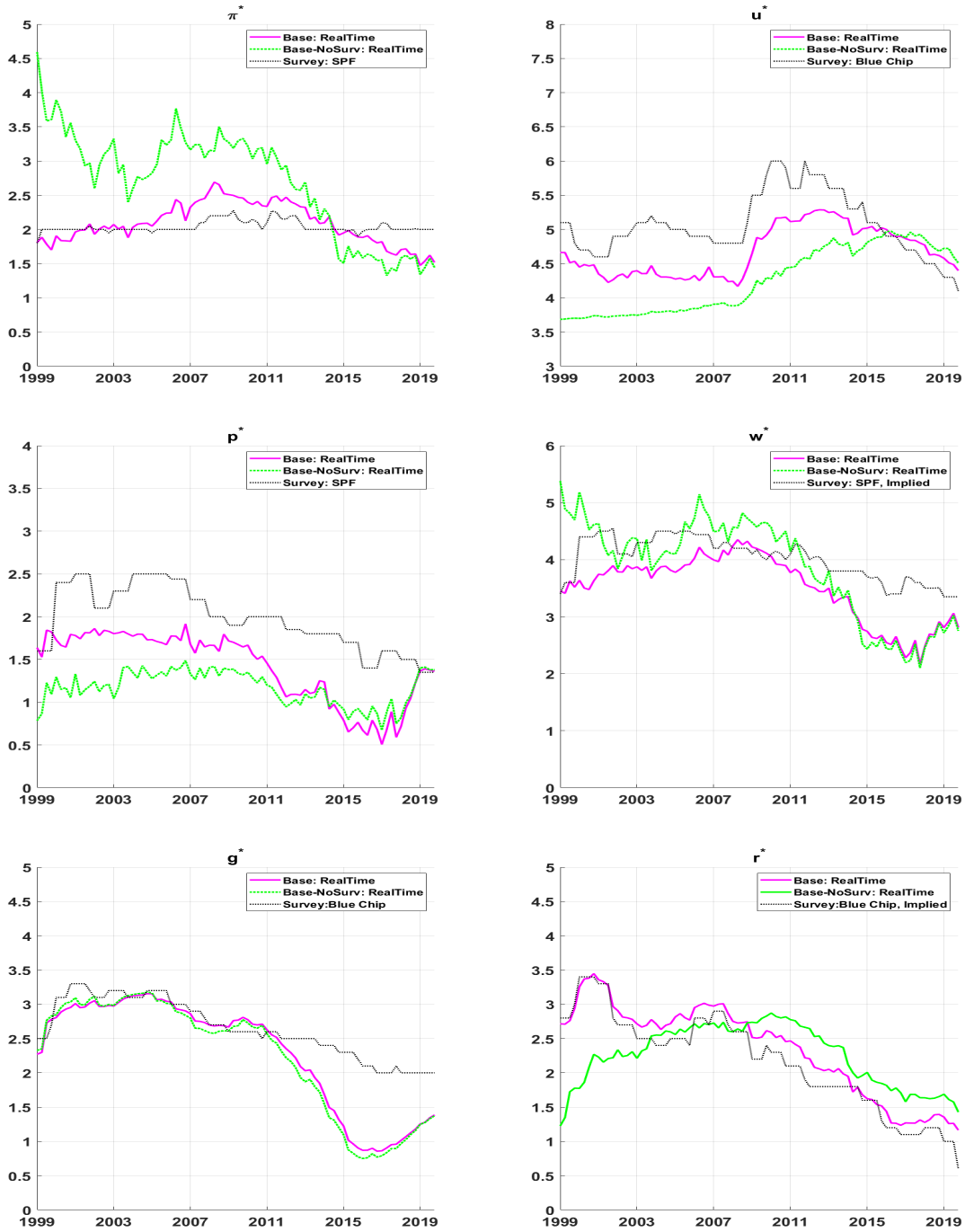

Notes: The plots correspond to real-time recursive estimates generated by estimating Base and Base-NoSurv models at different points in time, specifically 1999.Q1 through 2019.Q4. To facilitate comparison, real-time estimates from the survey either Blue Chip or Survey of Professional Forecasters (SPF) are also plotted.

A7. Estimated relationship between Survey and Stars

Figure A6: Estimated Link Between Survey Forecasts and Stars

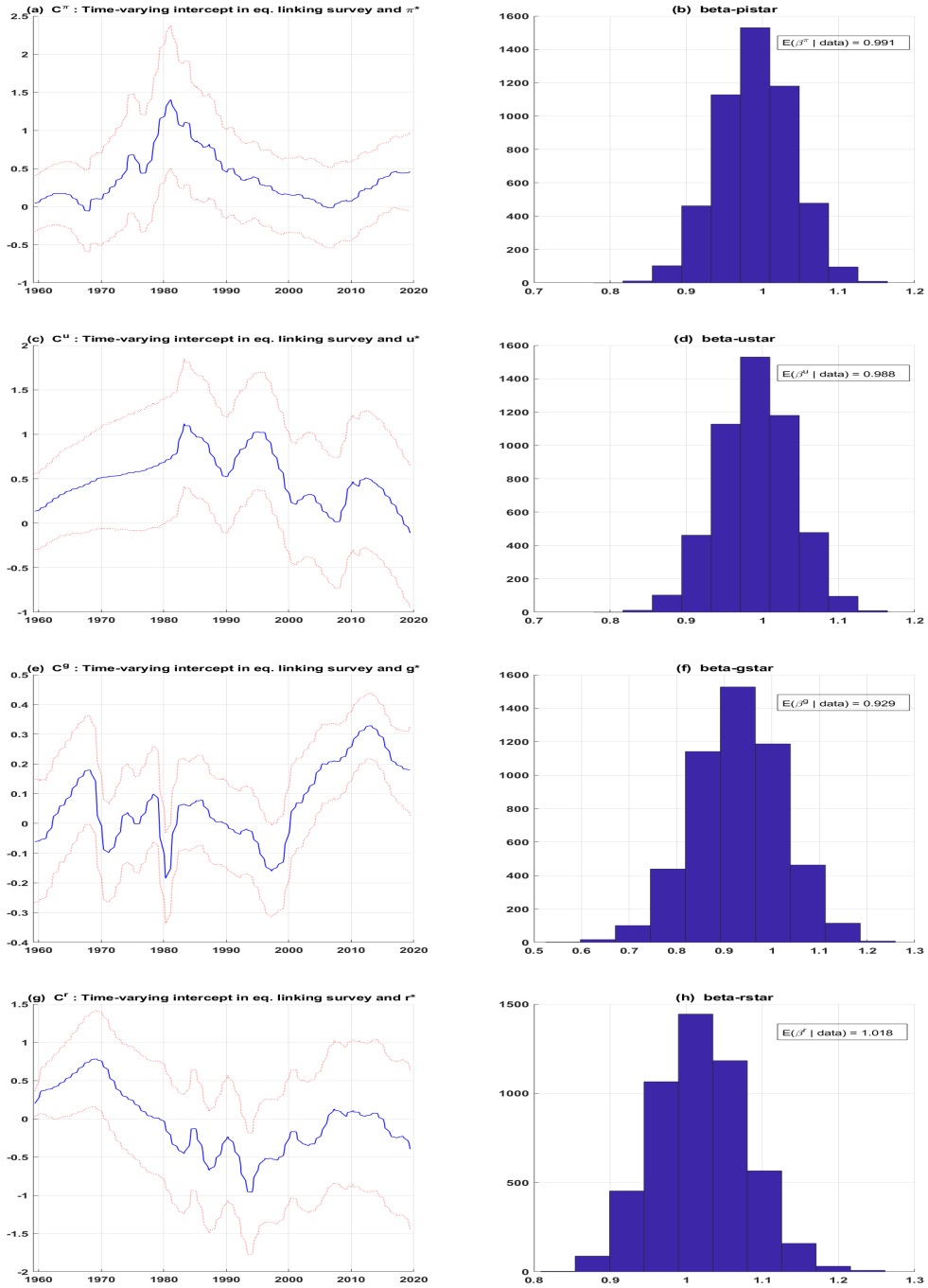

Notes: The posterior estimates are based on the full sample (from 1959Q4 through 2019Q4).

A8. Additional COVID-19 Pandemic Results

Figure A7 presents posterior estimates of u-star, g-star, and r-star from Base and Base-NoSurv models based on estimating data through 2020Q3. Also plotted to facilitate comparison are the corresponding posterior estimates based on estimation through 2019Q4. Figure A8, similarly, provides estimates of pi-star, p-star, and w-star. A visual inspection of the plots suggests the following four observations. First, estimates appear reasonable, indicating the model isn't blowing up. Second, adding pandemic data to the estimation sample has small effects on the historical estimates of stars in the Base model and, for the most part, also applies to the Base-NoSurv model. For u-star, there are some notable revisions in the estimates obtained from the Base-NoSurv model comparing between estimation pre-and post-pandemic recession. The considerable revision in the posterior mean of u-star is associated with decreased precision, as evidenced by the larger width of the 90% credible intervals; however, in the Base model, the estimation with pandemic data is associated with increased precision of u-star.

Third, in the case of g-star, estimation using pandemic data yields posterior mean estimates of g-star that are revised four-tenths higher starting 2000 onwards compared to estimation using pre-pandemic data. Fourth, as would be expected (see Carriero et al., 2021), the precision plots indicate an uptick in uncertainty towards the end of the sample period associated with pandemic data. Though except for p-star and w-star, the uptick in uncertainty is small. The Base model generally held up better because the survey forecasts help anchor the econometric estimates of stars to a reasonable range. Without it, extreme data movements in the unemployment rate profoundly influenced the econometric estimates of u-star in the Base-NoSurv model. In light of the discussion in the preceding paragraph, we view the uptick in uncertainty around p-star as a reasonable result.

We believe that the rich features of our models, which includes: (1) modeling the changing economic relationships via the implementation of time-varying parameters; (2) allowing for changing variance of the innovations to various equations (i.e., SV); (3) imposing bounds on some of the random walk processes; (4) joint modeling of the output gap and unemployment gap in particular; (5) and the use of survey forecasts; helped position our models to handle the pandemic data better.

Carriero et al. (2021) using monthly Bayesian VARs show models that allow for SV better handle pandemic observations than those without SV. But, even models with SV have a drawback in the context of pandemic data. This drawback arises from the standard approach to modeling SV, which assumes a random walk process or a very persistent AR process. So in the face of a temporary spike in volatility, the model will attribute this spike incorrectly to a persistent increase in volatility. Inspired by the outlier treatment method of Stock and Watson (2016) for UCSV models, Carriero et al. (2021) propose an outlier-adjusted SV method that models the VAR residuals as a combination of persistent and transitory changes in volatility.

We believe that this drawback of standard SV applies more to monthly VARs and to a lesser extent in quarterly models, as is the case here. However, we stress that Stock and Watson outlier treatment method can be conveniently implemented in our modeling framework. It would also require introducing SV in both the output gap and the unemployment gap equations. To keep the length of the paper manageable, we leave this extension for future research.

The COVID-19 pandemic provides an excellent real-time illustration of the importance of using survey expectations data in the econometric estimation of the stars. The unprecedented nature of the pandemic crisis and the extreme movements in the data induced by the pandemic are too volatile to provide a timely and credible signal about the long-run macroeconomic

consequences. Complicating the signal extraction problem from the data during the pandemic period is that consensus has been developing (perhaps rightly so) to treat macroeconomic data for the periods 2020Q2 and 2020Q3 as outliers in estimating the macro-econometric models; see Schorfhedie and Song (2020), Lenza and Primiceri (2020), Carriero et al. (2021), among others.

On the other hand, judgment assessment informed from past event studies and understanding of many decades of economics research indicates that the COVID pandemic is likely going to have implications on the long-run productivity growth (p-star), the growth rate of potential output (g-star), the natural rate of unemployment (u-star), the long-run real rate of interest (r-star); see Jorda, Singh, and Taylor (2020). As time rolls forward, and more is revealed about the possible long-term macroeconomic impacts of the pandemic on the underlying trends, the survey participants would judgmentally adjust their estimates of long-run projections in a more timely manner. And by extension, our Base model, which incorporates the long-run survey projections.

Base model vs. external sources: post-pandemic Recession

We next compare our Base model estimates with those produced by externals sources (and or models) to assess further the reliability of our Base model estimates post-pandemic recession. Figure A9 compares the estimates of the output gap (panel a), r-star (panel b), u-star (panel c), and pi-star (panel d) from the Base model to the outside estimates.[3] The estimates are based on data through 2020Q3 (specifically vintage of data corresponding to late November 2020). In the case of CBO, the projections correspond to an update as of late July 2020.

The plots in panel (a) indicate remarkable similarity between the posterior mean estimate of the base model's output gap and the CBO output gap. Compared with Morley and Wong (2020), even though before the pandemic, the base model's output gap estimates indicated less tight resource utilization, for 2020, they are quite similar. Morley and Wong (2020), based on a BVAR approach, could be viewed more flexibly than ours because it explicitly considers the possible error correlation across model equations. However, at the same time, their approach could be deemed less flexible than ours because it does not explicitly model time-variation in parameters and stochastic volatility – i.e., abstracts from the issue of "changing economic environment." Both the Base model and Morley and Wong (2020) estimates the output gap at -3.5% for 2020Q3, with CBO just a tenth higher at -3.6%.

Panel (b) plots the estimates of the r-star from various sources. Except for Laubach and Williams (2003) [LW], all others are based on information available as of late November 2020. LW estimate reflects information through August 2020. Comparing between 2019Q4 and 2020Q3, the Base model, Johannsen and Mertens (2019), and Del Negro et al. (2017), all three estimate r-star to have changed only a little; Base model: from 1.36% to 1.26%, Del Negro et al. (2017): from 1.11% to 1.08%, Johannsen and Mertens (2019): from 1.48% to 1.47%. In contrast, Lubik and Matthes (2015) have r-star increasing from 0.64% to 1.0%. However, in their estimate, r-star first falls from 0.64% to -0.68% and then bounces back to 1.0% in 2020Q3.

[3]Morley and Wong (2020) estimates are based on their updated work Berger, Morley, and Wong (forthcoming) and are available to download from outputgapnow.com. The estimates were downloaded in the last week of November, which included the nowcast estimate for 2020Q4 that we do not plot. Thank Murat Tasci, for providing the estimates of the u-star from the Tasci (2012) model. And also, thank Benjamin Johannsen for providing the r-star estimates from Johannsen and Mertens (2019). The LW estimates of r-star were downloaded from the New York Fed website. Del Negro et al. (2017) estimates of r-star were downloaded from github.com/FRBNY-DSGE/rstarBrookings2017. Lubik and Matthes estimates were downloaded from the Richmond Fed website in late November 2020.

Their estimate of r-star displays considerable volatility compared to others.

Panel (c) plots the estimates of the u-star from four sources, Base model, CBO, Tasci (2012), and Chan, Koop, and Potter (2016). Comparing between the Base model and CBO, the contours of the u-star plots are quite similar. But, the levels through 2010 are notably different, with CBO higher than the Base model. From mid-2013 onwards, the levels are quite similar, and in 2020Q3, both indicate u-star at 4.3% (Base) and 4.4% (CBO). Interestingly, both CBO and the Base model have u-star remaining mostly stable between 2019Q4 and 2020Q3, suggesting that they attribute most of the increase in the pandemic's unemployment rate to the cyclical component. It is worth highlighting that the (median) estimate of u-star reported in the September 2020 Summary of Economic Projections, which the Federal Reserve compiles, also indicated a stable u-star (at 4.1%) between 2019Q4 and 2020Q3.

Broadly speaking, the contour of the u-star implied by the CKP (bivariate Phillips curve) is similar to the Base model and CBO. But, the estimated level of u-star is significantly higher. According to the CKP model, the estimated u-star in 2020Q3 is 5.7%, just a tenth higher than 2019Q4. The Tasci (2012) model, which is based on the flow rates in-and-out of unemployment, is significantly impacted by the pandemic data, as the u-star is estimated to have increased from 4.7% in late 2019 to 5.2% in 2020Q3. Part of the explanation of more significant movements in u-star seen in the Tasci model in response to pandemic data is that the model is estimated using maximum likelihood methods, which are relatively known to have done a less well job in handling extreme pandemic induced movements in variables. More generally, Tasci (2019) document the challenges of estimating u-star in real-time with these models during crisis periods.

Panel (d) presents pi-star estimates from three sources: the Base model, CCK model, and CKP model. All three models indicate pi-star to have remained stable between 2019Q4 and 2020Q3. However, the pi-star estimates differ slightly across models, with the Base model at 1.65%, CCK at 1.50%, and CKP at 1.44% (in 2020Q3).

Figure A7: Estimates of Stars pre- vs. post-COVID Recession

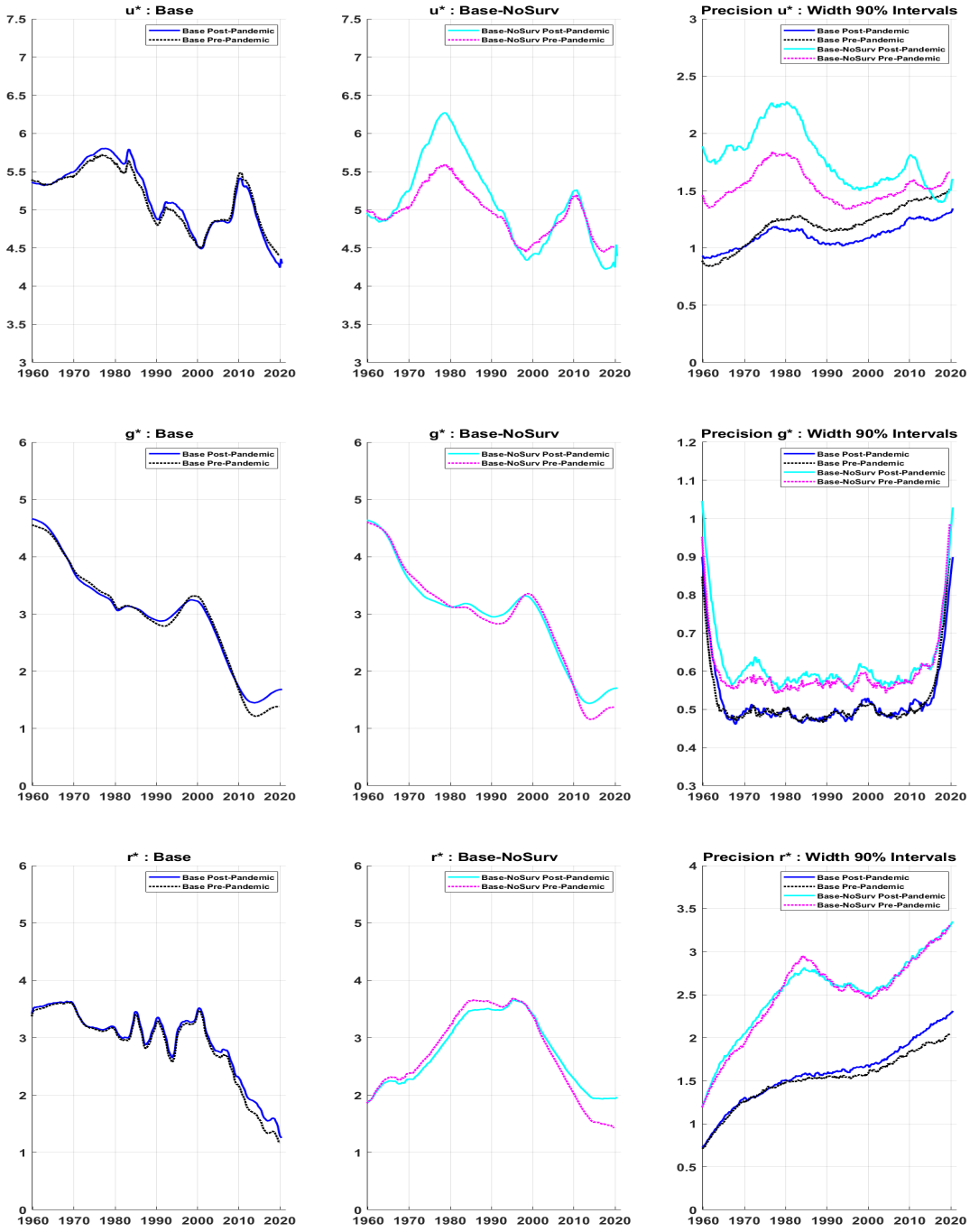

Notes: The plots labeled Pre Pandemic reflect posterior estimates based on information in the sample 1959Q4 through 2019Q4, and plots labeled Post Pandemic reflect posterior estimates based on the sample 1959Q4 through 2020Q3.

Figure A8: Estimates of Stars pre- vs. post-COVID Recession

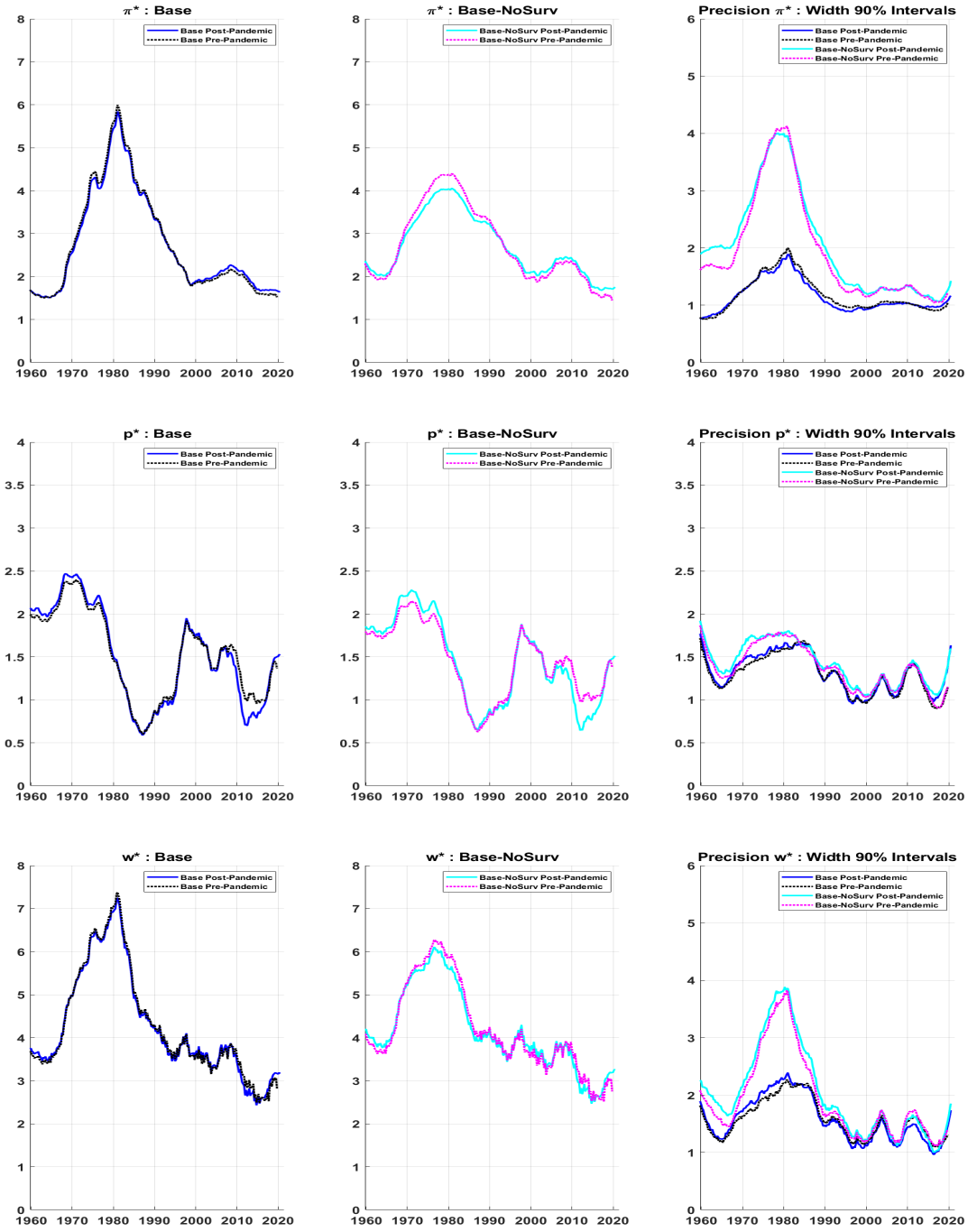

Notes: The plots labeled Pre Pandemic reflect posterior estimates based on information in the sample 1959Q4 through 2019Q4, and plots labeled Post Pandemic reflect posterior estimates based on the sample 1959Q4 through 2020Q3.

Figure A9: Estimates of Stars post-COVID Recession: Base vs. Outside

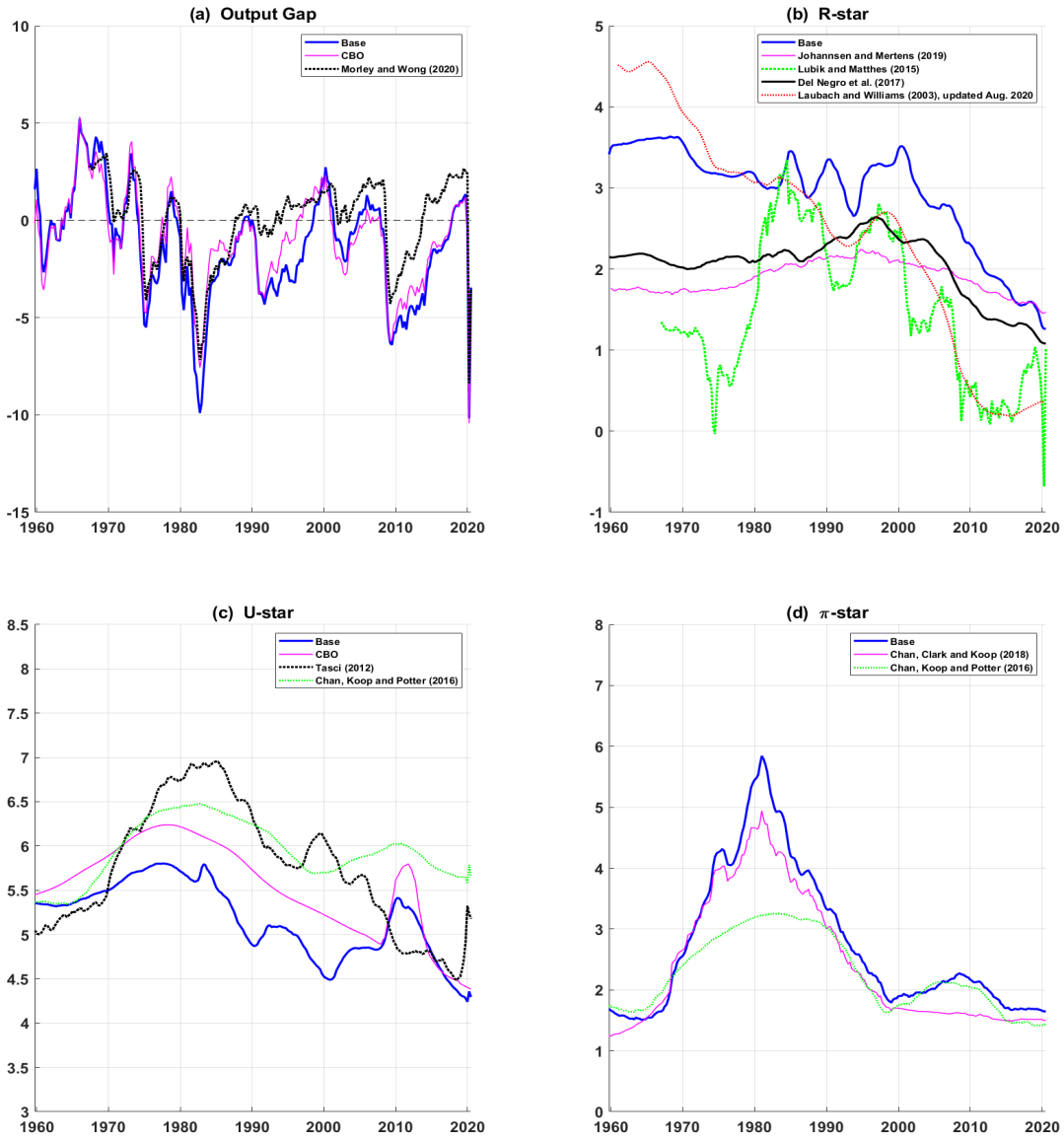

Notes: In the case of Johannsen and Mertens (2019), Del Negro et al. (2017), and Lubik and Matthes (2015), the estimates plotted are the posterior median, for all others it is the (posterior) mean estimate.

A9. R*: Backcast Survey R* from 1959-1982

The survey estimates of g-star, u-star, and pi-star are direct reads from the survey. In contrast, the r-star survey estimate is not a direct estimate. Instead, it is inferred from the Blue Chip survey long-run estimates of GDP deflator and short-term interest rates (3-month Treasury bill) using the long-run Fisher equation. Specifically, the long-run forecast of 3-month Treasury bill less the long-run forecast of GDP deflator. To this differential, we add +0.3 to reflect the average differential between the federal funds rate and the 3-month Treasury bill. (r-star refers to the long-run equilibrium federal funds rate)

Survey projections are not available before 1983Q1. To fill in estimates for the survey variables between 1959Q4 and 1982Q4, we use CBO long-run projections in the case of real GDP growth and the unemployment rate. In the case of inflation, we use the PTR series available from the Federal Reserve Board website; this series is used in many studies employing long-run expectations of inflation (e.g., CCK, Tallman and Zaman, 2020). We do not have a readily available historical source for long-run forecasts for interest rates (and r-star). So we backcast a particular time series of implied r-star using CBO's long-run projections of g-star. Specifically, we first fit a simple linear regression model over the post-1983 period that regresses survey r-star on a constant, its lags (2 lags), and a one-period lag "gap," defined as the difference between survey r-star and survey g-star. We use the estimated model and the CBO long-run projections of g-star over the sample 1959Q4 through 1982Q4 to backcast the implied survey r-star estimates. (When backcasting, the initial values of r-star for 1959Q2 and 1959Q3 are assumed identical to CBO g-star)

$$r_t^{*,Surv} = c + \beta_1 gap_{t-1}^{r*,g*,Surv} + \beta_2 r_{t-1}^{*,Surv} + \beta_3 r_{t-2}^{*,Surv} + \varepsilon_t^{*,Surv}, \quad \varepsilon_t^{*,Surv} \sim N(0, \sigma^2_{*,Surv}) \qquad (85)$$

where, $gap_t^{r*,g*,Surv} = g_t^{*,Surv} - r_t^{*,Surv}$

The OLS estimation yields, $c = -0.0745$; $\beta_1 = 0.06$; $\beta_2 = 1.167$; $\beta_3 = -0.148$

Figure A10 plots the survey g-star and r-star estimates in solid, and the CBO g-star and the backcast r-star in dashed lines.

Figure A10: Survey r* and g*

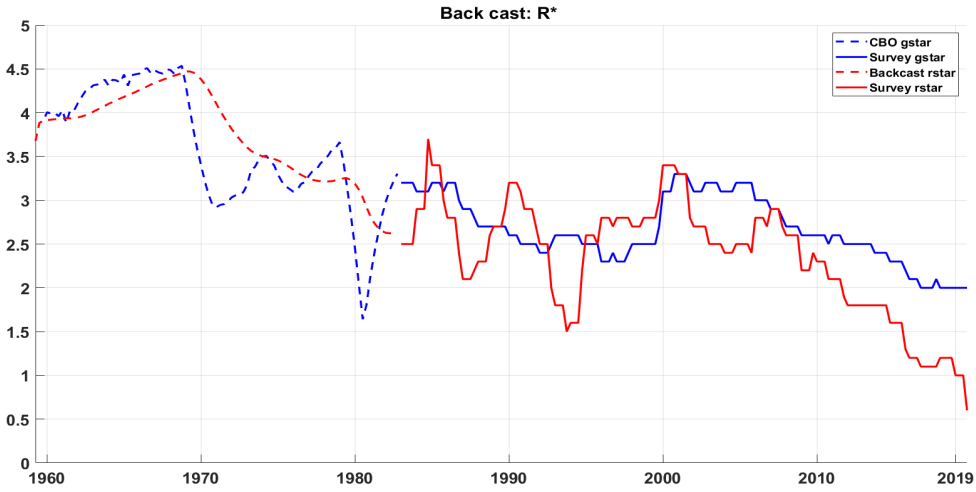

A10. R* : Additional Full Sample Results

A10.a. Role of data vs. prior in shaping r-star

Kiley (2020), using a model in which r-star follows a RW process, documents an essential finding that data provide very little information in shaping the r-star process. Hence, the model-based r-star estimate is mainly driven by the modeler's prior views. Our results generally confirm Kiley's findings. However, in our Base specification, where the variance of the g-star process influences both the prior and the posterior for the r-star process, the data does influence the r-star estimate; because we find evidence that data provide information about the g-star process. This latter evidence of data's influence on the identification of g-star is also noted by Kiley (2020).

We begin by comparing the prior and posterior estimates of the parameter σ^2_{r*}, which governs the shock variance of the r-star process, in the Base-R*RW and Base-NoSurvR*RW – both these specs model r-star as a RW similar to Kiley (2020). We set prior for $E(\sigma^2_{r*}) = 0.1^2$), which is the same as in Astudillo and Laforte (2020) but tighter than 0.25^2 used by Kiley.[4] (Our choice of tighter prior than Kiley is due to a significantly more complex model). Our model estimation yields posterior estimates of 0.09^2 (with 90% credible intervals 0.07^2 to 0.11^2) in Base-R*RW and 0.1^2 (with 90% interval 0.08^2 to 0.13^2) in Base-NoSurvR*RW, respectively. It appears that in the case of Base-NoSurv-R*RW, the prior setting of the r-star process is driving the trajectory as evidenced by the posterior mean of the parameter σ^2_{r*} identical to the prior. But in the case of Base, the posterior mean of the parameter σ^2_{r*} is slightly different from the prior mean, suggesting that by bringing survey data in the estimation, the data does play a role in shaping r-star.

We next confirm our finding by re-doing our exercise setting a looser prior for $E(\sigma^2_{r*}) = 0.25^2$), same as in Kiley (2020). The updated model estimation yields posterior estimates of $E(\sigma^2_{r*}) = 0.15^2$) (with 90% credible intervals 0.13^2 to 0.17^2) in Base-R*RW and $E(\sigma^2_{r*}) = 0.22^2$) (with 90% interval 0.18^2 to 0.27^2 in Base-NoSurvR*RW, respectively. The fit of these models to interest rate data (and other model data) is significantly worse compared to Base and Base-NoSurv.

We explored the impact on the r-star estimates of even more looser priors on the shock process governing r-star. We find that as the prior on the r-star process loosens, data becomes more informative in shaping the r-star estimate (echoing Lewis and Vazques-Grande, 2019). But it comes at the cost of worsening model fit, higher volatility in the r-star estimate, and worsening precision of r-star.

A10.b. Base vs. External models

In figure A11, the left panel plots r-star from Base (solid line) and two external models, the seminal model of LW (dashed line) and the more recent model developed in Del Negro et al. (2017) (dotted line). As is the case with most r-star estimates presented in the literature, the LW estimate shows a marked decline in r-star from 2000 and beyond. As shown in the figure, compared to the r-star estimate from the Base, the LW estimate is lower over this period. Part of the explanation of this difference in the estimates comes from the different estimates of g-star (not shown).

[4] We also explore a model specification in which prior variance is set at 0.25^2, the fit of this specification was significantly inferior, and the r-star estimate was quite volatile.

In the LW model, the mechanical reason for this steadily declining trajectory of r-star is coming from the fact that their model estimate of g-star has been steadily declining over the same period. Over this period, GDP grew just slightly above their estimate of g-star, even though the real short-term rate is significantly below zero over this period. The model explains the combination of moderate growth in GDP (suggesting a small positive output gap) and negative real short-term interest through a low level of r-star estimate so to obtain a negative real interest rate gap (see LW, 2016). In our Base (and Base-NoSurv) model, because the estimate of g-star is even lower than LW, which implies a more positive output gap (than LW), a less negative real interest rate gap (than LW) is required to explain the output gap. The less negative real interest rate gap (i.e., a smaller interest rate gap) implies a higher level of r-star than LW.

The r-star estimate from Del Negro et al. is stable around 2% from 1960 through early 1980 and then slowly move up, reaching 2.5% by late 1990. From thereon, it begins a gradual decline ending 2019 at 1.2%, identical to Base, and two-tenths lower than Base-NoSurv. It is worth noting that Del Negro et al. also utilize survey expectations on r-star to estimate r-star but their approach in how they model the link between the two is very different than ours.[5] They also assume a relationship between g-star (in their case, long-run productivity growth) and r-star. However, their model structure is different compared to ours. Shortly, we show an r-star estimate from our model specification with the tighter prior assumption for the r-star process, which is remarkably similar to Del Negro et al.

A10.c. Sensitivity of r-star to the prior setting

As just shown and noted by others (e.g., Kiley (2020)), the prior elicitation for the variance parameter of the shock process governing r-star has a notable influence on the dynamics of r-star. We briefly show another illustration highlighting the sensitivity of r-star to the prior setting. In figure A11, the right panel plots the posterior mean r-star obtained from model specification, Base-NoSurv-R*TightPrior, which is Base-NoSurv but with a tighter prior value for the parameter σ_d^2 (0.01^2 instead of 0.1^2). The parameter σ_d^2 refers to the variance of the shock process defining the "catch-all" component D. Also plotted are the posterior estimates of r-star from Base-NoSurv and Del Negro et al. (2017) model. Three things immediately stand out. First, imposing a tighter prior has a notable impact on r-star, as shown by comparing dashed and solid lines in the figure. Second, the model specification Base-NoSurv-R*TightPrior has the posterior mean of r-star near 2% from early 1960 through mid-1980, which is similar to the r-star estimate reported in Kiley (2020). Third, the entire trajectory of r-star from the Base-NoSurv-R*TightPrior is remarkably similar to the median estimate of r-star from the Del Negro et al. model. These results indicate that very different approaches could provide similar estimates, yet somewhat related approaches could yield very different estimates.

[5]Del Negro et al. use survey expectations from Survey of Professional Forecasters, which start from 1992 onwards. In addition, in their framework survey expectations is one of the several financial indicators that they use to extract a common trend. So arguably, in their approach, the survey expectations of r-star will be less influential in driving r-star than in our approach in which a direct connection between r-star and survey data is assumed.

Figure A11: R* estimates

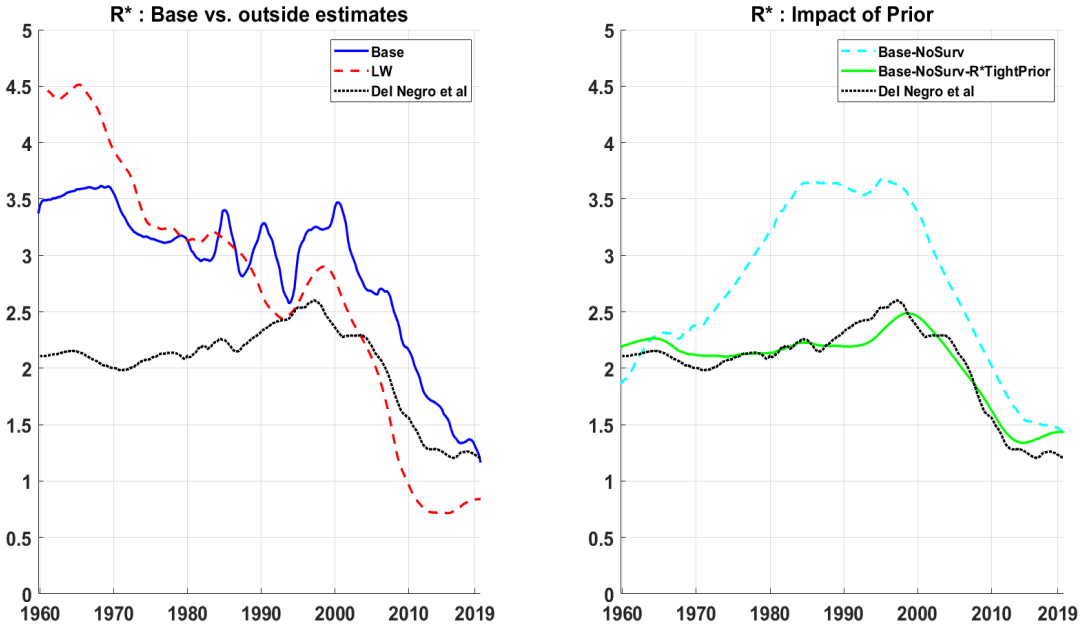

A10.d. The usefulness of the Taylor-rule equation and the equation linking r* to survey

In recent studies on estimating r-star, a Taylor-type rule equation is added to the model structure to improve the econometric estimation. Our Base model also includes a Taylor-type rule. As we now illustrate, this addition is crucial to improve precision and the plausibility of the r-star estimates significantly. The left panel in figure A12 plots three estimates of r-star obtained from model specifications Base (solid line), Base-NoR*Surv (dashed line), and Base-NoR*Surv-NoTRule (dotted line). The right panel plots the corresponding precision of the r-star estimates. The specification Base-NoR*Surv excludes the equation linking r-star to survey expectations from the model (but keeps equations relating other stars to survey). Doing so produces a trajectory of r-star similar to the Base-NoSurv spec; and not surprisingly, the precision of r-star is reduced relative to the Base spec, as evidenced by the plot corresponding to Base-NoR*Surv lying above the Base.

The specification Base-NoR*Surv-NoTRule excludes the equation linking r-star to survey expectations and the Taylor-rule equation. So in this spec, r-star is identified from the IS-curve equation, and the equation relating r-star to g-star. As expected, shrinking the model's structure further by excluding the Taylor-rule equation reduces the r-star estimate's precision dramatically, as evidenced by Base-NoR*Surv-NoTRule plot located above all the others in the left panel. Besides the impact on the precision, as would be expected, changes in the system's structure result in notable differences in the estimated level of the r-star. The posterior mean estimate of r-star, which has the r-star declining steadily over the sample, is substantially lower than both Base and Base-NoR*Surv. However, the uncertainty around the posterior mean is enormous complicating inference with a reasonable degree of certainty.

Figure A12: The Usefulness of Taylor Rule equation

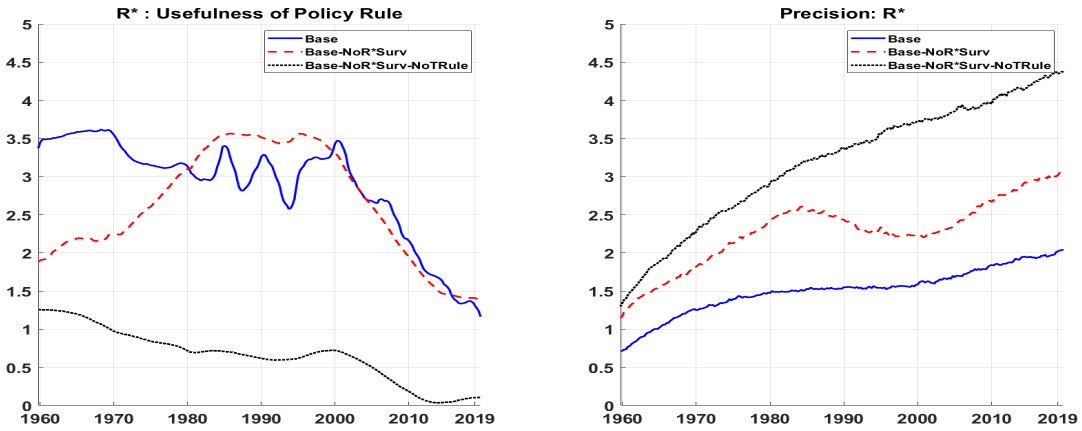

Notes: The posterior estimates are based on the full sample (from 1959Q4 through 2019Q4).

A11. Pi* : Additional Full Sample Results

A11.a. Pi-star comparison Base vs. outside models

In figure A13, panel (a) plots posterior mean estimates of pi-star from some related (smaller size) models from the literature alongside Base to facilitate comparison. In particular, estimates are shown for CKP, CCK, and the celebrated UCSV model of Stock and Watson (2007).[6] Panel (b) plots the corresponding precision estimates of pi-star.

There are some interesting similarities and differences across the pi-star estimates. Whereas UCSV displays very volatile and erratic estimates of pi-star, others show smoother evolution of pi-star. CKP indicates a lower estimate of pi-star than others from the early 1970s through the late 1980s. The primary factor contributing to lower pi-star in CKP is the model assumption of a bounded random walk for pi-star. As discussed in CKP, the addition of bounds on pi-star leads the model to attribute a substantial share of the high observed inflation of the 1970s to the increased persistence of the inflation gap and only a small increase in the pi-star. Hence, pi-star is estimated to have risen less than implied by other models. For instance, CCK model had pi-star peaking at 4.9%, Base at 6.0% and CKP at 3.2%. As alluded in CKP, this small rise in pi-star is consistent with a specific narrative that during the Great Inflation period, the Fed had a low implicit target for inflation but was either unable to or unwilling to correct large deviations of inflation from the target.

The contours of pi-star from Base is similar to CCK through 2000, but from 2000 to 2012, Base is identical to CKP, with CCK a touch lower. It is interesting to note that from the early 2000s through 2010, both Base and CKP indicate pi-star at 2%. From 2012 through 2019, both Base and CKP gradually drift lower to 1.5% (same as CCK) and 1.3%, respectively.

Panel (b), which plots the corresponding precision of pi-star, reveals some interesting patterns. First, the precision of the pi-star evolved generally with the level of pi-star. As pi-star increased during the Great Inflation, pi-star became more uncertain, i.e., more imprecise. Subsequently, as pi-star trended lower during the Volcker disinflation, so did the uncertainty about it (i.e., precision increased). Second, comparing across models, there is significant heterogeneity in the precision of pi-star. From 1960 through the mid-1970s, the Base model indicates the most precise pi-star, followed by CCK and CKP. UCSV model shows volatile estimates of precision, sharply fluctuating between the most precise to least precise. From the mid-1970s through 2019, the CCK model indicates the most precise (least uncertain) pi-star, followed by Base, CKP, and UCSV. CCK had the uncertainty of pi-star gradually trending down starting in the mid-1970s. In contrast, in others, the uncertainty continued to trend higher until peaking in the early 1980s.

Third, between 2000 and 2019, the uncertainty around pi-star implied by CCK and Base has been reasonably stable, an artifact of the use of survey data. During this period, the precision of pi-star implied by CCK is on average 40 basis points higher (i.e., uncertainty is lower) compared to Base. This improved precision of CCK is interesting because both CCK and Base utilize information from survey expectations of inflation. However, at the same time, compared to Base, which has a rich structure (hence more parameters), the CCK model is parsimonious, as it uses information from inflation and survey only to estimate pi-star.

An additional factor that could contribute to the differential in precision is that, unlike Base, CCK allows SV in the pi-star equation. A more in-depth inspection of the estimation results reveals the primary factor driving the superior precision of the CCK estimate of pi-star

[6] Whereas in estimating the UCSV model, Stock and Watson (2007) fix the parameters governing the smoothness of the SV processes, we estimate them.

compared to Base is tighter priors on the assumed relationship between survey forecast and pi-star. And that translates into a posterior estimate implying a stronger connection between survey forecast and pi-star in CCK than Base.

Figure A13: Pi* estimates: Base vs. External models

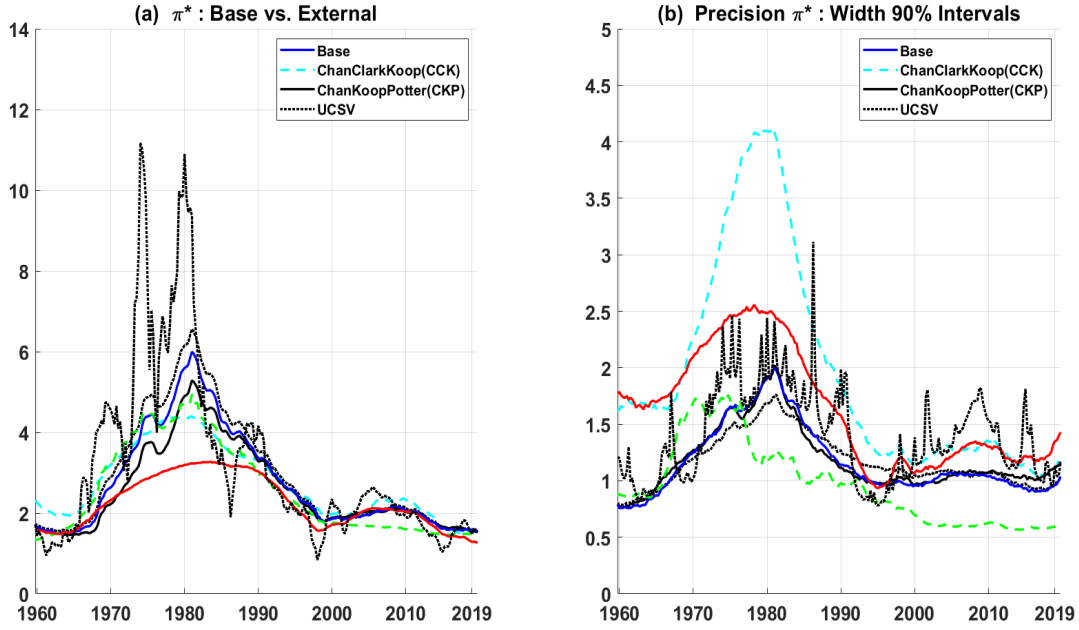

Notes: The posterior estimates are based on the full sample (from 1959Q4 through 2019Q4). In all cases, the inflation measure is the PCE inflation.

A11.b. Sensitivity of pi-star to modeling assumptions

Figure A14, panel (a) indicates the sensitivity of the pi-star estimates to modeling assumptions. The plot labeled Base-W*RW is the variant of the Base model that removes the theoretical restriction imposed by equation (28) and instead assumes a random walk assumption for w-star. Comparing the Base and Base-W*RW plots indicate the effects of the theoretical restriction on pi-star. As shown, the posterior mean estimate of pi-star from Base-W*RW is marginally lower than Base in the period 1970 through the early 1980s (Great Inflation period). However, from thereon, estimates of pi-star are identical. During the high-inflation period, compared to the Base model, the Base-W*RW allocates a higher share of the increase in inflation to the persistence component than pi-star (i.e., the random walk component); see figure A14. Hence, the lower level of pi-star in Base-W*RW than Base.

The plot labeled Base-NoPT is the variant of the Base model that eliminates the passthrough from prices to wages, modeled via equation (29b)—doing so results in a slightly higher pi-star (Base-NoPT) from 1970 through the early 1980s. However, thereafter, estimates of pi-star are identical between Base and Base-NoPT. During the high-inflation period, compared to the Base model, the Base-NoPT allocates a lower share of the increase in inflation to the persistence component than pi-star; hence, the higher level of pi-star in Base-NoPT than Base. Based on the model comparison, Base-W*RW model's fit to the inflation data and other data is inferior compared to Base. In the case of Base-NoPT, the fit to the inflation data is slightly higher than Base. However, the overall fit of the Base-NoPT is significantly worse than Base. The Base-NoPT model's reduced fit is the net effect of its reduced ability to fit wages and its improved ability to fit prices.

We also explored a variant of the Base model that allowed the passthrough from wages to prices in the price inflation equation, denoted Base-PT-Wage-to-Prices in table 1. The estimates of pi-star (and of other parameters) are identical to those of the Base; hence, they are not shown. Therefore, not surprisingly, as reported in table 8 (main paper), both models' ability to fit inflation data are very similar. We also highlight that allowing SV in the inflation equation is very important, as evidenced by a significantly reduced fit of the Base-NoSV model, which is the Base model variant that does not feature SV in any model equations.

Figure A14: More Estimates for Price inflation block

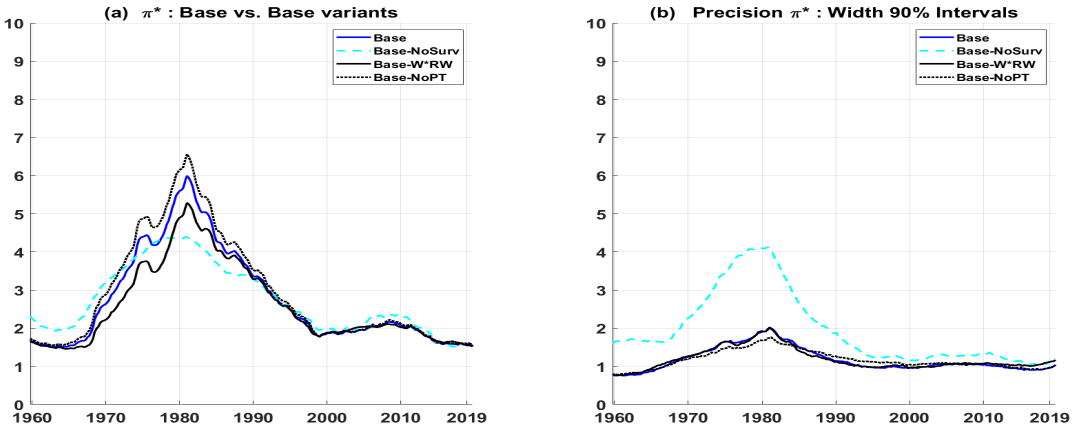

Notes: The posterior estimates are based on the full sample (from 1959Q4 through 2019Q4).

A11.c. Pi-star estimates for some variants of the Base model

Figure A15: Pi* estimates: Base vs. Base model variants

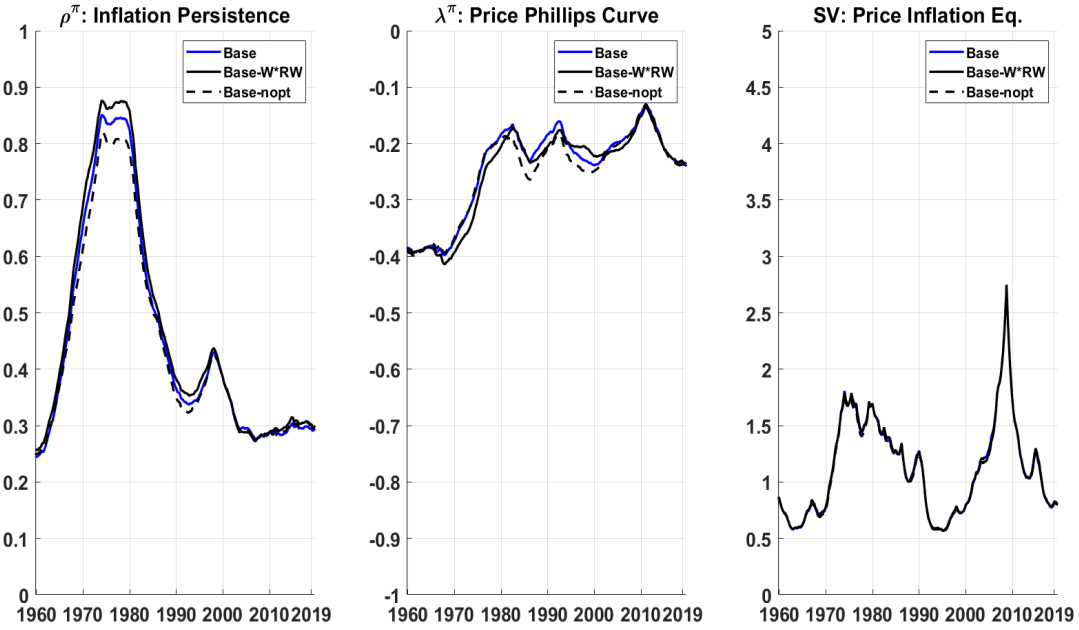

Notes: The posterior estimates are based on the full sample (from 1959Q4 through 2019Q4).

A12. P*: Base comparison with Kahn and Rich (2007)

In this section, we compare our model-based estimates of p-star with the narrative about p-star implied from the two-regime Markov switching model of Kahn and Rich (2007).[7] A regime-switching framework (as in Kahn and Rich) allows for deterministic values of p-star, where the number of deterministic values equals the number of possible regimes. Accordingly, in a 2-regime setup, the estimated p-star would periodically alternate from one-regime (e.g., low productivity regime) to the other regime (e.g., high productivity regime). In contrast, the random walk assumption for p-star adopted in this paper (and in others such as Roberts, 2001; Edge et al., 2007; Benati, 2007) allows for the possibility that p-star may be (slowly) changing in every period. This latter assumption implies that the possible values of p-star could equal the number of periods in the estimation sample. The differences in the stochastic conception between the two frameworks complicate direct comparison in p-star.

One possible albeit imperfect approach to comparing the implied p-star from two frameworks is to use the regime-switching model's identified regimes to assess how well those corroborate with p-star estimates implied from the RW assumption model. Specifically, for the RW model, compute the "average" p-star over the specific periods (identified regimes). Then assess the following: (1) whether the "average" rates imply characterization of regimes that corroborate with the identified regimes; (2) how close the "average" rates of p-star are to the deterministic values of p-star estimated in the regime-switching model. We use this approach to compare the estimates of p-star from our models to the p-star estimated by the Kahn and Rich model.

Figure A16 presents the comparison of p-star. Panel (a) compares the Base model with Kahn and Rich model, and panel (b) compares the Base-W*RW model with Kahn and Rich model. In the panels, the shaded areas refer to the two regimes identified by the Kahn and Rich model using the same vintage of data as our models. The lighter shaded area corresponds to the "high productivity regime," and the darker shaded area "low productivity regime." Their model identifies two subperiods of high productivity regimes: the beginning of our sample through 1974Q4 and 1996Q3 through 2004Q4. Similarly, two subperiods of low productivity regime: 1975Q1 through 1996Q2 and 2005Q1 through the end of the sample, 2019Q4. Based on the "average" rates of p-star computed for the specific two regimes from our models, if we assume a cutoff of 1.5%, with "average" rate of p-star <= 1.5% as defining low productivity regime, and "average" rate > 1.5% as defining high productivity regime, then the characterization of regimes (and in-turn the narrative) aligns perfectly with Kahn and Rich.

Next, we compare the "average" rates for the two-regimes implied by our models to Kahn and Rich model. The Base model implies for a low productivity regime an "average" rate of 1.3% (for both subperiods) and for a high productivity regime an "average" rate of 2.1% (subperiod beginning of our sample through 1974Q4) and 1.7% (subperiod 1996Q3 through 2004Q4). The Base-W*RW model implies for a low productivity regime an "average" rate of 1.5% (for both subperiods) and for a high productivity regime an "average" rate of 2.5% (in the first subperiod) and 2.3% (in the second subperiod). In comparison, Kahn and Rich's model implies a p-star of 1.33% for a low productivity regime for both subperiods – p-star are equal across subperiods by construction; and 2.96% p-star for a high productivity regime. For the low productivity regime, the implied p-star is similar between our models and Kahn and Rich, but for the high productivity regime, Kahn and Rich's model is on the higher side than our models.

[7] The estimates of p-star implied by the Kahn and Rich (2007) model are routinely updated and made available for download at James A. Kahn's website: http://sites.google.com/view/james-a-kahn-economics/home/trend-productivity-update

Overall, this illustration suggests that the two approaches provide generally similar inferences about developments in p-star, and we view this as a useful result for macroeconomists tasked with modeling and tracking productivity developments.

Figure A16: P* consistent with narrative from 2-Regime Markov-Switching Model

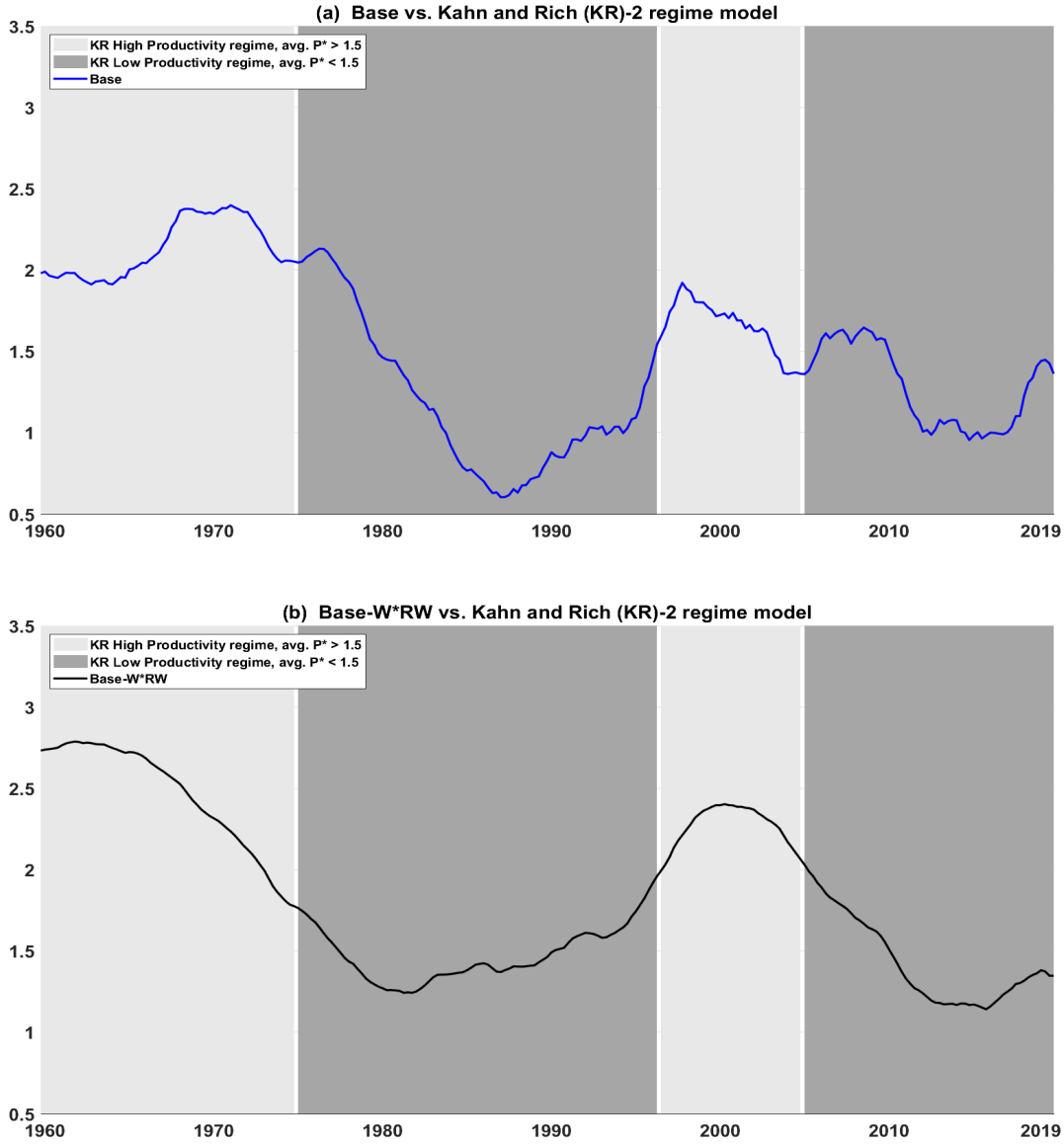

Notes: The shaded areas refer to the two regimes identified by the Kahn and Rich model using the same vintage of data as our models. The lighter shaded area corresponds to the "high productivity regime," and the darker shaded area "low productivity regime." The plots labeled Base and Base-W*RW are the posterior mean estimates based on the full sample (from 1959Q4 through 2019Q4).

A13. P* : Additional Full Sample Results

A13.a. Cyclical Productivity based on Output gap

Figure A17: Base-P*CycOutputGap model

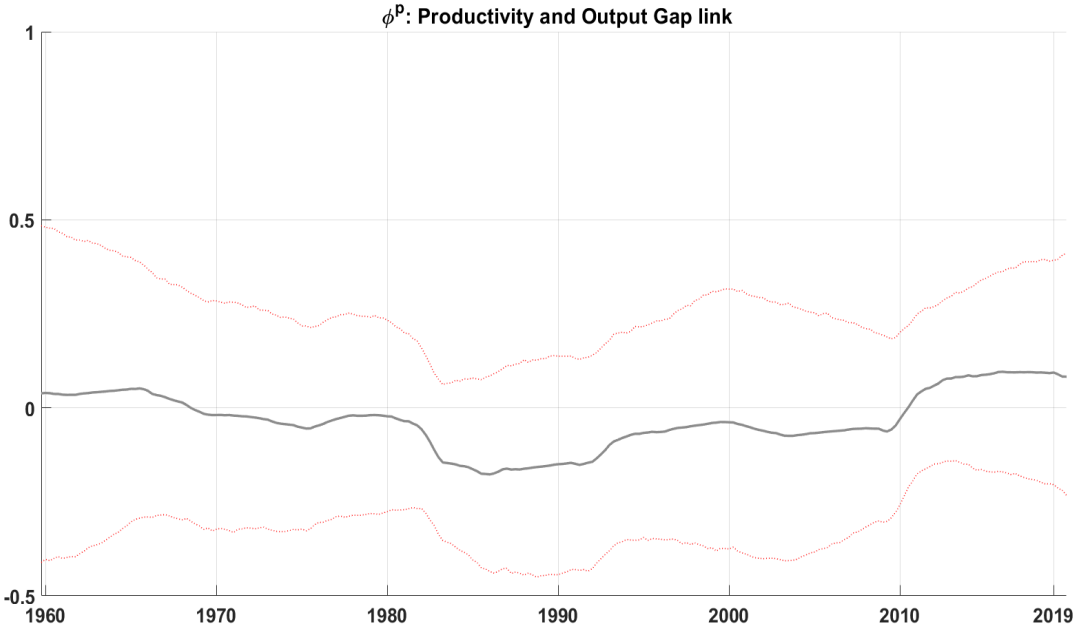

Notes: The posterior estimates are based on the full sample (from 1959Q4 through 2019Q4). The solid line represents the posterior mean and the dotted lines represent the 90% credible intervals.

References

[1] Benati, Luca (2007). Drift and breaks in labor productivity. *Journal of Economic Dynamics & Control*, 31(8): 2847-2877.

[2] Berger, Tino, Morley, James, & Benjamin Wong (forthcoming). Nowcasting the output gap. *Journal of Econometrics*

[3] Carriero, Andrea, Clark, Todd E., Marcellino, Massimiliano, & Elmar Mertens (2021). Addressing COVID-19 outliers in BVARs with stochastic volatility. Federal Reserve Bank of Cleveland, Working Paper No.21-02. https://doi.org/10.26509/frbc-wp-202102

[4] Chan, Joshua, Clark, Todd E., & Gary Koop (2018). A new model of inflation, trend inflation, and long-run inflation expectations. *Journal of Money, Credit, and Banking*, 50(1): 5-53

[5] Chan, Joshua, & Ivan Jeliazkov (2009). Efficient simulation and integrated likelihood estimation in state space models. *International Journal of Mathematical Modeling and Numerical Optimisation* 1: 101-120

[6] Chan, Joshua, Koop, Gary, Poirier, Dale J., & Justin Tobias L. (2019). Bayesian Econometric Methods 2nd edition. *Cambridge University Press*

[7] Chan, Joshua, Koop, Gary, & Simon M. Potter (2013). A new model of trend inflation. *Journal of Business and Economic Statistics* 31: 94-106

[8] Chan, Joshua, Koop, Gary, & Simon M. Potter (2016). A bounded model of time variation in trend inflation, NAIRU and the Phillips curve. *Journal of Applied Econometrics* 31: 551-565

[9] Chan, Joshua, & Rodney Strachan (2012). Estimation in non-linear non-Gaussian state-space models with precision-based methods. CAMA working paper series 2012-13.

[10] Del Negro, Marco, Giannone, Domenico, Giannoni, Marc, & Andrea Tambalotti (2017). Safety, liquidity, and the natural rate of interest. *Brookings Papers on Economic Activity*

[11] Edge, Rochelle M., Laubach, Thomas & John C. Williams (2007). Learning and shifts in long-run productivity growth. *Journal of Monetary Economics* 54: 2421-2438

[12] Geweke, John (1992). Evaluating the accuracy of sample-based approaches to the calculation of posterior moments, in *Bayesian Statistics 4* (ed. J.M. Bernardo, J.O. Berger, A.P. Dawid, A.F.M.Smith), 641-649. Oxford: Clarendon Press.

[13] Gonzalez-Astudillo, Manuel, & Jean-Philippe Laforte (2020). Estimates of r* consistent with a supply-side structure and a monetary policy rule for the U.S. economy. Finance and Economics Discussion Series Paper 2020-085

[14] Harvey, David, Leybourne, Stephen, & Paul Newbold (1997). Testing the equality of prediction mean squared errors. *International Journal of Forecasting*, 13: 281-291.

[15] Johannsen, Benjamin K., & Elmar Mertens (2019). A time series model of interest rates with the effective lower bound. *Journal of Money, Credit, and Banking*

[16] Jorda, Oscar, Singh, Sanjay R., & Alan M. Taylor (2020). Longer-Run economic consequences of pandemics. San Francisco Fed Working paper 2020-09

[17] Kahn, James A., & Robert W. Rich (2007). Tracking the new economy: Using growth theory to detect changes in trend productivity. *Journal of Monetary Economics* 54: 1670-1701

[18] Koop, Gary (2003). Bayesian Econometrics. *Chichester: Wiley.*

[19] Koop, Gary, Leon-Gonzalez, Roberto & Rodney W. Strachan (2010). Dynamic probabilities of restrictions in state space models: An application to the Phillips curve. *Journal of Business and Economic Statistics* 28(3): 370-379

[20] Korobilis, Dimitris (2017). Quantile regression forecasts of inflation under model uncertainty. *International Journal of Forecasting* 33(1): 11-20

[21] Kiley, Michael T. (2020). What can data tell us about the equilibrium real interest rate? *International Journal of Central Banking*, June 2020

[22] Knotek, Edward S. (2015). Difficulties forecasting wage growth. Federal Reserve Bank of Cleveland *Economic Trends*

[23] Laubach, Thomas & John C. Williams (2003). Measuring the natural rate of interest. *The Review of Economics and Statistics*, 85(4): 1063-1070

[24] Lewis, Kurt F. & Francisco Vazquez-Grande (2019). Measuring the natural rate of interest: A note on transitory shocks. *Journal of Applied Econometrics* 34: 425-436

[25] Lubik, Thomas A. & Christian Matthes (2015). Calculating the natural rate of interest: A comparison of two alternative approaches. *Richmond Fed Economic Brief*

[26] Morley, James, & Benjamin Wong (2020). Estimating and accounting for the output gap with large Bayesian vector autoregressions. *Journal of Applied Econometrics*, 35: 1-18

[27] Pescatori, Andrea, & Jarkko Turunen (2016). Lower for longer: Neutral rate in the U.S. *IMF Economic Review*, 64(4): 708-731

[28] Primiceri, Giorgio E. (2005). Time varying structural vector autoregressions and monetary policy. *Review of Economic Studies*, 72, 821-852 doi:10.1111/j.1467-937x.2005.00353.x

[29] Roberts, John. (2001). Estimates of the productivity trend using time-varying parameter techniques. *Contributions to Macroeconomics*, 1(1):3

[30] Schorfheide, Frank, & Dongho Song. (2020). Real-Time Forecasting with a (Standard) Mixed-Frequency VAR During a Pandemic. Philadelphia Fed Working paper 20-26.

[31] Stock, James H., & Mark W. Watson (2007). Why has U.S. inflation become harder to forecast? *Journal of Money, Credit and Banking*, 39: 3-33

[32] Stock, James H., & Mark W. Watson (2016). Core inflation and trend inflation. *Review of Economics and Statistics*, 98(4): 770-784

[33] Tallman, Ellis W., & Saeed Zaman (2020). Combining survey long-Run forecasts and nowcasts with BVAR forecasts using relative entropy. *International Journal of Forecasting*, 36(2): 373-398

[34] Tasci, Murat (2012).The ins and outs of unemployment in the long run: Unemployment flows and the natural rate. Federal Reserve Bank of Cleveland Working paper

[35] Tasci, Murat (2019). Challenges with estimating u star in real time. Federal Reserve Bank of Cleveland *Economic Commentary*, 2019-18

[36] Wright, Jonathan (2013). Evaluating real-time VAR forecasts with an informative democratic prior. *Journal of Applied Econometrics*, 28: 762-776 doi:10.1002/jae.2268

[37] Wright, Jonathan (2019). Some observations on forecasting and policy. *International Journal of Forecasting*, 35(3): 1186-1192